



<https://theses.gla.ac.uk/>

Theses Digitisation:

<https://www.gla.ac.uk/myglasgow/research/enlighten/theses/digitisation/>

This is a digitised version of the original print thesis.

Copyright and moral rights for this work are retained by the author

A copy can be downloaded for personal non-commercial research or study, without prior permission or charge

This work cannot be reproduced or quoted extensively from without first obtaining permission in writing from the author

The content must not be changed in any way or sold commercially in any format or medium without the formal permission of the author

When referring to this work, full bibliographic details including the author, title, awarding institution and date of the thesis must be given

Enlighten: Theses

<https://theses.gla.ac.uk/>  
[research-enlighten@glasgow.ac.uk](mailto:research-enlighten@glasgow.ac.uk)

**Post-translational Modification and Sequestration of  
cAMP-specific Phosphodiesterase 4 in  
Signalling Complexes**

A thesis submitted to the

FACULTY OF BIOMEDICAL AND LIFE SCIENCES

For the degree of

DOCTOR of PHILOSOPHY

**Xiang Li**

MRes. Molecular Functions in Disease

BSc. Pharmacy

Division of Biochemistry and Molecular Biology

Institute of Biomedical and Life Sciences

University of Glasgow

October 2006

ProQuest Number: 10391390

All rights reserved

INFORMATION TO ALL USERS

The quality of this reproduction is dependent upon the quality of the copy submitted.

In the unlikely event that the author did not send a complete manuscript and there are missing pages, these will be noted. Also, if material had to be removed, a note will indicate the deletion.



ProQuest 10391390

Published by ProQuest LLC (2017). Copyright of the Dissertation is held by the Author.

All rights reserved.

This work is protected against unauthorized copying under Title 17, United States Code  
Microform Edition © ProQuest LLC.

ProQuest LLC.  
789 East Eisenhower Parkway  
P.O. Box 1346  
Ann Arbor, MI 48106 – 1346

GLASGOW  
UNIVERSITY  
LIBRARY:

**This thesis is dedicated to my parents and grandparents.**

## **Acknowledgements**

So many people have helped my PhD study on its way that it seems invidious to single out individuals. However, certain people have had a direct impact on what follows. I acknowledge with gratitude the supervision of Professor Miles Houslay, for allowing me to carry out those exciting and forefront projects, for his guidance and support. I would particularly like to thank Dr. George Baillic, whose help has been extremely invaluable over the entire course of my PhD study. He has never been too busy to answer enquiries about any number of issues pertaining both to the science or life more generally and constantly provided the source of much amusement.

I would like to mention and thank Dr. Martin Lynch, Dr. Elaine Huston, Dr. Ahmed Mohammed, Mr. Derek Wallace, Dr. Angela McCahill and Mrs. Irene Gall for their generous advice, patient explication of the techniques and introduction of the Scottish jokes! Thank you Mrs. Nindy Bhari and Miss Amelie Gormand for your company in the lab. Thank you all the rest of the Gardiner Lab old and new for the help!

I wish to single out Miss Lida Teng and Miss Mridu Acharya, my best friends in U.K. for their constant encouragement, support and amusement. Also, thanks to Dr. Niall Fraser and Dr. Alastair Gardiner, who helped me more than they know! Equally supportive and forthcoming are my Chinese friends in Glasgow, without whom, of course...

I would also like to take this opportunity to thank the Wellcome Trust for the studentship. A big 'thank you' is also owed to Professor Bill Cushley and Professor Richard Cogdell for their generous help from the minute I arrived in Glasgow International Airport...

Finally, I would like to thank my dad, my mum and my grandparents for their patience, support and understanding. I owed you too much!

## Abstract

cAMP is a ubiquitous second messenger that is pivotal in controlling a wide array of cellular functions. The sole means to inactivate cAMP is to degrade it into 5'-AMP through the action of cyclic nucleotide phosphodiesterases (PDEs). It is now well appreciated that cAMP hydrolysis by PDEs is as important as its synthesis by adenylyl cyclases to achieve cAMP homeostasis in cells. The cAMP-specific phosphodiesterase-4 (PDE4) is encoded by four different genes (*PDE4A*, *PDE4B*, *PDE4C* and *PDE4D*), which generate over 16 different isoforms by alternative 5' mRNA splicing. This process gives rise to PDE4 isoforms with unique N-terminal region, complete or truncated UCR1/UCR2 modules, a central catalytic domain and an extreme C-terminal region. This plethora of PDE4 isoforms, complete with distinct N-terminal targeting domains and particular regulatory properties, confers compartmentalized action on cAMP signaling in various cell types. Understanding the distinct molecular mechanisms and functional outcomes of modification and sequestration of specific PDE4 isoforms can be expected to aid the development of more selective PDE4 inhibitor-based therapeutics.

I have assessed the involvement of PDE4 isoenzymes in the  $\beta_2$ -adrenergic receptor ( $\beta_2$ AR) desensitization process in Chapter 3. It has been previously shown that agonist-activated  $\beta_2$ ARs can recruit PDE4 isoforms in complex with  $\beta$ -arrestins and, in particular, PDE4D5 whereupon they undergo a dual desensitization. Using the PDE4-selective inhibitor rolipram or siRNA-mediated knockdown of PDE4B and PDE4D, I determined a new facet of PDE4-mediated process in the early stage of  $\beta_2$ AR desensitization. In HEKB2 cells (stably overexpressing  $\beta_2$ ARs) that have been pretreated with either rolipram or with siRNA to PDE4B and PDE4D, PKA phosphorylated GRK2 was accelerated in response to treatment with the  $\beta$ -agonist isoprenaline, as was isoprenaline-induced membrane translocation of GRK2, phosphorylation of the  $\beta_2$ AR by GRK2, membrane translocation of  $\beta$ -arrestins/PDE4D complex and internalization of  $\beta_2$ ARs, in comparison with the cells that were only challenged with isoprenaline. In the absence of isoprenaline, rolipram-induced inhibition of PDE4 activity in HEKB2 cells also stimulated the phosphorylation of GRK2 by PKA, with consequential effects on GRK2 membrane

recruitment and GRK2 phosphorylation of  $\beta_2$ AR. These results collectively suggest that PDE4 plays a fundamental role in influencing  $\beta_2$ AR functioning by gating for the ability of PKA to phosphorylate GRK2 in resting cells and thereby regulating the degree of feedback through this system in stimulated cells. This provides a finely tuned adaptive response for preventing inappropriate activation of GRK through fluctuations in the basal levels of cAMP in resting/unstimulated cells.

In Chapter 4 and 5 of this thesis, I analyzed the potential post-translational modification on one PDE4 isoform, namely PDE4D5. I have used site-directed mutagenesis to show that the ubiquitin-interacting motif (UIM) can confer the ability of PDE4D5 to undergo ubiquitination in response to extracellular stimuli. Furthermore, this ubiquitination was shown to be mediated by the E3 ligase Mdm2 that is brought in close proximity to PDE4D by the associated  $\beta$ -arrestin. My data shows that only a small subset of PDE4D5, namely that to which  $\beta$ -arrestins bind, is susceptible to ubiquitination. Using epitope-tagged ubiquitin mutants that can block specific type of ubiquitin chain formation, I determined the K48-linked polyubiquitin chain as the predominant form in conjugation to PDE4D5. This finding, together with the observation that PDE4D5 can interact with two subunits of 19S regulatory complex, suggests that ubiquitination can target PDE4D5 to 26S proteasome for degradation. Having compared the kinetics of PDE4D5 ubiquitination and its association with  $\beta$ -arrestins, I concluded that ubiquitination alters the ability of PDE4D5 to bind  $\beta$ -arrestins. I proposed that the time-dependent ubiquitination of PDE4D5 may serve to facilitate  $\beta_2$ AR desensitization.

In Chapter 5, I investigated another post-translational modification, namely sumoylation, on PDE4D5. From *in vitro* sumoylation studies it showed that a subpopulation of PDE4D5 exists in a sumo-conjugated state. I confirmed this modification *in vivo*, by showing that immunoprecipitated wild type PDE4D5, but not a PDE4D5 SUMO K site mutant, could be conjugated with SUMO-1 as tested by immunoblotting. Sequential immunoprecipitation analyses showed that the established binding partners of PDE4D5, namely  $\beta$ -arrestin, ERK2, and AKAP188, preferentially interact with sumoylated forms of PDE4D5. This was further confirmed when comparing the association of these proteins with the wild type PDE4D5 and

SUMO K mutated PDE4D5, respectively, by co-immunoprecipitation. All these data indicate that SUMO modification of PDE4D5 serves to enhance its binding to signal scaffolding proteins *in vivo*.

I further investigated protein-protein interactions involving PDE4D5 in Chapter 6. Overlay studies were carried out with PDE4D5 peptide array libraries. These showed that  $\beta$ -arrestin and SUMO E2 enzyme Ubc9 interact at distinct sites within the unique N-terminal region of PDE4D5 and at overlapping sites within the conserved PDE4 catalytic domain. Also that ERK2 binds this overlapping site within the conserved PDE4 catalytic domain. Screening scanning alanine substitution peptide array libraries revealed a common docking site on PDE4D5 catalytic domain for  $\beta$ -arrestin, Ubc9 and ERK2, suggesting that these signaling scaffold proteins might interact with PDE4D5 in a mutually exclusive manner and compete to sequester distinct 'pools' of PDE4D5.

The above studies collectively suggest that sequestration of cAMP specific phosphodiesterase PDE4D5 in different signaling complex by distinct signaling scaffold proteins ensures the fidelity and efficiency in activating PDE4D5 post-translational modification and signaling.

## Table of Contents

<b>Declaration</b>		II
<b>Acknowledgements</b>		III
<b>Abstract</b>		IV
<b>Table of contents</b>		VII
<b>List of Figures</b>		XII
<b>Abbreviations</b>		XV
<b>Chapter 1</b>	<b>General Introduction</b>	1
1.1	Cyclic nucleotide signalling pathways	2
1.1.1	The cAMP signalling pathway	2
1.1.2	G-proteins and G-protein coupled receptors	2
1.1.2.1	G proteins	2
1.1.2.2	G-protein coupled receptors (GPCRs)	3
1.1.2.3	Beta-adrenergic receptors ( $\beta$ ARs)	3
1.1.3	Adenylyl Cyclases (ACs)	6
1.1.3.1	Structure of AC	6
1.1.3.2	Diversity and Distribution of ACs	6
1.1.3.3	Regulation of ACs	6
1.1.3.3.1	Stimulation by $G_{\alpha s}$	7
1.1.3.3.2	Inhibition by $G_{\alpha i}$	7
1.1.3.3.3	Regulation by $G_{\beta\gamma}$	7
1.1.3.3.4	Regulation by $Ca^{2+}$	7
1.1.3.3.5	Regulation by other small molecules	8
1.1.3.3.6	Post-translational modification	8
1.1.3.4	Expression pattern and their physiological roles	8
1.1.3.5	Compartmentalisation of ACs	8
1.1.4	Effectors of cAMP pathways	9
1.1.4.1	Protein Kinase A (PKA)	9
1.1.4.2	cAMP-regulated GEFs (GTP-exchange factors)	10
1.1.4.3	cAMP-gated membrane ion channels (CNG Ion Channels)	10
1.1.5	Compartmentalization of cAMP	10
1.2	The 3'5' cyclic nucleotide phosphodiesterase (PDE) superfamily	11
1.2.1	The PDE1 enzyme family	14
1.2.1.1	Structure of PDE1	15
1.2.1.2	Regulation of PDE1	15
1.2.2	The PDE2 enzyme family	15
1.2.3	The PDE3 enzyme family	16
1.2.3.1	Structure of PDE3	16
1.2.3.2	Biological importance of PDE3 enzymes	17
1.2.4	The PDE4 enzyme family	18
1.2.5	The PDE5 enzyme family	19
1.2.6	The PDE6 enzyme family	21
1.2.7	The PDE7 enzyme family	22
1.2.8	The PDE8 enzyme family	22
1.2.9	The PDE9 enzyme family	23
1.2.10	The PDE10 enzyme family	24
1.2.11	The PDE11 enzyme family	24

1.2.12	PDE and diseases	25
1.3	Molecular biology and biochemistry of the PDE4 enzyme family	25
1.3.1	PDE4	25
1.3.1.1	Structure of PDE4 isoforms	26
1.3.1.2	Presence of signalling complexes involving PDE4s	28
1.3.1.2.1	RACK1	29
1.3.1.2.2	$\beta$ -arrestins	30
1.3.1.2.3	AKAPs	32
1.3.1.3	Inhibitors	34
1.3.1.4	Compartmentalization of cAMP and PDE4 enzymes	35
1.3.1.5	Short-term regulation of PDE4s	37
1.3.1.5.1	Phosphorylation	38
1.3.1.5.2	Ubiquitination	40
1.3.1.5.3	Sumoylation	42
1.3.1.6	cAMP gated long-term PDE4 expression	45
1.3.2	PDE4A	45
1.3.3	PDE4B	46
1.3.4	PDE4C	47
1.3.5	PDE4D	48
<b>Chapter 2</b>	<b>Materials and Methods</b>	59
2.1	Mammalian Cell Culture	60
2.1.1	Maintenance of cell lines	60
2.1.1.1	HFK293 cell line	60
2.1.1.2	COS-1 cell line	61
2.1.1.3	HEK-B2 cell line	61
2.1.2	Transfection	61
2.1.2.1	PolyFect transfection of HEK293 cells (and HEK-B2 cells)	61
2.1.2.2	DEAE-Dextran transfection of COS1 cell line	62
2.2	Biochemical techniques	63
2.2.1	Protein analysis	63
2.2.1.1	Whole Cell lysate	63
2.2.1.2	Protein quantification (Bradford assay)	63
2.2.2	Gel electrophoresis and Western blotting	64
2.2.2.1	Sample preparation	64
2.2.2.1.1	Cell lysis samples	64
2.2.2.1.2	Membrane Recruitment samples	64
2.2.2.2	Nu-Page™ gel system	65
2.2.2.3	Protein Transfer	65
2.2.2.4	Immunoblotting	66
2.2.3	Immunoprecipitation	66
2.2.3.1	Sepharose pre-wash	67
2.2.3.2	Pre-clearing	67
2.2.3.3	Pre-immunc	67
2.2.3.4	Binding of antibody and target protein complex to beads	67
2.2.4	Kinase Assays	68
2.2.4.1	PKA assay	68
2.2.4.1.1	Cell lysate extraction for PKA assay	68
2.2.4.1.2	PKA assay tube pre-incubation	68
2.2.4.1.3	PKA assay reaction	69

2.2.4.2	Phosphodiesterase activity assay	70
2.2.4.2.1	Activation of Dowex	70
2.2.4.2.2	Assay preparation	70
2.2.4.2.3	Determination of PDE4 activity	71
2.2.5	Expression and Purification of GST Fusion Proteins	71
2.2.5.1	Induction and Purification of GST Fusion Proteins	71
2.2.5.2	SDS PAGE	73
2.2.5.3	Staining of SDS Polyacrylamide Gels with Coomassie Brilliant Blue	73
2.2.5.4	Visualisation of Proteins	73
2.2.5.5	Drying SDS Polyacrylamide Gels	73
2.2.6	Peptide Array Analysis	73
2.2.7	<i>In vitro</i> Ubiquitination Assay	74
2.2.7.1	Ubiquitination Assay Pre-incubation	74
2.2.7.2	<i>In vitro</i> Ubiquitination reaction	75
2.3	Molecular Biology Techniques	75
2.3.1	Large-scale production of plasmid DNA	75
2.3.1.1	Production of a cleared lysate	75
2.3.1.2	Plasmid DNA purification	76
2.3.2	Small-scale production of plasmid DNA	76
2.3.3	Quantification of purified DNA	77
2.3.4	Site-Directed Mutagenesis	77
2.3.4.1	Primer designs	78
2.3.4.2	Mutant Strand Synthesis Reaction (Thermal Cycling)	78
2.3.4.3	Dpn I Digestion of the Amplification Products	79
2.3.4.4	Transformation of XL1-Bulue Supercompetent cells	80
2.3.4.5	Sequence Analysis	80
2.3.4.6	Glycerol Stocks	80
2.3.5	Agarose Gel Analysis of DNA	81
2.4	Laser Scanning Confocal Microscopy (LSCM)	81
2.4.1	Preparation of slides	81
2.4.2	Visualization of cells	82
<b>Chapter 3</b>	<b>The role of PDE4 in <math>\beta_2</math>-adrenergic receptor desensitization</b>	84
3.1	Introduction	85
3.2	Results	87
3.2.1	The isoprenaline-stimulated PKA phosphorylation of GRK2 is amplified by inhibition of PDE4	87
3.2.1.1	GRK2 is the major species among 7 GRKs in HEKB2 cells	87
3.2.1.2	Isoprenaline stimulates PKA phosphorylation of GRK2 in HEKB2 cells	87
3.2.1.3	PDE4 inhibition enhances isoprenaline-induced PKA phosphorylation of GRK2 in HEKB2 cells	88
3.2.1.4	PDE4 inhibition alone is able to cause time-dependent PKA phosphorylation of GRK2	89
3.2.2	The effect of PDE4 inhibition on PKA phosphorylation of GRK2 is not PDE4 subfamily-specific	90
3.2.3	PDE4 inhibition enhances isoprenaline-stimulated membrane translocation of GRK2	90
3.2.4	PDE4 inhibition accelerates phosphorylation of the $\beta_2$ AR by GRK2	92

3.2.5	PDE4 inhibition accelerates membrane recruitment of $\beta$ -arrestin and PDE4D	93
3.2.6	Analysis of PDE4 inhibition effect on ERK-phosphorylated GRK2	94
3.2.7	Analysis of PDE4 inhibition on the trafficking and GRK phosphorylation status of the $\beta_2$ AR in HEKB2 cells	95
3.2.8	Rolipram triggers PKA phosphorylation of GRK2 in cardiac myocytes	96
3.2.9	PDE4 inhibition enhances isoprenaline-stimulated PKA phosphorylation of $\beta_2$ AR	96
3.2.10	Isoprenaline-stimulated phosphorylation of $\beta_2$ AR by PKA is dependent upon AKAP79 but not gravin	97
3.2.11	Interaction with $\beta$ -arrestin is required for PDE4D to regulate isoprenaline-stimulated phosphorylation of ERK	99
3.3	Discussion	100
<b>Chapter 4</b>	<b>Analysis of ubiquitination of PDE4D5 and its functions in HEKB2 cells</b>	129
4.1	Introduction	130
4.2	Results	132
4.2.1	Isoprenaline-stimulated ubiquitination of PDE4D5 in HEKB2 cells	132
4.2.2	UIM of PDE4D5 is critical for ubiquitination	133
4.2.3	Vasopressin-stimulated ubiquitination of PDE4D5 in HEKB2 cells	134
4.2.4	Requirement of $\beta$ -arrestin binding for PDE4D5 ubiquitination	135
4.2.5	Interaction of the E3 Ub ligase Mdm2 with PDE4D5	135
4.2.6	The ubiquitination signals of VSV-PDE4D5 are composed of mono-ubiquitination and poly-ubiquitination	136
4.2.7	Isoprenaline stimulates the association of VSV-PDE4D5 with proteasome 19S regulatory subunits 19S1, 19S2 and 19S5a in a time-dependent manner	137
4.2.8	Isoprenaline promotes PDE4D5 interaction with $\beta$ arrestin in HEKB2 cells via a ubiquitination-dependent process	138
4.2.9	In vitro ubiquitination assay on peptide array of PDE4D5 identifies two regions where the ubiquitin acceptors reside	139
4.3	Discussion	140
<b>Chapter 5</b>	<b>Initial exploration of sumoylation of PDE4D5 in HEK293 cells</b>	166
5.1	Introduction	167
5.2	Results	169
5.2.1	Mutation of the potential lysine residue located within SUMO modification consensus sequence in PDE4D5 ablates its sumoylation in vitro	169
5.2.2	Modification of PDE4D5 by SUMO-1 in cells	170
5.2.2.1	Conditions that I have tried to detect sumoylation of PDE4D5 in cells	170
5.2.3	Effects of SUMO-1 modification on PDE4D5 interaction with its binding partners	173
5.3	Discussion	174

<b>Chapter 6</b>	<b>Analysis of the binding sites on PDE4D5 to <math>\beta</math>-arrestin, ERK2 and Ubc9</b>	186
6.1	Introduction	187
6.2	Results	189
6.2.1	Analyses of PDE4D5 binding to $\beta$ -arrestins	189
6.2.1.1	Purification of GST- $\beta$ -arrestin 1 and GST- $\beta$ -arrestin 2 fusion protein	189
6.2.1.2	Peptide arrays identify sites in PDE4D5 that interacts with $\beta$ -arrestin2	190
6.2.1.3	Peptide arrays identify sites in PDE4D5 that interacts with $\beta$ -arrestin1	191
6.2.1.4	Scanning substitution identifies individual amino acids on PDE4D5 that require for it to interact with $\beta$ -arrestin2	191
6.2.2	Analysis of PDE4D5 association with ERK2	192
6.2.2.1	Expression and purification of GST-ERK2 fusion proteins	192
6.2.2.2	Selective immunoprecipitation identifies the association between PDE4D5 and ERK2	193
6.2.2.3	Peptide array analysis identifies the interaction sites for ERK2 on PDE4D5	193
6.2.2.4	Scanning substitution identifies individual amino acids in the PDE4D5 required for it to interact with ERK2	195
6.2.3	Analyses of PDE4D5 binding to Ubc9	196
6.2.3.1	Selective immunoprecipitation analyses indicate PDE4D5 binds to Ubc9	196
6.2.3.2	Purification of GST-Ubc9 fusion proteins	197
6.2.3.3	Peptide arrays identify sites in the PDE4D5 that interacts with Ubc9	197
6.2.3.4	Alanine scanning substitution identifies individual amino acids in the PDE4D5 catalytic region that may contribute to a binding site for Ubc9	198
6.2.4	Analyses of $\beta$ -arrestin2 binding to Ubc9	198
6.2.4.1	Peptide array and scanning substitution array identify sites in the $\beta$ -arrestin2 that may allow interaction with Ubc9	199
6.3	Discussion	200
<b>Chapter 7</b>	<b>General Discussion</b>	224
	<b>References</b>	240
	<b>Publications</b>	

## List of Figures

<b>Chapter 1</b>	
Figure 1.1 General schematic of cAMP signalling pathway initiated by G-protein coupled receptors (GPCRs)	51
Figure 1.2 Cyclic nucleotide hydrolysis by cyclic nucleotide phosphodiesterases	52
Figure 1.3 Table of phosphodiesterases superfamily	53
Figure 1.4 Schematic of the PDE4 isoenzymes	54
Figure 1.5 The effects of PKA and ERK2-mediated phosphorylation on PDE4 long isoforms	55
Figure 1.6 Compartmentalization of PDE4s	56
Figure 1.7 Schematic of $\beta_2$ -adrenergic receptor ( $\beta_2$ AR) desensitization	57
Figure 1.8 Table of the differences between Ubiquitin and SUMO families	58
<b>Chapter 2</b>	
Figure 2.1 Table of antibodies and inhibitors produced by companies other than SIGMA.	83
<b>Chapter 3</b>	
Figure 3.1 A schematic of GRK2 ( $\beta$ ARK1)	105
Figure 3.2 Existence of GRKs in HEKB2 cells	106
Figure 3.3 GRK2 is phosphorylated by PKA in HEKB2 cells	107
Figure 3.4 Differential PKA phosphorylation of GRK2 following PDE4 or PDE3 inhibition in HEKB2 cells	109
Figure 3.5 PKA phosphorylation of GRK2 in PDE4 isoform-knockdown HEKB2 cells	110
Figure 3.6 Membrane translocation of GRK2 in HEKB2 cells	111
Figure 3.7 Phosphorylation status of GRK2 in HEKB2 membrane fractions	112
Figure 3.8 Phosphorylation of the $\beta_2$ AR in HEKB2 cells by GRK2	113
Figure 3.9 Rolipram induced GRK2 phosphorylation of $\beta_2$ AR in HEKB2 cells	114
Figure 3.10 Phosphorylation of $\beta_2$ AR by GRK2 in siRNA mediated PDE4B and PDE4D knockdown HEKB2 cells	115
Figure 3.11 Membrane translocation of $\beta$ -arrestins and PDE4D	116
Figure 3.12 Rolipram alone induced membrane recruitment of $\beta$ -arrestins and PDE4D	117
Figure 3.13 Membrane ERK-phosphorylated GRK2 in HEKB2 cells	118
Figure 3.14 Membrane translocation of activated ERK1/2 in HEKB2 cells	119
Figure 3.15 ERK activation in HEKB2 cells	120
Figure 3.16 PKA phosphorylation of GRK2 in cardiac myocytes	121
Figure 3.17 Membrane recruitment of GRK2 in cardiac myocytes	122
Figure 3.18 PKA phosphorylation of $\beta_2$ AR in HEKB2 cells	123
Figure 3.19 AKAP79-mediated isoprenaline activation of phosphorylation of $\beta_2$ AR in HEKB2 cells	124
Figure 3.20 Gravin-mediated isoprenaline activation of phosphorylation of $\beta_2$ AR in HEKB2 cells	125
Figure 3.21 $\beta$ -arrestin-scaffolded PDE4D5 is fundamental to regulate $\beta_2$ AR	126

switching	
Figure 3.22 GRK2 phosphorylated $\beta_2$ AR trafficking in HEKB2 cells	127
Figure 3.23 PKA phosphorylated $\beta_2$ AR trafficking in HEKB2 cells	128
<b>Chapter 4</b>	
Figure 4.1 The ubiquitination pathway	147
Figure 4.2 Different forms of ubiquitin modification	148
Figure 4.3 Characterization of the UIM	149
Figure 4.4 Isoprenaline-stimulated ubiquitination of PDE4D5	150
Figure 4.5 Isoprenaline-stimulation of HEKB2 cells failed to lead to ubiquitination of PDE4A5, PDE4B1, PDE4B3, PDE4B4 and PDE4C1	151
Figure 4.6 Absence of ubiquitination of PDE4D3 in response to isoprenaline in HEKB2 cells	152
Figure 4.7 The extreme C-terminal of PDE4D5 contains a UIM domain essential for ubiquitination	153
Figure 4.8 Vasopressin-stimulated ubiquitination of PDE4D5-VSV in HEKV2 cells	154
Figure 4.9 $\beta$ -arrestin-mediated PDE4D5 ubiquitination in HEKB2 cells	155
Figure 4.10 PDE4D5 interacts with Mdm2 via a $\beta$ -arrestin-dependent manner	156
Figure 4.11 A mixture of K29-linked, K48-linked and K63-linked polyubiquitin chains on PDE4D5 in response to isoprenaline in HEKB2 cells	157
Figure 4.12 Isoprenaline-stimulated wild type PDE4D5 interaction with proteasome 19S1, 19S2 and 19S5a in a time-dependent manner in HEKB2 cells	159
Figure 4.13 Loss of ability of VSV-tagged PDE4D5 UIM mutant 723E to interact with proteasome 19S regulatory complex in HEKB2 cells in response to isoprenaline	160
Figure 4.14 Ubiquitination of PDE4D5 enhances its binding to $\beta$ -arrestin	161
Figure 4.15 <i>In vitro</i> ubiquitination assay determines PDE4D5 putative ubiquitination sites	163
Figure 4.16 The <i>in vitro</i> ubiquitination of sequential alanine substitution version of a peptide 10-derived peptide	164
Figure 4.17 Organization and structure of the 26S proteasome and 19S regulatory particles	165
<b>Chapter 5</b>	
Figure 5.1 Enzymatic conjugation mechanism of sumoylation	179
Figure 5.2 PDE4D5 amino acid sequence alignment	180
Figure 5.3 PDE4D5 is a substrate for SUMO-1 and SUMO-2 conjugation <i>in vitro</i>	181
Figure 5.4 Exogenously expressed VSV-tagged PDE4D5 is modified by SUMO-1 <i>in vivo</i>	182
Figure 5.5 Illustration of sumoylated form of PDE4D5 preferentially binding to $\beta$ -arrestin, RACK-1, FRK2, and AKAP18	183
Figure 5.6 SUMO-1 conjugation enhances PDE4D5 interaction with $\beta$ -arrestins, RACK-1, ERK and AKAP18 $\delta$	184

<b>Chapter 6</b>	
Figure 6.1 Schematic of long isoform PDE4D5	206
Figure 6.2 Sequence alignments of the residues of full-length $\beta$ -arrestin1 and $\beta$ -arrestin2	207
Figure 6.3 Over-expression and purification of recombinant proteins of GST- $\beta$ -arrestin1 and GST- $\beta$ -arrestin2	208
Figure 6.4 Detection of protein-protein interaction by using Peptide Array Analysis and subsequent Alanine Substitution Analysis	209
Figure 6.5 Probing PDE4D5 peptide array for $\beta$ -arrestin2 interaction sites	210
Figure 6.6 The binding of $\beta$ -arrestin2 to sequential alanine substituted version of a RAID1-containing peptide	211
Figure 6.7 Purification of recombinant protein of GST-ERK2	212
Figure 6.8 Association of PDE4D5 with ERK2 in HEK293 cells	213
Figure 6.9 Probing PDE4D5 peptide array for ERK2 interaction sites	214
Figure 6.10 The binding of ERK2 to sequential alanine substituted version of a FQF-containing peptide	215
Figure 6.11 The binding of $\beta$ -arrestin2 and ERK2 to sequential alanine substituted version of a FQF-containing peptide	216
Figure 6.12 Association of PDE4D with Ubc9 in HEK293 cells	217
Figure 6.13 Purification of recombinant protein of GST-Ubc9	218
Figure 6.14 Probing PDE4D5 peptide array for Ubc9 interaction site	219
Figure 6.15 The binding of Ubc9 to sequential alanine substituted versions of Ubc9-interacting PDE4D5 peptides	220
Figure 6.16 Probing $\beta$ -arrestin2 peptide array for Ubc9 interaction sites	221
Figure 6.17 The binding of Ubc9 to sequential alanine substituted versions of Ubc9-interacting $\beta$ -arrestin2 peptide	222
Figure 6.18 Predicted structure of catalytic domain in PDE4D	223
<b>Chapter 7</b>	
Figure 7.1 Schematic of PDE4D5	239

## Abbreviations

AC	adenylyl cyclase
AKAP	A kinase anchoring protein
ATP	adenosine triphosphate
Ca/CaM	calcium/calmodulin
cAMP	cyclic 3'5' adenosine mono phosphate
cGMP	cyclic guanosine mono phosphate
cDNA	complementary DNA
DEAE	Dicthyl aminoethyl
DMEM	Dulbecco's modification of Eagle's Medium
DMSO	dimethylsulphoxide
DNA	deoxyribonucleic acid
dNTP	deoxynucleotide triphosphate
DTT	dithiothreitol
ECL	enhanced chemiluminescence
EDTA	diaminoethanetetra-acetic acid
EGTA	ethylene glycol-bis( $\beta$ -aminoethyl ether)-N,N,N',N'-tetraacetic acid
ELISA	enzyme linked immunosorbent assay
FCS	foetal calf serum
GPCR	G-protein coupled receptor
G-protein	guanine nucleotide binding regulatory protein
GRK	G-protein coupled receptor kinase
GST	glutathione S-transferase
GTP	guanosine triphosphate
HEPES	N-2-Hydroxyethylpiperazine-N'-2-ethanesulfonic acid
IBMX	isobutylmethylxanthine
IPTG	isopropyl- $\beta$ -D-thiogalactopyranoside
KHEM	potassium (K), HEPES, EGTA, Magnesium
K <sub>m</sub>	Michaelis-Menten constant (mathematically equivalent to the concentration of substrate at which the initial reaction rate is half of V <sub>max</sub> )
LB	Luria-Bertoni
LR	linker-region
MAP kinase	mitogen activated protein kinase
mRNA	messenger RNA
ORF	open reading frame
PBS	phosphate buffered saline
PCR	polymerase chain reaction
PDE	phosphodiesterase
PKA	protein kinase A
PKC	protein kinase C
RNA	ribonucleic acid
SDS	sodium dodecyl sulphate
SH2 domain	Src homology 2 domain
SH3 domain	Src homology 3 domain
TAE	tris/acetate/EDTA
TBS	tris buffered saline
TE	tris/EDTA
UCR	upstream conserved region
V <sub>max</sub>	The maximum initial rate of an enzyme catalysed reaction under defined conditions

## **Chapter 1**

### **General Introduction**

## **1. General Introduction**

### **1.1 Cyclic nucleotide signalling pathways**

Two types of cyclic nucleotides exist, cyclic adenosine 3',5'-monophosphate (cAMP) and cGMP. The amplitude and duration of cAMP and cGMP signals are controlled by their rates of synthesis by adenylyl and guanylyl cyclases, respectively, and their degradation by 3',5'-cyclic nucleotide phosphodiesterases (PDEs). While some PDEs hydrolyse only cAMP or cGMP, others hydrolyse both. Major differences between phosphodiesterases are observed in substrate affinity, turnover of substrate and inhibitor sensitivity.

#### **1.1.1 The cAMP signalling pathway**

Cyclic adenosine 3',5'-monophosphate (cAMP) is one of the oldest signalling molecules known (Tasken and Aandahl 2004; Beavo and Brunton 2002; Scott et al. 2000). This ubiquitous second messenger of hormone action is produced from ATP by adenylyl cyclases at the plasma membrane (Cooper 2003) and is degraded solely through the action of phosphodiesterases to 5'AMP (Houslay and Adams 2003). In cells, cAMP controls metabolism, cytoskeleton function, gene expression, muscle contraction and memory (Dumaz N. and Marais R. 2005; Tasken and Aandahl 2004; Beavo and Brunton 2002; Scott et al. 2000). It is also involved in regulating inflammation (Asirvathan et al. 2004; Steiner and Branco 2003; Castro et al. 2004; Moore and Willoughby 1995). cAMP-dependent protein kinase holoenzyme (PKA), cyclic nucleotide gated ion channels (CNGCs) and exchange proteins regulated by cAMP (EPACs) are three major but different effectors of cAMP and mediate distinct cAMP signalling pathways in many cells and tissues (Baillie et al. 2005) (Figure 1.1). Every focal point along each cAMP signalling pathway has the potential to be integrated with some other specific signalling proteins, which is achieved not only temporally, but also spatially. This leads to a more complexed signalling cross-talk than was at first appreciated (Dumaz and Marais 2005; Houslay and Baillie 2003; Tasken and Aandahl 2003).

#### **1.1.2 G-proteins and G-protein coupled receptors**

##### **1.1.2.1 G-proteins**

Heterotrimeric guanine nucleotide-binding proteins (G-proteins) relay a variety of signals across the plasma membrane by sequential interaction with their cognate receptors and effectors, such as adenylyl cyclases and ion channels (Luttrell 2006). After the receptors are activated, the exchange of GDP for GTP is catalysed on the  $\alpha$  subunit of their cognate G-proteins, leading to the conformational changes in the G-protein  $\alpha$  subunits (Hepler and Gilman 1992) and the dissociation of  $\alpha$  subunit from its high affinity binding complex of  $\beta\gamma$  subunits. These dissociated subunits then couple to their individual effectors, initiating the distinct signal transduction pathways. After specific cell signals have been initiated, GTP hydrolysis returns  $G\alpha$  to the GDP-bound state, allowing reformation of the inactive heterotrimer. To date, 16 distinct  $\alpha$  subunit genes have been identified in human. This gives rise to isoform multiplicity, which may explain the multitude of cAMP-induced physiological responses activated by the same stimuli in different cells. Based on the amino acid sequence and their functions, G-protein  $\alpha$  subunits can be categorised into four classes:  $G\alpha$ ,  $G_i$ ,  $G_q$  and  $G_{12}$  (Berman and Gilman 1998), among which cAMP signalling is largely regulated by activation of adenylyl cyclase through  $G_s$  and inhibition through  $G_i$ .

### **1.1.2.2 G-protein coupled receptors (GPCRs)**

G-protein coupled receptors (GPCRs) are cell-surface receptors. They have 7 transmembrane helices, bind effectors at the external surface of the plasma membrane and interact with G-proteins at the cytosolic surface (Jacoby et al. 2006). They respond to a wide range of extra-cellular stimuli, such as light, odour, chemoattractants, peptides, neurotransmitters, lipids, and hormones. They constitute one of the largest protein families in the human genome, with at least 600 putative members (Pierce et al. 2002; Maudsley et al. 2005). These GPCRs serve to translate extracellular messages by increasing or decreasing levels of second messengers, such as cAMP or cytosolic  $Ca^{2+}$ . GPCRs are of great interest for pharmaceutical industries and account for nearly 40% of all current therapeutic targets (Brink et al. 2004).

### **1.1.2.3 Beta-adrenergic receptors ( $\beta$ ARs)**

$\beta$ -adrenergic receptors ( $\beta$ ARs) are  $G_s$ -coupled receptors, activation of which leads to the increase in cAMP production in cells (Rockman et al. 2002). Three types

of  $\beta$ ARs,  $\beta_1$ ,  $\beta_2$ , and  $\beta_3$ AR have been cloned to date, each of which has its own molecular characteristics and functions (Jahns et al. 2006; Johnson 2006; Lamba and Abraham 2000; Babol and Blasiak 2005).

Best known are  $\beta_1$ AR and  $\beta_2$ AR.  $\beta_1$ AR shares a 54% amino acid homology with  $\beta_2$ AR (Freedman et al. 2005) and undergoes a similar but not identical desensitisation, internalisation, down-regulation and re-sensitization process to the  $\beta_2$ AR (Rapacciuolo et al. 2003; Gardner et al. 2004; Jockers et al. 1999; Freedman et al. 1995; Luttrell and Lefkowitz 2002). The  $\beta_1$ AR and  $\beta_2$ AR represent the primary targets for sympathetically derived catecholamines in the heart and are fundamental to the overall regulation of cardiovascular homeostasis (Rockman et al. 2002). Alterations, for example, desensitisation and down-regulation, in  $\beta$ AR function are associated with cardiac hypertrophy and the development of heart failure (Lefkowitz et al. 2000). Therefore, manipulation of  $\beta$ AR signalling constitutes a route for therapeutic strategies in treating heart failure (Petrofski and Koch 2003).

Although the  $\beta_1$ AR and  $\beta_2$ AR have differential effects on cardiac myocyte apoptosis, with  $\beta_1$ -AR appearing to be pro-apoptotic and  $\beta_2$ AR anti-apoptotic, they both undergo Gs/Gi switching upon agonist stimuli in a PKA-dependent manner as explained below (Martin et al. 2004; Baillie et al. 2003). Thus  $\beta_2$ ARs localise within caveolae in the membrane of cardiac myocytes (Xiang et al. 2002). Following stimulation of adenylyl cyclase via  $G_{\alpha s}$ , cAMP production results in PKA activation. Phosphorylation of the PKA consensus sites within the third intracellular loop (Ser261, Ser262) and C-terminal tail (Ser345, Ser346) of the  $\beta_2$ AR causes an attenuation of receptor-Gs coupling and facilitates the coupling of receptor to Gi proteins, leading to the activation of the MAP kinase pathway. Pertussis toxin, which ADP-ribosylates the  $G_{i\alpha}$  subunit and prevents receptor- $G_{i\alpha}$  coupling, is generally used to inhibit  $\beta_2$ AR switching-mediated MAP kinase activation (Daaka et al. 1997).

In addition to the well-studied  $\beta_2$ AR, vasoactive intestinal peptide receptors (Luo X. et al. 1999) and prostacyclin receptors (Lawler et al. 2001) also have the ability to undergo Gs/Gi switching after agonist stimuli, providing independent

evidence for the prevalence of the cell-used strategy in mediating multiple signal transduction cascades via the same receptor.

A cell model (HEKB2 cells) that over-expresses FLAG and GFP tagged  $\beta_2$ ARs, a prototype of GPCRs, is used in many of the experiments described in this thesis. HEKB2 cells provide a well-established model system for studying the  $\beta_2$ AR signalling pathway in which cAMP-specific phosphodiesterases 4 (PDE4s) have been shown to influence  $\beta_2$ AR functioning, in particular the phosphorylation of the  $\beta_2$ AR by PKA (Perry et al. 2002).

Various investigators have shown that activation of  $\beta_2$ AR can lead to the activation of ERK pathway via two pathways, both of which utilize a common upstream pathway to activate PKA in the presence of increased levels of cAMP due to the stimulation of adenylyl cyclases by activated  $\beta_2$ AR (Lefkowitz et al. 2002). The differences emerge from the downstream of PKA activation. In one pathway, cAMP-mediated ERK activation is achieved through PKA activation of B-raf and consequent activation of MEK and ERK. The details of this activation are unclear at present. There have been competing theories, such as EPAC/Rap1-mediated B-Raf activation and the largely discredited PKA phosphorylation of Rap1, which leads to B-Raf activation. Undoubtedly mechanisms differ in various cell types and much more work is needed to clarify these mechanisms (Housaly and Kolch 2000). In another pathway, the coupling of PKA phosphorylated  $\beta_2$ AR switches from Gs to Gi. This leads to a Src-dependent Ras/c-Raf1/MEK/ERK cascade activation (Lefkowitz et al. 2002).

$\beta_2$ AR signalling is seen in very many cell-types, including peripheral blood T lymphocytes, which are involved in mediating immune responses. In this cell type GRK2 activation is achieved through Src-mediated phosphorylation, and is followed by phosphorylation of  $\beta_2$ AR by GRK2,  $\beta$ -arrestin binding, as well as a switching from Gs to Gi. This mechanism by which GRK2 is activated appears to be different from that in HEK293 cells where GRK2 is activated by PKA (Cong et al. 2001; Heijink et al. 2005).

### **1.1.3 Adenylyl Cyclases (ACs)**

A single polypeptide that would both recognize hormone and synthesize cAMP was first shown to exist by Sutherland and Rall (Sutherland and Rall 1960), and is now known as adenylyl cyclases (ACs). ACs is a critically important family that is responsible for the conversion of ATP into cAMP, a ubiquitous intracellular second messenger (Antoni 2000). This biological process is used in virtually all types of organisms from prokaryotes to eukaryotes (Danchin 1993).

#### **1.1.3.1 Structure of AC**

AC is an integral membrane protein composed of an N-terminus, two tandemly repeated trans-membrane segments (unlike GC which has only one transmembrane domain) connected by a cytoplasmic loop, and another C-terminal cytoplasmic loop (Antoni 2000). The N-termini of the two cytoplasmic domains are highly conservative and dimerize to form the catalytic site.

#### **1.1.3.2 Diversity and Distribution of ACs**

Molecular cloning techniques have identified nine mammalian genes that encode membrane-bound ACs, and one gene encoding a soluble isoform (Cooper 2003). These ten AC isoforms can be categorized into five distinct families according to their primary structure similarity and functional attributes (Sunahara and Taussig 2002): AC1, AC3, and AC8, are a class of  $\text{Ca}^{2+}$ -CaM sensitive forms; AC2, AC4 and AC7 are a class of  $G_{\beta\gamma}$ -stimulatory forms; AC5 and AC6 are a class that shows sensitivity to inhibition by both  $\text{Ca}^{2+}$  and G $\alpha$ i isoforms (G $\alpha$ 0, G $\alpha$ i1, G $\alpha$ i2, G $\alpha$ i3, and G $\alpha$ z); while AC9 is distinguished from the other membrane-bound ACs by its insensitivity to the small molecule forskolin; and sAC, a soluble enzyme, is incapable of responding to stimuli such as GTP, G proteins, and forskolin.

#### **1.1.3.3 Regulation of ACs**

ACs are susceptible to many modes of regulation depending on their specific cellular compartment and propensity to associate with scaffolding proteins. Such regulation can impart their signalling specificity and discrimination.

### 1.1.3.3.1 Stimulation by $G_{\alpha s}$

Adrenaline, dopamine, prostaglandin PGE<sub>2</sub>, adenosine, and glucagon are a few examples of many hormones that activate AC to initiate the generation of cAMP. This activation occurs primarily through the receptors coupling to GTP-bound  $G_{\alpha s}$ . Although there are three splice variants of  $G_{\alpha s}$ , only  $G_{\alpha s}$ -short and  $G_{\alpha s}$ -long are able to mediate this effect upon hormone stimuli (Klemke et al. 2000).

### 1.1.3.3.2 Inhibition by $G_{\alpha i}$

$G_{\alpha i}$  has five isoforms,  $G_{\alpha i1}$ ,  $G_{\alpha i2}$ ,  $G_{\alpha i3}$ ,  $G_{\alpha i0}$ , and  $G_{\alpha z}$ . Among the ACs that have been tested for the inhibition by  $G_{\alpha i}$ , AC1, AC5, AC6, and AC8 are inhibited by  $G_{\alpha i}$ , with selectivity for AC5 and AC6; while AC2, AC3 and AC7 are not (Cooper 2003).  $G_{\alpha i}$  subunits are subjected to long-chain acyl (myristoyl) and thioacyl (palmitoyl) post-translational modification, and its myristoylation has been shown prerequisite for  $G_{\alpha i}$ -mediated inhibition of AC (Sunahara and Taussig 2002).

### 1.1.3.3.3 Regulation by $G_{\beta\gamma}$

G-protein  $\beta\gamma$ -subunits also regulate ACs, but in an AC subtype-specific manner. In the case of AC2, AC4 and AC7,  $G_{\beta\gamma}$ -subunits stimulate their activities; as for AC1 and AC8,  $G_{\beta\gamma}$ -subunits inhibit their activities (Sunahara and Taussig 2002). The effect of  $G_{\beta\gamma}$  on AC2, AC4 and AC7 is only substantial in the presence of  $G_{\alpha s}$  (Antoni 2000). Since  $G_{s\alpha}$  is relatively less than  $G_{i\alpha}$  and  $G_{o\alpha}$  in the plasma membrane, it is thought of  $G_{\beta\gamma}$  from Gi or Go as the co-activator of  $G_{\alpha s}$ , conferring a positive 'cross talk' by simultaneous activation of Gs- and Gi-coupled receptors. Less is understood about the relationship between  $G_{\beta\gamma}$  and AC5 and AC6. However, Bayewitch et al. (Bayewitch et al. 1998) have suggested that they exert an indirect inhibitory action on AC5 and AC6 through  $G_{\beta\gamma}$ .

### 1.1.3.3.4 Regulation by $Ca^{2+}$

$Ca^{2+}$  also has isoform-specific effects on ACs.  $Ca^{2+}$ /CaM activates isoforms AC1, AC8 and possibly AC3 (Krupinski et al.1989; Cali et al.1994; Choi et al.1992), while AC5 and AC6 are inhibited by a concentration of  $Ca^{2+}$  within a physiological concentration range (Cooper 2003). Strikingly,  $Ca^{2+}$ -sensitive AC isoforms are able

discriminate the source of increased intracellular  $\text{Ca}^{2+}$  before regulation can occur. For example, AC1 and AC8 are only sensitive to voltage-gated  $\text{Ca}^{2+}$  channels or capacitative  $\text{Ca}^{2+}$  entry (CCE, the entry of  $\text{Ca}^{2+}$  that is triggered by depletion of  $\text{Ca}^{2+}$ ) but not  $\text{IP}_3$  released  $\text{Ca}^{2+}$  (Fagan et al. 2000; Gu and Cooper 2000), while AC5 and AC6 are only sensitive to CCE (Cooper 2003). Although it is uncertain if AC9 is regulated by  $\text{Ca}^{2+}$  in systems mainly expressing AC9, cAMP synthesis is inhibited by  $\text{Ca}^{2+}$  through calcineurin (Antoni 2000).

#### **1.1.3.3.5 Regulation by other small molecules**

The diterpene, forskolin is known to potentially activate all known isoforms of membrane-bound ACs, except for AC9 (Sunahara et al. 1996), while pyrophosphate and P-site inhibitor negatively regulate AC activities (Sunahara and Taussig 2002).

#### **1.1.3.3.6 Post-translational modification**

ACs can undergo phosphorylation and this can alter their activities (Cooper 2003). For example, PKA directly phosphorylates AC5, resulting in its reduced activity; PKC has also been shown to regulate ACs in an isoform-specific manner. This is supported by evidence that phorbol ester treatment can stimulate the activities of AC1, AC2, AC3 and AC5, but inhibit that of AC4 and AC6 (Sunahara and Taussig 2002).

#### **1.1.3.4 Expression pattern and their physiological roles**

The physiological importance of ACs has been related to learning and memory (AC1 and AC8) (Kandel and Schwartz 1982), drug dependency (AC7) and sperm capacitation (Sunahara and Taussig 2002). Generally, AC isoforms have broad distribution, however, some isoforms are expressed tissue specifically. For example, AC1 and AC3 are only expressed in brain (Xia et al. 1992); AC5 is at its highest level in striatum and cardiac tissue; AC9 is highly abundant in the brain (Antoni 2000), whereas sAC is expressed predominantly in the testis (Sunaharah 1996).

#### **1.1.3.5 Compartmentalisation of ACs**

The susceptibility of ACs to multiple modes of regulation raises the problem of signalling specificity and confidelity. However, compartmentalisation of the

relevant factors in close proximity helps ensure a particular regulatory context (Cooper 2003). GPCRs, the  $\alpha$ -subunits of G-proteins, and ACs have been found in phospholipid rafts (Huang et al. 1997), and  $\text{Ca}^{2+}$ -sensitive AC co-localise with and respond to capacitative  $\text{Ca}^{2+}$  entry CCE (Goraya and Cooper 2004). Similarly, the endogenous AC5 and AC6 and  $\beta_2\text{AR}$  of cardiac myocytes were suggested to co-abide in caveolae (Rybin et al. 2000; Ostrom et al. 2000), to allow orchestration of cAMP signalling. In neuronal tissue, ACs are rich in post-synaptic densities (PSDs) and thus conveniently interact with other PSDs-related scaffolding proteins to relay specific signals (Cooper et al. 1998). In addition to the constraints exerted by co-expression in lipid microdomains, scaffolding proteins, such as PKA-anchoring proteins (AKAPs) can also achieve an organised compartmentalisation (Baillie et al. 2005).

#### **1.1.4 Effectors of cAMP pathways**

##### **1.1.4.1 Protein Kinase A (PKA)**

Protein kinase A (PKA) is the most well known cAMP effector. This serine/threonine specific protein kinase, is composed of two catalytic subunits (C) and two regulatory subunits (R). The R-subunits maintain PKA in an inactive state. However, cAMP binding to two sites on each R subunit releases active C subunits and the activated PKA can now phosphorylate specific substrates with R/K, R/K, X, S/T, X<sub>hydrophobic</sub> consensus sequence (Tasken and Aandahl 2003).

Based on the differences within the R subunit, PKA isoenzymes are categorized into type I and type II holoenzymes. A further heterogeneity is achieved as three isoforms of catalytic subunit ( $C\alpha$ ,  $C\beta$ ,  $C\gamma$ ) and four ( $R\text{I}\alpha$ ,  $R\text{I}\beta$ ,  $R\text{II}\alpha$ ,  $R\text{II}\beta$ ) of regulatory subunits are found in mammals (Dumaz and Marias 2005). RI and RII subunit have different affinities for cAMP and distinct subcellular localizations: RI holoenzymes have a higher affinity for cAMP, and are mainly cytoplasmic; whereas RII holoenzymes are typically particulate and confined to cell structures and organelles by virtue of anchoring to A-kinase anchoring proteins (AKAPs). NMR solution structures of the PKA regulatory subunits delineates the molecular mechanism of PKA R subunits binding to AKAP by which an AKAP amphipathic

helix interacts with the hydrophobic groove in the dimerization domain of the PKA R subunit (Tasken and Aandahl 2003).

#### **1.1.4.2 cAMP-regulated GEFs (GTP-exchange factors)**

The exchange protein directly activated by cAMP (Epacs), is another category of cAMP effectors (Tasken and Aandahl 2003). So far, two proteins in this family, Epac1 and Epac2 have been identified. Epac1 and Epac2 share a similar organisation structure, with the slight difference that Epac1 has one cAMP binding site, whereas Epac2 contains two binding moieties (De Rooij et al. 2000). The binding of cAMP to Epac via its cAMP binding domain leads to the allosteric activation of its GEF domain (Rehmann et al. 2003), therefore promoting its ability to activate Rap1, a small Ras-like GTPase (Vossler et al. 1997; Dumaz and Marias 2005; Bos et al. 2003). In order to discriminate PKA and Epac-mediated effects, a novel synthesized analogue, 8pCPT-2'OMe-cAMP is widely used to specifically activate Epac (Bos et al. 2003).

#### **1.1.4.3 cAMP-gated membrane ion channels (CNG Ion Channels)**

The third set of cAMP effectors is cyclic nucleotide-gated (CNG) cation channels. These channels open in response to the direct binding of cAMP/cGMP, therefore regulating the membrane potential and intracellular  $Ca^{2+}$  levels (Kaupp and Seifert 2002). Retinal rod photoreceptor, which is directly activated by cGMP, an ion channel in olfactory transduction, which binds both cAMP and cGMP, as well as the most recently reported GatSper that is involved in cAMP-mediated sperm motility, comprise currently known CNG ion channels (Fesenko et al. 1985; Nakamura and Gold 1987; Ren et al. 2001).

### **1.1.5 Compartmentalization of cAMP**

In the 1980s, a study on cardiomyocytes in which different Gs-coupled receptors were found to selectively activate type I and type II PKA holoenzymes, brought up a new concept — compartmentalization of cAMP (Buxton and Brunton 1983). Evidence for the existence of cAMP microdomains has since been obtained in cardiac myocytes (Brunton 2003; Zaccolo and Pozzan 2002; Vandecasteele et al. 2006) as well as other cell types (Cooper 2003; Karpen and Rich 2001). It is now well

recognized that cAMP signalling responses are compartmentalized (Houslay and Adams 2003; Baillie and Houslay 2005; Cooper 2005; Cooper and Crossthwaite 2006). Recently, the use of fluorescence resonance energy transfer (FRET), based on either PKA or Epac, cAMP-gated ion channels, or the selective activation of AKAP anchored PKA isoforms (Baillie and Houslay 2005), consolidated this hypothesis by visualising spatial and temporal gradients of cAMP in living cells (Zaccolo and Pozzan 2002).

Indeed, the molecular mechanisms behind cAMP compartmentalization are far more complex than previously recognised. The components of the cAMP-generating pathway (GPCRs, adenylyl cyclases) are localized to specific regions of the plasma membrane. PKA, which detects cAMP, and PDEs, which degrades cAMP, are also targeted to specific regions within the cell. This allows cAMP gradients to form within the 3-D matrix of the cell whereby the cAMP concentration is highest nearest the membrane and least in areas that contain the highest levels of PDEs. Thus, the activation of a certain GPCRs can increase the cAMP levels within discrete compartments in the cell and cause unique physiological responses (Hayes et al. 1982). In addition to PKA isoenzymes, A-kinase anchoring proteins (AKAPs) are also shown to be able to assemble signalling complexes to include other proteins such as cAMP phosphodiesterases, PKC and protein phosphatases that are targeted to specific subcellular compartments. Thus AKAPs provide scaffolds for the four-dimensional organization of cAMP signalling in both space and time (Baillie et al. 2005).

## **1.2 The 3'5' cyclic nucleotide phosphodiesterase (PDE) superfamily**

Cyclic nucleotide phosphodiesterases (PDEs) are a class of enzymes responsible for the hydrolysis of the cyclic nucleotides cAMP and cGMP to 5'AMP and 5'GMP, respectively (Figure 1.2). The function of PDEs in cells is to control the resting level of cyclic nucleotides, to restore the steady state levels after cAMP or cGMP-stimulating events and to form and shape intracellular gradients of these cyclic nucleotides. This superfamily of enzymes plays a key regulatory role in the orchestration of signalling cross-talk, desensitisation and compartmentalisation of cAMP (Houslay and Adams 2003). PDEs were first identified by Sutherland and co-workers (Rall et al. 1958). An increasing number of studies have suggested PDEs as

putative therapeutic targets, with this gaining global recognition upon the development of Viagra as a selective PDE5 inhibitor used to originally treat penile erectile dysfunction and, more recently, infantile pulmonary hypertension (Kulkarni and Patil 2004). To date, a number of PDE inhibitors have been in clinical trials, and some have already entered the market place. In particular, the PDE3 selective inhibitor cilostazol (Pletal) is widely used as a drug for the reduction of symptoms of intermittent claudication and PDE5 inhibitors sildenafil (Viagra), vardenafil (Levitra) and tadalafil (Cialis) are used for the treatment of male erectile dysfunction. Selective PDE inhibitors appear to have a potentially broad application in treating various diseases, such as asthma, chronic obstructive pulmonary disease, heart failure, atherosclerotic peripheral arterial disease and neurological disorders (Tasken and Aandahl 2003; Jeon et al. 2005).

PDEs are made up of 11 families based on their amino acid sequence identities, substrate specificities, allosteric regulatory characteristics, and pharmacological properties (Tasken and Aandahl 2003) (Figure 1.3). 8 PDE families generate over 30 different isoforms that are able to hydrolyse cAMP (Houslay and Adams 2003). This is due to the multiple genes encoded, as well as additional alternative mRNA splicing (Baillie and Houslay 2005). The existence of multiple PDE isoforms underscores their individual functional importance. Despite the heterogeneity across the superfamily, all PDE isoforms share a modular architecture, with a surprising degree of homology within their catalytic domains (in proximity to the COOH terminus), but with distinct regulatory domains and targeting domains invariably located at the NH2 terminus (Francis et al. 2001).

The catalytic domains of PDEs are well conserved, with slight structural differences in their catalytic domains determining if the PDE is cAMP-specific (PDE4, PDE7, PDE8), cGMP-specific (PDE5, PDE6, PDE9) or has dual substrate specificity (PDE1, PDE2, PDE3, PDE10, PDE11 (Goraya and Cooper 2005). This highlights the importance of achieving a precise understanding of the catalytic domains of PDEs, which can provide a molecular basis for rational drug design of competitive inhibitors. So far, several three-dimensional (3D) structures of the catalytic domains of PDEs in the presence of their inhibitors or substrates have been

resolved, and this includes PDE1, PDE2, PDE3, PDE4, PDE5 and PDE9 (Jeon et al. 2005; Scapin et al. 2004).

Compared to the evolutionarily conservative catalytic domains of PDEs, the N-terminal regions of PDEs are highly divergent in both amino acid sequences and their family-specific determinants. These family-specific determinants are: (1) calmodulin binding sites (PDE1), (2) non-catalytic cGMP binding (GAF) sites (PDE2, PDE5, and PDE6), (3) membrane targeting sites, protein-protein interaction sites and regulatory (UCR) sites (PDE4), (4) hydrophobic membrane associate sites (PDE3), and (5) phosphorylation sites for either the calmodulin-dependent kinase (PDE2), the cAMP-dependent kinase (PDE1, PDE3, and PDE4), or the cGMP dependent-kinase (PDE5) (Iffland 2005). Therefore, N-terminal regions of PDEs provide an important platform where the multiple PDE isoforms are subjected to specific protein interactions and response to distinct regulatory signals. PDE8 isoforms contain an N-terminal REC and a PAS domain that are not found in other PDEs, however, the functions of these REC and PAS domains are not known at present (Bender and Beavo 2006).

In line with the tight compartmentalization of cAMP/cGMP (Zaccolo et al. 2002), PDE isoforms have their distinct patterns of regulation and intracellular localization, which were observed through either fractionation techniques or histoimmunofluorescence techniques. PDEs, in most cases, are associated with the particulate and/or cytosolic fraction (Houslay 2001), but a few reports have shown nuclear localisation. Nuclear localisation has, however, been shown for PDE4 enzymes, which have been observed on the nuclear envelope (Kapiloff et al. 2001) and in perinuclear regions (Verde et al. 2001).

PDE regulation also occurs at the level of transcription and translation (Conti et al. 2002). Increases in cAMP levels seem to up-regulate PDEs so that the induction of PDEs will combat the augmented cAMP effect and adaptation to chronic activation will be realised. This type of regulation has been seen with PDE3, PDE4 and PDE7 (Seybold et al. 1998; D'Sa et al. 2002; Lee et al. 2002), and is likely due to the cAMP-response elements as well as other elements involved in transcription found in the promoters of these genes (D'Sa et al. 2002; Torras-Llort and Azorin 2003).

### 1.2.1 The PDE1 enzyme family

3',5'-cyclic nucleotide phosphodiesterase 1 (PDE1) was the first PDE to be discovered, cloned and characterized (Kakiuchi et al. 1970). PDE1 consists of a family of enzymes that are  $\text{Ca}^{2+}$ -calmodulin ( $\text{Ca}^{2+}$ -CaM)-dependent, and this family mediates the cross talk between cAMP and  $\text{Ca}^{2+}$  signalling. PDE1s are encoded by three distinct genes (PDE1A, PDE1B, and PDE1C), with further complexity arising from alternative mRNA splicing (Giembycz 2005). Two 5'-splice variants have been identified for bovine PDE1A, namely PDE1A1 and PDE1A2, with different affinities for CaM. In humans, six different PDE1A isoforms (PDE1A1 through PDE1A6) arising from the 5' or 3' mRNA splicing were isolated and were validated by both RT-PCR and tissue expression (Peter et al. 1999). PDE1B generates two splice variants (PDE1B1 and PDE1B2). The amino termini of PDE1B1 and PDE1A2 show close homology, which might explain the similarity in their CaM binding affinity (Mark et al. 2001). Despite the similarity in their N-termini, PDE1A and PDE1B have tissue-specific distribution (Mark et al. 2001).

PDE1C has been suggested to be involved in smooth muscle proliferation (Rybalkin et al. 2002) which is characteristic of COPD and other airway inflammatory diseases (Giembycz 2005). Compared to PDE1A and PDE1B, which preferentially hydrolyse cGMP, PDE1C degrades both cAMP and cGMP with high affinity (Giembycz 2005). To date, five alternatively spliced products of PDE1C gene have been identified in mouse (PDE1C1, PDE1C2, PDE1C3, PDE1C4, and PDE1C5). These related isoforms showed similar high affinities and  $V_{\max}$  for both cAMP and cGMP, although responded to  $\text{Ca}^{2+}$  stimulation differently (Chen 1996).

Pharmacological data have shown that the compound vinoxetine is able to inhibit all PDE1 isoforms, but inhibits PDE1C with less potency (Chen et al. 1996). The inhibitors specific to PDE1 are suggested to alter sperm motility and capacitation in humans. Recently, Giembycz (2005) advocated the development of dual-specific inhibitors of PDE1C and PDE4, the application of which could effectively target proliferating airway smooth muscle cells by retarding the remodelling process through PDE1C inhibition and arresting inflammation by way of PDE4 inhibition.

### 1.2.1.1 Structure of PDE1

The overall structure of PDE1 isoforms is well conserved. PDE1 isoforms are composed of dual CaM binding domains, called CaM1 and CaM2, at the N-termini together with an inhibitory domain and a catalytic domain at the C termini (Goraya and Cooper 2004). Although the mechanism by which the PDE1 inhibitory domain maintains basal low activity state is still debatable, it has been suggested that in the presence  $\text{Ca}^{2+}/\text{CaM}$  creates a large hydrophobic cleft on the surface of each of its lobes, which can accommodate the amphipathic  $\alpha$  helices of PDE1 and relieve auto-inhibition.

### 1.2.1.2 Regulation of PDE1

Like  $\text{Ca}^{2+}$ -sensitive ACs, PDE1 is activated almost exclusively through extracellular  $\text{Ca}^{2+}$  influx in intact cells (Goraya and Cooper DMF 2004), although this may not occur exclusively via CCE channels (capacitative  $\text{Ca}^{2+}$  entry). PDE1 can undergo phosphorylation and this reduces the affinity of PDE1 for CaM and its sensitivity to  $\text{Ca}^{2+}$  (Rajendra 1991). In addition, dephosphorylation by  $\text{Ca}^{2+}/\text{CaM}$ -dependent protein phosphatase essentially reactivates PDE1. Thus, such regulation confers a possible scenario *in vivo* whereby increased cAMP induced by hormonal stimulation temporarily inhibits PDE1 (through PKA). This would generate a positive feedback loop to evoke a physiological response before  $\text{Ca}^{2+}$  influx-activated  $\text{Ca}^{2+}/\text{CaM}$ -dependent protein phosphatase overrides the inhibition of PDE1 by PKA. The net effect of this is to return the high cAMP level back to normal (Goraya and Cooper 2004). This hypothesis has been supported by a study in olfactory receptor cells where both AC3 and PDE1C were expressed.

## 1.2.2 The PDE2 enzyme family

3',5'-cyclic nucleotide phosphodiesterase 2 (PDE2) is encoded by a single gene. It is sensitive to both cAMP and cGMP and is able to hydrolyse both (Yang et al. 1994). PDE2 is highly expressed in the brain and heart, and is also found in lung, kidney, and liver (Rosman et al. 1997).

The family-specific N-terminal domain of the full length PDE2A contains a phosphorylation site for calmodulin-dependent kinase, as well as two GAF domains,

one being responsible for the activation of PDE2 enzymes in response to cGMP, another promoting dimerization of PDE2A (Martinez et al. 2002). Full length PDE2A hydrolyzes both cAMP and cGMP, with a slight preference to cGMP under basal conditions; however, following the binding of cGMP to the allosteric GAF domain, the enzyme undergoes a conformational change that leads to its activation and results in a 10-fold lower  $K_m$  for cAMP (Iffland et al. 2005).

To date, two generations of compounds have been used to specifically inhibit PDE2: the first generation PDE2-selective inhibitor EHNA (erythro-9-(2-hydroxy-3-nonyl) adenine) and the more selective second generation PDE2 inhibitor BAY 31-9472 (Netherton and Maurice 2005). The application of EHNA to cardiac myocytes has been shown to increase L-type  $Ca^{2+}$  currents (Vandecasteele et al. 2001). Recently, Iffland et al. determined the crystal structure of the catalytic domain of human PDE2A at 1.7Å and identified the active site residues involved in inhibitor and substrate selectivity in PDE2A. This study provides a rational explanation for the potent inhibition of PDE2A by EHNA, but not by rolipram, and provides insights into the dual substrate specificity of PDE2A enzymes (Iffland et al. 2005).

### **1.2.3 The PDE3 enzyme family**

The 3',5'-cyclic nucleotide phosphodiesterase 3 (PDE3) family comprises two subfamilies, PDE3A and PDE3B, both of which can catalyse the hydrolysis of cAMP and cGMP. Although PDE3 binds to both cAMP and cGMP with high affinities, the apparent lower  $V_{max}$  for hydrolyzing cGMP than that for cAMP allows cGMP to act as a potent competitive inhibitor of cAMP hydrolysis by PDE3 (Aizawa et al. 2003), thus cGMP is considered to inhibit PDE3 (Manganiello et al. 1995).

Three isoforms PDE3A1, PDE3A2, and PDE3A3 are generated from PDE3A gene due to the alternative splicing, while only one isoform of the PDE3B gene has been identified so far (Movsesian et al. 2002; Wechsler et al. 2002).

#### **1.2.3.1 Structure of PDE3**

The structural organization of PDE3A and PDE3B proteins is identical and follows the typical pattern of all the PDE family members (Degerman et al. 1997).

The catalytic domain of PDE3 is flanked by a divergent N-terminal region and a hydrophilic C-terminal region. Although the amino acid sequence of the N-terminal portions of PDE3A and PDE3B are different, both are indicated in the potential membrane targeting and regulation by PKA (Leroy et al., 1996). Within the catalytic domain of PDE3 is a 44 amino acid insert that has no counterpart in the cognate domain of other PDEs, this distinguishes PDE3 from other PDEs and may also distinguish the two subfamilies of PDE3 (Degerman et al 1997). It has been speculated that the unique insertion within the PDE3 catalytic region may contribute part, if not all, to the differences in substrate and inhibitor specificities between PDE3 and other PDEs (Tang et al. 1997), or even between PDE3 subfamilies. Recently, the presentation of a three dimensional structure of the catalytic domain of human PDE3B by Scapin et al. (Scapin et al. 2004) provides supportive evidence for this. Although the functional role of this unique insert is not fully understood, it has been suggested that this PDE3 specific insert region is important to maintain the effective structure of the catalytic domain of PDE3 enzymes (Tang et al. 1997).

### **1.2.3.2 Biological importance of PDE3 enzymes**

The two PDE3 subfamilies, PDE3A and PDE3B, are highly homologous, but they show a tissue-specific expression pattern (Beavo 1995). PDE3A is mainly expressed in vascular smooth muscle, platelets, and cardiac muscle, whereas PDE3B is predominately identified in adipose and liver. This different distribution thus confers their individual effects on different organisms and different cAMP pathways.

Ding et al. (2005) have shown that the expression and activity of PDE3A are significantly reduced in human failing hearts and suggested that PDE3A plays a unique role in the regulation of cardiomyocyte apoptosis through the proapoptotic transcriptional repressor inducible cAMP early repressor (ICER). This action is unique to PDE3 family, as the inhibition of only PDE3, but not PDE4 which is also largely present in cardiomyocytes, promoted cardiomyocyte apoptosis, indicating that PDE3 and PDE4 regulate distinct pool of cAMP in cardiomyocytes. This concept is consistent with the previous observation that PDE3 and PDE4 inhibitors elicited different cAMP dynamics when real-time imaging of cAMP in situ via fluorescence resonance energy transfer was applied in live cardiomyocytes (Mongillo et al. 2004).

Although PDE3A is the major PDE3 isoform in cardiac muscle and PDE3 inhibitors show great effects on cardiac contractility, interestingly, mice lacking PDE3A (PDE3A<sup>-/-</sup>) are viable with no other obvious deficiencies except that female PDE3A<sup>-/-</sup> mice are completely sterile due to cAMP/PKA dependent meiotic arrest of the oocyte (Maurice et al. 2003; Masciarelli et al 2004). This may be explained by the fact that depletion of PDE3A alone may not be sufficient to induce cardiac injury in vivo, and additional challenge with chronic pressure overload might be required.

It has long been believed that the major PDE3 isoform in cardiomyocytes is PDE3A. However, a recent study suggested that PDE3B is also important in the regulation of cardiac function (Patrucco et al. 2004) via the interaction with phosphoinositide 3-kinase  $\gamma$  (PI3K $\gamma$ ), albeit this direct interaction is not sufficient to drive PDE3B activation. PDE3B is indicated as a key agent in the stimulatory action of cAMP on pancreatic  $\beta$ -cell exocytosis and insulin release (Harndahl et al. 2002), and the increased activity of PDE3B in  $\beta$ -cells dramatically decreases insulin release. PDE3B thus is a candidate for therapeutic intervention in type 2 diabetes. It has also been reported that PDE3B is involved in lipolysis and metabolic turnover, and therefore may provide a target for obesity treatment (Scapin et al. 2004).

A number of commercial PDE3 inhibitors exist, such as cilostamide, milrinone and amrinone, all of which have a pyridazinone core that has been shown to be important for selectivity over other PDEs (eg. PDE2, PDE4, and PDE7) (Edmondson et al. 2003). However, inhibitors that distinguish between PDE3A and PDE3B are limited. So far, MERCK1 is one such compound that selectively inhibits PDE3B. Recently, the crystal structure of human PDE3B was resolved by Scapin et al. (2004) and this finding can be expected to aid in the design of future improved PDE3 selective inhibitors.

#### **1.2.4 The PDE4 enzyme family**

3',5'-cyclic nucleotide phosphodiesterase 4 (PDE4) is one of the members of the superfamily that specifically hydrolyses cyclic adenosine monophosphate (cAMP). Another characteristic of this family is their selective inhibition by the compound, rolipram (Houslay et al. 1998). Selective inhibitors of PDE4 form the largest group of

inhibitors for any PDE family and have been studied as anti-inflammatory drugs targeting asthma and chronic obstructive pulmonary disease (COPD) and also as therapeutic agents for rheumatoid arthritis, multiple sclerosis, type II diabetes, septic shock, and atopic dermatitis (Giembycz 2000; Souness et al. 2000; Huang et al. 2001; Piaz and Giovannoni 2000; Barnette and Underwood 2000; Sturton and Fitzgerald 2002). The prototypical PDE4 selective inhibitor roflumilast has shown to exhibit antidepressant and memory-enhancing properties (Scott et al. 1991). The development of dual-specific compounds that can inhibit PDE4 and either PDE1, 3, 5 or 7 may be desirable because of their potential benefit for the treatment of COPD (Giembycz 2005). The most advanced compound in clinical trials for the treatment of asthma and COPD is Altana's pumafentriene (roflumilast).

Mammalian PDE4 genes are orthologous for the *dunce* gene in the fruitfly *Drosophila melanogaster* (Conti et al. 2003), and they encode four subfamilies, called PDE4A, PDE4B, PDE4C, and PDE4D. Like *Drosophila*, mammalian PDE4 genes are composed of multiple transcriptional units and multiple promoters. So far, a total of at least 20 open reading frames for PDE4 genes have been identified, each of which is characterised by a unique N-terminal region (Houslay et al. 1997; Houslay and Adams 2003).

### 1.2.5 The PDE5 enzyme family

3',5'-cyclic nucleotide phosphodiesterase 5 (PDE5) is one of the members of superfamily that specifically cleaves cyclic guanosine monophosphate (cGMP), a key intracellular second messenger. In smooth muscle, PDE5 is the most expressed cGMP-hydrolysing PDE and plays a pivotal role in NO/cGMP signalling, which modulates smooth muscle tone (Corbin and Francis, 1999). Recently, PDE5 has also been suggested to play a critical role in tubule function and regulate the cGMP signalling that is important for epithelial fluid transport in *Drosophila* (Broderick et al. 2004).

PDE5 is composed of 875 amino acids and was first identified in lungs, vascular tissue and platelets (Kulkarni and Patil, 2004). PDE5 comprises a C-terminal catalytic domain of ~250 amino acids that are well conserved between mammalian

PDEs and an N-terminal cGMP-binding domain (GAF) which is also present in PDE2 and PDE6 (Stacey et al. 1998). To date, only one gene, PDE5A is identified for the PDE5 family. This gene generates two alternatively spliced variants, PDE5A1 and PDE5A2 (Corbin and Francis, 1999). In large pulmonary arteries, synthesis of PDE5A2 protein has been suggested to account for the decreased cGMP levels and subsequent decrease in acetylcholine-induced vasodilation under chronic hypoxic conditions (Murray et al. 2002), providing a molecular mechanism by which PDE5 inhibitors exert their beneficial effects.

PDE5 exists as a dimer, and the N-terminal region of each monomer contains one phosphorylation site (Ser92), two allosteric cGMP binding sites of ~110 amino acids arranged in tandem, and at least a small portion of the dimerisation domain (McAllister-Lucas et al. 1995; Corbin and Francis, 1999). Like the other known mammalian PDEs, PDE5 contains two sequences (HX<sub>3</sub>HX<sub>n</sub>(E/D)) that resemble the Zn<sup>2+</sup> binding sites in the catalytic domain, which are involved in the catalysis function of the enzyme (Francis et al. 1994). In the catalytic domain, a cGMP-binding substrate site is also present. The binding of cGMP at the catalytic site precedes the binding of cGMP at the allosteric binding sites and this is required for the specific phosphorylation of Ser92 by PKG or PKA which results in the subsequent activation of PDE5 (Corbin and Francis, 1999; Burns et al. 1992). This implies a negative feedback regulation of cGMP levels in the cells. Recently, it has been identified that PDE5 can interact with recombinant PDE6 $\gamma$  and this interaction serves to prevent the activation of PDE5 by PKA (Lochhead et al. 1997). In addition, caspase-3 has also been shown to either directly or indirectly interact with PDE5A1, leading to the cleavage and inactivation PDE5A1 via caspase-3 activated proteases, (Frame et al. 2003). Interestingly, rod PDE $\gamma$  was found to interact with PDE5A1 and therefore promote this cleavage of PDE5A1 by caspase-3 (Frame et al. 2001).

Sildenafil (Viagra®), a potent and reversible inhibitor of PDE5 (IC<sub>50</sub> ~4 nM), is highly selective for this PDE when compared with other known PDE families (Ballard et al. 1998) and is used as a clinical treatment for male erectile dysfunction. Recently, other PDE5 inhibitors that are functioning in vascular smooth muscle have also been reported they have been shown to amplify the pulmonary vasodilator

response to inhaled prostacyclin (Schermuly et al. 1999). These include tadalafil (Cialis<sup>TM</sup>) and vardenafil (Levitra<sup>TM</sup>) (de Tejada et al. 2001; Eardley and Cartledge, 2002). As PDE5 is also involved in a number of maladies, such as angina, hypertension, in addition to erectile dysfunction, new and selective inhibitors are now being intensely explored (Kulkarni and Patil, 2004).

### 1.2.6 The PDE6 enzyme family

3',5'-cyclic nucleotide phosphodiesterase 6 (PDE6) is known as the photoreceptor cGMP phosphodiesterase. It is cGMP specific and highly concentrated in the internal membrane of the rod and cone photoreceptors of the retina (Cote 2004). This family of PDEs has been shown to play important role in vertebrate phototransduction by mediating the photoresponse from rhodopsin to cGMP-gated ion channels. This results in vision through neuronal activities (Arshavsky et al. 2002). Compared to other PDE families, PDE6 is unique in its composition, because it is a tetrameric protein, composed of two catalytic subunits and two identical inhibitory  $\gamma$  subunits. For rod PDE6 enzymes, the two catalytic subunits ( $\alpha$  and  $\beta$ ) form a heterodimer, while for retinal PDE6, the two catalytic subunits are identical (two  $\alpha$ s) forming a homodimer (Artemyev et al. 1998). Each catalytic subunit of PDE6 contains three distinct domains, a catalytic domain and two GAF domains (responsible for allosteric cGMP binding) (Cote 2004). The inhibitory subunits of rod and cone PDE6 are different in their N-terminal regions (Wan et al. 2001). In response to light, GTP-bound G-protein (transducin) binds to the PDE $\gamma$  subunits and displaces them, thereby activating the PDE6 catalytic subunits. Recently, it has been suggested that rod and cone PDE $\gamma$  are also expressed in lung, kidney, testes, liver, heart, airway, pulmonary smooth muscle and even HEK293 cells. Intriguingly, it has been shown that PDE $\gamma$  serves as a novel, non-receptor phosphorylation substrate for GRK2, allowing it to interact with dynamin II so as to regulate p42/p44 MAPK signaling in human embryonic kidney 293 cells (Wan et al. 2001). In addition, PDE6 is also known as an effector for the Wnt/ $Ca^{2+}$ /cGMP-signalling pathway crucial in development (Wang et al. 2004). This represents another non-visual function of PDE6.

PDE6 resembles PDE5 with a degree of homology in amino-acid sequence as well as in three-dimensional structure of the catalytic dimer. Both also have the ability

to bind cGMP at the regulatory GAF domains. This might explain the observation that a number of compounds that inhibit PDE5 also inhibit PDE6 (Cote 2004).

### **1.2.7 The PDE7 enzyme family**

3',5'-cyclic nucleotide phosphodiesterase 7 (PDE7) is a cAMP-specific enzyme, insensitive to cGMP and refractory to inhibitors of PDE3 and PDE4 (Michaeli et al.1993). This family of enzymes was first isolated at the gene level in 1993 from a human glioblastoma cDNA library and expressed in a cAMP-deficient strain of the yeast *Saccharomyces cerevisiae*. To date, two PDE7 genes, PDE7A and PDE7B, have been identified in humans. Transcription of *PDE7A* gives rise to three isoenzymes (PDE7A1, PDE7A2, and PDE7A3) due to alternative mRNA splicing; while PDE7B exists as a single isoenzyme with about 70% sequence similarity to PDE7A (Smith et al. 2004). Except for PDE7A2 that has not been detected at protein level, PDE7A isoforms and PDE7B have distinct expression patterns, indicating their non-overlapping, tissue-specific functions (Gardner et al. 2000). PDE7A1 is distributed ubiquitously across human proinflammatory and immune cells, PDE7A3 is mainly expressed in human T-lymphocytes, while PDE7B has a broader distribution pattern, and is found in brain, liver, heart, thyroid glands, and skeletal muscles (Gardner et al. 2000).

Although the physiological role of PDE7 is not well understood, the development of PDE7 inhibitors has progressed over the past several years because the distribution of PDE7A1 across human proinflammatory and immune cells mirrors the expression pattern of PDE4 and that a PDE7A inhibitor increased anti-proliferative and cAMP elevating activity of rolipram in T cells without itself achieving such effects (Smith et al. 2004). There may be a use for developing a novel class of therapeutic inhibitors which can inhibit both PDE7 and PDE4. This may also reduce the significant side effect of emesis from PDE4 inhibitor treatment in the treatment of a wide variety of immune and inflammatory diseases.

### **1.2.8. The PDE8 enzyme family**

3',5'-cyclic nucleotide phosphodiesterase 8 (PDE8) is a class of PDEs which has high affinity for cAMP and are IBMX-insensitive (Fisher et al. 1998). Unlike

classical PDEs such as PDE 1-6, PDE8 was identified using a bioinformatics approach. Little detailed studies have, however, been done on PDE8 and our understanding of this recently discovered PDEs function is poor. PDE8 is known to have characteristic features that include the PAS (Period, Arnt, Sim) domain and REC domain, N-terminal to the PDE catalytic domain. However, the functions of these domains regarding PDE8 are not known yet.

In humans, the PDE8 family is encoded by two genes, PDE8A and PDE8B (Kobayashi et al. 2003), which are 68% identical in sequence. So far, PDE8A cDNAs has been isolated from humans and mice, and PDE8B cDNAs have been isolated from humans and rats. Human PDE8A1 is expressed at protein levels in testis, spleen, colon, small intestine, ovary, placenta and kidney; while human PDE8B is expressed in a unique tissue-restricted pattern, which is confined to the thyroid gland. Hayashi et al. have shown that recombinant PDE8B is not inhibited by various PDE inhibitors including vinpocetine, a PDE1 inhibitor; milrinone, a PDE3 inhibitor; rolipram, a PDE4 inhibitor, but dipyridamole, at a concentration of 40  $\mu$ M, inhibited PDE8B by 50% (Hayashi et al. 1998).

### **1.2.9 The PDE9 enzyme family**

3',5'-cyclic nucleotide phosphodiesterase 9 (PDE9) is a class of cGMP-specific PDEs. It is encoded by a single gene PDE9A in humans and mice (Wang et al. 2003). The transcriptional gene product with alternative N-terminal splicing gives rise to five isoforms, PDE9A1, PDE9A2, PDE9A3, PDE9A4, and PDE9A5 (Guipponi 1998; Wang et al. 2003). These five splice variants have distinct tissue distribution and subcellular localisation pattern, implying their differential cGMP-hydrolysing ability within specific cellular compartments in appropriate tissues. Recently, Wang et al. (2003) reported that PDE9A is highly expressed in immune tissues and cells, indicating a pivotal role for PDE9A in the regulation of immune functions.

Interestingly, as a high affinity cGMP-hydrolysing PDE, PDE9A lacks a region homologous to the allosteric cGMP binding domain found in other cGMP-binding PDEs, such as PDE2, PDE5 and PDE6 (Fisher et al. 1998).

PDE9A was shown to be insensitive (up to 100  $\mu\text{M}$ ) to a variety of commonly used PDE inhibitors including rolipram, vinpocetine, SKF-94120, dipyridamole, and IBMX, but was inhibited by zaprinast, which inhibits various cGMP PDEs (Fisher et al. 1998).

### **1.2.10 The PDE10 enzyme family**

3',5'-cyclic nucleotide phosphodiesterase 10 (PDE10), a dual specificity PDE, was identified by a bioinformatics approach (Fujishige et al. 1999). PDE10 can hydrolyse both cGMP and cAMP, but has been suggested to function as a cAMP-inhibited cGMP PDE (Soderling et al. 1999).

PDE10A contains two conserved GAF domains at its N-terminus, similar to their counterparts in PDE2, PDE5, or PDE6 (Soderling et al. 1999). The phosphorylation site of cAMP- or cGMP-dependent kinase in the N-terminal region of PDE10A is absent but in its place a putative protein kinase C (PKC) phosphorylation site was observed, suggesting that PDE10A may be regulated by PKC (Fujishige et al. 1999). PDE10A has a tissue specific expression pattern, and was found particularly abundant in the putamen and caudate nucleus regions of brain as well as in thyroid and testis. To date, not much is known about the physiological role of PDE10. However, selective inhibitors are actively being sought to treat affective disorders.

Sequence analogy study reveals a high degree of homology in the catalytic domain of PDE10A to that of PDE5A (47%) and PDE2A (42%). This might lead to a conclusion that inhibitors of PDE5 or PDE2 can inhibit PDE10 isoenzymes. Indeed, only cGMP PDE inhibitors (zaprinast, E4021, SCH51866, and dipyridamole), but not PDE2 inhibitor (EHNA) or non-selective PDE inhibitor (IBMX), antagonized PDE10A activity efficiently (Fujishige et al. 1999).

### **1.2.11 The PDE11 enzyme family**

3',5'-cyclic nucleotide phosphodiesterase 11 (PDE11) is the most recently discovered member of the PDE superfamily. So far, only one gene, PDE11A, has been discovered. In common with various other PDE family gene members, PDE11A encodes four isoforms by virtue of alternative splicing, and these isoforms are named

PDE11A1, PDE11A2, PDE11A3, and PDE11A4. PDE11A1 possess an incomplete GAF domain, PDE11A3 has a complete GAF domain and an incomplete GAF domain, while PDE11A4 contains two complete GAF domains (Yuasa et al 2000; Fawcett et al. 2000). To date, only two of the isoforms, PDE11A3 and PDE11A4 were detected at the level of protein. PDE11A3 transcripts are specifically expressed in the testis, while PDE11A4 transcripts are found in human prostate, pituitary, heart and liver, but not in blood vessels, cardiac myocytes, skeletal muscle, testis or penis. The physiological role of PDE11A has not been determined, but a PDE5A inhibitor, Tadalafil (Cialis®), has been shown to partially inhibit PDE11.

### **1.2.12 PDE and diseases**

Mutations in subunits of PDE6 in the retina are the basis of some forms of hereditary retinitis pigmentosa and stationary night blindness (Dryja et al. 1999; Gal et al. 1994). Differential expression of PDE4 isoforms has been described in lung macrophages from patients with COPD, with an increased expression of PDE4A4 transcripts (Barber et al. 2004). Recently, the PDE4D gene has been identified as the most likely candidate susceptibility gene for cardiogenic and carotid ischemic stroke (Gretarsdottir et al. 2003). Although the precise pathogenic mechanism of the dysregulation of PDE4D expression for stroke is still not clear, it is known that PDE4D is expressed in many cells that are important for the pathogenesis of atherosclerosis, an important risk factor in stroke. More recently, a PDE4B gene disrupted by a balanced translocation has been identified in a subject diagnosed with schizophrenia and a relative with chronic psychiatric illness. This finding therefore provides a primary evidence for PDE4B as a genetic susceptibility factor for schizophrenia (Millar et al. 2005).

## **1.3 Molecular biology and biochemistry of the PDE4 enzyme family**

### **1.3.1 PDE4**

PDE4 is encoded by four genes, PDE4A, PDE4B, PDE4C, and PDE4D. PDE4A, 4B, 4D are expressed in inflammatory cells such as T cells, B cells, eosinophils, neutrophils, airway epithelial cells and endothelial cells (Burnouf and Pruniaux 2002). The expression of PDE4C is usually weak in these cases. In HEK293

cells, PDE4B and PDE4D are predominantly expressed, while PDE4C was hardly detected (Lynch et al. 2005). PDE4 isoforms have been suggested (Houslay et al. 2005) to have non-overlapping functions in the cells, and the understanding of this is much accelerated with the advent of gene knockout approaches (Hansen et al. 2000; Jin and Conti 2002; Ariga et al. 2004), and crucially, the development of both dominant-negative (Baillie et al. 2003; McCahill et al. 2005) and siRNA-mediated knockdown strategies (Lynch et al. 2005). These approaches have helped to discern the functional role of individual PDE4 isoforms. siRNA-mediated knock down can be used to target either entire PDE4 subfamilies or specific isoforms, dependent on the probe design (Lynch et al. 2005), whereas dominant negative strategies exploit the targeting of specific isoforms by overexpressing a catalytic inactive forms to displace the tethered endogenous active species from the functionally relevant site in the cell (Baillie et al. 2003; Baillie and Houslay 2005).

### **1.3.1.1 Structure of PDE4 isoforms**

The 16~18 different PDE4 isoenzymes that are expressed in mammalian cells have closely related kinetic properties and ion requirement (Conti et al. 2003). Products of any single PDE4 gene all have a common unit, consisting of a highly conserved catalytic domain together with a PDE4 subfamily-specific C-terminal domain. The signature of each isoenzyme is a unique variant-specific N-terminal region (Houslay and Adams 2003). In most cases, the N-terminal region is encoded by a single 5' exon, although two such 5' exons are present in PDE4C1 (Sullivan et al. 1999). The promoters that drive the generation of these isoenzymes are shown to lie immediately upstream of the 5' exon that encodes their N-terminus (Houslay and Adams 2003; Rena et al. 2001; Wallace et al. 2005). The four PDE4 subfamilies, PDE4A, PDE4B, PDE4C and PDE4D are each encoded by large genes around 50 kb consisting of multiple exons.

Functional PDE4s can be categorized into three groups, namely long PDE4 isoenzymes that exhibit both upstream conserved region 1 and 2 (UCR1 and UCR2), short PDE4 isoenzymes that lack UCR1 but have intact UCR2, and supershort PDE4 isoenzymes that not only lack UCR1, but have a NH<sub>2</sub>-terminally truncated UCR2 (Houslay and Adams 2003). UCR1 is adjacent to the N-terminal of long isoenzyme,

while UCR2 is adjacent to the N-terminal of the catalytic unit. These two modules are joined together through linker region 1 (LR1) and LR2, both of which vary in the four PDE4 subfamilies (Figure 1.4).

Uniquely, the PDE4A gene encodes an isoform, PDE4A7 that lacks PDE activity. Inspection of the gene sequence has suggested that the molecular basis of this phenomenon is due to the mRNA splicing at both the 5' and 3' end (Horton et al. 1995; Johnston et al. 2004).

UCR1 and UCR2 function as a regulatory domain that controls the catalytic unit, and confers regulatory functions on PDE4 by orchestrating the functional outcome of phosphorylation by PKA and ERK (Houslay and Adams 2003). This gives a key insight into the existence and importance of alternative mRNA splicing variants (Beard et al. 2000; Mackenzie et al. 2000; Sette and Conti 1996). Biochemical pull-down and two-hybrid analyses show that it is the hydrophobic C-terminal portion of UCR1 that interacts with the hydrophilic N-terminal region of UCR2 (Beard et al. 2000), and the direct contact of UCR2 with the catalytic unit may exert an inhibitory effect on the activity of the PDE4 catalytic unit. This was found in both PDE4D (Lim et al. 1999; Jin et al. 1992) and PDE4A5 (Beard et al. 2002). In brief, long PDE4 isoforms are phosphorylated by PKA at a site present in the N-terminal of UCR1 leading to an increase in  $V_{max}$  of the enzyme. The interaction of UCR1 and UCR2 is thought to be relevant to the mechanism of enzyme activation by PKA phosphorylation. Moreover, PKA phosphorylation also enhances the sensitivity of PDE4D3 and PDE4A4 to stimulation by  $Mg^{2+}$  (Houslay and Adams 2003).

All PDE4 subfamilies, except for PDE4A, contain a single ERK consensus motif (Pro-Xaa-Ser-Pro) within their third subdomain of the catalytic unit. This serine residue is subject to phosphorylation by ERK both *in vitro* and *in vivo* (MacKenzie et al. 2000). Flanking this motif are two ERK docking sites, one of which is a common docking site ('KIM'), utilized by both ERK and JNK, another is specific for ERK, called 'FQF' motif. More complicated than PKA phosphorylation, ERK phosphorylation of PDE4s leads to different activity changes due to the nature of PDE4 isoforms as well as the cell type, the nature of the prevailing stimuli and temporal window over which analyses are made (Houslay and Adams 2003). In PDE4

long isoforms, a novel feedback regulatory system exists, where the transient inhibition of PDE4 by ERK is rapidly overturned by the subsequent activation of PKA (Hoffmann et al. 1999). Interestingly, ERK was shown to mediate PKA activation of PDE4D isoforms in aortic smooth-muscle cells through a different pathway involving COX2 (Baillie et al. 2001; Liu and Maurice 1999).

### **1.3.1.2. Presence of signalling complexes involving PDE4s**

The plethora of PDE4 isoforms are uniquely characterized by their distinct N-terminal region, which can confer intracellular targeting, as well as interaction with putative binding partners. Thereby they may form spatially constrained signalling complexes that underpin the compartmentalization of cAMP and integrate with other signalling pathways. These properties can be seen in the binding of Src family tyrosyl kinases to PDE4A4/5 (McPhee et al. 1999) and PDE4D4 (Beard et al. 1999), of RACK1 to PDE4D5 (Yarwood et al. 1999; Bolger et al. 2002); of  $\beta$ -arrestin to PDE4D5 (Bolger et al. 2003); of myomegalin to PDE4D3 (Verde et al. 2001); of the immunophilin XAP2 to PDE4A5 (Bolger et al. 2003) and of DISC1 to PDE4B1 (Millar et al. 2005).

The ability of PDE4D3 to interact with mAKAP through its unique N-terminal region has also been shown (Dodge et al. 2001). This offers a signalling complex with potential for controlling a unique negative feedback. Thus, as cAMP level rise and mAKAP-associated PKA activated, it will phosphorylate and activate PDE4D3, which in turn lowers cAMP levels then facilitates the de-activation of mAKAP-bound PKA and the subsequent dephosphorylation of PDE4D3. In cardiac myocytes under hypertrophic conditions, the spatial redistribution of PDE4D3, due to the dynamic interaction with mAKAP, is thought to contribute partly to the altered cellular functioning seen subsequent to heart failure. In addition to mAKAP, another AKAP, called AKAP450, has also been shown to interact with PDE4D3, but differently as their interaction is carried out through the UCR2 module of PDE4D3 (Tasken et al. 2001).

Interestingly, the super-short form PDE4A1 is entirely membrane-associated and its bilayer association is attributable to the novel microdomain, called 'TAPAS-1'

(tryptophan anchoring PA selective domain 1), which confers  $\text{Ca}^{2+}$  gated insertion and shows a preferential binding for net -2 charge phosphatidic acid (Baillie et al. 2002).

PDE4 isoforms interact with signalling or scaffolding proteins not only via their N-terminal or UCR2 regions, as demonstrated above, but also through the catalytic domains with which they provide the substrate domain for ERK (MacKenzie et al. 2000) and  $\beta$ -arrestin (Perry et al. 2002). As the catalytic domain in each PDE4 isoform is well conserved across PDE4 subfamilies, these interactions are not reckoned to be isoform-specific.

### 1.3.1.2.1 RACK1

RACK1 was originally identified as a scaffolding protein for activated C-kinase (Ron et al. 1994), but its role has been expanded through identification of a number of novel binding partners (McCahill et al. 2002), ranging from protein kinases (Yaka et al. 2002; Ron et al. 1999; Kiely et al. 2002; Chang et al. 2002), the phosphodiesterase PDE4D5 (Yarwood et al. 1999) to numerous receptors (Yaka et al. 2002; Kiely et al. 2002; Geijzen et al. 1999; Thornton et al. 2004). This variety of RACK-binding partners suggest that RACK1 is a multi-purpose protein that is involved in various biological functions, such as the regulation of heart contraction by noradrenaline (Johnson et al. 1996), glucose-stimulated insulin secretion in pancreatic  $\beta$  cells (Yedovitzky et al. 1997), NMDA channel function (Thornton 2004), and integration of adhesion and insulin-like growth factor I signalling and cell migration (Kiely et al. 2005).

RACK1 is a 36-kDa protein that contains seven tryptophan/aspartate (WD) repeats that are believed to form a seven-bladed  $\beta$ -sheet propeller structure, conferring the availability of multiple protein interaction surfaces (Sondek et al. 1996). Recent biochemical and structural studies have shown that at least two of the WT repeats are important for RACK1 self-regulation. One is the 4<sup>th</sup> repeat which is involved in the formation of RACK1-homodimer (Kiely et al. 2005), another is the 6<sup>th</sup> WD repeat where two highly conserved tyrosines are phosphorylated by Src kinase (Chang et al. 2002). In addition, WD repeats 5, 6, and 7 have recently been shown to provide a bifurcated trough that can accommodate PDE4D5 through its RAID1 (RACK1

interaction domain) located within its unique N-terminal region (Steele et al. 2001). Although G $\beta\gamma$  shares a highly identical sequence homology with RACK1, it does not interact with PDE4D5 (Yarwood et al. 1999). The interaction sites on both RACK1 and PDE4D5 has been extensively explored, however, the functional consequences of their interaction are still an enigma. Nevertheless, the most possible role of their interaction has been proposed that the recruitment of PDE4D5 to RACK1-containing complex controls cAMP levels in the close proximity of this complex and therefore regulates the PKA-phosphorylation status of RACK1-associated proteins within the same complex (Houslay and Adams 2003).

### 1.3.1.2.2 $\beta$ -arrestins

Two visual arrestins,  $\beta$ -arrestin1 and  $\beta$ -arrestin2 comprise a family of intracellular proteins that play a vital role in the desensitization of many GPCRs (Luttrell and Lefkowitz 2002). Visual arrestin is 60% and 65% identical in amino acid composition to  $\beta$ -arrestin1 and  $\beta$ -arrestin2 respectively and predominantly localized in rod photoreceptor cells of the retina. The  $\beta$ -arrestins are 78% identical in amino acid sequence and widely expressed in tissues, but their expression level varies in a cell-specific fashion (Attramadal et al. 1992; Sterne-Marr et al. 1993).

In the classic paradigm of receptor desensitization, agonist-occupied and activated  $\beta_2$ AR couples to Gs, leading to the activation of membrane-bound ACs and generation of cAMP. This process is rapidly desensitized when G-protein-coupled receptor kinases (GRKs) phosphorylate the activated  $\beta_2$ AR, which promotes the recruitment of cytosolic  $\beta$ -arrestins to the plasma membrane and thus uncouples the further interaction between  $\beta_2$ AR and Gs (Luttrell and Lefkowitz 2002). Recent studies add a new facet of  $\beta$ -arrestin function to this  $\beta_2$ AR desensitization process as  $\beta$ -arrestin has been shown to form a complex with PDE4 enzymes (Perry et al. 2002). This provides a means of delivering a cAMP-degrading enzyme to the site of cAMP synthesis and quenching the existing cAMP at the plasma membrane in an agonist-dependent manner (Figure 1.7). Indeed, all PDE4 isoenzymes bind  $\beta$ -arrestin, independent of agonist treatment, through a common site located within their conserved catalytic domain (Bolger et al. 2003; Perry et al. 2002). In addition, PDE4D5 preferentially interact with  $\beta$ -arrestin through an extra  $\beta$ -arrestin binding

region located within its unique N-terminal region (Bolger et al. 2003). The functional significance of this interaction was clearly demonstrated using an overexpressed catalytically inactive PDF4 construct, which resulted in a selective amplification of agonist-induced PKA activation towards  $\beta_2$ AR and the subsequent Src-regulated Gi switching which allowed activation of ERK pathway (Baillie et al. 2003).

Following desensitization, GPCRs are removed from the cell surface by a process of internalization (also termed endocytosis or sequestration). GRK-mediated phosphorylation and  $\beta$ -arrestin binding facilitates many GPCRs internalization. This includes  $\beta_2$ AR, angiotensin II type 1a, m2-m5 muscarinic cholinergic endothelin A, D<sub>2</sub> dopamine, follitropin, monocyte chemoattractant protein-1, CCR5 and CXCR1 receptors (Ferguson 2001). More than one mechanism is involved in mediating internalization of GPCRs, which are clathrin-coated vesicles, caveolae and uncoated vesicles (Claing et al. 2002). The extent of  $\beta$ -arrestin involvement is dependent on the receptor, agonist and cell type. In general, many GPCRs interact with  $\beta$ -arrestins and undergo internalization via clathrin-coated pits. Thus,  $\beta$ -arrestins both desensitizes agonist-activated receptors and promotes their internalization through clathrin-coated pits by binding to clathrin (von Zastrow and Kobilka 1994). In addition,  $\beta$ -arrestin links directly to the  $\beta_2$ -subunit of the clathrin-AP2 (adaptor protein 2) complex, a complex that targets many receptors to the clathrin endocytic machinery and is involved in the initiation of clathrin-coated pit formation (Laporte et al. 2000). Therefore, by binding to both clathrin and AP2,  $\beta$ -arrestin facilitates the targeting of the activated receptors to the endocytic machinery. Based on the pattern of  $\beta$ -arrestin-mediated GPCRs trafficking in the cells, GPCRs are classified into two groups (Oakley et al. 2000). Class A receptors include  $\beta_2$ AR,  $\alpha_{1b}$ -adrenergic receptor,  $\mu$ -opioid receptor, endothelin ET1A receptor and dopamine D<sub>1</sub> receptor, the binding of which to  $\beta$ -arrestin is transient during internalization. On the other hand, Class B receptors, represented by the angiotensin AT<sub>1a</sub>, neurotensin 1, vasopressin 2, thyrotropin-releasing hormone and neurokinin NK-1 receptors, form stable complexes with  $\beta$ -arrestin and traffic together during endocytosis. Recently, Lefkowitz et al. have reasoned that these distinct intracellular trafficking patterns of the two classes of receptors may be due to the different kinetics of  $\beta$ -arrestin ubiquitination and de-ubiquitination (Lefkowitz and Whalen 2004).

Research on arrestins has rapidly expanded over the past few years. There has been very considerable interest in how it links to the activation of ERK. This rose from demonstrations that the Src family non-receptor tyrosine kinase was shown to bind  $\beta$ -arrestin (Luttrell et al. 1999). Recently, the components of MAP kinases including ERKs, JNKs, and p38 (Marinissen and Gutkind 2001), the downstream elements of highly conserved cascades of MAPKKKs and MAPKKs that lead to the activation of the MAP kinases (Reiter and Lefkowitz 2006), have all been found to bind to  $\beta$ -arrestins. Due to the heterogeneity and diversity of kinases of each level of the MAPK cascades (for example, there are five ERKs, four p38 and three JNKs),  $\beta$ -arrestins have been suggested to function as scaffolding molecules to ensure fidelity and efficiency in activating specific MAPK molecules.

Furthermore,  $\beta$ -arrestins have also been shown to be involved in cell motility, chemotaxis and apoptosis (Lefkowitz and Shenoy 2005), which require  $\beta$ -arrestin-dependent activation of ERK or p38 MAPK (Wei et al. 2003; Azzi et al. 2003; Sun et al. 2002).

### **1.3.1.2.3 AKAPs**

AKAPs are a large family of structurally unrelated proteins that bind to PKA (Michel and Scott 2002). This interaction is carried out through the amphipathic helix from the AKAP and the hydrophobic pocket formed at the dimerization interface of the RII regulatory (cAMP binding) subunit of PKA. Functioning as other scaffolding proteins, AKAPs constrain PKA pools at different subcellular localizations, therefore conferring the compartmentalized response on PKA substrates that are either within the same complex or in their close proximity. Recently, a number of studies on AKAPs have broadened the list of the identification of AKAP-associated proteins. This includes other kinases (eg. PKC) (Klauck et al. 1996), phosphodiesterases (Houslay and Adams 2003), phosphatases (Smith et al. 2006), GPCRs (Malbon et al. 2004) and G proteins (Diviani et al. 2006).

One of the properties of AKAPs is to target signaling intermediates to a specific microenvironment where they can respond to upstream signals. This has been demonstrated extensively for PDE4D3 and mAkap (muscle-selective AKAP).

mAKAP uses a site distinct from its PKA-R subunit interaction site to bind to the unique N-terminal region of PDE4D3 and facilitates the phosphorylation and activation of PDE4D3 by localized PKA (Houslay and Adams 2003). This provides a unique negative feedback loop. Indeed, when cAMP levels rise and mAKAP-PKA is activated, PDE4D3 that is located in the same signaling complex is consequently activated by the phosphorylation by PKA. This activation thus amplifies the ability of PDE4D3 to degrade cAMP, hence decreasing the activity of mAKAP-bound PKA. As such, the system resets itself to the basal condition (McConnachie 2006). The PDE4D3-mAKAP-PKA module in a spatially localized self-regulatory system has been suggested to have clinical importance in the altered cellular function seen after heart failure (Dodge et al. 2001).

AKAP450 has the same complex of PDE4D and PKA RII (Tasken et al. 2001) in Sertoli cells of the testis, located in the centrosome. The interaction site on PDE4D for AKAP450 was mapped to its UCR2, indicating that other long PDE4 isoenzymes may also bind to AKAP450 (Tasken et al. 2001). Additional components of this signaling complex, such as PP1 and PP2A have also been suggested as AKAP450 can bind to these phosphatases (Westphal et al. 1999).

Recently, it has been suggested that PDE4D3 is in complex with the  $\text{Ca}^{2+}$  channel RyR, PKA, mAKAP and PP1 in cardiomyocytes (Marx et al. 2000; Kapiloff et al. 2001).

In addition, AKAP79, which constitutively anchors PKA to the  $\beta_2\text{AR}$ , and gravin that binds the  $\beta_2\text{AR}$  in an agonist-dependent manner, are both involved in an exquisite orchestration of spatial and temporal downstream signaling (Tao et al. 2003; Cong et al. 2001).

In Jurkat T cells, another PDE isoform PDE7A which is has been identified to be associated with AKAP149 at the nuclear membrane, with AKAP95 in the nucleus and with novel Golgi associated AKAPs derived from the myeloid translocation gene (MTG) (Asirvatham et al. 2004). This new evidence of functional

PDE-AKAP complexes present in real cells underpins the importance of such complexes in tightly controlling compartmentalized cAMP signaling.

### 1.3.1.3 Inhibitors

Selective inhibitors of PDE4 form the largest group of inhibitors for any PDE family, and have been studied as potential therapeutic reagents for many diseases (see review: Lipworth 2005). Rolipram, a highly selective first generation of PDE4 inhibitor, has been used for many years as a research tool to chemically ablate PDE4 activity and investigate the role of PDE4. Recently, Sanz et al. (2005) have reviewed the anti-inflammatory and anti-immunomodulatory effects of rolipram. It is now generally accepted that PDE4 has at least two conformations, HARBS and LARBS, for which rolipram has high and low binding affinities, respectively (Houslay and Adams 2003). While PDE4L is associated with anti-inflammatory activity, HARBS, which is generally expressed in the central nervous system, has been linked to the high levels of adverse effects, such as nausea and vomiting triggered by rolipram treatment (Chung 2006). This limitation by class-associated side effects thus calls for a need for a PDE4 inhibitor with a wide therapeutic ratio.

New second generation PDE4 inhibitors have now been developed with the hope of providing a wider therapeutic ratio, particularly with respect of overcoming nausea and vomiting (Burnouf and Pruniaux 2002). These inhibitors include cilomilast, roflumilast, arofylline, C-3885 etc. However, currently, among these inhibitors, only two of them, cilomilast and roflumilast, have reached phase III clinical trial stage (Chung 2006; Lipworth 2005).

In addition, PDE4 inhibitors have been investigated in the mediation of memory (Zhang et al. 2005) and infection-induced preterm labour (Oger et al. 2004).

Selective inhibitors of PDE4 sub-families may represent a favourable pharmacological strategy for the treatment of TNF- $\alpha$  mediated diseases such as rheumatoid arthritis, Crohn's disease and septic shock. PDE4D-specific inhibitors are used in the treatment of airway diseases associated with smooth muscle contraction, such as asthma and chronic obstructive pulmonary disease (Mehats et al. 2003); while

targeting of PDE4B gene revealed an essential role of this isoform in the innate immune response mediated by TNF- $\alpha$ .

Recently, it has been suggested that nausea and emesis, the most common side effect of PDE4 inhibitors, may be caused by the inhibition of PDE4D in the brain (Robichaud et al. 2002). However, this has yet to be proven. In addition, an increasing amount of evidence has indicated the non-redundant functions between PDE4 isoforms. Thus design of inhibitors selective for specific PDE4 subtypes is strongly desired. Undoubtedly, the understanding of these PDE4 subtypes at the atomic level, would greatly facilitate the design of PDE4 isoenzyme-specific inhibitors with reduced side effects and improved therapeutic use in a varieties of diseases. To date, several papers have elucidated the isoenzyme structure of PDE4 family members, including PDE4B (Xu et al. 2000) and PDE4D (Huai et al. 2003; Lee et al. 2002). These structures reveal that the selective binding of rolipram to PDE4s, shows a conserved variation of inhibitor binding residues across the PDE families, suggesting that the inhibitor specificity is determined by the chemical nature of amino acids and the conformational variation of the binding pockets (Houslay and Adams 2003; Card et al. 2004; Huai et al. 2003). Zhang et al. (2004) have described the mechanism of nucleotide selectivity based on the co-crystal structure of PDE4B and PDE4D with AMP, PDE5A with GMP, and the apostructure of PDE1B. In their study, an invariant glutamine has been suggested as the key specificity determinant for recognizing the purine moiety in cAMP or cGMP, and the surrounding residues contribute to anchoring the glutamine in different orientations for cAMP and for cGMP. In addition, the crystal structure of the human PDE4D2 catalytic domain in complex with AMP was obtained independently by another group, and it has been suggested that a hydroxide ion or water bridging two metal ions may serve as the nucleophile for the hydrolysis of the cAMP phosphodiester bond (Huai et al. 2003). This structural information on PDE4 in complex with AMP/GMP sheds light on the hydrolysis action of PDE4, provides insight into how more specific PDE4 inhibitors can be rationally designed (Zhang et al. 2004).

#### **1.3.1.4 Compartmentalization of cAMP and PDE4 enzymes**

The pioneering work of Brunton and colleagues (Brunton et al. 1998) has led to recognition of the paradigm for cAMP signalling compartmentalization. They showed that in cardiac myocytes, various Gs-coupled receptors caused different physiological outputs via the compartmentalized changes in cAMP and the subsequent selective activation of 'pools' of PKA. In some instances, PKA and PDE have been shown to be part of the same scaffold signalling complex where a negative feedback loop can be rapidly activated (Tasken et al. 2001; Dodge et al. 2001). The recruitment of PDE4 to activated receptors, as seen in cardiac myocytes and T cells (Bolger et al. 2003; Arp et al. 2003), contributes to the degradation of cAMP near the site of synthesis. This delimits the spatial-temporal wave of cAMP propagation in combination with intracellular molecular and physical barriers to diffusion.

The advances in development of visualisation techniques using FRET probes, based on either PKA or EPAC, cAMP gated ion channels, or the selective activation of AKAP-anchored PKA isoforms, have helped overcome the difficulties in visualizing compartmentalized cAMP (Zaccolo and Pozzan 2002; Zhang et al. 2001; Bos 2003; Nikolaev 2004).

Adenylyl cyclases and PDEs are pivotal in shaping and controlling intracellular cAMP gradients in cells (Baillie and Houslay 2005; Houslay and Adams 2003). ACs are located at the plasma membrane, and activation of AC sub-populations found in distinct plasma membrane sub-domains by specific Gs-coupled receptors is suggested to generate spatially segregated 'clouds' of cAMP from different plasma membrane locales. However, the plethora of PDE4 isoforms, together with their individual defined intracellular micro-environments and particular regulatory properties, make them predominant players in compartmentalizing cAMP and regulating inputs from other signalling pathways (Baillie et al. 2005) (Figure 1.6). Indeed, selective chemical knockout of PDE4 activity, coupled with the use of dominant negative PDE4 constructs, has identified this family of isoenzymes as a key contributor in modulation of isoprenaline-stimulated gradients of cAMP in cardiac myocytes and cultured cells (Rochais et al. 2004; Mongillo et al. 2004; Lynch et al. 2005). That PDE4s can associate with other proteins, allowing them to be strategically anchored throughout the cells (Houslay and Adams 2003) further confirms their role in shaping the cAMP gradients. Furthermore, as the importance of PDE4 in

engineering compartmentalised cAMP gradients is recognised in a number of papers, the use of selective PDE4 inhibitors as drugs to combat a number of human diseases looks likely (Baillie et al. 2003; Lynch et al. 2005; McCahill et al. 2005; Abrahamsen et al. 2004).

More recently, Karpen and coworkers have shown that a pool of cAMP below the plasma membrane does not equilibrate rapidly within the bulk of the cytoplasm, and more importantly, that PDE4 activity is crucial for this 'microdomain'-concentrated cAMP regulation. Thus, PDE4 regulation is likely to be involved in controlling cAMP access to its effectors close to the plasma membrane (Rich et al. 2001). A similar cAMP microdomain modulated by PDE4 has also been demonstrated in cardiac myocytes where cAMP accumulation in response to  $\beta$ -adrenergic agonists occurs preferentially in a region covering the Z band and the T-tubules (Zaccolo and Pozzan 2002). This is consistent with the observation that myomegalin serves to anchor long isoforms of PDE4 close to the Z band in proximity to the L-type channels, RyR and PKA (Marx et al. 2000; Verde et al. 2001).

### **1.3.1.5 Short-term regulation of PDE4s**

Post-translational modification often governs short-term regulation of proteins. Responses to many extracellular and intracellular stimuli often elicit post-translational modification on a variety of cellular proteins, which in turn further propagates the signal downstream. This can be achieved via the activation of several signalling pathways, alterations in subcellular localization, and the formation of physical protein-protein interactions (Jesen 2004). So far, almost every cellular pathway discovered uses post-translational protein modifications to generate and transmit signals in response to growth signals, stresses and chemical stimuli (Johnson 2004). Until recently, only large molecule moieties that covalently attach to cellular proteins had been studied extensively. Such modifications, triggered by cellular responses involved phosphates, various lipids, acetate or sugars (Muller et al. 2001). Among those modifications, protein phosphorylation is best understood (Hunter 1995). All PDE4 isoforms from four subfamilies (apart from PDE4A) can be phosphorylated by ERK and all long isoforms are shown to be susceptible to PKA phosphorylation (Baillie et al. 2000; Houslay and Adams 2003). The outcome of a specific

phosphorylation event varies dependent on the category of the PDE4 isoform, as well as the identity of the protein kinase. Much is known about the functional consequences of activity regulation of PDE4s resulting from phosphorylation post-translational modifications.

In the past two decades, ubiquitination and sumoylation have been identified as novel and important post-translational modifications that contribute to the altered functioning of the modified proteins. Sequence analysis of PDE4 genes during my PhD studies has revealed that some specific PDE4 gene products may have the potential to undergo ubiquitination and sumoylation. These two post-translational modifications and their characteristics are further discussed with respect to PDE4 in Chapters 4 and 5.

#### **1.3.1.5.1 Phosphorylation**

Recently, PDE4 has been identified as a key modulator of integrin-induced actin assembly at the cell periphery, which, in turn, controls cell migration and this effect is PKA dependent (Fleming et al. 2004).

The activity of the PDE4 isoenzymes can be regulated by phosphorylation at certain key sites and the mode of this regulation has been shown to be rapid and transient. The best example comes from the studies on the PDE4D3 isoform. PDE4D3 is a long PDE4 isoform, which contains a conserved single serine residue Ser54 at the N-terminal of UCR1 within the PKA consensus motif, RRESF. In mammals, such phosphorylation increases PDE4D3 activity (Sette and Conti 1996). This was confirmed by the observation that replacement of Ser54 with an aspartate residue, which mimicked the phosphorylation at this site, led to a 3~fold increase in enzymatic activity (Hoffmann et al. 1998). It has been suggested that this phosphorylation results in a conformational change in the catalytic domain, therefore increasing the PDE4D3 affinity towards rolipram. Recently, the function of another PDE4D3 serine (Ser13) phosphorylation was revealed. This phosphorylation modification promoted the binding of PDE4D3 to mAkap (Carlisle Michel et al. 2004), which can provide part of the cellular desensitization mechanism of cAMP signalling.

In addition to being phosphorylated by PKA in its N-terminal and UCR1 region, PDE4D3 is able to undergo phosphorylation by ERK2 at its COOH-terminal end of the catalytic domain (Figure 1.5) (Hoffmann et al. 1999). Activation of ERK pathway by epidermal growth factor (EGF) in COS-1 or HEK293 cells resulted in a rapid (within 5 min) drop in the activity of recombinant PDE4D3, and this inhibition was indicated as the result of being phosphorylated by ERK2 at its Ser579. However, over 20 minutes this inhibitory effect on PDE4D3 was reversed due to the feedback action of PKA that activated PDE4D3 by phosphorylating its Ser54. Therefore, PDE4D3 provides a perfect point of crosstalk between the ERK pathway and cAMP pathway.

As the UCR1 single serine Ser54 in PDE4D3 is found in all long PDE4 isoforms, it confers the ability of these enzymes to be phosphorylated by PKA (Houslay and Adams 2003). Indeed, long PDE4 isoforms from all four sub-families (PDE4A8, PDE4B1, PDE4C and PDE4D3/5) have been shown to be phosphorylated at a single serine residue in UCR1 by PKA in COS1 cells (MacKenzie et al. 2002) and this serves to increase their activity, modulate Rolipram affinity,  $Mg^{2+}$  sensitivity and the re-programming of the functional output of ERK phosphorylation (Houslay and Adams 2003).

Interestingly, the ERK2 phosphorylation site (Pro-Xaa-Ser-Pro) at the third subdomain of the catalytic unit is present in all PDE4D, PDE4B and PDE4C isoforms, to confer these isoforms the ability to be phosphorylated by ERK2. The exception to this is PDE4A that contains a slightly different sequence (RXSP), and fails to provide a substrate for ERK2 (Hoffmann et al. 1999). Indeed, PDE4A5 can in fact be phosphorylated after growth hormone treatment through a process that lies downstream of both PI-3 kinase and p70S6 kinase (MacKenzie et al. 1998). Interestingly, ERK2 phosphorylation has profoundly different functioning outcomes for the three different categories of PDE4 isoenzymes. For example, phosphorylation of long PDE4 isoforms that contain both UCR1 and UCR2 by ERK2 leads to the catalytic inhibition, and such inhibition causes a localized increase in cAMP levels. In contrast, short PDE4 isoforms such as PDE4D1 that lacks UCR1 but contains an intact UCR2 are stimulated by ERK2 phosphorylation. Furthermore, super short PDE4 isoforms, represented by PDE4D2 that lack all the UCR1 and the first 32 amino

acids of UCR2, are inhibited by ERK2 phosphorylation, but to a lesser extent than that seen with PDE4 long isoforms (MacKenzie et al. 2000; Houslay and Adams 2003). All these suggest an intrinsic inhibitory role of UCR2 in regulating PDE4 activity (Figure 1.5).

### 1.3.1.5.2 Ubiquitination

Ubiquitin (Ub) is a 76-amino acid protein which is highly conserved in all eukaryotes and present in most organisms studied (Hatakeyama and Nakayama 2003). It is a very stable protein and recalcitrant to high temperature and acid or alkaline exposure. Ubiquitin is synthesised as a precursor protein, the C-terminal of which needs to be processed by specific proteases to expose a double glycine end. The covalent attachment of Ub molecule to a substrate protein is called ubiquitination. Ubiquitination is a chemically complex process that forms an isopeptide bond between the COOH-terminal glycine of Ub and  $\epsilon$ -amino group of a lysine residue in the substrate (Di Fiore et al. 2003). Ub, as its name suggests, is ubiquitously expressed and regulates a number of fundamental cellular processes, including metabolic homeostasis, protein quality control, transcription, translation, signal transduction, response to hypoxia, cell cycle progression, DNA repair, protein trafficking, chromatin remodelling, viral budding and immune responses (Van Demark and Hill 2002; Passmore and Barford 2004).

Protein ubiquitination involves a sequential action of three enzyme families, E1 activating enzyme, E2 conjugating enzyme, and E3 ubiquitin ligase (Di Fiore et al. 2003; Hershko and Ciechanover 1998). This enzymatic reaction starts from the activation of ubiquitin by E1 in an ATP-dependent manner: the E1 adenylates the C-terminal glycine of Ub and then forms a thioester bond between the ubiquitin C-terminus and a catalytic E1 cysteine residue. The thioester-linked ubiquitin is then transferred from E1 to a similar cysteine residue in the active site of an E2, where it again forms a thioester bond. With the direct or indirect help of an E3, the transfer of ubiquitin is promoted from a thioester linkage within the E2 to an amide linkage within a substrate. Substrate specificity in the ubiquitination pathway is mostly contributed by E3s as E3s are able to recognize and bind to specific substrate sequences directly (Hershko and Ciechanover 1998; Pickart 2001; Cilckman and

Ciechanover 2002). A combination of E2 and E3 determines the synthesis of a specific topology of the ubiquitin chain (Passmore and Barford 2004).

Based on the primary structure and enzymatic mechanism, E3s are categorised into two groups: HECT (homology to E6-AP carboxyl terminus) domain E3s and RING (really interesting new gene) domain E3s. HECT E3 uses their HECT domain to bind Ub-conjugated E2, and accept this ubiquitin moiety from Ub-E2 complex to form a covalent E3-Ub thioester intermediate before Ub is transferred to the substrate (Scheffner et al. 1995). Many HECT E3s, but not E6-AP, share the feature of having the WW domain and an amino-terminal C2 domain that function as protein protein interaction motif (Wang et al. 1999; Kanelis et al. 2001). Distinct from HECT E3s, RING E3s do not function as a catalyst, but rather work as a molecular scaffold to bring ubiquitin-conjugated E2 and substrate in close proximity (Passmore and Barford 2004), without forming a Ub-E3 thioester intermediate (Joazeiro and Weissman 2000).

The large number of RING E3s are further divided into single subunit E3s where the RING domain and the substrate recognition elements are on the same polypeptide and multisubunit E3s where the RING finger domain is organized to form a complex with other subunits on a member of cullin family based scaffold (VanDemark and Hill 2002; Weissman 2001). The single subunit E3s include the oncoprotein Mdm2 (Fang et al. 2000; Shenoy et al. 2001; Lin et al. 2002), protooncoprotein c-Cbl (Waterman et al. 1999), the inhibitors of apoptosis (IAPs) (Yang et al. 2000) and Parkin (Tanaka et al. 2004). RING finger E3 complex is found in SCF E3s, APC/cyclosome and VCB-CUL2 E3s (Weissman 2001). In SCF E3s, the F box protein executes the substrate protein recognition by recognizing those substrates that have a phosphorylated serine or threonine on their sidechains.

More recently, U box domain E4 has been identified and suggested to mediate substrate polyubiquitin chain elongation (Namekata et al. 2002).

Strictly regulated like phosphorylation, ubiquitination is a reversible process, in which deubiquitinating enzymes (DUBs) serve to catalytically remove the ubiquitin or ubiquitin chains from the modified substrates (Wilkinson 2000). DUBs fall into

two groups: ubiquitin carboxyl-terminal hydrolases (UCHs) and ubiquitin-specific processing enzymes (UBPs), both of which are thiol proteases. UCHs preferentially work on small fusion proteins to remove the carboxyl-terminal from ubiquitin (a subset of ubiquitin that is translated as a fusion protein), while UBPs are generally responsible for removing ubiquitin from residual peptides or multiubiquitin chains (Papa and Hochstrasser 1993; Lam et al. 1997).

Numerous cellular proteins are post-translationally modified by ubiquitin, but the functions conferred by this vary. It is now clear that different types of ubiquitin conjugation decide the fate of the substrates. Mono-ubiquitination, where a single ubiquitin is added to a substrate (Schlessinger 2000), is often implicated in non-proteolytic functions, such as endocytic trafficking, virus budding, vacuolar sorting, DNA repair, histone activity and transcriptional regulation (Hicke 2001). In contrast, poly-ubiquitin chains formed by Lysine 48 of two adjacent ubiquitin targets modified substrates for proteasomal degradation (Weissman 2001). In addition, other modes of lysine conjugation (eg. Lysine 63) used by poly-ubiquitin chains have been shown to function differently (Koegl et al. 1999; Spence et al. 1995; Spence et al. 2000).

To date, six conserved ubiquitin binding modules exist (Schnell and Hicke 2003), the structures of five of which have been determined. These include the UIM (ubiquitin interacting motif) (Hofmann and Falquet 2001), UBA (ubiquitin-associated domain) (Mueller et al. 2004), UEV (ubiquitin E2 variant domain) (Pornillos et al. 2002), NZF (npl4 zinc finger domain) (Meyer et al. 2002), and CUE (coupling of ubiquitin conjugation to ER degradation domain) (Ponting 2000). These motifs have been shown to be able to bind ubiquitin *in vitro*, and adopt interactions with Ub via the same hydrophobic patch on the surface of the five stranded  $\beta$ -sheet of Ub (Mueller et al. 2004). The centre of the binding site on Ub is mapped to Ile44.

### **1.3.1.5.3 Sumoylation**

Small ubiquitin-related modifier (SUMO) is a protein of 97 amino acids. Due to multiple independent discoveries, it has been called by other names, like Smt3p, Pmt2p, PIC-1, GMP-1, Ubl1 and sentrin (Melchior 2000). SUMO was first found in mammalian cells where it was found to be covalently conjugated to the GTPase

activating protein RanGAP1 (Matuni et al. 1996), and since then, more than 60 target proteins have been sequentially identified to be able to conjugate to SUMO under different conditions (Seeler and Dejean 2003). Although only one gene encodes SUMO in yeast species and invertebrate, eight and four genes in plants and mammals, respectively, have been identified to date. The four genes encoded in mammalian cells are termed SUMO-1, SUMO-2, SUMO-3 and SUMO-4. SUMO-4 is most recently identified and shown to express in a tissue-specific manner (Bohren et al. 2004). SUMO-2 and SUMO-3 are very similar in sequence (95% sequence identity for the human proteins), whereas SUMO-1 only shares 47% identical to SUMO2/3 (Melchior 2000; Muller et al. 2004). In addition to the sequence homology, SUMO-1 and SUMO-2/3 are also differ in their substrate specificities (Johnson 2004), as well as the ability to form SUMO chains *in vitro* (Seeler and Dejean 2003; Bohren et al. 2004; Tatham et al. 2001), indicating their different functions (Gill 2004).

As its name indicates, SUMO is related to Ub to some extent (Figure 1.8). It shares a similar protein fold that is characterized by  $\beta\beta\alpha\beta\beta\alpha\beta$ , a similar three-dimensional structure (Bayer et al. 1998), and a similar conjugation pathway (Hilgarth et al. 2004). The route of SUMO conjugation to target proteins, termed sumoylation, involves four discrete steps: maturation, activation, conjugation and ligation (Hilgarth et al. 2004). Like Ub, all SUMO isoforms are initially synthesized as inactive precursors, which need to be C-terminal proteolytic cleaved by SUMO-specific carboxyl-terminal hydrolase to produce a C-terminal diglycine motif. This motif is required for the formation of an isopeptide bond between the carboxyl terminus of SUMO with an  $\epsilon$ -amino group of a lysine residue within a target protein. After maturation, the conjugation to proteins involves the ATP-dependent dimeric SUMO activating E1 enzyme (SAE1/SAE2 in humans) and the E2 conjugating enzyme Ubc9. Sumoylation is also highly dynamic and reversible (Dohmen 2004). SUMO-specific proteases are involved in both SUMO maturation and SUMO detachment from its substrate proteins (Melchior et al. 2003).

Many differences exist between ubiquitin and SUMO functionality (Dohmen 2004). This is apparent in the enzymes they use to become conjugated to/deconjugated from, target proteins and the fates of the proteins that they modify

(Dohmen 2004; Johnson 2004; Li and Hochstrasser 1999). Instead of targeting the substrates for degradation, SUMO conjugation exerts effects relating to changes in transcription (Nakagawa and Yokosawa 2002; Yang and Sharrocks 2004), subcellular localization (Lin et al. 2003; Muller et al. 2001), antagonism of ubiquitination (Desterro et al. 1998), cell cycle, maintenance of genome integrity and viral replication (Hay 2005). Compared to Ub, SUMO has a short flexible N-terminal extension that is absent in Ub. This extension, which varies among different SUMO proteins, is rich in charged amino acids like glycine and proline, providing excellent candidates for specific protein-protein interactions (Wilson and Rangasamy 2001). In contrast to the numbers of Ub E1 and E2 enzymes, single SUMO-E1 and SUMO-E2 exist in most organisms and are required for the conjugation of all SUMO isoforms. Most strikingly, SUMO E2 Ubc9 can directly interact with substrate proteins via their sumoylation consensus sequence  $\psi$ KXE ( $\psi$  is a large hydrophobic residue and preferably L, I, or V; E is an acidic amino acid, such as D or E; K is the site of SUMO conjugation) in most cases (Sampson et al. 2001) and imparts partiality on substrate selection.

Although not required for sumoylation *in vitro* (Bernier-Villamor et al. 2002), SUMO E3 ligases are important in regulating substrate selection *in vivo*, especially for the substrates that lack SUMO attachment consensus sequence. To date, three unrelated SUMO E3 ligases have been identified: the PIAS proteins, RanBP2, and the polycomb group protein Pc2. PIAS family is composed of four members, PIAS1, PIAS3, PIASx and PIASy (Hay 2005). Although there is still in controversy in the identification of substrate specificities between different PIAS proteins, it is known that p53, jun (Schmidt and Muller 2002), Lef-1 (Sachdev et al. 2001), nuclear androgen receptor (Kotaja et al. 2002), Mdm2, Sp3, and Tcf-4 (Dohmen 2004) undergo sumoylation via this family of E3 proteins. In addition, RanBP2 has been shown to exert SUMO E3 ligase activity for the promyelocytic leukaemia (PML) nuclear body (NB) protein, sp100 (Pichler et al. 2002), the histone deacetylase HDAC4 (Kirsh et al. 2002), and Mdm2 (Miyauchi et al. 2002), while Pc2 is the SUMO E3 ligase for transcriptional corepressors CtBP1 and CtBP2 (Kagey et al. 2003). The different substrate specificities of these SUMO E3 ligases are consistent with their distinct subcellular localization (Johnson 2004; Hay 2005).

### **1.3.1.6 cAMP gated long-term PDE4 expression**

In addition to the short-term regulation of PDE4 due to post-translational modifications, PDE4 expression is also regulated at the transcriptional level. Both PDE4B and PDE4D genes contain promoters that include several potential cAMP regulatory elements. In vitro and in vivo data have shown that increased intracellular cAMP largely induces mRNA levels for both PDE4B and PDE4D, as well as their corresponding short isoform proteins (Swinnen et al. 1989; Swinnen et al. 1991; Le Jeune et al. 2002). The function of this feedback regulation of PDE4D from sustained cAMP signalling has been linked to the growth and maturation of the follicle in the ovary because ablation of PDE4D gene causes a 75% decrease in the rate of ovulation and consequent reduced fertility (Jin et al. 1999). In addition, the Toll-receptor-related signalling pathway activated by LPS in macrophages or monocyte cells can cause a large increase in PDE4B2 mRNA and its protein (Jin and Conti 2002). This has helped identify a function for PDE4B2 as in PDE4B gene knockout mice, the induction of PDE4B2 by LPS is a positive feedback regulation required to remove a negative cAMP constraint (Jin and Conti 2002).

### **1.3.2 PDE4A**

The human PDE4A gene is mapped to chromosome 19p-31.1 in man (Sullivan et al. 1998). To date, five isoforms of human PDE4A gene have been cloned. This includes a short form, PDE4A1 (Sullivan et al. 1998), the long form PDE4A4B (Bolger et al. 1993), PDE4A5 (McPhee et al. 1995), and PDE4A10 (Rena et al. 2001) and a catalytically inactive N- and C-terminally truncated PDE4A7 (Johnston et al. 2004). Specific PDE4A isoforms have been suggested to have distinct roles in the brain, thus providing valid targets for therapeutic interventions (McPhee et al. 2001).

The changes in the expression of PDE4A isoforms seem to correlate with the status of the cells. PDE4A4B long isoform is found upregulated in macrophages from smokers with chronic obstructive pulmonary disease (Barber et al. 2004), and PDE4A10 seems to be up-regulated upon differentiation of monocytes to macrophages (Shepherd et al. 2004).

To date, PDE4A7 is the only PDE4 isoform that is generated from both 5' and 3' domain swaps, providing both a unique N-terminal and C-terminal region (Sullivan et al. 1998), and it is this unique C-terminal region that leads to the lack of crucial phenylalanine, thus lack of the catalytic activity in PDE4A7 (Johnston et al. 2004).

### 1.3.3 PDE4B

PDE4B is a key enzyme in mediating TNF- $\alpha$  production. It has been shown that PDE4B is involved in LPS-induced TNF- $\alpha$  production in macrophage (Jin et al. 2005), as well as in Abeta peptide-induced TNF- $\alpha$  production in Alzheimer's disease (AD) patients (Sebastiani et al. 2005). As this regulation of TNF- $\alpha$  production was specific for PDE4B, consistent with the study in PDE4B null mice (Jin and Conti 2002), it suggests the non-overlapping functions between PDE4 isoforms. In addition, a combination of pharmacological and genetic strategies provides evidence that PDE4B and PDE4D genes are non-redundant and complementary in neutrophil recruitment to the lung, even though PDE4B has greater impact than PDE4D (Ariga et al. 2004). This further indicates that PDE4B and PDE4D control two different pools of cAMP in neutrophils.

In addition to pro-inflammatory outcomes, PDE4B is also involved in other biological process. PDE4B3 has been reported to change its translational and transcriptional regulation during hippocampal long-term potentiation (LTP), suggesting a possible molecular model where it plays an important role in learning and memory formation (Ahmed et al. 2004). Targeting of PDE4B2 to the immunological synapse through its N-terminus interaction with lipid rafts has been shown to regulate TCR-mediated interleukin-2 production. Thus, dynamic redistribution of PDE4B2 seems to regulate the T-cell activation during immunological synapse formation (Arp 2003).

Recently, Millar et al. reported a primary evidence for PDE4B as a genetic susceptibility factor for Schizophrenia. They found that the disrupted in schizophrenia 1 (DISC1) interacts with the UCR2 domain of PDE4B in a compartmentalized manner, and that only when the cellular cAMP is elevated will sequestered PDE4B

dissociate from DISC1 and retain its activity. Any functional variation in DISC1 and/or PDE4 is therefore speculated to have a concomitant physiological and psychiatric outcome (Millar et al. 2005).

It is well accepted that inhibitors with increased selectivity toward one PDE4 isoform may have advantages over non-selective PDE4 inhibitors due to the decreased side effect. Recently Robichaud et al. (Robichaud et al. 2002) indicated that the main contribution to the emetic side effects may involve PDE4D, but not PDE4B. Therefore, a compound that preferentially inactivates PDE4B is much favourable, because PDE4B inactivation should retain some of the beneficial properties of PDE4D inactivation, such as blockade of neutrophil adhesion and chemotaxis and can be used in a higher dose (Robichaud et al. 2002).

The expression level of PDE4B is regulated under different conditions with different mechanisms. Nitric oxide has been shown to increase PDE4B expression in rat pulmonary artery smooth muscle cells via a mechanism that requires cGMP synthesis (Busch et al. 2005). In diffuse large B-cell lymphoma (DLBCL), PDE4B is up-regulated through phosphatidylinositol 3-kinase (PI3K)/AKT pathway mediated apoptosis that is induced by cAMP, highlighting the useful development of PDE4 and PI3K/AKT inhibitor in treating the B-lymphoid malignancies (Smith et al. 2005).

### **1.3.4 PDE4C**

PDE4C is one of the four mammalian genes that encode multiple PDE4 isoforms which are inhibited by rolipram. Unlike other PDE4 species, PDE4C is restrictly expressed in certain tissues, indicating their distinct function roles (Sullivan et al. 1999).

The human PDE4C gene was reported to localize on chromosome 19p, where PDE4A gene is also present. However, the relative location and any possible linkage between PDE4A and PDE4C are still poorly understood (Sullivan et al. 1999).

To date, four cDNAs of PDE4C have been isolated, which represent three different PDE4C long isoforms, PDE4C1, PDE4C2, and PDE4C3 (Engels et al. 1995;

Oberholte et al. 1997; Owens et al. 1997). Compared to the short forms of PDE4A, PDE4B and PDE4D characterized at cDNA and protein levels, no PDE4C short forms have been reported so far. The absence of PDE4C short forms can be explained by the analysis of the sequence where introns separating PDE4C exon 5, 6 and 7 equivalents are unlikely contain either additional exons or alternative promoters (Sullivan et al. 1999), which is reminiscent of the *Drosophila dunce* gene that does not produce short isoforms (Qiu 1991).

### 1.3.5 PDE4D

PDE4D is the predominant PDE4 form in tracheal extracts and airway epithelia and plays a crucial role in balancing relaxant and contractant cues in airway smooth muscle (Mehats et al. 2003; Barnes et al. 2005). It has been suggested that a PDE4D subtype inhibitor has important therapeutic implications for resolution of asthmatic bronchoconstriction (Giembycz 2000). Indeed, it has been shown that mice deficient in PDE4D exhibited absence of muscarinic cholinergic airway responses (the tone of which has been associated with clinical asthma) and this is thought to be due to the impaired muscarinic cholinergic receptors M2 and M3 signalling pathway (Hansen et al. 2000). In the same mice deficient in PDE4D, delayed growth as well as reduced viability and female fertility were also observed (Jin et al. 1999), suggesting that the activity of this isoenzyme is also required for the regulation of growth and fertility.

PDE4D is known to play an important role in regulating vascular smooth muscle and endothelial cells that are involved in atherosclerosis (Gretarsdottir et al. 2003). Recently, a number of independent groups have reported the association between PDE4D variants and ischemic stroke (Gretarsdottir et al. 2003; Meschia et al. 2005), which appear to converge on PDE4D as an ischemic stroke risk factor gene. However, no identified 'at-risk' single nucleotide polymorphisms or haplotypes has been reported to date. Indeed, it is not clear that any specific PDE4D variant will be found associated with stroke in replication studies. In addition, a recent new study records the possibility of the association of PDE4D gene with cardioembolic stroke and despite the failure of showing that PDE4D is a major risk factor for ischemic stroke, the authors could not exclude a connection (Bevan et al. 2005).

Although until now there have been no reports implicating any member of the PDE4 gene family in human osteoporosis, an association between a variation in PDE4D gene and bone mineral density has been indicated (Rencland et al. 2005). In addition, PDE4D has been suggested to be involved in impaired memory in a water maze task (Giorgi et al. 2004).

To date, nine PDE4D isoforms have identified, PDE4D1 through to PDE4D9, which are further categorized into short isoforms (PDE4D1), long isoforms (PDE4D3, 4, 5, 7, 8 and 9), and supershort isoforms (PDE4D2 and 6) (Richter et al. 2005; Wang et al. 2003). Compared to the high restricted tissue distribution of PDE4D4, PDE4D6 (in brain), PDE4D7 (in cortex, testis and kidney) and PDE4D8 (in lung, heart and liver), PDE4D1, PDE4D2, PDE4D3, PDE4D5 and PDE4D9 are all widely distributed and present to some extent in most tissues in rat (Richter et al. 2005). PDE4D1 and PDE4D2 have been shown to be up-regulated in activated vascular smooth muscle cells (VSMC) (Tilley and Maurice 2005). As the induction of these specific PDE4 isoforms seems to serve to desensitise the susceptibility of activated VSMC to the inhibitory action of cAMP, inhibitors of these two specific isoforms are desirable for the treatment of adjunctive pharmacotherapy after percutaneous coronary interventions (Tilley and Maurice 2005). PDE4D7 is a long isoform and it has been suggested its putative promoter is associated with Icelandic stroke (Gretarsdottir et al. 2003; Houslay 2005).

PDE4D enzymes are the major PDE4 isoforms found in a variety of cells, with the PDE4D3 and PDE4D5 long isoforms predominating (Conti et al. 2003; Houslay 2001). Conti and co-workers, together with Houslay's lab, have shown that PDE4D3 is phosphorylated at Ser54, PDE4D5 at Ser126, both sites located at the beginning of UCR1 and this activates these isoforms (Hoffmann et al. 1998; Sette et al. 1994; MacKenzie et al. 2002). PDE4D3 and PDE4D5 are also phosphorylated by ERK2, at Ser579 and S651, respectively, and this inhibits enzyme activity (Hoffmann et al. 1999; MacKenzie et al. 2000; Baillie et al. 2001). As the various PDE4D isoforms provide a panel of enzymes that can be differentially regulated to different extents by ERK2 phosphorylation, together with their distinct subcellular distribution properties, they offer the potential to tailor cAMP signalling in specific cell types, as well as in discrete intracellular domains. This may explain why cells might choose to

express particular PDE4 isoforms and adds the PDE4 enzymes to the growing list of machinery responsible for cAMP signalling compartmentalization (MacKenzie et al. 2000).

It has been reported recently that during  $\beta_2$ AR desensitisation, the cytoplasmic adaptor  $\beta$ -arrestin recruits the PDE4D isoforms to the plasma membrane (Perry et al. 2002) where they may regulate the receptor coupling to G proteins (Baillie et al. 2003). PDE4D5 has been shown to preferentially bind to two sites in  $\beta$ -arrestin2 through its unique N-terminal region, as well as the common PDE4 catalytic domain. And it has been suggested that it is this unique N-terminal region of PDE4D5 that allows it for the binding specificity over PDE4D3, which accounts for the observation that more PDE4D5 compared to PDE4D3 is recruited with  $\beta$ -arrestin to the membrane fraction upon  $\beta$ -agonist stimulation in HEKB2 cells. Whereas in HEKB2 cells the total protein level of PDE4D3 is greater than that of PDE4D5, challenge of these cells with isoprenaline leads to more PDE4D5 than PDE4D3 translocation to membrane fraction (Bolger et al. 2003).

Xiang et al. have identified the selective role of PDE4D in impacting  $\beta_2$ AR subtype-specific signalling in neonatal cardiomyocytes, therefore favouring the view that PDE4D controls a functionally and perhaps physically discrete pool of cAMP (Xiang et al. 2005). Indeed, this might be partially due to the fact that  $\beta_2$ AR has more binding affinity than  $\beta_1$ AR towards arrestin which recruits PDE4D to the plasma membrane (Shiina et al. 2000; Xiang et al. 2005).

Recently, Robichaud and colleagues have provided evidence that PDE4D mediates the known emetic effects of PDE4 inhibitors through a sympathetic pathway by mimicking the pharmacological actions of yohimbine, a  $\alpha_2$ -adrenocceptor antagonist (Robichaud et al. 2002). Although this is an unfortunate finding because the most clinically advanced PDE4 inhibitors are selective for PDE4D, the data may readily account for the poor tolerability of these compounds in clinical trials.

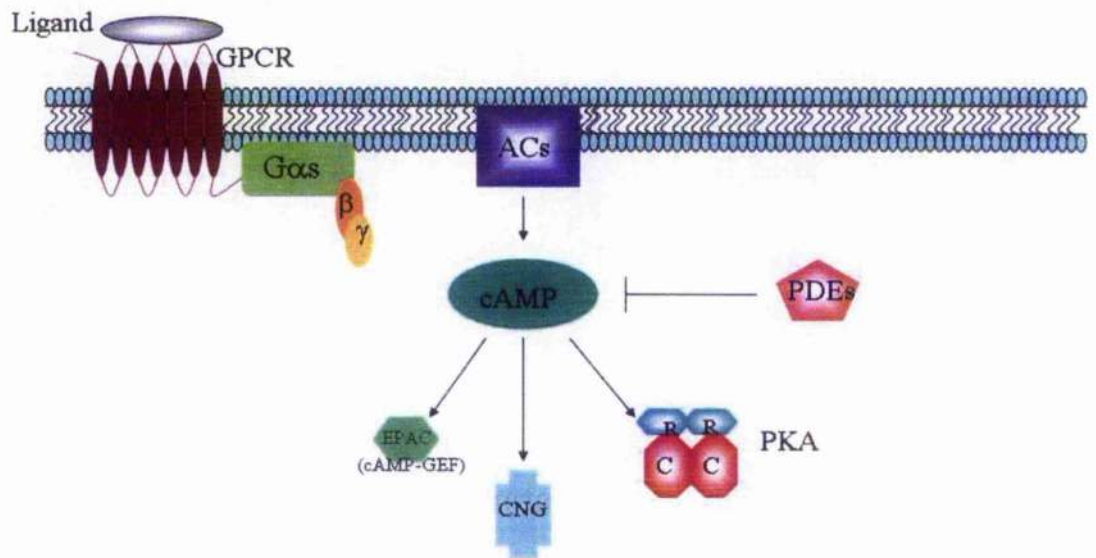


**Figure 1.1 General schematic of cAMP signalling pathway initiated by G-protein coupled receptors (GPCRs).**

An appropriate ligand binds to and activates GPCRs, which results in the dissociation of the G $\alpha$ s subunit. G $\alpha$ s subunit can stimulate adenylyl cyclases (ACs), therefore generating cyclic AMP (cAMP). The cAMP signalling can be mediated by PKA, EPAC or cyclic nucleotide gated ion channels. The sole means to inactivate cAMP is through cyclic nucleotide phosphodiesterases (PDEs) that hydrolyse cAMP into 5'-AMP. PKA, Protein Kinase A; Epac, exchange protein activated by cAMP; CNG, cyclic nucleotide-gated channels.

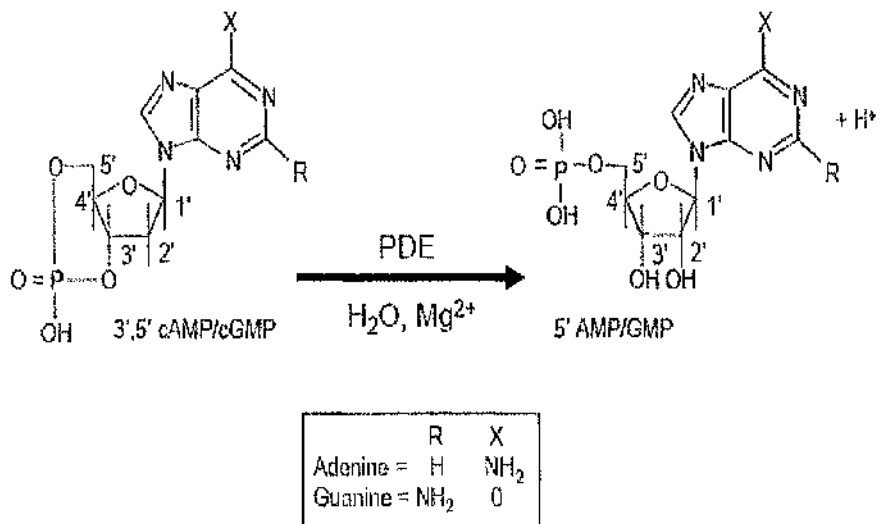


**Figure 1.2 Cyclic nucleotide hydrolysis by cyclic nucleotide phosphodiesterases.**

PDE family	Regulatory domains	Substrate specificity	Property	Specific inhibitors
<b>PDE1</b>	Ca <sup>2+</sup> /CaM binding	cAMP/cGMP	Ca <sup>2+</sup> /CaM-activated	Nimodipine
<b>PDE2</b>	cGMP binding GAF domain	cAMP/cGMP	cGMP-activated	EHNA
<b>PDE3</b>	Transmembrane domain	cAMP specific	cGMP-inhibited	Cilostamide, milrinone
<b>PDE4</b>	UCR1 and UCR2	cAMP specific	PKA/ERK-phosphorylated	Rolipram, Ro 20-1724, roflumilast
<b>PDE5</b>	cGMP binding GAF domain	cGMP specific	PKA/PKG-phosphorylated	Zaprinast, DMPP0, E4021, Sildenafil
<b>PDE6</b>	cGMP binding GAF domain	cGMP specific	Transducin-activated	Zaprinast, DMPP0, E4021, Sildenafil
<b>PDE7</b>		cAMP specific	Rolipram-insensitive	BRI. 50481, IC1242
<b>PDE8</b>	PAS domain	cAMP specific	Rolipram-insensitive IBMX-insensitive	Unknown
<b>PDE9</b>	Unknown	cGMP specific	IBMX-insensitive	Unknown
<b>PDE10</b>	cGMP binding GAF domain	cAMP/cGMP	Unknown	Unknown
<b>PDE11</b>	cGMP binding GAF domain	cAMP/cGMP	Unknown	Unknown

**Figure 1.3 Table of phosphodiesterases superfamily (adapted from Lugnier review, 2006).**

All human PDE gene families identified to date are listed.

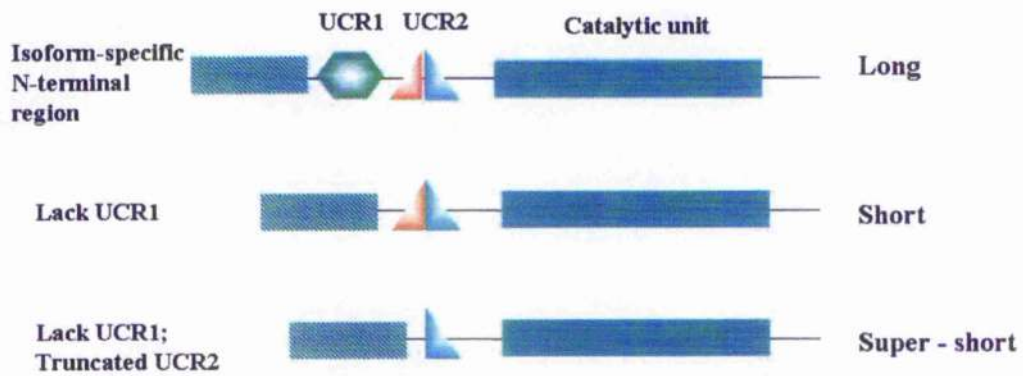


**Figure 1.4 Schematic of the PDE4 isoenzymes.**

Functional PDE4 isoforms are divided into three categories: long, short, and super-short isoforms dependent on the combined presence of upstream conserved regions (UCRs). Long isoforms possess both UCR1 and UCR2, short isoforms lack UCR1, whereas super-short isoforms lack UCR1 and only have a truncated UCR2.

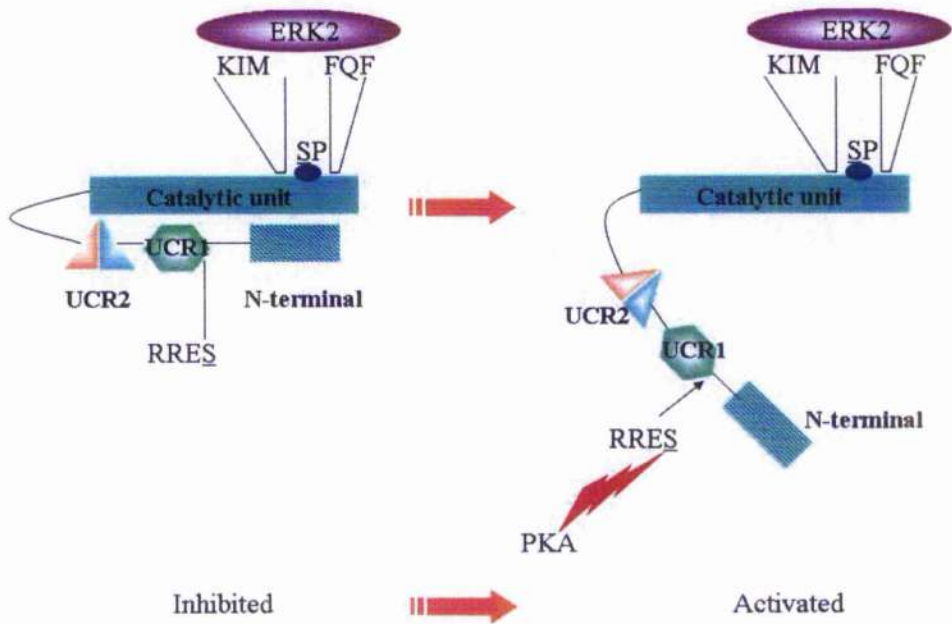


**Figure 1.5 The effects of PKA and ERK2-mediated phosphorylation on PDE4 long isoforms.**

PDE4 long isoforms processes both UCR1 and UCR2. ERK2-mediated phosphorylation of PDE4 long isoforms leads to their enzymatic inhibition, whereas PKA-mediated phosphorylation increases their enzymatic activity.

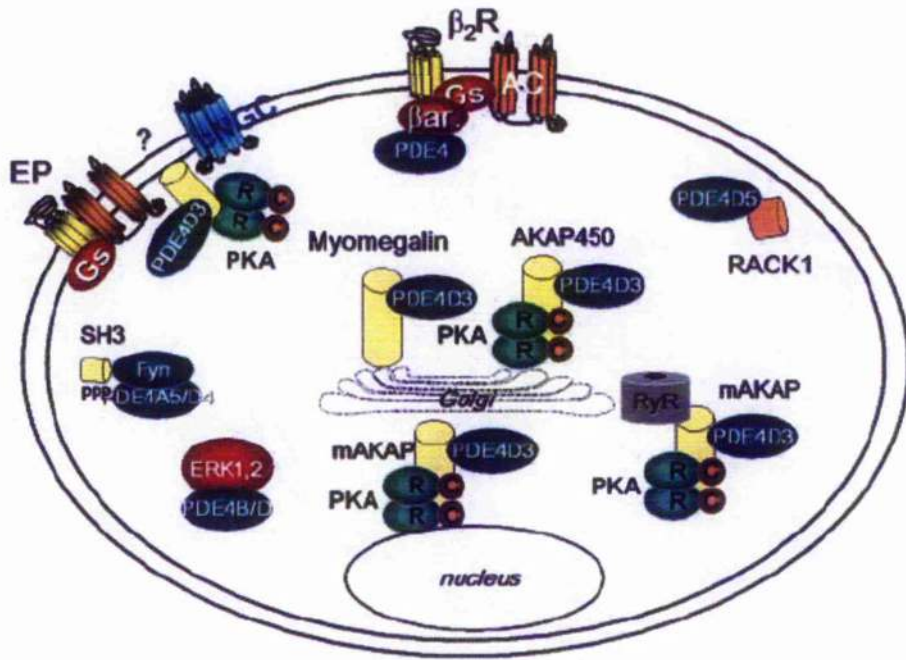


**Figure 1.6** Compartmentalization of PDE4s.

The known sequestration of PDE4 in signalling complexes and their subcellular localization are depicted in a hypothetical cell. The yellow barrels represent the scaffolding proteins. (Taken from Conti et al. 2003).

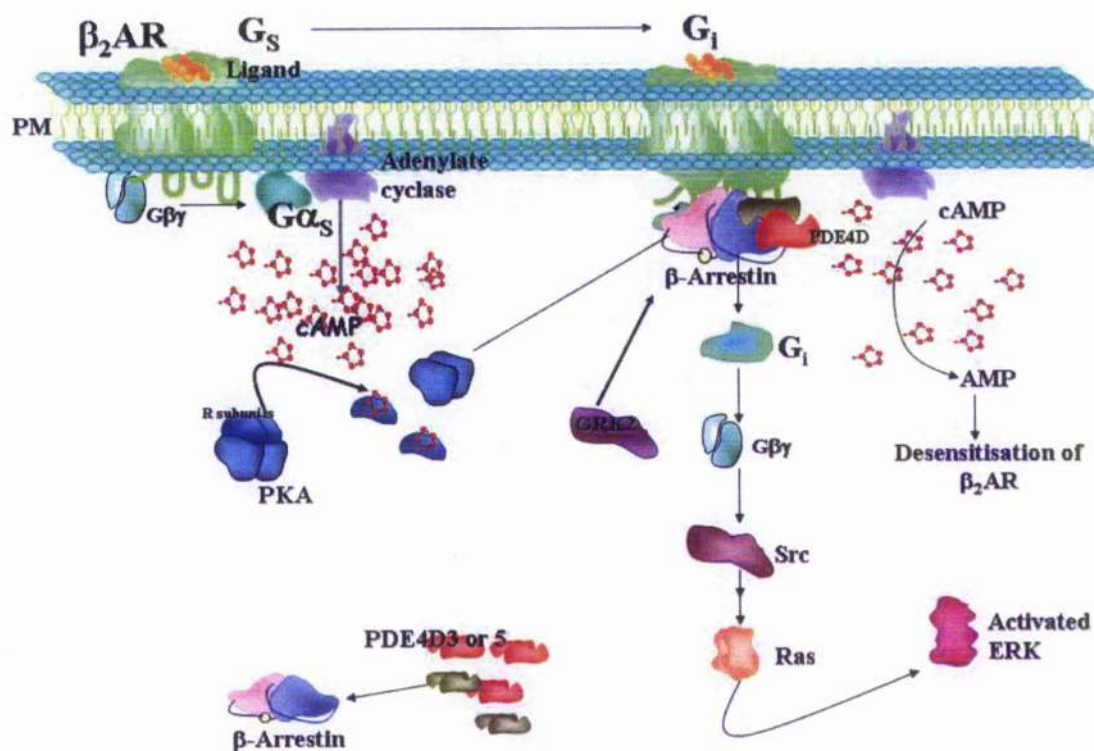


**Figure 1.7 Schematic of  $\beta_2$ -adrenergic receptor ( $\beta_2$ AR) desensitization.**

Agonist occupancy of the  $\beta_2$ AR initiates PKA and GRK mediated phosphorylation of the receptor. PKA phosphorylation of  $\beta_2$ AR leads to the switching of  $\beta_2$ AR signalling from  $G_s$  to  $G_i$ , and hence the activation of ERK. This switching is mediated by  $\beta$ -arrestin delivered PDE4D isoforms. GRK mediated phosphorylation of  $\beta_2$ AR results in the membrane recruitment of  $\beta$ -arrestin/PDE4 complexes.  $\beta$ -arrestin serves to sterically blocks coupling of the  $\beta_2$ AR to  $G_s$ , whereas delivered PDE4 isoforms actively degrade cAMP in the prime site of cAMP generation.

	Ubiquitin	SUMO
Size	9 kDa	11 kDa (~20 amino acids longer in an N-terminal extension)
Surface charge	Positive	Negative
Family members	One ubiquitin isoform	Four members: SUMO-1, SUMO-2, SUMO-3 and SUMO-4
Polymeric chains	Both <i>in vivo</i> and <i>in vitro</i> , with different topology	SUMO2, 3 and 4 are found to form chains <i>in vitro</i> so far
E1 enzymes	Single UBA1	SAE1(AOS1)-SAE2 (UBA2) heterodimer
E2 enzymes	Multiple, including UBC4 and UBC7, which have negative or neutral potentials	Single UBC9, the surface of which is mainly positively charged, functions in substrate recognition
E3 ligases	Classified into: HECT domain E3s and RING domain E3s.	Three types: RanBP2, the PIAS proteins, and the Pc2.
Substrate specificity	No consensus site	ψKXE consensus sequence
Cleaving enzymes	Cystein proteases	Distantly related to viral cystein proteases and shows no similarity to ub-cleaving enzymes

**Figure 1.8 Table of the differences between Ubiquitin and SUMO families.**

## **Chapter 2**

### **Materials and Methods**

Throughout the following methods the names of the companies used for the purchase of specific reagents or materials are given in parentheses. Where no company is mentioned, the reagent was purchased from Sigma-Aldrich. All reagents were of analytical grade.

#### *Plasmids used in this study:*

Plasmids encoding N-terminally 6his-tagged human SUMO1 (6His-SUMO-1), N-terminally 6his-tagged SUMO2 (6His-SUMO-2) and C-terminally SV5 tagged Ubc9 (Ubc9-SV5) in pcDNA3.1 vectors, those encoding N-terminally haemagglutinin tagged mouse PIASy (HA-PIASy) in pKW2T, and those encoding GST fusion protein of Ubc9 were kindly gifted by Dr. R. Hay (University of Dundee, UK). The plasmid encoding C-terminally VSV-tagged human PDE4D3 (PDE4D3-VSV) in pCInco was created by Dr. R. Hoffmann (Sandoz, Switzerland). Plasmids encoding C-terminally VSV-tagged human wild type PDE4D5 and C-terminally VSV-tagged R34A PDE4D5 mutant in pcDNA3.1, those encoding GST fusion protein of  $\beta$ -arrestin2 in pGEX-5X-3 were created and gifted by Dr. G. Bolger (University of Alabama, USA). The plasmid encoding N-terminally HA-tagged human ubiquitin (HA-Ub) in BSSK<sup>+</sup> was a gift from Dr. D. Bohnamm. The plasmid encoding a GST fusion protein of  $\beta$ -arrestin1 in pGEX4T was created by Dr. R.J. Lefkowitz (Duke University, USA). The plasmid encoding GST fusion protein of ERK2 (p42) was subcloned into pGEX-2T by Dr. W. Kolch (Beatson Institute, Glasgow). Plasmids encoding C-terminally VSV-tagged PDE4A5, PDE4B1, PDE4B3, PDE4B4 and PDE4C1 in pcDNA3 were generated previously by others working in the Houslay Laboratory. Plasmids encoding N-terminally HA-tagged UbK48R, UbK63R and UbK29, 48, 63R in pcDNA3 were generated by Dr. Martin Lynch in the Houslay Laboratory.

## **2.1 Mammalian Cell Culture**

### **2.1.1 Maintenance of cell lines**

#### **2.1.1.1 HEK293 cell line**

HEK293 cell line (ATCC CRL 1573) is a human embryonic cell with an epithelial cell morphology. Cells were maintained in Dulbecco's Modified Eagles Medium (DMEM) supplemented with 2mM Glutamine, 10% foetal bovine serum (FBS) and 1% penicillin/streptomycin (100 units/ml) in an atmosphere of 5% CO<sub>2</sub> and

37°C. When cells were passaged at 80-90% confluency, they were split 1:5. To passage the cells they were rinsed with pre-warmed sterile PBS and 1-2mls of pre-warmed 0.25% trypsin/0.03% EDTA solution were added. Flasks were incubated at 37°C until cells detached. Cells were collected by adding 10mls of culture media and centrifugation at 72.8 x g for 3 min. The cells were then resuspended in fresh culture media and transferred into new culture flasks at approximately 10<sup>5</sup> cells/ml final volume.

#### **2.1.1.2 COS-1 cell line**

The COS-1 cell line (ATCC CRL 1650) is an African green monkey derived cell line, with a fibroblast morphology transformed with the SV40 virus. This cell line was maintained and passaged as with the HEK293 cell line.

#### **2.1.1.3 HEKB2 cell line**

The HEKB2 cell line was derived from HEK293 cell line, with stably over-expressing FLAG and GFP- tagged  $\beta_2$  adrenergic receptors and is resistant to the G418 antibiotic. Cells were maintained in Dulbecco's Modified Eagles Medium (DMEM) supplemented with 2mM glutamine, 10% newborn calf serum (NCS), 1% penicillin/streptomycin (100units/ml) and 1mg/ml G418 antibiotic in an atmosphere of 5% CO<sub>2</sub> and 37°C. G418 here was used to select the cell generations with GFP tagged  $\beta_2$  adrenergic receptors expressed. Cells were passaged at 90-100% confluency with a split ratio of 1:4. To passage the cells, they were rinsed with pre-warmed sterile PBS and then 2ml of pre-warmed 0.25% trypsin/0.03% EDTA solution was added to the 75mm flasks. Flasks were incubated at 37°C until cells detached. Cells were then collected by addition of 8ml of culture media and subsequent centrifugation at 72.8 x g for 3 minutes. The cells were resuspended in fresh medium and transferred into new culture flasks at approximately 10<sup>5</sup> cells/ml final volume.

### **2.1.2 Transfection**

#### **2.1.2.1 PolyFect transfection of HEK293 cells (and HEKB2 cells)**

Transfection of HEK293 cells was carried out using PolyFect reagent (Qiagen). 1.2 x 10<sup>6</sup> cells per 100 mm dish were seeded in 7 ml of DMEM supplemented with 2mM glutamine, 10% newborn calf serum (NCS) and 1%

penicillin/streptomycin (100 units/ml) in an atmosphere of 5% CO<sub>2</sub> and 37°C. Once the cells reached 40-80% confluency the transfection was carried out. For each transfection, 8µg of DNA was dissolved in TE buffer (10mM Tris-HCl pH7.5, 1mM ethylenediaminetetra-acidic acid (EDTA)) with DMEM containing no serum protein or antibiotics to a total volume of 300µl. The solution was mixed well for a few seconds to remove drops from the top of the tube containing this DNA. 80µl of Polyfect Transfection Reagent was then added to the DNA solution, which was followed by mixing by pipetting up and down 5 times. The DNA complex was formed when it was incubated for 10min at room temperature (20-25°C). While complex formation took place, the growth medium from the 100mm dish was gently aspirated and replaced with 7 ml of fresh cell growth medium (containing serum and antibiotics). After being mixed by pipetting up and down twice, the formed DNA transfection complexes were transferred from the reaction tube to the cells in the 100mm dish. Then the dish was gently swirled to ensure uniform distribution of the complexes before put into the incubator at 37°C and 5% CO<sub>2</sub> to allow for gene expression. The cells were harvested 48-72 hr after transfection.

#### **2.1.2.2 DEAE-Dextran transfection of COS1 cell line**

The cells were split the day prior to transfection and allowed to grow to 50-70% confluency. 10µg of the plasmid DNA was diluted in TE buffer (1mM ethylenediaminetetra-acidic acid (EDTA), 10mM TrisCl, pH 7.5) to a total volume of 250µl in a sterile 15ml centrifuge tube. To this tube, 200µl of sterile DEAE Dextran (10mg/ml in PBS) was added, mixed and incubated at room temperature for 15 minutes. Meanwhile, the culture media in the 100mm dish seeded with COS1 cells was replaced with medium and 100µM chloroquine (filter sterilized) was added. Once the DNA complexes formed, the DNA-DEAE dextran mixture was dropped onto the cells and mixed by swirling. The cells were then incubated at an atmosphere of 5% CO<sub>2</sub> and 37°C for 3-4 hours. Following this incubation, the media were removed and replaced with 5ml sterile PBS supplemented with 10% DMSO. Cells were incubated in this 10% DMSO for 2 minutes and washed with 5ml fresh sterile PBS twice. Then 7ml of fresh culture media was added to the cells that were then incubated for 48hours at 37°C in an atmosphere of 5% CO<sub>2</sub>. The cells were then harvested. Mock

transfections were performed by treating the cells exactly as described above except adding the DNA into the mixture.

## **2.2 Biochemical techniques**

### **2.2.1 Protein analysis**

#### **2.2.1.1 Whole Cell lysate**

Cell culture dishes were maintained on ice and all buffers used were ice-cold to minimize protein degradation and denaturing of enzymes. The cell growth media was aspirated and the cells washed with PBS. The PBS was drained and approx 100 $\mu$ l/100 mm dish 3T3 lysis buffer (20mM N-2-hydroxyethylpiperazine-N'-2-ethanesulfonic acid (HEPES), pH7.4, 50 mM NaCl, 50mM NaF, 10% glycerol, 1% Triton X-100, 10mM ethyleneglycol-bis(P-aminoethylether)-N,N,N',N'-tetra-acetic acid (EGTA), 30mM sodium pyrophosphate and Roche proteases inhibitor cocktail) was added. The cells were scraped, transferred to a 1.5 ml eppendorf tube and snap-frozen. The cell samples were then thawed at 4°C and subjected to mechanical disruption using a micropestle (Eppendorf). The cell debris was removed by centrifugation at 18,000 x g for 3 min. The cell lysates were stored at -20°C until required for use.

#### **2.2.1.2. Protein quantification (Bradford assay)**

All protein assays were carried on 96 well titre plates, with triplet samples loaded as indicated below. Different amount of 100 $\mu$ g/ $\mu$ l BSA was diluted in distilled water to a total volume of 50 $\mu$ l, which was used for making the standard concentration curve. 10 $\mu$ l of each cell extract was diluted in 490 $\mu$ l distilled water, mixed well, and 50 $\mu$ l of the mixture was loaded into the Elisa 96-well plate in triplicate. Once all the standards and samples were loaded, 200 $\mu$ l of 20% Bio-Rad protein assay reagent (5ml in 20ml distilled water) was added to each well. The 96-well plate was then analysed using the Revelation Program and an MRX microtitre plate reader (absorbance read at 590 nm). Protein concentrations were obtained by plotting the standard curve and using least regression analysis to obtain the line of best fit. The equation of the line of calculated best fit was used to determine the protein concentration of samples in  $\mu$ g/ $\mu$ l.

	1	2	3	4	5	6	7	8	9	10	11	12
A 0µl BSA	0µl BSA	0µl BSA	50µl sample1	50µl sample1	50µl sample1	Sample 9	Sample 9	Sample 9	Sample 17	Sample 17	Sample 17	
B 5µl BSA	5µl BSA	5µl BSA	50µl sample2	50µl sample2	50µl sample1	Sample 10	Sample 10	Sample 10	Sample 18	Sample 18	Sample 18	
C 10µl BSA	10µl BSA	10µl BSA	50µl sample3	50µl sample3	50µl sample3	Sample 11	Sample 11	Sample 11	Sample 19	Sample 19	Sample 19	
D 15µl BSA	15µl BSA	15µl BSA	50µl sample4	50µl sample4	50µl sample4	Sample 12	Sample 12	Sample 12	Sample 20	Sample 20	Sample 20	
E 20µl BSA	20µl BSA	20µl BSA	50µl sample5	50µl sample5	50µl sample5	Sample 13	Sample 13	Sample 13	Sample 21	Sample 21	Sample 21	
F 30µl BSA	30µl BSA	30µl BSA	50µl sample6	50µl sample6	50µl sample6	Sample 14	Sample 14	Sample 14	Sample 22	Sample 22	Sample 22	
G 40µl BSA	40µl BSA	40µl BSA	50µl sample7	50µl sample7	50µl sample7	Sample 15	Sample 15	Sample 15	Sample 23	Sample 23	Sample 23	
H 50µl BSA	50µl BSA	50µl BSA	50µl sample8	50µl sample8	50µl sample8	Sample 16	Sample 16	Sample 16	Sample 24	Sample 24	Sample 24	

## 2.2.2 Gel electrophoresis and Western blotting

### 2.2.2.1 Sample preparation

#### 2.2.2.1.1 Cell lysis samples

Cell lysates were obtained by using lysis buffer or needle/syringe passaging, followed by centrifugation at 18,000 x g for 3 min. The supernatants were assayed for protein concentration as described above. Then equal amounts of protein were taken and diluted 1/5 with 5x Laemmli sample buffer (260mM TrisCl, pH 6.7, 55.5% glycerol, 8.8% SDS, 0.007% bromophenol blue, 11.1% 2-mercaptoethanol), which was boiled for 3-5 minutes to cause proteins to denature.

#### 2.2.2.1.2 Membrane Recruitment samples

Once the cells were treated as indicated in experimental text, medium was taken off and the plates to which the cells adhered were put on ice. The cells were washed with ice cold KHEM (50mM Hepes KOH, pH7.4, 50mM KCl, 10mM EGTA, 1.92mM MgCl<sub>2</sub>) twice and the excess wash fluid was removed by tapping. To a 100mm dish, 300µl of complete KHEM (50mM Hepes KOH, pH7.4, 50mM KCl, 10mM EGTA, 1.92mM MgCl<sub>2</sub>, 1mM DTT, Roche protease inhibitor) was added. Cells were scraped with complete KHEM into new Eppendorf microcentrifuge tubes and kept on ice. Then cells were broken by passaging 10 times using 26G gauge needles. The resulting lysate was centrifuged at 366 x g for 3 minutes to isolate the P1

fraction (enriched in nuclear and cytoskeletal components). The supernatants were then removed to ultracentrifuge tubes and further centrifuged at 245,000 x g for 30 minutes to make the P2 fraction (enriched in plasma membrane, vesicles formed from the Golgi apparatus and the endoplasmic reticulum, lysosomes and endosomes). The supernatants were kept as S fraction (enriched in cytosolic proteins), and the pellets were carefully washed in 750µl complete KHEM, followed by further centrifugation at 245,000 x g for 30 minutes. The pellets were resuspended in 200µl complete KHEM as P2 fractions. Protein concentrations were then determined by above description, and equal amount of proteins were loaded with sample buffer to the Nu-PAGE gel.

#### **2.2.2.2 Nu-Page™ gel system**

Pre-cast 4-12%, 10-well, 12-well or 15-well Bis-Tris 1.0mm gels (Invitrogen) were used for all the western blotting. The gels were assembled in *Xcell SureLock™* tanks (Invitrogen) according to the manufacturer's instruction. Depending on the molecular weight of protein interest, either NuPage™ MOPS SDS running buffer or NuPage™ MES SDS running buffer (Invitrogen) was used to fill the tank. 2µl of Bio-Rad prestained broad range precision protein marker was loaded in the front lane as a standard to determine protein migration weight, and an appropriate volume of pre-boiled samples, according to the capacity of the gel type, was loaded into each following well. The gels were run at 160V constant (operated by POWER-PAC 300 (Bio-Rad) for around 1 hour.

#### **2.2.2.3 Protein Transfer**

The SDS gel was disassembled from the gel cassette and placed onto a piece of Whatmann 3MM paper pre-soaked in 1x NuPage Transfer Buffer (Invitrogen). A piece of nitrocellulose paper (Schleicher& Schuell), pre-soaked with the 1x NuPage Transfer Buffer, was overlaid on the SDS gel, while ensuring the absence of bubbles between the layers. The nitrocellulose was, in turn, covered by another pre-soaked Whatmann 3MM paper to result in a sandwich that was later placed in *Xcell II™* Blot Module between two pieces of foam soaked in 1x Transfer Buffer. The module was placed with the nitrocellulose to the positive electrode in the *Xcell SureLock™* tank,

filled with 1x NuPage Transfer Buffer. The proteins were transferred with an applied voltage of 25V for 1 hour or 10V overnight.

#### **2.2.2.4 Immunoblotting**

Once transferred onto the nitrocellulose, Ponceau S stain (0.1% Ponceau S, 3% Trichloroacetic Acid) was used to visualise the proteins. The Ponceau S was added to the nitrocellulose for a few minutes until the proteins became stained, then the nitrocellulose membrane was washed with distilled water. 5% skimmed milk powder was dissolved in TBS-tween20 (137mM NaCl, 20mM TrisCl, pH 7.6, 0.1% Tween20), and the unoccupied protein binding sites on the nitrocellulose membrane were blocked in 5% skimmed milk powder for 1 hour at room temperature with agitation. After 1 hour blocking, the appropriate primary antibody was added to the membrane with a dilution 1:1000 (for polyclonal antibody) or 1:5000 (for monoclonal antibody) in 1% skimmed milk powder in TBS-Tween20. This incubation was carried out for 2 hours with vigorous shaking. Then the nitrocellulose membrane was washed three times in TBS-Tween20, each time for 10 minutes. A secondary antibody was diluted 1:5000 in TBS-Tween20, added to the membrane and incubated with the membrane for 1 hour with vigorous shaking. The secondary antibody was an anti-immunoglobulin (IgG) antibody conjugated to horse-radish peroxidase (HRP) and directed against the primary antibody. After 1-hour secondary antibody incubation, the nitrocellulose membrane was washed in TBS-tween20 three times, each time 10 minutes. Then the membrane was incubated with ECL reagents (Amersham) for 1 minute, according to the manufacturers instruction, followed by subjection to a piece of x-ray film (Kodak) in a dark room, which was then developed using a Kodak X-moat machine.

#### **2.2.3 Immunoprecipitation**

Depending on which source is the antibody generated, either Protein G Sepharose (Amersham Biosciences) or Protein A Agarose (Invitrogen) was used to immunoprecipitate the target protein. Among all the animal sources, Protein A Agarose can only be used when the antibody against the target protein is generated from mouse, human, rabbit, guinea pig; while Protein G sepharose can be used for any type of animal-generated antibody. For optimal precipitation, protein G sepharose was

preferred to immunoprecipitate a monoclonal antibody or a polyclonal antibody raised in a sheep, while Protein A Agarose was chosen to immunoprecipitate any other polyclonal antibodies.

#### **2.2.3.1 Sepharose pre-wash**

50 $\mu$ l of the appropriate beads were washed in 700 $\mu$ l of a decent buffer that was used for harvesting the cells, and recovered by centrifugation at 18,000 x g for 1 minute at 4°C (Heraeus refrigerated bench-top centrifuge). This was carried out three times. After the final wash, the supernatant was thrown away, and the same volume of the decent buffer as the spun beads was added to resuspend the beads.

#### **2.2.3.2 Pre-clearing**

For 400 $\mu$ l of cell extracts (approx 400  $\mu$ g), 25  $\mu$ l of 50% (v/v) pre-washed beads was added and this mixture was incubated with end-over-end rotation at 4°C for 30 minutes. The sample was then centrifuged at 18,000 x g for 1 minute at 4°C to recover the beads.

#### **2.2.3.3 Pre-immune**

If a pre-immune antibody was available, it was incubated with the cell lysate with end-over-end rotation at 4°C for 30 minutes. 25 $\mu$ l of pre-washed beads were then added to the lysate and again incubated with end-over-end rotation at 4°C for 30 minutes. The beads were recovered by centrifugation.

#### **2.2.3.4 Binding of antibody and target protein complex to beads**

After pre-clearing/incubation with pre-immune antibody, the beads were collected by centrifugation at 18,000 x g at 4°C for 1 minute, and the supernatant was removed to a fresh 1.5ml-Eppendorf tube as the pre-cleared cell extract. To this fresh tube, 1-5 $\mu$ l of the antibody (depending on the quality of the antibody provided, but usually ~ 2 $\mu$ g) against the target protein that was in the cleared cell extract was added, and this tube was rotated end-over-end at 4°C for 1 hour, to enable the binding of the protein to the antibody. Then, 25 $\mu$ l of pre-washed protein beads were added to the sample and rotated end-over-end for at least 2 hours at 4°C. The beads were isolated from solution by centrifugation at 18,000 x g at 4°C for 1 minute and washed with

750µl of cell harvesting buffer. The resuspended beads in the wash buffer were recovered by the same speed centrifugation, and the supernatant was thrown away. This wash was performed twice to minimise any non-specifically bound protein to the beads. The third time wash of the beads was carried out in 20mM TrisCl, pH 7.4, if the protein was to be used for a PDE assay. For later western blotting, the beads were diluted 1/5 with 5x Laemmli Sample Buffer. The sample was boiled for 3 minutes to release the target protein from the beads. For optimal release, the Eppendorf tube containing the sample was inverted several times during the boiling. The beads were then recovered again by a 18,000 x g speed centrifugation at room temperature, and an appropriate amount of supernatant was subjected to the Nu-Page™ gel for immunoblotting. The following procedures were performed as above described for western blotting.

## **2.2.4 Kinase Assays**

### **2.2.4.1 PKA assay**

#### **2.2.4.1.1 Cell lysate extraction for PKA assay**

Mammalian cells were grown and treated as required, after which time the cell media was removed, the cells were washed with PBS once, followed by another wash by extraction buffer (5mM EDTA, 50mM Tris, pH7.5). The extraction buffer was poured off, and the cells were drained by pipetting out the left-over extraction buffer in the plates where the cells were growing. This gives a high concentration of cells in which the PKA is also concentrated. The monolayer of cells were snap-frozen and thawed in the ice, which was followed by homogenisation achieved by drawing the cell suspension through a 26 gauge needle around 10 times. The cell debris was then removed by centrifugation for 2 mins at 18,000 x g at 4°C (Heraeus refrigerated bench-top centrifuge) and the supernatant was transferred into new 1.5ml Eppendorf tubes to be used for a PKA assay.

#### **2.2.4.1.2 PKA assay tube pre-incubation**

For each cell lysate, the following was set up on ice in 1.5ml Eppendorf tubes. The cell extracts were added last, and then mixed well by vortexing. The cells were incubated on ice for 20 mins to allow the inhibitor to bind PKA. N.B. due to the

time restrictions, during the assay, a maximum of 9 different lysates can be analysed at any one time:

Tube	Cell Extract	Diluent	4x PKA inhibitor	4x PKA Activator
A	10µl	20µl	0µl	0µl
B	10µl	10µl	10µl	0µl
C	10µl	10µl	0µl	10µl
D	10µl	0µl	10µl	10µl

4x PKA Inhibitor-4µM PKI(6-22) amide, 50mM Tris, pH 7.5.

4x PKA Activator-4µM cAMP, 50mM Tris, pH 7.5.

#### 2.2.4.1.3 PKA assay reaction

To 1 ml of the 4x PKA substrate (200µM Kemptide, 400µM ATP, 40mM MgCl<sub>2</sub>, 1mg/ml BSA, 50mM Tris, pH 7.5) 6000µCi/mmol of [ $\gamma$ -<sup>32</sup>P]ATP (Amersham Biosciences) was added whilst maintained on ice. To the first assay tube (1A), 10µl of radioactive 4x PKA substrate solution was added; the contents were mixed gently before being placed in a rack within a water bath at 30°C for 10mins. 15 seconds after substrate addition to the first tube, 10µl of the radioactive substrate was added to the next tube (1B), which was then mixed and incubated. This method of addition of substrate to tubes every 15 seconds continued until all the tubes with substrate were incubated at 30°C. After the 10min incubation of the first tube, 15µl of the reaction mix was removed from the water bath and spotted onto a pre-marked piece of ion exchange phosphocellulose paper P81 (Whatman). This was carried out for each tube after they had each undergone the 10 min incubation with the substrate. The phosphocellulose pieces were then placed into a larger beaker containing 1% (v/v) phosphoric acid (H<sub>3</sub>PO<sub>4</sub>) and washed for 3 min with slight agitation. The waste acid was removed and the acid wash repeated. The phosphocellulose was then washed twice in dH<sub>2</sub>O before being placed in 1.5ml Eppendorf tubes, to which 1ml scintillation fluid was added. The <sup>32</sup>P incorporated into the peptide bound to the phosphocellulose was counted on the Wallac 1409 liquid scintillation counter. To two

separate vials 10µl of the radioactive 4x PKA substrate was added to scintillation fluid, to enable the determination of the total counts from the substrate solution.

#### **2.2.4.2 Phosphodiesterase activity assay**

A cAMP hydrolysis assay was used to measure phosphodiesterase activity, which was modified based on the two step procedure of Thompson and Appleman (Thompson and Appleman 1971) and Rutten et al, as described previously by Marchmont and Houslay (Marchmont and Houslay, 1980). The principles of this two-step assay are illustrated in Figure 2.2. In the first step, the samples to be assayed were incubated with 1 µM 8-<sup>3</sup>H-labelled cAMP substrate. In the second step, the <sup>3</sup>H-labelled product of cAMP hydrolysis, 5'AMP, was dephosphorylated to adenosine by incubation with 0.2 mg/ml snake venom that has 5'-nucleotidase activity. The conditions were such that complete conversion took place within the snake venom incubation time. The negatively charged unhydrolysed cAMP was then separated from the uncharged adenosine by incubation with Dowex ion exchange resin. The amount of unbound <sup>3</sup>H-adenosine in the supernatant was determined by scintillation counting in order to calculate the rate of cAMP hydrolysis.

##### **2.2.4.2.1 Activation of Dowex**

To activate, 400g of the Dowex 1 X8-400 resin was suspended in 4 litre of NaOH and incubated at room temperature for 15 minutes with gentle mixing. The resin was allowed to settle by gravity, after which the 1M NaOH was removed. The resin was then extensively washed with 4 litre of distilled water (30 washes). After the last wash, the resin was resuspended in 4 litre of 1M HCl and incubated at room temperature for 15 minutes with gentle mixing before being allowed to settle by gravity. The 1M HCl was removed and the activated resin was resuspended 1:1 in distilled water and stored at 4°C until required.

##### **2.2.4.2.2 Assay preparation**

Samples of cell lysate (0.1-50 µg depending on activity) were placed into 1.5 ml Eppendorf tubes and made up to a volume of 25 µl with 20 mM Tris-HCl, pH 7.4. Each sample was assayed in triplicate. All tubes were set up on ice, and remained on ice until all components for the assay had been added. To every tube, 50 µl of 2 µM

cAMP containing 3  $\mu\text{Ci}$  [ $^3\text{H}$ ]-cAMP in 20 mM Tris/HCl/10mM  $\text{MgCl}_2$  pH 7.4 was added, the tubes were vortexed and incubated at 30 °C for 10 min. After this time, the tubes were boiled for 2 min to terminate the reaction and cooled on ice. 25  $\mu\text{g}$  snake venom (either *Ophiophagus Hannah* or *Crotalus atrox* venom) in 25  $\mu\text{l}$  20 mM Tris/HCl, pH 7.4 was added to each tube, mixed by vortexing and incubated at 30 °C for 10 min. The tubes were cooled on ice and 400  $\mu\text{l}$  Dowex/ethanol/distilled water, in a 1:1:1 ratio was added and mixed. The tubes were then further incubated on ice for at least 20 min. The tubes were vortexed and the Dewex separated from supernatant by centrifugation at 18,000 x g for 2 min (Heracus bench top centrifuge). Finally, 150  $\mu\text{l}$  of the clear supernatant was added to 1 ml Opti-scint scintillation fluid (Fisons Chemicals Ltd) and the [ $^3\text{H}$ ]-adenosine in these samples was counted for 1 min in a Wallac 1409 liquid scintillation counter. The cps for each sample were corrected for a background using a blank reaction (containing no PDE). The corrected counts were used to determine the initial rate of reaction (pmol cAMP hydrolysed/min). Determination of the protein content of the samples allowed the results to be expressed in units of pmol cAMP/min/mg protein.

#### **2.2.4.2.3 Determination of PDE4 activity**

The PDE4 family is specifically inhibited by the compound rolipram. Rolipram was dissolved in DMSO as 10 mM stock and this inhibitor was diluted in PDE assay dilution buffer (20 mM Tris/HCl/10 mM  $\text{MgCl}_2$  pH 7.4) for use in assay. DMSO itself does not affect PDE activity at the concentration used. Measurement of PDE4 activity with and without rolipram (10  $\mu\text{M}$ ) present gave the contribution of PDE4 in total PDEs.

### **2.2.5. Expression and Purification of GST Fusion Proteins**

#### **2.2.5.1 Induction and Purification of GST Fusion Proteins**

A sample of the plasmid DNA of interest from glycerol stock was put into a 50ml falcon tube that contained 30ml of L-Broth (170mM NaCl, 0.5% (w/v) Bacto Yeast Extract, 1% (w/v) Bacto-Tryptone pH 7.5) and 100 $\mu\text{g/ml}$  ampicillin and cultured at 37°C overnight. The next day the overnight culture was inoculated into 450ml of L-broth containing 100 $\mu\text{g/ml}$  ampicillin and left for growing to  $\text{OD}_{600}$  between 0.6 and 1.0 at 37°C. The protein that the interest plasmid DNA encodes were

then induced by the addition of IPTG to a final concentration of 0.2mM, shaken in the incubator for a further 2-5 hours at 25°C-30°C at 200 rpm. 1ml of the samples at 2.5hr intervals were taken to pellet at 18,000 x g and analysed by SDS-PAGE to monitor the induction. The cells after 5hr IPTG addition were pelleted at 2,400 x g at 4°C for 10min and frozen at -80°C overnight (In this step, the cells can be kept in -80°C for at least one month). The next day the frozen cells were thawed on ice, resuspended with 10ml of ice cold resuspension buffer (50mM TrisCl pH8.0, 10mM sodium chloride, 1mM EDTA, 10mM  $\beta$ -mercaptoethanol, 1x Roche protease inhibitor tablet) and transferred to 'oak ridge' centrifuge tubes. 1/10 volume of 10mg/ml Lysozyme was then added to the resuspended cells, and the mixture was incubated on ice for 15min. The cells were sonicated at power level 4 on ice (4x 30secs with 30sec rest). 1/500 volume of 10% Triton X-100 was added to each oak ridge tube, mixed and centrifuged at 12,000 x g at 4°C for 15 minutes. The supernatant was transferred to 10/15ml ccntrifuge tube and 1 ml of glutathione beads pre-equilibrated in wash buffer (50mM TrisCl pH8.0, 10mM sodium chloride, 1mM EDTA, 10mM  $\beta$ -mercaptoethanol, 1x protease inhibitor tablet, 0.05% NP-40). The mixture was incubated at 4°C, end over end, for 1 hour, followed by centrifugation at 366 x g at 4°C for 2 min. The supernatant was carefully removed and the beads were washed in 5 ml wash buffer. The beads were centrifuged at 366 x g at 4°C for 2 min, and the supernatant was removed. 1 ml wash buffer was then used to transfer the beads to a 2-ml Eppendorf, and the beads were given a further 3x wash in 1 ml wash buffer. It is very important to keep the sample on ice as much as possible. The GST tagged fusion proteins were eluted from Glutathione Sepharosc 4B (Amersham Biosciences) with 10mM glutathione in 50mM TrisCl pH 8.0. The beads were resuspended in 600 $\mu$ l of elution buffer (10mM glutathione, 50mM TrisCl, pH 8.0), incubated at 4°C end over end for 20 min, and centrifuged at 18,000 x g in micro-centrifuge tubes for 10 seconds. The supernatant was carefully removed to a fresh eppdorf tube. This elution step was kept repeating another 2-3 more times, and the elutes were pooled into a new 2-ml Eppendorf tube. Again, during this procedure, the samples were kept icecold. In order to get rid of the free glutathione in the elutes, the pooled elutes in Slide-A-Lyzer<sup>®</sup> Dialysis Cassette (0.5-3.0ml capacity) (PIERCE) were dialyscd in 650ml of chilled dialysis buffer (50mM TrisCl pH8.0, 100mM NaCl, 5% glycerol), with three

buffer changes. The dialysed fusion protein was collected and subject to protein concentration assay.

#### **2.2.5.2 SDS PAGE**

Samples of each stage from induction to purification were diluted 1/5 with 5x Laemmli sample buffer (260mM TrisCl, pH 6.7, 55.5% Glycerol, 8.8% SDS, 0.007% Bromophenol Blue, 11.1% 2-mercaptoethanol), and boiled for 3 minutes to denature. 30µl of each sample was loaded into each well of the 4-12% Bis-Tris NuPage gel. The gel was run at a constant voltage until the dye front reached the bottom of the gel.

#### **2.2.5.3 Staining of SDS Polyacrylamide Gels with Coomassie Brilliant Blue**

Following separation by gel electrophoresis, the gel was incubated in at least 5 volumes of Coomassie Blue (1.25mg/ml Blue R250, 44.4% methanol, 5.6% acetic acid, 50% distilled water) with gentle shaking at room temperature for at least 4 hours. The limit of detection for protein on Coomassie stained gel is 0.3-1.0µg.

#### **2.2.5.4 Visualisation of Proteins**

Protein bands were visualised by incubation of the stained gel with Destain Buffer (44.4% methanol, 5.6% acetic acid, 50% distilled water) overnight at room temperature with gentle shaking. After destaining, the gel was rehydrated by incubating in 1% glycerol for 30 minutes at room temperature with gentle shaking.

#### **2.2.5.5 Drying SDS Polyacrylamide Gels**

Gels were dried on a Bio-Rad gel drier. The gel was placed on a wetted piece of filter paper, on top of which covered a cling film. The filter paper was facing the drying surface of the drier, and the cover sheet of the drier was then laid over the cling film. A vacuum was applied so the cover sheet made a tight seal over the gel. The lid of the drier was then closed and the gel was dried at 63°C for 2 hours.

### **2.2.6 Peptide Array Analysis**

Peptide libraries were produced by automatic SPOT synthesis (Kramer and Schneider-Mergener 1998). Peptide libraries were synthesized on continuous cellulose membrane supports on Whatman 50 cellulose membranes according to standard

protocols by using Fmoc-chemistry with the AutoSpot-Robot ASS 222 (Intavis Bioanalytical Instruments AG, Koln, Germany).

Fresh peptide array membranes were immersed in pure ethanol for activation and then washed with 1x TBST (137mM NaCl, 20mM TrisCl, pH 7.6, 0.1% tween20) for 5 min, 3 times to get rid of the ethanol. The non-specific protein binding sites on the membrane were blocked with 5% skimmed milk powder in 1x TBST for 2 hrs at room temperature with agitation. The interaction of spotted peptides with either GST or the indicated GST fusion proteins was tested by overlaying the cellulose membrane with 10 µg/ml of recombinant protein overnight at 4 °C with vigorous shaking. The next day, the membrane was washed with 1x TBST for 5 min, 3 times, followed by incubation with rabbit antisera for the indicated protein species at room temperature for 2 hrs with vigorous shaking. Then the membrane was again washed with 1x TBST for 5 min, 3 times and subject to secondary anti-rabbit horseradish peroxidase coupled antibody incubation at room temperature for 1 hr with vigorous shaking, after which the membrane was washed three times in TBST. The membrane was then incubated with ECL reagents (Amersham Biosciences), according to the manufacturers' instructions. The membrane was exposed to X-ray film (Kodak) in a darkroom and then developed using a Kodak X-omat.

### 2.2.7 *In vitro* Ubiquitination Assay

A Ubiquitination Kit (Biomol) was used in this procedure.

#### 2.2.7.1 Ubiquitination Assay Pre-incubation

Assay components were added to a 15ml falcon tube in order shown below. All enzymes were kept on ice throughout the assay.

Components	Volume / µl
dH <sub>2</sub> O	700
10x Ubiquitination Buffer	250
IPP (100U/ml)	500
DTT (50mM)	50
Mg-ATP (0.1M)	125

20x E1 (2 $\mu$ m)	125
10x Ubc5Hb (0.5mg/ml)	250
20x GST-Mdm2 (2 $\mu$ M)	125
20x Bt-Ub (50 $\mu$ M)	125

### 2.2.7.2 In vitro Ubiquitination reaction

The contents in the falcon tube was mixed gently and then incubated with a PDE4D5 peptide array membrane at 37°C for 60 minutes. Reaction was stopped by washing the membrane with 1x TBST. Detection of the ubiquitin moieties on the peptide array was carried out as described above in Peptide Array Analysis, with the antibody that is specifically against the Ub.

## 2.3 Molecular Biology Techniques

All molecular biology techniques were carried out with sterilised equipment and buffers, to prevent contamination.

### 2.3.1 Large-scale production of plasmid DNA

Wizard Plus<sup>®</sup> Maxipreps (Promega) were used in this procedure.

#### 2.3.1.1 Production of a cleared lysate

A pinch of plasmid DNA from glycerol stock was sub-cultured in 5 ml L-broth (170mM NaCl, 0.5% (w/v) Bacto Yeast Extract, 1% (w/v) Bacto-Tryptone pH7.5) containing 100 $\mu$ g/ml ampicillin, shaken at 200 rpm 37°C for 4 hours. Then the subculture was inoculated into 500ml L-broth containing the same concentration of antibiotics for overnight culture. The next day, the cells were harvested by centrifuging at 3754 x g using the JA-14 rotor in the Beckman refrigerated centrifuge for 10 minutes at room temperature. The supernatant was thrown away and the pellet was finely resuspended in 15ml Cell Resuspension Solution. 15ml Cell Lysis Solution was added to the cells that were then mixed by gently and thoroughly inverting. Once the solution became clear and viscous, 15ml Neutralization Solution was added to the cells and the centrifuge bottle which contained the mixed solution was immediately and gently mixed by gently inverting several times. The undesired cell debris was isolated by centrifugation at 5,000 x g for 10 minutes in room temperature. 30ml of

cleared supernatant was transferred by filtering through a Muslin cloth into a clean 50ml centrifuge tube. 18ml of room temperature isopropanol was added into this tube, and mixed by inversion. The mixture was then subject to centrifugation at 14,000 x g for at least 2 hours in room temperature. The supernatant was discarded and the DNA pellet was resuspended in 2 ml of distilled water.

### **2.3.1.2 Plasmid DNA purification**

10ml of Wizard<sup>®</sup> Maxiprep DNA purification Resin that was incubated in a 37°C water bath beforehand was added to the resuspended DNA solution and swirled to mix. The resin/DNA mix was then transferred into the Maxicolumn that was connected with a vacuum manifold port. A vacuum of at least 15 inches of Hg was applied to pull the resin/DNA mix into the Maxicolumn. 25ml of Column Wash Solution was added to the Maxicolumn and a vacuum was applied to draw the solution through the Maxicolumn. To rinse the resin, 5ml of 80% ethanol was added to the Maxicolumn and a vacuum was applied to draw the ethanol through the Maxicolumn. To allow all the ethanol removed, additional 1 minute was taken to vacuum the column. The undesired fraction was centrifuged at 1,300 x g with a swinging bucket rotor (Thermo Life Sciences) for 5 minutes and discarded. The resin was then dried by applying to a vacuum for 5 minutes. The Maxicolumn was placed in a clean 50ml centrifuge tube and added 1.5ml of preheated (65-70°C) nuclease-free water. To elute the DNA, the Maxicolumn/50ml centrifuge tube were let stand for 1 minute, followed by centrifugation at 1,300 x g for 5 minutes in a centrifuge with a swinging bucket rotor. The eluted DNA was then subject to DNA concentration determination and kept frozen in at least -20 °C.

### **2.3.2 Small-scale production of plasmid DNA**

QIAprep Spin Miniprep Kit was used in this performance. A pinch of plasmid DNA from glycerol stock was cultured in 5 ml of L-broth medium containing desired antibiotics with shaking at 200 rpm 37°C overnight. The next day, the cells were pelleted by a microcentrifuge at full speed for 10 minutes (18,000 x g). The pelleted bacterial cells were then resuspended in 250µl Buffer P1 and transferred to a 1.5ml microcentrifuge tube. 250µl Buffer P2 was added into this tube, and the tube was gently inverted 4-6 times to mix. Then 350µl Buffer N3 was added, followed by

another immediate gentle inversion 4-6 times. A compact white pellet formed after the tube was centrifuged at 18,000 x g for 10 minutes in a tabletop microcentrifuge. The supernatant was applied to the QIAprep Spin Column that was then subject to centrifuge at full speed for 1 minute. The flow-through was discarded. In order to remove trace nuclease activity, 500µl Buffer PB was added to the QIAprep Spin Column and centrifuged at full speed for 1 minute. Again, the flow-through was discarded. Then the QIAprep Spin Column was washed by addition of 750µl Buffer PE and centrifuged at full speed for 1 minute. After the flow-through was discarded, additional 1 minute was taken for spinning down the residual wash buffer at full speed. The QIAprep column was then placed in a clean 1.5ml microcentrifuge tube. To elute DNA from the column, 50µl Buffer EB (10mM TrisCl, pH 8.5) was added to the center of each QIAprep Spin Column, let stand for 1 minute, and centrifuged for 1 minute at full speed (18,000 x g) to get the purified DNA that was collected in the microcentrifuge tube.

### **2.3.3 Quantification of purified DNA**

The DNA concentrations were measured using a WPA light wave spectrophotometer blanked with distilled water. 5µl of DNA was diluted in 1 ml f distilled water and the absorbance measurements were taken at 260nm and 280nm.

The concentration of the DNA was then calculated using the following approximations:

An absorbance of 1 at 260nm correspond to 50µg/ml double stranded DNA  
37µg/ml single stranded DNA

Easily, the concentrations of the plasmid DNA stored from the lab would be equal to 10 times the number of the absorbance at 260nm.

The ratio between the absorbance measurements at 260nm and 280nm provided an indication of the purity of the DNA. In solution, DNA should have an  $A_{260}:A_{280}$  ratio around 1.8. If the absorbance ratio is significantly less than 1.8, it indicates that the DNA may be impure.

### **2.3.4 Site-Directed Mutagenesis**

### 2.3.4.1 Primer designs

For optimal 5'-primer design, the desired nucleotide bases that encode the new amino acid were chosen as identical to those that encode the parent amino acid as possible. The length of the flanking nucleotide sequence was varied dependent on the estimated melting temperature. Generally, between 45 and 50 nucleotides in length containing the desired mutation and flanked by unmodified nucleotide sequence with the estimated melting temperature around 75 °C was considered good. G or C was always chosen for the first and the last nucleotide in the primer.

The following formula is commonly used for estimating the melting temperature  $T_m$  of the primers:

$$T_m (^{\circ}\text{C}) \approx 2 (N_A + N_T) + 4 (N_G + N_C)$$

Where N equals the number of primer adenine (A), thymidine (T), guanidine (G), or cytosine (C) bases.

The 5'- and 3'-primers designed for PDE4D5 UIM mutant (PDE4D5 723E) and that for PDE4D5 SUMO K mutant (PDE4D5K323R) were shown as follows:

	5'-primer	3'-primer
723E	CTTGATGAACAGGTT <u>G</u> CAGCG <u>G</u> CGGCAGTAGGGGAAGAA	TTCTTCCCCTACTGCCGCGCTGC AACCTGTTCAATCAAG
K323R	CCCAAGGTTTGGAGTT <u>C</u> GAACT GAACAAGAAGATGTCC	GGACATCTTCTTGTTCAAGT <u>C</u> GAAAC TCCAAACCTTGGG

The mutated nucleotides were underlined.

### 2.3.4.2 Mutant Strand Synthesis Reaction (Thermal Cycling)

Site directed mutagenesis was performed using the QuickChange Site-Directed Mutagenesis Kit from Stratagene. For each mutant, two complimentary oligonucleotides containing the desired mutation and flanked by unmodified nucleotide sequence were synthesized and purified by high-pressure liquid chromatography

(HPLC). The sample reactions were then prepared in Thermo-tubes (Abgene) as indicated below:

- 5  $\mu$ l of 10x reaction buffer (supplied with the kit);
- x  $\mu$ l (5-50 ng) of dsDNA template;
- x  $\mu$ l (125 ng) of oligonucleotide primer #1 (sense primer);
- x  $\mu$ l (125 ng) of oligonucleotide primer #2 (antisense primer);
- 1  $\mu$ l of dNTP mix (supplied with the kit);
- Sterile, deionised H<sub>2</sub>O to a final volume of 50 $\mu$ l;

NB: a series of sample reactions were set up with various concentrations of dsDNA template ranging from 5 to 50 ng (eg., 5, 10, 20, and 50 ng of dsDNA template) while the primer concentration was kept constant.

Then 1 $\mu$ l of PfuTurbo DNA polymerase (2.5U/ $\mu$ l) was added into each tube, followed by a good mix by gently vortexing. The reactions were cycled in a Techgene thermocycler PCR machine by using the cycling parameters outlined in Table II.

**TABLE II.**

Cycling Parameters for the QuickChange Site-Directed Mutagenesis Method

Segment	Cycles	Temperature	Time
1	1	95°C	30 seconds
2	12	95°C	30 seconds
		55°C	1 minute
		68°C	2 minutes/kb of plasmid length

Following temperature cycling, the reactions were placed on ice for 2 minutes to cool the reaction under 37°C.

#### 2.3.4.3 Dpn I Digestion of the Amplification Products

1 $\mu$ l of the Dpn I restriction enzyme (U/ $\mu$ l) (Stratagene) directly was added to each amplification reaction using a small pointed pipette tip. Each reaction mixture was gently and thoroughly mixed by pipetting the solution up and down several times.

The reaction mixtures were then centrifuged at 18,000 x g in a microcentrifuge for 1 minute and immediately incubated at 37°C for 1 hour to digest the parental supercoiled dsDNA.

#### **2.3.4.4 Transformation of XL1-Blue Supercompetent cells**

The XL1-Blue supercompetent cells (Stratagene) were gently thawed on ice. For sample reaction to be transformed, 50µl of the supercompetent cells were aliquoted to a pre-chilled Falcon® 2059 polypropylene tube. 1µl of the Dpn I-treated DNA was then carefully transferred from each sample reaction to separate aliquots of the supercompetant cells, and the transformation reactions were swirled gently to mix and incubated on ice for 30 minutes. Heat pulse was performed to the transformation reactions by incubating those reaction samples in the water bath with temperate 42°C for 45 seconds, and then the reactions were placed on ice for 2 minutes. 0.5ml of the preheated to 42°C NZY+ broth (10g casein hydrolysate, 5g yeast extract, 5g sodium chloride, in 1 litre, pH 7.5, autoclaved and supplemented with the filter-sterilized 12.5ml Magnesium chloride, 12.5ml magnesium sulphate and 10ml 2M glucose) was added and the transformation reactions were incubated at 37°C for 1 hour with shaking at 200 rpm. For each sample mutagenesis, 250µl of each transformation reaction was placed on an agar plates containing 100µg/ml ampicillin and incubated at 37° for around 16 hours. The single colony was picked for further DNA extraction by using QIAprep Spin Miniprep Kit. The mutated DNA was sent to sequence before it was used in the later experiment.

#### **2.3.4.5 Sequence Analysis**

Routine DNA and deduced amino acid sequence analysis were performed on the Gene Jockey II programme. The identity of the sequences within 500 kilo-base pairs length of either side of the mutated site to the DNA templates was thought to be good.

#### **2.3.4.6 Glycerol Stocks**

A single colony was picked from an agar plate and was inoculated with 5ml of L-broth supplemented with a selection antibiotic (usually 100µg/ml ampicillin). The culture was grown overnight at 37°C. After 16 hours, 1 ml of the overnight

culture was transferred into a sterile eppendorf tube where was 500 $\mu$ l of sterile glycerol (Riedel-deHaën) on the bottom. The glycerol stock was immediately frozen by dry ice and then stored at -80°C.

### **2.3.5 Agarose Gel Analysis of DNA**

DNA was visualised using agarose gel electrophoresis. 1% agarose was dissolved in 1x TBE (9M Tris base, 20mM EDTA, 0.9M Boric acid) by heating in the microwave, during which the bottle that contained the mixture was gently swirled to reduce the bubbles in the solution. To this solution, 0.01% ethidium bromide was added, which enables visualisation of the DNA under a UV light source. A comb and end stoppers were then set up in the gel apparatus, according to the manufacturer's instruction. Once the ethidium bromide was well mixed in the agarose solution, it was poured into the set up gel apparatus and allowed to set completely. The comb and end stoppers were then carefully removed, and the gel tank was filled with 1x TBE until the TBE buffer covered the solid gel. 5 $\mu$ l of standard 1Kb DNA ladder marker (Roche) was added to the first lane to enable the prediction of the size of DNA fragments, and all the diluted DNA samples 6:1 with 6x Blue/Orange loading dye (Promega) were added sequentially from the second lane onto the gel. The gel was run at 50v until the dye front migrated along the gel and the fragments of DNA were separated. Then the gel was carefully removed from the tank and subject to UV light.

## **2.4 Laser Scanning Confocal Microscopy (LSCM)**

### **2.4.1 Preparation of slides**

HEK-B2 cells were plated onto poly(L-lysine)-treated coverslips (18mm x 18mm) at approx. 40% confluence in 6 well tissue culture plates. After treatment with the indicated ligands, cells were fixed for 10 min in 4% (w/v) paraformaldehyde (dissolved in Tris buffered saline (TBS) (150 mM NaCl, 20 mM Tris, pH 7.6) and the coverslips were washed three times, for 5 min each time, in TBS. Cells were then permeabilized in 0.2% Triton-contained TBS for 15 min, and blocked in a blocking solution (10% goat serum, 4% BSA dissolved in TBS) at room temperature for 1hr. The primary antibody used specifically to detect phosphorylation of the  $\beta_2$ AR on Ser355/356 by GRK2 or on Ser345/346 by PKA was diluted to the required concentration in diluting buffer (blocking buffer dilute 1:1 with TBS) and 200  $\mu$ l of

the primary antibody solution was added to each slide. This incubation time was around 2 hrs at room temperature. The cells were washed three times with 5 min incubations in blocking solution and incubated with 200  $\mu$ l of 1:400 diluted Alexa Fluor 594 fluorophore-conjugated IgG (Molecular Probes) for 1 hr. Cells were then washed extensively with TBS (~5 times), and mounted on microscope slides with Immunomount (Sandon).

#### **2.4.2 Visualization of cells**

The cells were visualized using a Plan-Apo 40 x 1.4 NA oil immersion objective and the Zeiss Pascal laser-scanning confocal microscope (Zeiss, Oberkochen, Germany). The Alexa 594-conjugated antibody was excited at 543 nm and detected at 590 nm. The GFP tagged on the  $\beta_2$ AR was excited at 495 nm and detected at 518 nm.

Companies	Antibodies
Abcam	Anti-Proteasome 19S S5A; Anti-Proteasome 19S S1; Anti-Proteasome 19S S2; Anti-Proteasome 19S S6; Anti-Proteasome 19S S12
Affinity BioReagents	Anti-arrestin (Pan)
Amersham Biosciences	Anti-mouse IgG peroxidase conjugate
BD Pharmingen™	Anti-Mdm2
BD Transduction Laboratories™	Anti-RACK1; Anti-Ubc9
Cell Signalling Technology	Phospho-p44/42 MAP Kinase (Thr202/Tyr204); p44/42 MAP Kinase antibody; Phospho-(Ser/Thr) PKA substrate antibody
CALBIOCHEM	Anti-GFP
GENESIS	Anti-GST
ICOS	Anti-PDE4D
Santa Cruz Biotechnology	p-β <sub>2</sub> -AR (Ser345/Ser346) antibody; p-β <sub>2</sub> -AR (Ser355/Ser356) antibody; β <sub>2</sub> -AR (H-20) antibody; Anti-GRK1 (C-20); Anti-GRK2 (C-15); Anti-GRK3 (C-14); Anti-GRK4 (H-70); Anti-GRK5 (C-20); Anti-GRK6 (C-20) Anti-Ub (P4D1)
SAPU	Anti-PDE4B
UPSTATE	Anti-AKAP79; Anti-gravin
Zymed Laboratories Lnc.	Anti-GMP-1 (SUMO-1); anti-Sentrin 2 (SUMO-3)

Companies	Inhibitors
Calbiochem	UO126 (for MEK); H89 (for PKA); MG-132
	Rolipram
	Cilostomide

**Figure 2.1 Table of antibodies and inhibitors produced by companies other than SIGMA.**

## **Chapter 3**

### **The Role of PDE4 in $\beta_2$ -adrenergic Receptor Desensitization**

### 3.1 Introduction

Extracellular signals provided by molecules such as hormones and neurotransmitters are relayed into cells through a large family of membrane receptors known as GPCRs (G protein-coupled receptors) (Lefkowitz and Whalen 2004). These agonist-occupied GPCRs are activated, adopting new conformations to confer coupling to membrane-localized G proteins, and thus promoting the dissociation of membrane bound heterotrimeric G proteins into  $G\alpha$  and  $G\beta\gamma$  subunits. The activated G protein subunits then amplify and transduce signals within cells to modulate the activity of effector molecules, such as adenylyl cyclases, phospholipases and ion channels (Shenoy and Lefkowitz 2003). In order to prevent the potential harmful effects resulting from persistent receptor stimulation, an adaptive response used by cells to constrain G protein signaling, a process known as 'desensitization' is initiated, and the intensity of the functional response to hormone wanes over time. For most of GPCRs that have been studied, desensitization follows a universal mechanism that involves two families of proteins, the GRKs (G protein coupled receptor kinases) and the arrestins (Lefkowitz and Whalen 2004).

In the case of the prototypic  $\beta_2$ -adrenergic receptor ( $\beta_2$ AR), agonist stimulation leads to its binding to and activating the G protein,  $G_s$  (Pierce et al. 2002). While the freed  $G\alpha$  subunit activates membrane-localized adenylyl cyclases and generates compartmentalized cAMP near plasma membrane, the resultant  $G\beta\gamma$  subunits recruit GRK2 to the membrane, allowing it to phosphorylate the  $\beta_2$ AR at residues on its carboxyl terminus (Lodowski et al. 2003). This phosphorylation promotes the high affinity binding of cytosolic  $\beta$ -arrestins and triggers the recruitment of these arrestins to the membrane-bound, GRK2-phosphorylated  $\beta_2$ AR. Such binding of  $\beta$ -arrestin to the  $\beta_2$ AR prevents further coupling to its cognate  $G_s$  proteins, and mediates the clathrin-dependent internalization of  $\beta_2$ AR (Lefkowitz and Shenoy 2005). Additionally, phosphorylation of  $\beta_2$ AR appears to play another important mechanism for its desensitization, which involves a feedback loop in which the increased cAMP generated by the agonist stimulated  $\beta_2$ AR, activates PKA that switches the  $\beta_2$ AR coupling to the G protein,  $G_i$ , and ultimately attenuates production

of the cAMP (Daaka et al. 1997). This PKA mediated phosphorylation of  $\beta_2$ AR and subsequent switching also leads to the activation of ERK1/2 (extracellular signal-regulated kinases 1/2) pathway.

PDEs (phosphodiesterases) provide the sole means to degrade cAMP in cells (Houslay and Adams 2003). Currently, there is much interest in members of the cAMP-specific PDE4 family, because PDE4 selective inhibitors have potential therapeutic benefits for treating asthma and chronic obstructive pulmonary disease, and they can also act as cognitive enhancers and anti-depressants (Houslay et al. 2005; O'Donnell and Zhang 2004).

The PDE4 family is encoded by four genes, called PDE4A, PDE4B, PDE4C, and PDE4D (Houslay and Adams 2003). Each gene generates a number of isoforms due to the different transcriptional starting site as well as alternative mRNA splicing. These isoforms are expressed on a tissue and cell type-specific basis (Houslay and Adams 2003; Conti et al. 2003). A feature of PDE4 isoforms is their ability to target to distinct intracellular sites. This feature can be due to their forming signaling complexes with a variety of scaffolding or signaling proteins and thus integrating with other signaling pathways. So far, there are a number of proteins that are identified to interact with specific PDE4 isoforms, such as Src family tyrosine kinases (McPhee et al. 1999), RACK1 (receptor for activated C-kinase 1) (Yarwood et al. 1999), myomegalin (Verde et al. 2001) and AKAPs (McCahill et al. 2005; Tasken et al. 2001; Dodge et al. 2001). Recently, Perry et al. demonstrated that the  $\beta$ -arrestins bind PDE4D family, and in particular, PDE4D5 (Perry et al. 2002). These complexes exist in the cytosol and are recruited to the plasma membrane in an agonist-dependent manner by virtue of  $\beta$ -arrestin translocation. The functional importance of this  $\beta$ -arrestin-delivered PDE4D is to hydrolyse localised cAMP around the activated receptor at an enhanced rate, thus slow the rate of PKA activation and subsequent  $\beta_2$ AR Gi switching with consequential ERK activation. In doing so,  $\beta$ -arrestin plays a dual role in desensitizing  $\beta_2$ AR as it not only slows the rate of  $\beta_2$ AR/Gs-stimulated cAMP generation, but in a coordinated fashion increases the rate of cAMP degradation in proximity to receptor-adenylyl cyclase signalling unit.

Several recent studies have shown that receptor phosphorylation by GRK2 is modulated by other kinases, such PKA, PKC, Src and ERK1/2 (Figure 3.1) (Kohout and Lefkowitz 2003). The effects of a particular phosphorylation event are dependent on what sites are being phosphorylated. Phosphorylation effects include the changes in GRK2 catalytic activity, protein binding affinity and its turnover rate. Among these phosphorylating kinases, PKA has been shown to phosphorylate GRK2 at Ser685 and increase its binding affinity towards free G $\beta\gamma$ , rather than directly enhance its activity, thereby accelerate the recruitment of active GRK2 to the plasma membrane. This facet of GRK2 regulation provides a fundamental step in the  $\beta_2$ AR desensitization. In the case of PKA, its activity is mediated by the intracellular levels of cAMP that is shaped by PDEs in HEKB2 cells. Thus, PDE4 may be acting as a guardian that coordinates this event that is crucial to the initial stages of  $\beta_2$ AR desensitization.

The experiments outlined in this chapter, investigate whether PDE4 activity can regulate GRK2 phosphorylation by PKA, and whether PDE4 activity can influence the rate of  $\beta_2$ AR desensitization through its direct action on GRK2 distribution.

## **3.2 Results**

### **3.2.1 The isoprenaline-stimulated PKA phosphorylation of GRK2 is amplified by inhibition of PDE4**

#### **3.2.1.1 GRK2 is the major species among 7 GRKs in HEKB2 cells**

So far, 7 members of GRK family have been identified. As GRK1 and GRK7 are almost exclusively expressed in retina, so detection of the expression of the other five GRK species was attempted in HEKB2. Endogenous GRK2-GRK6 were analysed in resting HEKB2 cells by Western blotting using antisera specific against GRK2, GRK3, GRK4, GRK5 and GRK6, respectively. In contrast with that of GRK2, antisera against GRK3, GRK4, GRK5 and GRK6 failed to detect these species in HEKB2 cells (Figure 3.2), suggesting that GRK2 is the major species in these cells. Thus, in this chapter, I will only focus on the effect of PDE4 on GRK2.

#### **3.2.1.2 Isoprenaline stimulates PKA phosphorylation of GRK2 in HEKB2 cells**

Cong et al. have shown that GRK2 can be phosphorylated at Ser685 by PKA *in vitro*, so I set out to investigate whether this phosphorylation can occur in HEKB2 cells when the  $\beta$ -agonist isoprenaline was added.

HEKB2 cells were subjected to an isoprenaline time course (0-10min), and harvested in 3T3 lysis buffer. As no phospho-antibody to the PKA phosphorylation site on GRK2 was available, GRK2 was immunopurified and then blotted with an antibody that specifically detects PKA phosphorylated substrates. Once the lysates were obtained, GRK2 was immunoprecipitated from HEKB2 cells using a GRK2-specific antibody. The resultant immunoprecipitate was probed with anti-GRK2 (Figure 3.3 a, lower panel), and anti-PKA substrate antibody (Figure 3.3 a, upper panel), respectively. GRK2 migrated as a single immunoreactive species at 79 kDa. In the presence of isoprenaline, the anti-PKA substrate antibody revealed a time-dependent appearance of PKA-phosphorylated GRK2 (Figure 3.3 a,b). Similarly, when the anti-PKA substrate was used to immunoprecipitate PKA-phosphorylated proteins from HEKB2 cells, followed by probing the immunopurified samples with anti-GRK antibody, a single 79 kDa species was detected following 5 min of isoprenaline treatment (Figure 3.3 c,d). Both these experiments confirm that isoprenaline causes a time-dependent PKA phosphorylation of GRK2 in HEKB2 cells.

### **3.2.1.3 PDE4 inhibition enhances isoprenaline-induced PKA phosphorylation of GRK2 in HEKB2 cells**

PDEs provide the sole means of hydrolyzing cAMP in cells (Houslay and Adams, 2003). In HEKB2 cells, approximately 60% of the cAMP PDE activity is contributed by PDE4 (Perry et al. 2002; Lynch et al. 2005). The functional importance of PDE4 family can be assessed by chemical ablation of PDE4 activity using the PDE4-selective inhibitor rolipram (Houslay and Adams, 2003). In order to determine whether PDE4 is involved in the PKA phosphorylation of GRK2, the PDE4-selective inhibitor rolipram was used to chemically ablate PDE4 activity in HEKB2 cells. Cells were pre-incubated with 10 $\mu$ M rolipram for 10 min, and then challenged with isoprenaline for a 1-10 min time course. Then these treated cells were harvested in 3T3 lysis buffer at the indicated time, followed by centrifugation to pellet cell debris at 18,000 x g. Supernatants were then analysed. In all experiments the protein

concentration of the lysates for each time point was normalized. In similar experiments to those described above but this time using a rolipram pre-incubation, I observed that the presence of the PDE4-selective inhibitor rolipram accelerated the ability of isoprenaline to cause PKA phosphorylation of GRK2 (Figure 3.3 a, c).

In order to confirm that the enhanced PKA phosphorylation of GRK2 mediated by PDE4 inhibition was actually PKA-dependent, a specific PKA inhibitor H89 (1 $\mu$ M) was pre-incubated together with rolipram for 10 min before the isoprenaline challenge. Doing this, no PKA phosphorylation of GRK2 was detected (Figure 3.3 a, c).

#### **3.2.1.4 PDE4 inhibition alone is able to cause time-dependent PKA phosphorylation of GRK2**

In the studies above, HEKB2 cells were challenged with isoprenaline after a 10 min pre-incubation with rolipram. However, PKA phosphorylation of GRK2 was clearly evident in rolipram-pretreated cells before the addition of isoprenaline (zero time; Figure 3.3 a, c). Thus, I set out to examine if the addition of rolipram alone can elicit PKA phosphorylation of GRK2 and if this phosphorylation is time-dependent. HEKB2 cells were subjected to rolipram treatment alone (0~10 min time course) and GRK2 phosphorylation by PKA was observed as before. The results here showed that addition of rolipram alone can cause the time-dependent PKA phosphorylation of GRK2 (Figure 3.4 upper panel), and that PKA inhibitor H89 ablated this effect (Figure 3.4 lower panel).

Interestingly, despite the fact that 40% of total cAMP PDE activity in HEKB2 cells is contributed by PDE3 (Lynch et al. 2005), the PDE3-selective inhibitor, cilostamide, failed to trigger such a PKA phosphorylation of GRK2 (Figure 3.4 lower panel). This suggests that PDE3 exerts different compartmentalized actions from PDE4 in HEKB2 cells. Indeed, in many cell types, it has been shown that selective inhibition of PDE3 and PDE4 result in very different functional outcomes (Maurice et al. 2003; Huang et al. 2001).

### **3.2.2 The effect of PDE4 inhibition on PKA phosphorylation of GRK2 is not PDE4 subfamily-specific**

Recently, Lynch et al. developed siRNA reagents and transfection conditions that allow for the selective ablation (>95%) of expression and activity of PDE4B, (PDE4B2), which contributes 30% of the total PDE4 activity in HEKB2 cells, and PDE4D, (PDE4D3 and PDE4D5), which provide 60% of the total PDE4 activity in HEKB2 cells. Although the use of rolipram can assess the functional importance of PDE4 action, it cannot discriminate between the actions of PDE4 subfamilies. Thus, in order to evaluate the individual contribution of PDE4B and PDE4D to the PKA phosphorylation of GRK2, I used HEKB2 cells that were treated with siRNA against PDE4B, PDE4D, or both PDE4B and PDE4D.

Ablation of either PDE4B or PDE4D subfamilies resulted in an enhanced agonist triggered PKA phosphorylation of GRK2 (Figure 3.5 upper panel). Such results support the data obtained from chemical ablation of PDE4 activity (Figure 3.3 a, c). However, in contrast to the detection of increased PKA phosphorylation of GRK2 in resting HEKB2 cells (Figure 3.4 upper panel), siRNA-mediated knockdown of either PDE4B or PDE4D alone failed to achieve this effect (Figure 3.5 upper panel). Interestingly, knockdown of both PDE4B and PDE4D together did achieve such an increase (Figure 3.5 lower panel). Indeed, such a combined knockdown resembles that of rolipram, which inhibits both of these PDE4 families. Thus, it appears that the effect of PDE4 on PKA phosphorylation of GRK2 is not subfamily-specific.

### **3.2.3 PDE4 inhibition enhances isoprenaline-stimulated membrane translocation of GRK2**

PKA phosphorylation of GRK2 has been previously suggested (Cong et al. 2001) to increase the binding affinity of GRK2 towards free G $\beta$  $\gamma$  subunits near the plasma membrane. This event occurs after activation of the agonist-occupied receptor, promoting membrane recruitment of GRK2 and subsequent GRK2 phosphorylation of the receptor. As inhibition of PDE4 enhances isoprenaline-stimulated PKA phosphorylation of GRK2, I investigated the functional consequences of this and

examined whether enhanced PKA phosphorylation of GRK2 resulted in changes in GRK2 membrane translocation.

HEK293 cells were treated with 10  $\mu$ M isoprenaline in the absence/presence of 10  $\mu$ M rolipram, and harvested at indicated times. Membrane fractions were obtained as described in Materials and Methods, and analysed by Western blotting with a specific anti-GRK2 antibody. The amount of GRK2 which had translocated to the membrane under different treatments was quantified by densitometry. Here, I show that challenge of HEK293 cells with isoprenaline elicited a time-dependent membrane translocation of cytosolic GRK2 (Figure 3.6 a, left panel). However, if the cells were pre-treated with rolipram, this recruitment was not only accelerated, but also was clearly transient in nature (Figure 3.6 a, left panel).

This surprising change in the kinetics of GRK2 membrane recruitment led me to examine further the factors that might directly mediate this process. Considering the other kinases that can regulate GRK2 by direct phosphorylation, ERK was chosen to study as it has been shown (Penn 2000) that ERK phosphorylation of GRK2 decreases its binding affinity to G $\beta$  $\gamma$  subunit and thus potentially promotes its release from the plasma membrane back to the cytosol. By additionally treating cells with the MEK (mitogen-activated protein kinase/ERK kinase) inhibitor, UO126, I observed that such transient translocation of GRK2 to membrane, after rolipram pre-incubation, was abolished and GRK2 was maintained in the plasma membrane throughout the time course (Figure 3.6 a, right panel).

Again, it was evident that rolipram pre-treatment alone sufficed to stimulate GRK2 translocation (Figure 3.6 a, left panel; zero time). In order to investigate the kinetics of the rolipram induced translocation, a 0~10 min time course was carried out using 10  $\mu$ M rolipram (Figure 3.6 b, upper panel). As a control, 1  $\mu$ M H89 was added 10 min before rolipram challenge, and this ablated GRK2 recruitment to the membrane fraction (Figure 3.6 b, lower panel). Thus, treatment of HEK293 cells with rolipram alone can cause both the PKA phosphorylation of GRK2 (Figure 3.4) and its time-dependent membrane translocation (Figure 3.6 b).

In order to further assess the PKA phosphorylation status of GRK2 at the plasma membrane, I combined both membrane fractionation and subsequent immunoprecipitation (as described in Materials and Methods) after treating the HEKB2 cells (3 min isoprenaline challenge; 10 min Roli+H89 pre-treatment, followed by 3 min isoprenaline challenge; or 10 min rolipram pre-treatment plus 3 min isoprenaline challenge). Similar to the results obtained from experiments using cell lysates, the PKA phosphorylated form of GRK2 was shown to be membrane recruited following isoprenaline treatment, and accumulate more in the presence of rolipram. Recruitment was abolished by pre-treatment with H89 (Figure 3.7) reinforcing the absolute requirement of activated PKA for this process to occur.

#### **3.2.4 PDE4 inhibition accelerates phosphorylation of the $\beta_2$ AR by GRK2**

One of the functions of membrane-localized GRK2 is to phosphorylate  $\beta_2$ AR and mediate the subsequent desensitisation process. Since PDE4 inhibition has been shown to result in enhanced and more transient membrane translocation of GRK2, I set out here to study the GRK2 phosphorylated status of  $\beta_2$ AR.

HEKB2 cells were challenged with isoprenaline during a 0~10 min time course, and harvested in 3T3 lysis buffer. Clear lysates were obtained after 18,000 x g centrifugation and normalised to equal protein levels. These normalised lysates were then subjected to Western blotting and probed with a specific phospho-antiserum against the GRK2 phospho site on the  $\beta_2$ AR, Ser 355/356. It was clear that isoprenaline challenge of HEKB2 cells led to the time-dependent phosphorylation of  $\beta_2$ AR by GRK2 (Figure 3.8 a). This action was ablated upon siRNA-mediated knockdown of GRK2 (Figure 3.8 b), confirming the requirement of GRK2.

In order to assess the effect of PDE4 inhibition on GRK2-phosphorylation of the  $\beta_2$ AR, HEKB2 cells were pretreated with rolipram before isoprenaline challenge at indicated times. This treatment appeared to accelerate the ability of isoprenaline to trigger the phosphorylation of the  $\beta_2$ AR by GRK2 (Figure 3.8 a), indicating that PDE4 gates the action of GRK2 on  $\beta_2$ AR after agonist binding.

Indeed, challenge with rolipram alone can also cause the time-dependent GRK2 phosphorylation of the  $\beta_2$ AR (Figure 3.9 a). This corresponded well with the observed recruitment of GRK2 after rolipram treatment (Figure 3.6 b, upper panel). The ability of rolipram to promote the GRK2 phosphorylation of  $\beta_2$ AR was ablated upon GRK2 knockdown (Figure 3.9 b).

Results shown earlier in this chapter suggested that the combined effects of PDE4B and PDE4D contributed to the change in PKA phosphorylation of GRK2, which mimicked rolipram action. Using siRNA I investigated whether the combined action of PDE4B and PDE4D also resulted in increased phosphorylation of  $\beta_2$ AR by GRK2.

Control cells and cells pre-treated with specific siRNA to PDE4B and PDE4D were challenged with 10  $\mu$ M isoprenaline during a 0~5 min time course. The lysates were subjected to Western blotting by specific antibodies against PDE4B and PDE4D, respectively. And it was observed that 95% of PDE4B and PDE4D were knocked down. Following siRNA-mediated knockdown of both PDE4B and PDE4D, the lysates were probed with antiserum specific against the  $\beta_2$ AR phospho Ser355/356. As was the case with GRK2 recruitment to the membrane (Figure 3.6 a), GRK2-mediated phosphorylation of  $\beta_2$ AR increased when both PDE4B and PDE4D were genetically ablated (Figure 3.10).

Consistent with previous data from rolipram experiments, siRNA-mediated ablation of PDE4B and PDE4D also increased the GRK phosphorylation of the  $\beta_2$ AR in resting (unstimulated) cells (Figure 3.10, zero time).

### **3.2.5 PDE4 inhibition accelerates membrane recruitment of $\beta$ -arrestin and PDE4D**

Perry et al. have shown that isoprenaline stimulates the time-dependent, transient and concomitant membrane recruitment of both  $\beta$ -arrestin and PDE4D in HEKB2 cells (Perry et al. 2002). I confirmed this in the present study by probing the membrane fraction from each time point with antiserum against  $\beta$ -arrestin and PDE4D respectively. Additionally, I showed that in isoprenaline-challenged cells that

had been pre-treated with 10 $\mu$ M rolipram for 10 min, the transient membrane recruitment of  $\beta$ -arrestin and PDE4D, occurred more rapidly (Figure 3.11).

Indeed, I noticed that challenge of HEKB2 cells with rolipram alone sufficed to cause membrane recruitment of both  $\beta$ -arrestin and PDE4D3/D5 (Figure 3.12, left panel). Comparing these time courses to experiments when GRK2 translocation was examined under the same conditions, it was apparent that the concomitant membrane recruitment of  $\beta$ -arrestin and PDE4D3/D5 occurred later than the recruitment of GRK2 (Figure 3.6 b) and GRK phosphorylation of the  $\beta$ 2AR (Figure 3.9 a). These kinetics make sense as others have shown that the recruitment of arrestin is dependent on the phosphorylation of the receptor by GRK2 (Lefkowitz and Shenoy 2005). All such rolipram-induced translocations were ablated by H89 (Figure 3.12, right panel).

### **3.2.6 Analysis of PDE4 inhibition effect on ERK-phosphorylated GRK2**

HEKB2 cells were challenged with isoprenaline in the absence/presence of rolipram over a 0~10 min time course and harvested in KHEM buffer. Membrane fractions were obtained and subjected to Western blotting with the specific antiserum against phospho-GRK2 Ser670 (which is the site of ERK phosphorylation on GRK2). It was shown that challenge of HEKB2 cells with isoprenaline caused a time-dependent increase in the level of ERK-phosphorylated GRK2 at the membrane (Figure 3.13, upper panel), and that in the presence of rolipram, such an increase was not only accelerated, but was also shown to be profoundly transient in nature (Figure 3.13, lower panel). In fact, the transience of this effect bears similarities with the time-dependent membrane recruitment of GRK2 (Figure 3.6 a). However, in contrast with this observation (Figure 3.6 b), I did not detect any signal for ERK phosphorylated GRK2 from the 10 min rolipram alone-treated HEKB2 cells (Figure 3.13), as indicated by the zero time point in the isoprenaline challenge time course with 10 min rolipram pre-incubation.

The two distinct observations on the effect of sole PDE4 inhibition in regulating GRK2 membrane recruitment and ERK phosphorylation status of GRK2 can be further explained by the different actions of PKA and ERK.

In the absence of isoprenaline, rolipram alone is sufficient to stimulate PKA and subsequently, induces PKA phosphorylated GRK2 (Figure 3.4, upper panel), triggering GRK2 membrane translocation (Figure 3.6 b). However, inhibition of PDE4 by rolipram was not able to cause ERK activation (Figure 3.14, zero time point; negative time course of 0~10 min, 10  $\mu$ M rolipram), which is due to the lack of  $\beta_2$ AR switching from Gs to Gi. Indeed, challenge of HEKB2 cells with isoprenaline is known to be required to activate ERK (Figure 3.15) (Baillie et al. 2003; Lynch et al. 2005). Rolipram pre-treatment of isoprenaline-challenged cells markedly enhanced the magnitude and kinetics of this process (Figure 3.15). This may explain the more rapid ERK phosphorylation of membrane associated GRK2 that ensues in rolipram pre-treated cells challenged with isoprenaline (Figure 3.13).

### **3.2.7 Analysis of PDE4 inhibition on the trafficking and GRK phosphorylation status of the $\beta_2$ AR in HEKB2 cells**

To evaluate the contribution of PDE4 to the development of  $\beta_2$ AR phosphorylation by GRK and to visualize internalization by confocal immunohistochemistry, I examined the ability of the PDE4-selective inhibitor to affect these processes in an agonist dependent manner. GRK-phosphorylated  $\beta_2$ AR (Ser355/356) can be detected using a specific antibody which has been extensively characterized by others (Tran et al. 2004). Thus, I used this reagent to define the temporal and spatial dynamics of the GRK2-phosphorylated form of the  $\beta_2$ AR in HEKB2 cells (Figure 3.22). In these studies, the green fluorescent channel detects the GFP-tagged  $\beta_2$ AR, and the red channel detects the GRK2-phosphorylated  $\beta_2$ AR. Therefore, the merged images of the two channels will identify the GRK2-phosphorylated form of  $\beta_2$ AR as a yellow signal (Figure 3.22). Here, I observed that challenge of HEKB2 cells with isoprenaline leads to a steady increase in  $\beta_2$ AR phosphorylation by GRK over the time course (Figure 3.22, upper panel). Also evident is that internalisation of the  $\beta_2$ AR began after 8 min of isoprenaline stimulation and a major fraction of the  $\beta_2$ AR population is internalised some 16 min after isoprenaline challenge (Figure 3.22, upper panel). In the presence of rolipram, the increases in both  $\beta_2$ AR phosphorylation and internalisation are seen earlier throughout the time course. Additionally, basal GRK phosphorylation of the  $\beta_2$ AR

and internalisation in HEKB2 cells pre-treated with rolipram (without agonist) are evident, indicating that rolipram alone can affect the kinetics of GRK-phosphorylation of this receptor (Figure 3.22, lower panel), which is consistent with the biochemical data presented previously (Figure 3.3 a, c).

### **3.2.8 Rolipram triggers PKA phosphorylation of GRK2 in cardiac myocytes**

It is known that impaired  $\beta_2$ AR signalling, especially impaired desensitisation resulting from persistent GRK2 activation, leads to the pathogenesis of heart failure (Penn et al. 2000; Tachibana et al. 2005). It is also known that PDE4D gene inactivation in mice can lead to accelerated heart failure after myocardial infarction (Kehnart et al. 2005). Consequently, work in this chapter sought to investigate whether the underlying trend that PDE4 activity could gate PKA phosphorylation of GRK2 and influence subsequent downstream signalling events could also be envisaged in cultured neonatal cardiac myocytes. To this end I performed similar biochemical techniques in these cells to those employed for HEKB2 cells. The results showed that challenge of cardiac myocytes with isoprenaline caused the time-dependent PKA phosphorylation of GRK2 (Figure 3.16), and also caused membrane recruitment of GRK2 (Figure 3.17). These responses were amplified by pre-incubation with rolipram (Figure 3.16, Figure 3.17). Consistent with the previous data obtained in HEKB2 cells, treatment of cardiac myocytes with 10  $\mu$ M rolipram alone sufficed to trigger both PKA phosphorylation of GRK2 (Figure 3.16) and membrane recruitment of GRK2 (Figure 3.17). As a negative control, 1  $\mu$ M H89 was added before challenge with rolipram, which ablated the actions of rolipram (Figure 3.16 and Figure 3.17, right panel), confirming the role of rolipram in gating PKA actions on GRK2 in cardiac myocytes. This provides further evidence of the crucial role of PDE4 in preventing inappropriate activation of GRK2 in cardiac myocytes. These observations may have potential for the development of novel therapies to treat heart failure.

### **3.2.9 PDE4 inhibition enhances isoprenaline-stimulated PKA phosphorylation of $\beta_2$ AR**

The  $\beta$ -agonist, isoprenaline, elicits the phosphorylation of the  $\beta_2$ AR both by GRK and by PKA (Pierce et al. 2002; Pronin et al. 2002; Perry and Lefkowitz 2002;

Lefkowitz et al. 2002). Both kinases contribute to  $\beta_2$ AR desensitization, via different molecular mechanisms. As I have already studied the role of PDE4 in GRK2-mediated  $\beta_2$ AR desensitization, here, I will focus on its effect in the PKA-mediated pathway.

HEKB2 cells were challenged with 10  $\mu$ M isoprenaline in the absence/presence of 10  $\mu$ M rolipram during a 0-10 min time course. Cells were harvested and protein levels were normalised. The PKA phosphorylation of  $\beta_2$ AR was analyzed using a specific phospho-antiserum against the phospho- $\beta_2$ AR at Ser345-346. As previously noted (Baillie et al. 2003), isoprenaline challenge of these cells causes the transient phosphorylation of the  $\beta_2$ AR (Figure 3.18 a). However, the added presence of rolipram, profoundly potentiates both the speed and magnitude of this response (Figure 3.18 a, b). This amplification was ablated upon treatment of PKA inhibitor I189 (Figure 3.18 c). A specific antiserum against total  $\beta_2$ AR was used as a loading control (Figure 3.18 a).

To study this effect further, I employed confocal immunohistochemistry to analyse these effects visually. The PKA-phosphorylated  $\beta_2$ AR (Ser345/346) can be detected using a specific antibody. Thus, I used this reagent to define the temporal and spatial accumulation of the PKA-phosphorylated form of the  $\beta_2$ AR in HEKB2 cells (Figure 3.23). In these studies, the green fluorescent channel detects the GFP-tagged  $\beta_2$ AR, and the red channel detects the antibody against the PKA-phosphorylated  $\beta_2$ AR. Therefore, the merged images for both channels will identify the PKA-phosphorylated form of  $\beta_2$ AR as a yellow signal (Figure 3.23). Here, I show that without rolipram pre-treatment, no detectable PKA-phosphorylated  $\beta_2$ AR is seen under basal conditions. However, addition of isoprenaline caused the  $\beta_2$ AR to become quickly phosphorylated and, subsequently, internalised. Furthermore, rolipram treatment alone could induce PKA phosphorylation of the receptor and agonist induced effects were both faster and more profound (Figure 3.23, lower panel), when rolipram was present (Figure 3.23, upper panel). Taken together, the biochemical and immunohistochemical data support each other and suggest that PDE4 has a role in controlling the PKA phosphorylation of the  $\beta_2$ AR.

### **3.2.10 Isoprenaline-stimulated phosphorylation of $\beta_2$ AR by PKA is dependent upon AKAP79 but not gravin**

Gradients of cAMP in cells are sampled by anchored forms of PKA that bind to members of a family protein known as AKAPs (Tasken and Aandahl 2004; Michel and Scott 2002). Although AKAPs are structurally unrelated, they all interact with PKA in the same manner through the dimerization interface of the regulatory subunits (Newlon et al. 1999).

It has been shown previously that the  $\beta_2$ AR can be co-immunoprecipitated from rat brain with AKAP150, the rodent homologue of human AKAP79 (Fraser et al. 2000), indicative of a constitutive interaction between these two species. Here, I show that in HEKB2 cells, the  $\beta_2$ AR can be co-immunoprecipitated with endogenous AKAP79 (Figure 3.19 a, left panel). Indeed, AKAP79 appears to be constitutively associated with the  $\beta_2$ AR in HEKB2 cells, and the level of its association with the  $\beta_2$ AR is seemingly unaffected by challenge of cells with isoprenaline or isoprenaline plus rolipram over a period (5min) (Figure 3.19 a, right panel). Such conditions suffice, however, to allow for the activation of PKA, PKA phosphorylation of the  $\beta_2$ AR (Figure 3.19 b, upper panel), and the recruitment of  $\beta$ -arrestin-PDE4D complex to the  $\beta_2$ AR/membrane fraction (Perry et al. 2002; Bolger et al. 2003). Similarly, over this time of challenge there was no change in the amount of AKAP79 associated with the P2 membrane fraction. The siRNA-mediated knockdown of AKAP79, in HEKB2 cells, ablated either isoprenaline or isoprenaline plus rolipram initiated PKA phosphorylation of the  $\beta_2$ AR (Figure 3.19 b).

In A431 human epidermoid carcinoma cells, it has been shown that isoprenaline challenge elicits the PKA phosphorylation of gravin (AKAP250) (Lin et al. 2000; Tao et al. 2003). This allows for the membrane recruitment of gravin where it can interact with the  $\beta_2$ AR. Data presented here, demonstrates that, in contrast to AKAP79, gravin was not constitutively associated with either the  $\beta_2$ AR or the plasma membrane fraction in HEKB2 cells (Figure 3.20 a; zero time). However, challenge of HEKB2 cells with isoprenaline alone or isoprenaline plus rolipram confers the translocation of gravin to the P2 membrane fraction, which was maximal after 3 min (Figure 3.20 a, right panel). Although challenge with isoprenaline or isoprenaline plus

rolipram also allowed gravin to translocate to the  $\beta_2$ AR (Figure 3.20 a, left panel), the maximal recruitment was delayed till 5 min after agonist challenge (Figure 3.20 a, left panel). Again, unlike the effect of knockdown of AKAP79, the siRNA-mediated knockdown of gravin did not alter the ability of isoprenaline alone or isoprenaline plus rolipram to cause the PKA phosphorylation of the  $\beta_2$ AR (Figure 3.20 b, upper panel). This suggests that isoprenaline-stimulated PKA phosphorylation is via the scaffolding of AKAP79 near the receptor.

### **3.2.11 Interaction with $\beta$ -arrestin is required for PDE4D to regulate isoprenaline-stimulated phosphorylation of ERK**

It has been previously suggested that ectopic  $\beta$ -arrestin2 confers isoprenaline-stimulated PDE4 membrane translocation, which attenuates switching of  $\beta_2$ AR coupling from Gs to Gi and subsequent ERK pathway activation (Baillie et al. 2003). In order to investigate further the role of PDE4 in the regulation of this switching, I used catalytically inactive mutants in a dominant negative strategy. Single point mutations of PDE4D5 (in the catalytic domain) were generated producing catalytically inactive forms which were still able to bind  $\beta$ -arrestins. A dominant negative role was assumed by displacement of active endogenous PDE4D from  $\beta$ -arrestins, as seen by its ability to enhance isoprenaline-stimulated phospho-ERK formation (Baillie et al. 2003).

HEKB2 cells were transfected with an empty vector or catalytically inactive PDE4D5, and then stimulated with 10  $\mu$ M isoprenaline at the indicated times. Cell lysates were harvested in 3T3 lysis buffer and subjected to Western blotting with specific antiserum against phospho-ERK. The same blot was stripped and probed with anti-ERK antibody as a loading control. Anti-VSV antibodies were used to for expression of PDE4D5 D/N. Expression of catalytically inactive PDE4D5 (DN-PDE4D5), in HEKB2 cells, markedly increased the ability of isoprenaline to activate ERK1/2 (Figure 3.21). However, when the catalytically inactive PDE4D5 was further mutated in its isoform-specific N terminal region where  $\beta$ -arrestins preferentially interacts (Arg34 $\rightarrow$ Ala) (Bolger et al. 2003), their unique interaction was efficiently ablated. The potentiating effect of dominant negative PDE4D5 on isoprenaline-stimulated ERK phosphorylation was abolished when an Arg34 $\rightarrow$ Ala form of

PDE4D5 was transfected into the HEKB2 cells (Figure 3.21). This shows that the potentiating effect of dominant negative PDE4D5 on this response is dependent upon its ability to interact with  $\beta$ -arrestins.

### 3.3 Discussion

Previous studies have shown that the functioning of GRK2 in the  $\beta_2$ AR desensitization process can be regulated by the activity of other kinases, which directly phosphorylate GRK2 (Kohout and Lefkowitz 2003). The effects of these phosphorylations vary, depending on the identity of the specific kinase. PKA (Cong et al. 2001), as well as PKC (Krasel et al. 2001), has been shown to phosphorylate GRK2, thereby increasing the ability of GRK2 to interact with  $G\beta\gamma$  subunits (Lodowski et al. 2003; Kozasa 2004). This enhances GRK2 membrane recruitment and the ability of GRK2 to phosphorylate GPCRs (Kohout and Lefkowitz 2003). In contrast, phosphorylation of GRK2 by ERK dramatically reduces its activity as well as its membrane association (Pitcher et al. 1999). In the present study, I identified a novel role for PDE4s, showing that they play a significant part in the regulation of GRK2 in the receptor desensitisation process.

Data presented here indicates that inactivation of PDE4 by the PDE4 selective inhibitor rolipram enhances the isoprenaline-induced PKA phosphorylation of GRK2 (Figure 3.3 a, c) and the subsequent membrane recruitment of GRK2 (Figure 3.6 a, left panel). It is also shown that, in response to isoprenaline, the added presence of rolipram facilitates  $\beta$ -arrestin translocation from the cytosol to the plasma membrane, leading to an increased rate of receptor internalization (Figure 3.11 a). Interestingly, whilst PDE4D provides around 60% of the total PDE4 activity in HEKB2 cells, and PDE4B around 30% (Perry et al. 2002; Lynch et al. 2005), the effect of PDE4 on the enhancement of the isoprenaline-induced PKA phosphorylation of GRK2 and subsequent GRK2-mediated phosphorylation of  $\beta_2$ AR seems not subfamily-specific, as siRNA-mediated knockdown of either PDE4B or PDE4D subfamilies is sufficient to facilitate the ability of isoprenaline to cause PKA phosphorylation of GRK2 (Figure 3.5). The lack of any selective effects in this instance is likely to be because cytosolic GRK2 is being phosphorylated by cytosolic

PKA and thus subject to global rather than compartmentalized cAMP actions, which both PDE4B and PDE4D are able to influence.

Following rolipram inhibition of PDE4, it is clear that isoprenaline-induced GRK2 recruitment to the plasma membrane is more transient in nature (Figure 3.6 a). GRK2 is a phosphoprotein and constitutively phosphorylated by ERK1/2 at its Ser670 under basal conditions (Pitcher et al. 1999). Before agonist stimulation, GRK2 is maintained in its inactive state. Only when the agonist stimuli reaches GPCRs, will GRK2 quickly be dephosphorylated by an un-identified phosphatase and translocate to the plasma membrane where it phosphorylates GPCRs. The phosphorylation of GPCRs by GRK2 is highly regulated as when it is in complex with the activated receptor and G $\beta$  $\gamma$  subunits, GRK2 quickly associates with ERK1/2 (Elorza et al. 2000) and becomes phosphorylated again (Pitcher et al. 1999). This phosphorylation then dramatically decreases its activity, as well as the affinity of binding to G $\beta$  $\gamma$  subunits, promoting its release from the plasma membrane back to the cytosol. By controlling the phosphorylation of GRK2 by PKA, and thereby its affinity binding towards G $\beta$  $\gamma$  subunit, ablation of PDE4 activity will promote the ability of isoprenaline to initiate membrane recruitment of GRK2. However, PDE4 inhibition will also lead to increased PKA phosphorylation of the  $\beta_2$ AR (Figure 3.18) and the switching of its signaling to the activation of ERK (Figure 3.15) (Baillie et al. 2003). In the present study, when HEKB2 cells were challenged with isoprenaline and rolipram together, such increases in activated ERK in the cytosol appear to result in greater but more transient ERK activation in the membrane fraction (Figure 3.14). This can be expected to subsequently, transiently phosphorylate GRK2 (Figure 3.13). Such actions are likely to control the transience of GRK2 membrane association. Consistent with ERK underpinning the release of GRK2 (Kohout and Lefkowitz 2003), under conditions of isoprenaline challenge and PDE4 inhibition, I observed that, if ERK is inhibited with UO126, a MEK inhibitor, then GRK2 remains membrane associated (Figure 3.6 a).

I also show here that PKA phosphorylation of GRK2 (Figure 3.4), GRK2 membrane recruitment (Figure 3.6 b) and GRK phosphorylation of  $\beta_2$ AR (Figure 3.9) can all occur in the absence of agonist in HEKB2 cells, following inactivation of

PDE4. This would suggest that PDE4 could prevent inappropriate membrane recruitment of GRK2 in unstimulated cells. Unsurprisingly, effects caused by rolipram alone in these cells were not as pronounced as those seen in the added presence of isoprenaline. Rolipram induced PKA phosphorylation of GRK2 and consequent membrane recruitment was not confined to HEK293 cells, but was also observed in cardiac myocytes (Figure 3.16 and Figure 3.17).

Current dogma dictates that GRK2 recruitment to the membrane is agonist-dependent. However, no one so far has reported the effects of PDE4 inhibition on GRK2 distribution. Observations described in this chapter are reminiscent of studies into the PKC phosphorylation of GRK2 induced by phorbol esters (Krasel et al. 2001). It is now well established that GPCRs, such as the  $\beta_2$ AR, exist in an equilibrium between active and inactive states and that agonist binding drives this equilibrium towards the activate state (Milligan 2003). Thus, under basal conditions, such equilibrium allows for the generation of a small pool of activated G $\alpha$ s, which is responsible for basal adenylyl cyclase activity, together with free G $\beta\gamma$  subunits (Dupre et al. 2004). In the cells used here, it would appear that basal adenylyl cyclase activity, in the presence of PDE4 inhibition, is sufficient to allow global cAMP levels to reach a magnitude whereby PKA can phosphorylate GRK2, increasing its affinity for G $\beta\gamma$  subunits and facilitating recruitment of GRK2 to the membrane.

That ERK activation is not stimulated by rolipram treatment alone in HEK293 cells (Figure 3.15, zero time; negative result from rolipram alone time course) indicates that agonist stimulation is essential to allow coupling of the PKA phosphorylated  $\beta_2$ AR to Gi and consequential ERK. This is consistent with previous data obtained via siRNA mediated knockdown of PDE4D, which has been shown to be the functionally relevant PDE in mediating the switching of  $\beta_2$ AR to the activation of ERK (Lynch et al. 2005). Thus, in HEK293 cells challenged with rolipram alone, which do not lead to ERK activation, the recruitment of GRK2 to the membrane is sustained (Figure 3.6 b).

As shown in the present study for the first time, PDE4 activity, in regulating PKA phosphorylation of GRK2, may, at least in certain cells, provide a means of

influencing the membrane recruitment of GRK2. There are three distinct facets to this. First, PDE4 activity is set to regulate the degree of feedback in the regulating PKA phosphorylation of GRK2 in stimulated cells, thereby influencing the rate of agonist-triggered desensitization. Secondly, PDE4 activity may modulate the degree of isoprenaline-stimulated ERK activation, which influences the release of GRK2 from membranes and the reversal of desensitization. Finally, PDE4 activity ensures that, under normal conditions, GRK2 is prevented from phosphorylation by fluctuations in basal PKA owing to intracellular cAMP levels, and only when agonist challenge breaches the threshold for PKA phosphorylation of GRK2 set by PDE4, will GRK2 translocation occur. As this system is also applicable in cardiac myocytes, it would appear that the potential importance of PDE4 in preventing inappropriate activation of GRK2 in cardiac myocytes may have functional relevance to heart failure, as both GRK2 and PDE4D are suggested being involved in heart failure (Tachibana et al. 2005; Harding et al. 2001; Lehnart et al. 2005).

Apart from GRK, PKA phosphorylation of  $\beta_2$ AR is another important route by which  $\beta_2$ AR desensitisation is regulated. Phosphorylated and activated  $\beta_2$ AR switches its coupling from Gs-mediated activation of adenylyl cyclase to Gi-mediated inactivation of adenylyl cyclase, therefore decreasing the rate of production of cellular cAMP (Daaka et al. 1997). Key to gating this phosphorylation process is the activation of anchored PDEs, such as enzymes of PDE4 family (Baillie et al. 2003) (Figure 3.18). More recently, it has been shown that  $\beta$ -arrestin-recruited PDE4D controls the cAMP-mediated activation of PKA involved in a defined, compartmentalized process focused on  $\beta_2$ AR (Perry et al. 2002). This underpins the possible existence of PKA tethering to some specific AKAPs as disruption of AKAP-PKA complexes resulted in the attenuation of isoprenaline-induced ERK activation in HEKB2 cells (Lynch et al. 2005). Interestingly, the  $\beta_2$ AR itself has been shown to be capable of interacting with specific AKAPs, such as AKAP79 (Fraser et al. 2000). AKAP79 is constitutively associated with  $\beta_2$ AR in transfected cells whereas gravin exhibits dynamic interaction with  $\beta_2$ AR following PKA phosphorylation of gravin (Lin et al. 2000; Tao et al. 2003). I show here that  $\beta_2$ AR can interact with endogenously expressed forms of both AKAP79 (Figure 3.19 a, left panel) and gravin (Figure 3.20 a, left panel) in HEKB2 cells. Consistent with previous data obtained in

different systems, I show that the interaction of  $\beta_2$ AR with AKAP79 is indeed constitutive (Figure 3.19 a, right panel), whereas that with gravin is only observed upon isoprenaline challenge (Figure 3.20 a, right panel). Using for the first time siRNA against these AKAPs, I show here that the ability of isoprenaline to cause the PKA-mediated phosphorylation of the  $\beta_2$ AR, is abolished upon knockdown of AKAP79 but not upon knockdown of gravin (Figure 3.19 b and Figure 3.20 b). This indicates that the activity of a discrete pool of AKAP79-tethered PKA is responsible for agonist-triggered phosphorylation of the associated  $\beta_2$ AR. Although it is uncertain of the role of recruited gravin, the selective siRNA-mediated knockdown of AKAP79 and gravin highlights the functional differences between the membrane bound forms of these AKAPs in HEK293 cells.

In contrast to the PDE4 effect on GRK phosphorylation of  $\beta_2$ AR, which is not subfamily specific, as indicated by non-subfamily specific PKA phosphorylation of GRK2, PDE4 control of PKA phosphorylation of the  $\beta_2$ AR and consequential switching of its signalling from activation of adenylyl cyclase to activation of ERK (Baillie et al. 2003) is PDE4D5-specific (Lynch et al. 2005). In order to support siRNA data, I used a dominant negative strategy to show that overexpression of catalytically inactive PDE4D5 enhances isoprenaline-stimulated ERK phosphorylation (Figure 3.21), consistent with previous data (Baillie et al. 2003). Unsurprisingly, however, such an action is clearly ablated when a PDE4D5-specific site for interaction with  $\beta$ -arrestin is disrupted (Figure 3.21). This indicates that the unique desensitisation process provided by  $\beta$ -arrestin-mediated delivery of PDE4D5 can be negated by disruption of this active complex. In this context, it is important to note that the presence of AKAP79 and  $\beta$ -arrestin-associated PDE4 has a profound effect on the ability of the  $\beta_2$ AR to become phosphorylated by PKA. This affects switching to  $G_i$ , and alters downstream signalling and this might be linked to heart disease (Xiang et al. 2004).

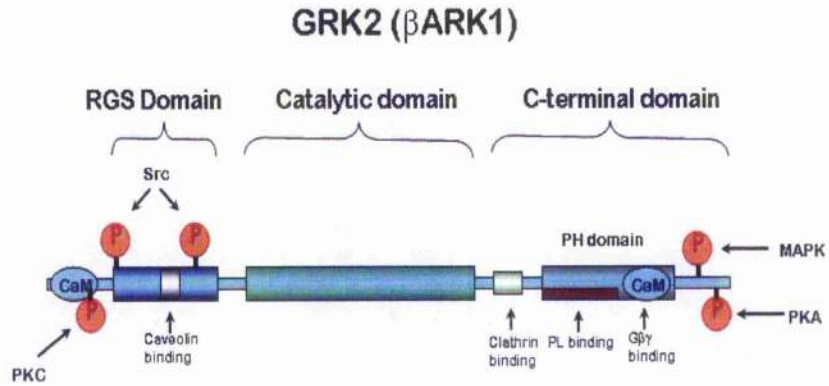


**Figure 3.1 A schematic of GRK2 ( $\beta$ ARK1).**

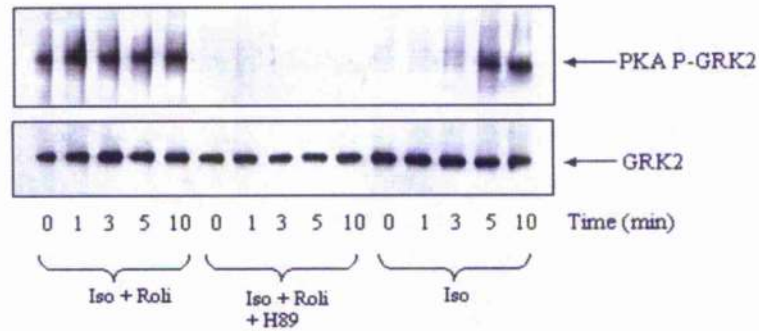
GRK2 is a multi-domain protein able to interact with a variety of cellular proteins. Such interactions allow for its different cellular functions and also contribute to modulate its activity and subcellular targeting. The figure depicts the regions where the regulatory phosphorylation takes place and the interactions sites with other proteins are mapped. RGS, regulators of G protein signalling; CaM, calcium-calmodulin; PL, phospholipids; PH, pleckstrin homology.



**Figure 3.2 Existence of GRKs in HEKB2 cells.**

HEKB2 cells were harvested when confluent in 3T3 lysis buffer. Clear lysates were divided into five equal volumes. The five volumes were subjected to western blotting probed for GRK2, GRK3, GRK4, GRK5 and GRK6, respectively.

(a)



(b)

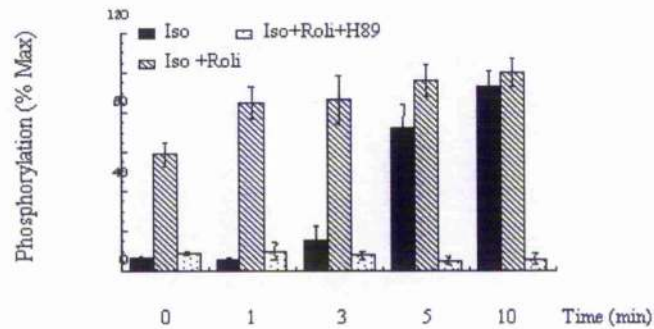
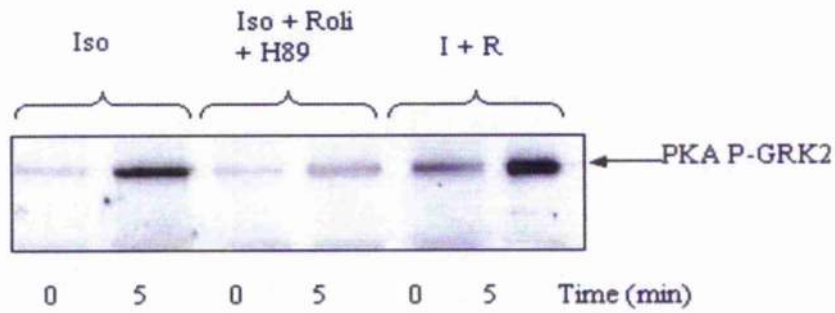


**Figure 3.3 GRK2 is phosphorylated by PKA in HEK293T cells.**

(a) HEK293T cells were treated with either isoprenaline (10 $\mu$ M) alone or isoprenaline following a 10 min pre-incubation with rolipram (10 $\mu$ M) in the presence and absence of the PKA inhibitor H89 (1 $\mu$ M). Cells were harvested in RNeasy lysis buffer and lysates were subjected to immunoprecipitation with an anti-GRK2 antibody, followed by probing with an anti-(phosphor-PKA substrate) antibody. Upper panel shows the GRK2 that has been phosphorylated by PKA in the immunoprecipitates; lower panel shows the equal GRK2 loading in the immunoprecipitates. (b) Quantification of three such independent experiments (means $\pm$  S.D.) from the western blots. Data was normalized for loading and represented as fold change basal.

(c)



(d)

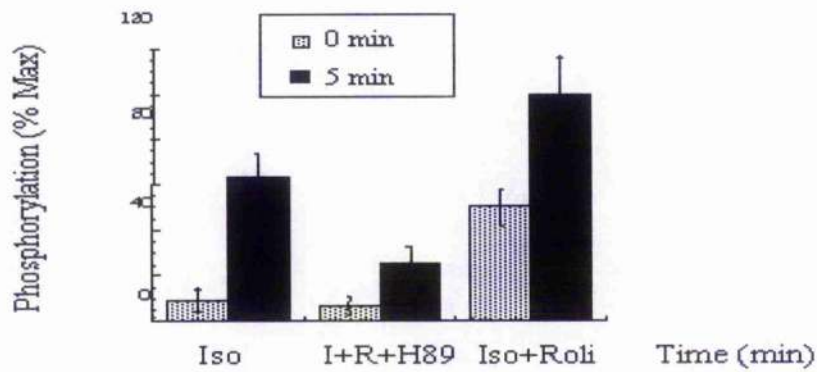


**Figure 3.3 GRK2 phosphorylation by PKA in HEKB2 cells.**

(c) HEKB2 cells were treated with either isoprenaline (10 $\mu$ M) alone or isoprenaline following a 10 min pre-incubation with rolipram (10 $\mu$ M) in the presence and absence of the PKA inhibitor H89 (1 $\mu$ M). Cells were harvested in 3T3 lysis buffer and lysates were subjected to immunoprecipitation with an anti-(phosphor-PKA substrate) antibody, followed by probing with an anti-GRK2 antibody. (d) Quantification of three such independent experiments (means $\pm$  S.D.) from the western blots as shown in (c). Data was normalized for loading and represented as fold change basal.

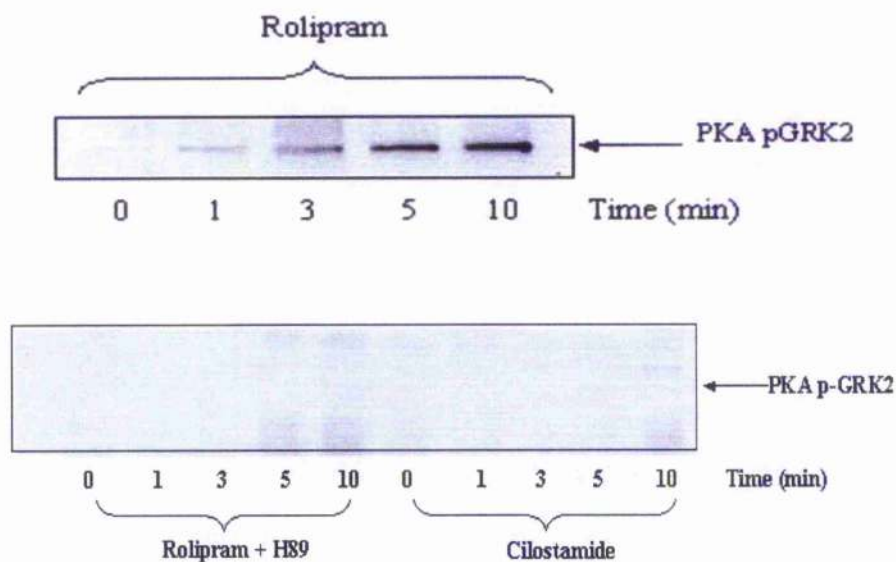


**Figure 3.4 Differential PKA phosphorylation of GRK2 following PDE4 or PDE3 inhibition in HEK293 cells.**

HEK293 cells were treated with either rolipram (10  $\mu$ M) alone, rolipram and H89 (1  $\mu$ M) or cilostamide (1  $\mu$ M) alone for the indicated time. Cells were harvested in RNeasy lysis buffer and subjected to immunoprecipitation with an anti-(phospho-PKA substrate) antibody, followed by western blotting probed with anti-GRK2 antibody. Upper panel shows the PKA phosphorylated GRK2 under single rolipram treatment; lower left panel shows the PKA phosphorylated GRK2 under rolipram treatment following a 10 min pre-incubation of H89; lower right panel shows the PKA phosphorylated GRK2 under single cilostamide treatment.

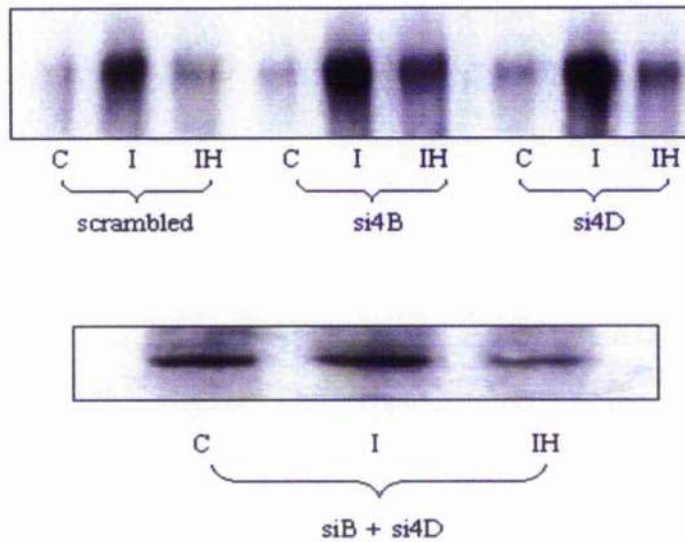
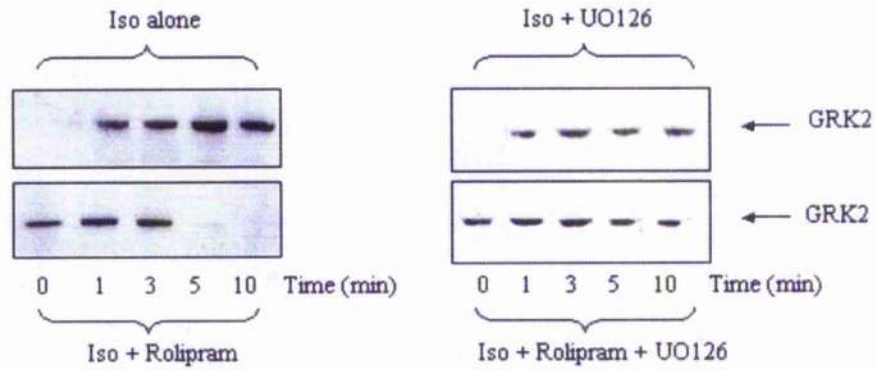


**Figure 3.5 PKA phosphorylation of GRK2 in PDE4 isoform-knockdown HEKB2 cells.**

HEKB2 cells were transfected with either scrambled siRNA, siRNA specific for PDE4B, siRNA specific for PDE4D, or siRNA specific for both PDE4B and PDE4D. After efficient transfections, cells were challenged either with isoprenaline (10  $\mu$ M) for 5 min or with isoprenaline (10  $\mu$ M) for 5 min following 10 min pretreatment with H89 (1  $\mu$ M), and then harvested in 3T3 lysis buffer. Clear cell lysates were subjected to immunoprecipitation with an anti-GRK2 antibody, and then western blotting probed with an anti-(phosphor PKA substrate) antibody. The cell proteins in upper panel were normalized, so were those in lower panel, but separately. C, resting conditions; I, isoprenaline; IH, isoprenaline plus H89; si4B, siRNA specific for PDE4B; siD, siRNA specific for PDE4D; si4B+si4D, siRNA specific for both PDE4B and PDE4D. Blots here are typical of separate experiments performed three times.

(a)



(b)

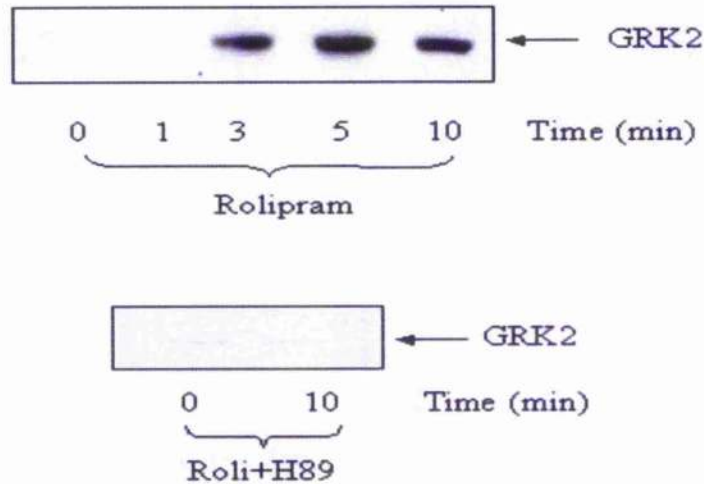


**Figure 3.6 Membrane translocation of GRK2 in HEKB2 cells.**

(a) HEKB2 cells were challenged with isoprenaline (10  $\mu$ M) at the indicated time in either the presence or absence of ERK upstream kinase MEK inhibitor UO126 (10  $\mu$ M), and either with or without rolipram (10  $\mu$ M) pre-incubation for 10 min. Cells were harvested in KHEM buffer and subjected to membrane fractionation. Membrane (P2 fraction) proteins were normalized and blotted for GRK2 in each case. (b) HEKB2 cells were treated with rolipram (10  $\mu$ M) for the indicated times in the absence and presence of H89 (1  $\mu$ M) and normalized membrane fractions were subjected to western blotting probed with an anti-GRK2 antibody. Iso, isoprenaline; UO126, a MEK inhibitor; Roli, rolipram; H89, a PKA inhibitor

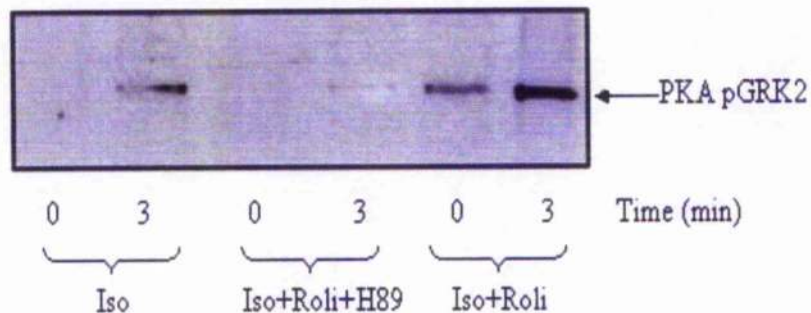


**Figure 3.7 Phosphorylation status of GRK2 in HEKB2 membrane fractions.**

HEKB2 cells were challenged with either isoprenaline (10  $\mu$ M) alone or isoprenaline after pre-incubation of rolipram (10  $\mu$ M) for 10 min or isoprenaline after pre-incubation of both rolipram (10  $\mu$ M) and H89 (1  $\mu$ M) together for 10 min. Cells were then subjected to membrane fractionation, followed by protein normalization. The membrane fractions were solubilized in 3T3 lysis buffer, and PKA-phosphorylated proteins existing in the plasma membrane were immunopurified using an anti-(phosphor-PKA substrate) antibody, followed by SDS-PAGE and immunoblotted for GRK2. Iso, isoprenaline; Roli, rolipram.

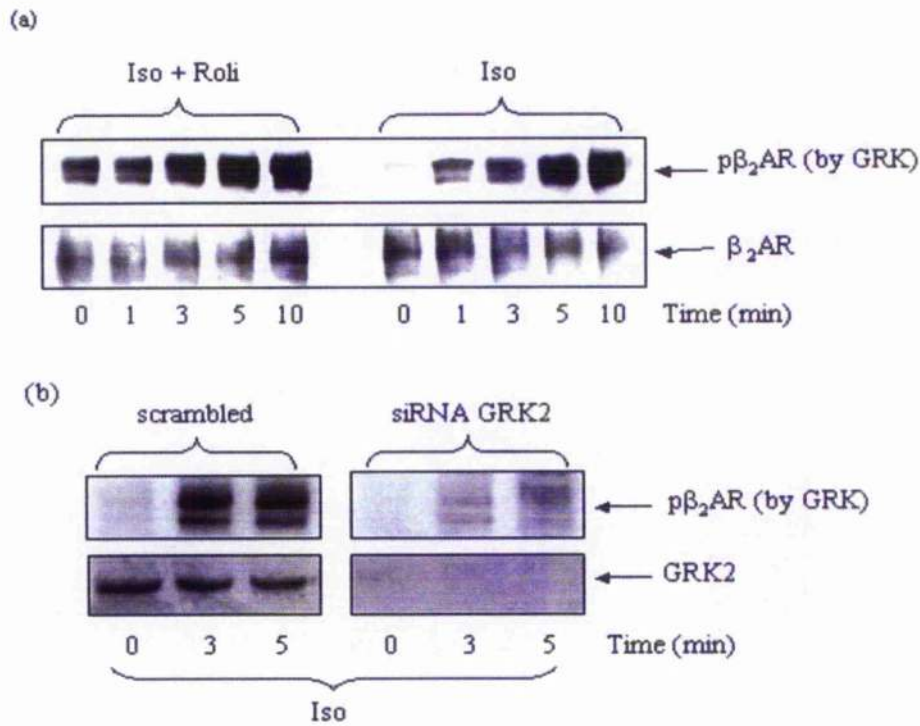


**Figure 3.8 Phosphorylation of the  $\beta_2$ AR in HEKB2 cells by GRK2.**

(a) HEKB2 cells were challenged with isoprenaline (10  $\mu$ M) for the indicated times either with or without rolipram (10  $\mu$ M) pre-treatment (10 min). Cells were harvested in 3T3 lysis buffer and normalized to have the equal protein levels in each time point. Clear lysates were subjected to SDS-PAGE and probed for either phosphorylation of the  $\beta_2$ AR by GRK2 on its Ser355/356 or for total  $\beta_2$ AR. (b) HEKB2 cells were transfected with scrambled siRNA or siRNA specific for GRK2 and then challenged with isoprenaline (10  $\mu$ M) at the indicated time. Cells were harvested in 3T3 lysis buffer and the clear lysates were probed for GRK2 and phosphorylation of  $\beta_2$ AR by GRK2 at Ser355/356 individually. Upper panel shows the effect of siRNA mediated GRK2 knockdown on  $\beta_2$ AR phosphorylation by GRK2; lower panel shows the efficiency of siRNA mediated knockdown. Iso, isoprenaline; p $\beta_2$ AR, phosphorylated  $\beta_2$ AR.

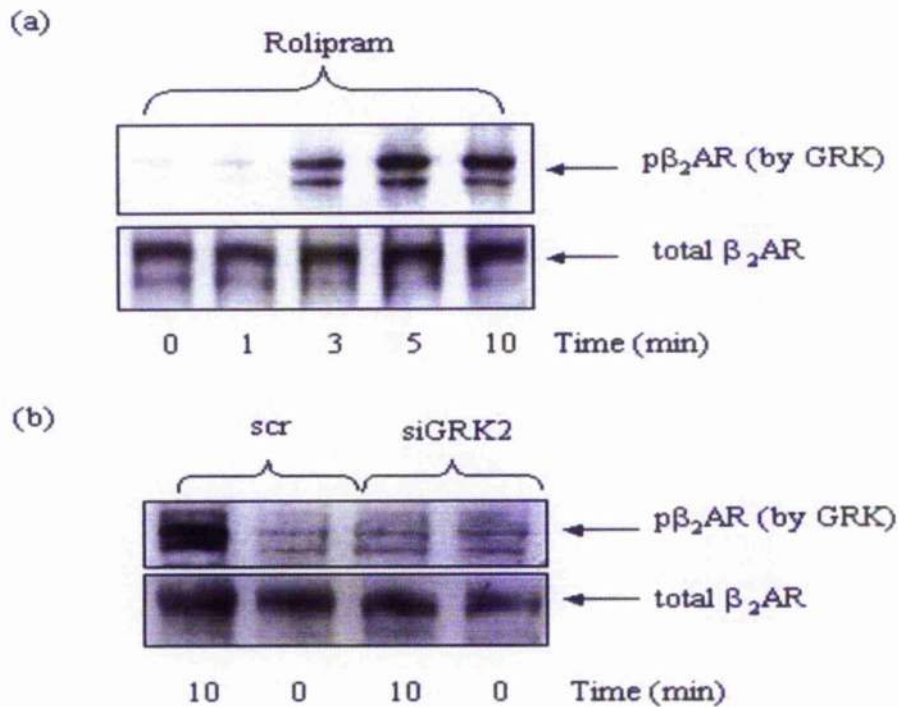


**Figure 3.9 Rolipram induced GRK2 phosphorylation of  $\beta_2$ AR in HEKB2 cells.**

(a) HEKB2 cells were treated with rolipram (10  $\mu$ M) at the indicated time and harvested in 3T3 lysis buffer. Protein levels were normalized and clear lysates were subjected to western blotting probed with a specific anti-phospho  $\beta_2$ AR (Ser355/356). The same blot was then stripped by stripping buffer and probed for total  $\beta_2$ AR. (b) HEKB2 cells were transfected with scrambled siRNA as a control and with siRNA specific for GRK2 as a test. Cells were treated with rolipram (10  $\mu$ M) for the indicated times and harvested in 3T3 lysis buffer. Normalized lysates were probed for phosphorylation of  $\beta_2$ AR by GRK2 and total  $\beta_2$ AR individually. p $\beta_2$ AR, phosphorylated  $\beta_2$ AR; scr, scrambled siRNA; siGRK2, siRNA specific for GRK2.

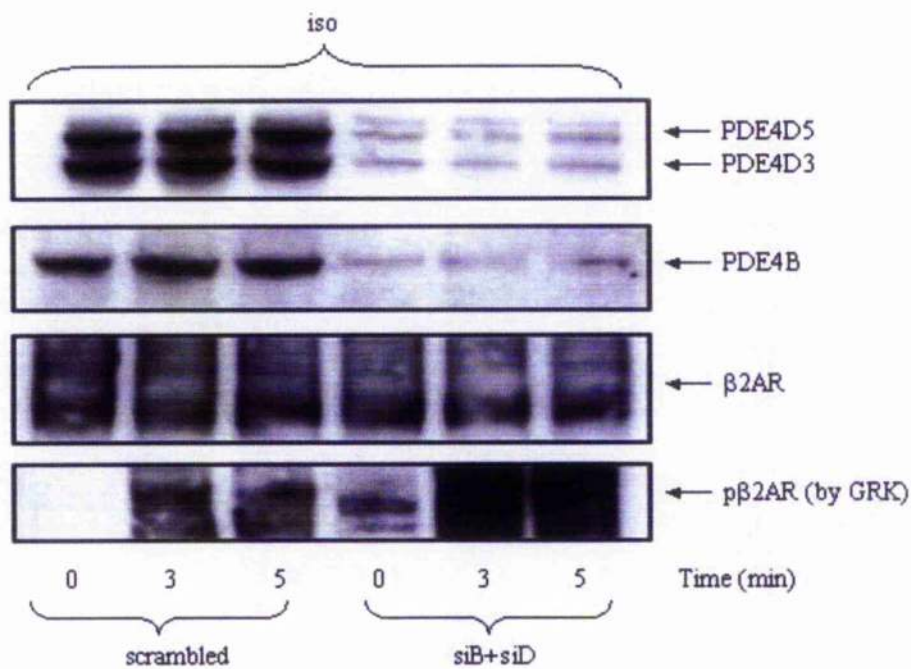


**Figure 3.10 Phosphorylation of  $\beta_2$ AR by GRK2 in siRNA mediated PDE4B and PDE4D knockdown HEK293T cells.**

Control cells pretreated with scrambled siRNA and cells pretreated with specific siRNA to PDE4B and PDE4D, were challenged with isoprenaline (10  $\mu$ M) at the indicated time. Cells were harvested and normalized to equal protein levels. Clear cell lysates were probed for PDE4D (upper panel), PDE4B (second upper panel),  $\beta_2$ AR (second lower panel) and phosphorylation of  $\beta_2$ AR by GRK (lower panel) individually. iso, isoprenaline; siB, siRNA to PDE4B; siD, siRNA to PDE4D; p $\beta_2$ AR, phosphorylated  $\beta_2$ AR.

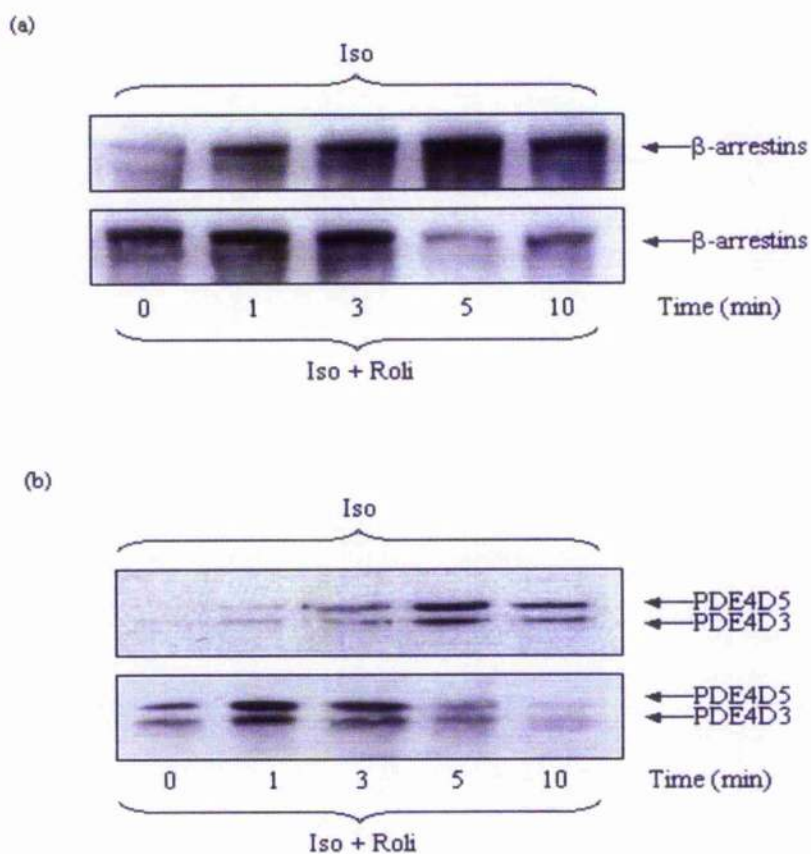


**Figure 3.11 Membrane translocation of  $\beta$ -arrestins and PDE4D.**

(a) HEK293 cells were challenged with isoprenaline ( $10 \mu\text{M}$ ) for the indicated times either with or without 10 min rolipram pre-treatment. Cells were harvested in KHEM buffer and subjected to membrane fractionation. Membrane (P2) fractions were normalized and probed for  $\beta$ -arrestins. (b) Cells were treated as in (a) and subjected to western blotting probed with anti-PDE4D. Iso, isoprenaline; Roli, rolipram.

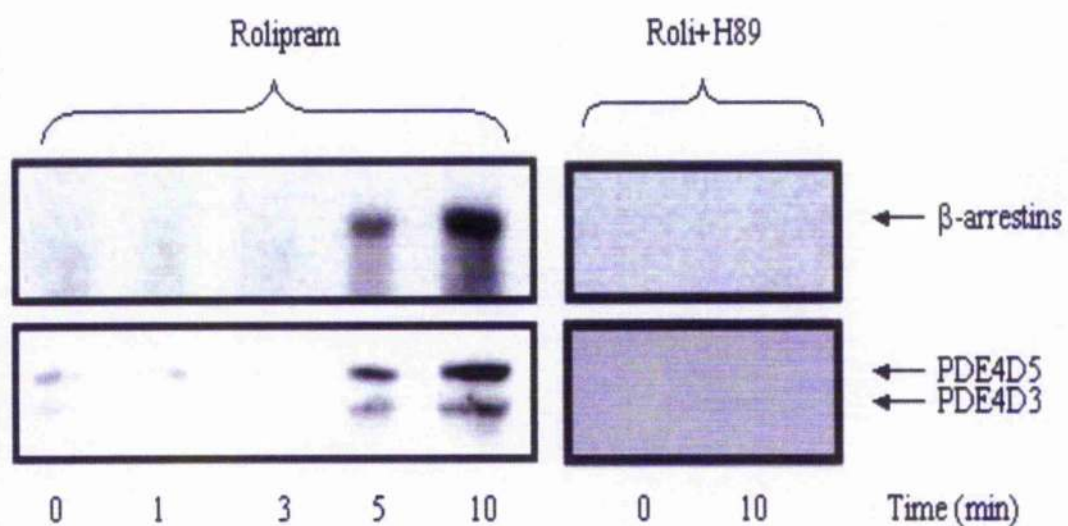


**Figure 3.12 Rolipram alone induced membrane recruitment of  $\beta$ -arrestins and PDE4D.**

HEKB2 cells were treated with rolipram (10  $\mu$ M) in a 0~10 min time course, in the presence or absence of 10 min H89 (1  $\mu$ M) pretreatment as indicated. Cells were then harvested in KHEM buffer and subjected to membrane fractionation. Membrane (P2) fractions were normalized and blotted for  $\beta$ -arrestin and PDE4D individually. Roli, rolipram.

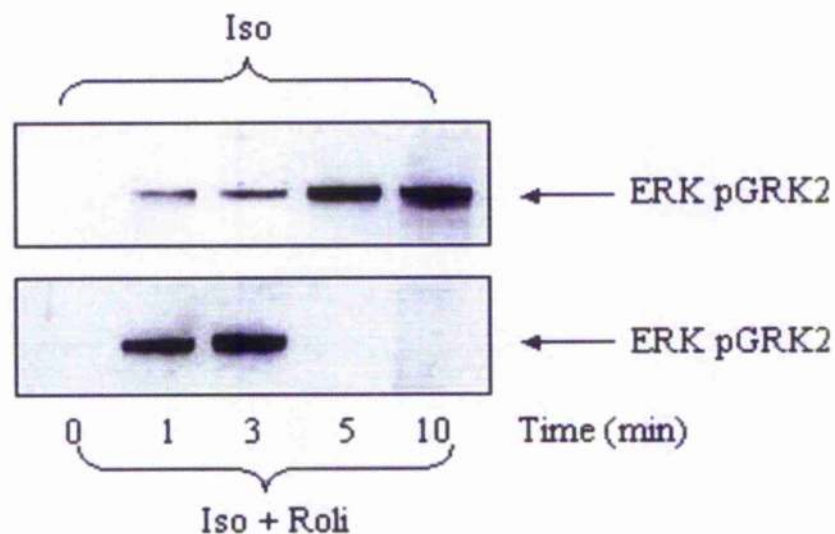


**Figure 3.13 Membrane ERK-phosphorylated GRK2 in HEKB2 cells.**

HEKB2 cells were challenged with isoprenaline (10  $\mu$ M) for the indicated times either with or without, as indicated, 10 min rolipram (10  $\mu$ M) pre-treatment. Cells were harvested in KHEM buffer and subjected to membrane fractionation. Equal amount of membrane proteins were obtained and subjected to western blotting probed for ERK phosphor-GRK2 Ser670. Iso, isoprenaline; Roli, rolipram.

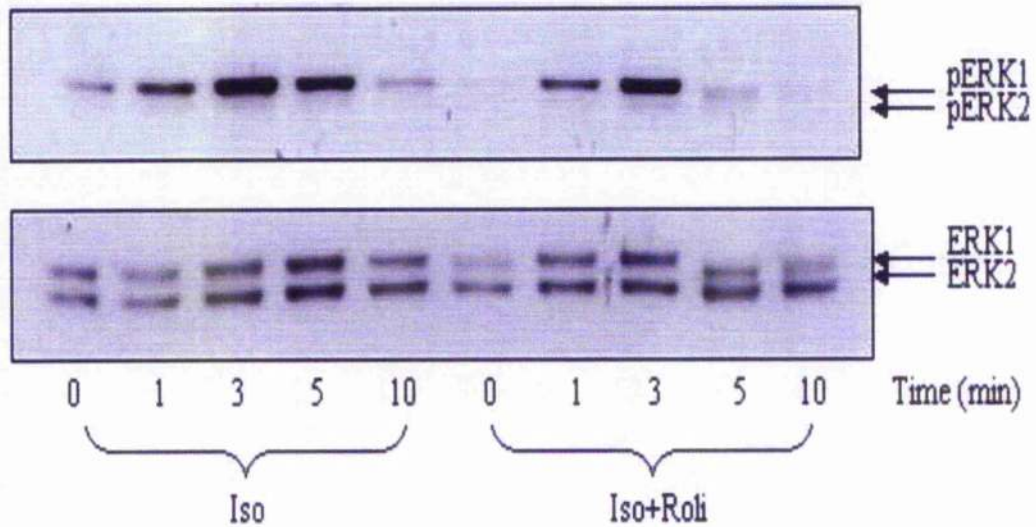


**Figure 3.14 Activation of ERK1/2 in membrane fraction of HEKB2 cells.**

HEKB2 cells were challenged with isoprenaline (10  $\mu$ M) for the indicated times either with or without, as indicated, 10 min rolipram (10  $\mu$ M) pre-treatment. Cells were harvested in KHEM buffer and subjected to membrane fractionation. Equal amount of membrane proteins were obtained and subjected to western blotting probed for phospho-ERK1/2. The same blot was then stripped and probed with an anti-ERK1/2 antibody. Iso, isoprenaline; Roli, rolipram.

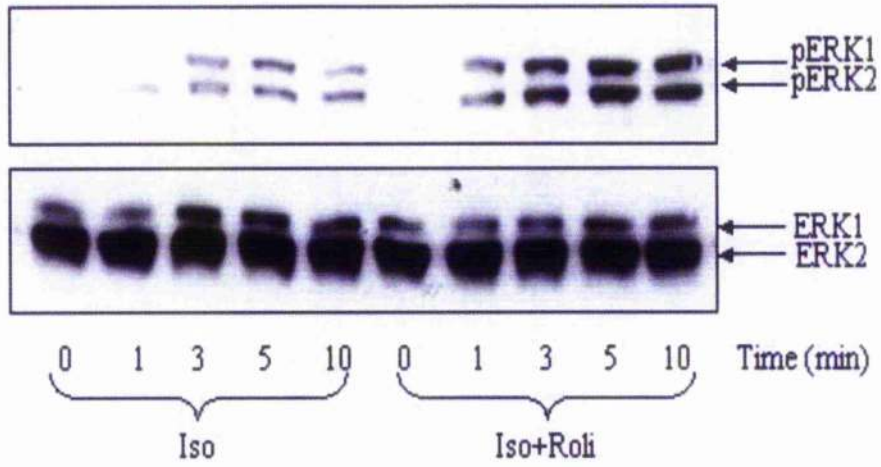


**Figure 3.15 ERK activation in HEKB2 cells.**

HEKB2 cells were challenged with isoprenaline ( $10 \mu\text{M}$ ) for the indicated times either with or without, as indicated, 10 min rolipram ( $10 \mu\text{M}$ ) pre-treatment. Cells were harvested in 3T3 lysis buffer and subjected to western blotting probed for phospho-ERK1/2. The same blot was then stripped and probed for total ERK1/2. Upper panel shows the ERK activation in each instance; lower panel shows the equal loading by checking the level of ERK1/2.

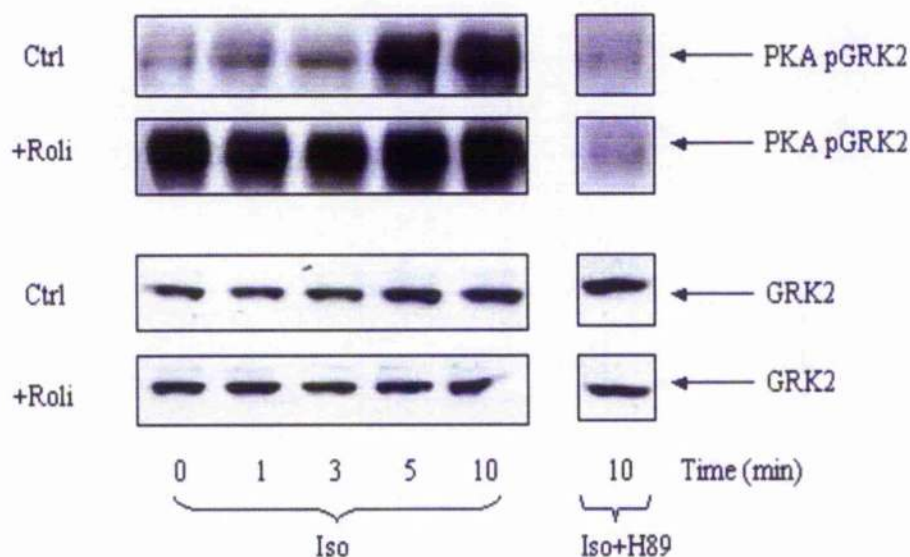


**Figure 3.16 PKA phosphorylation of GRK2 in cardiac myocytes.**

Cardiomyocytes were challenged with isoprenaline ( $10 \mu\text{M}$ ) for the indicated times either with or without, as indicated, 10 min rolipram ( $10 \mu\text{M}$ ) pre-treatment, in the presence or absence of H89 ( $1 \mu\text{M}$ , 10 min). Cells were harvested in 3T3 lysis buffer. Clear, normalized cell lysates were then subjected to immunoprecipitation using an anti-GRK2 antibody, followed by western blotting probed for phosphor-PKA substrate. The same blot was stripped and probed for GRK2 to check the loading.

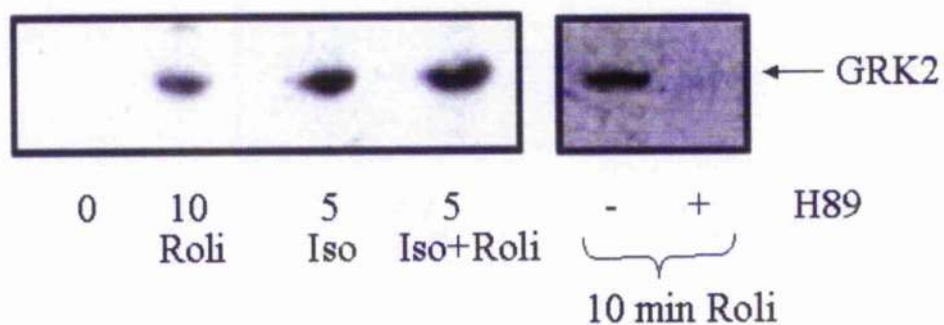


**Figure 3.17 Membrane recruitment of GRK2 in cardiac myocytes.**

Cardiomyocytes were challenged with the indicated combination of isoprenaline (10  $\mu$ M) and/or Rolipram (10  $\mu$ M) and H89 (1  $\mu$ M) for the indicated times. When rolipram or/and H89 was added together with isoprenaline, cells were then pre-incubated with rolipram or/and H89 for 10 min before the addition of isoprenaline for the indicated times. Cells were harvested in KHEM buffer and subjected to membrane fractionation. Equal amount of membrane (P2) fraction proteins were obtained and subjected to western blotting probed for GRK2. Ctrl, control; Iso, isoprenaline; Roli, rolipram.

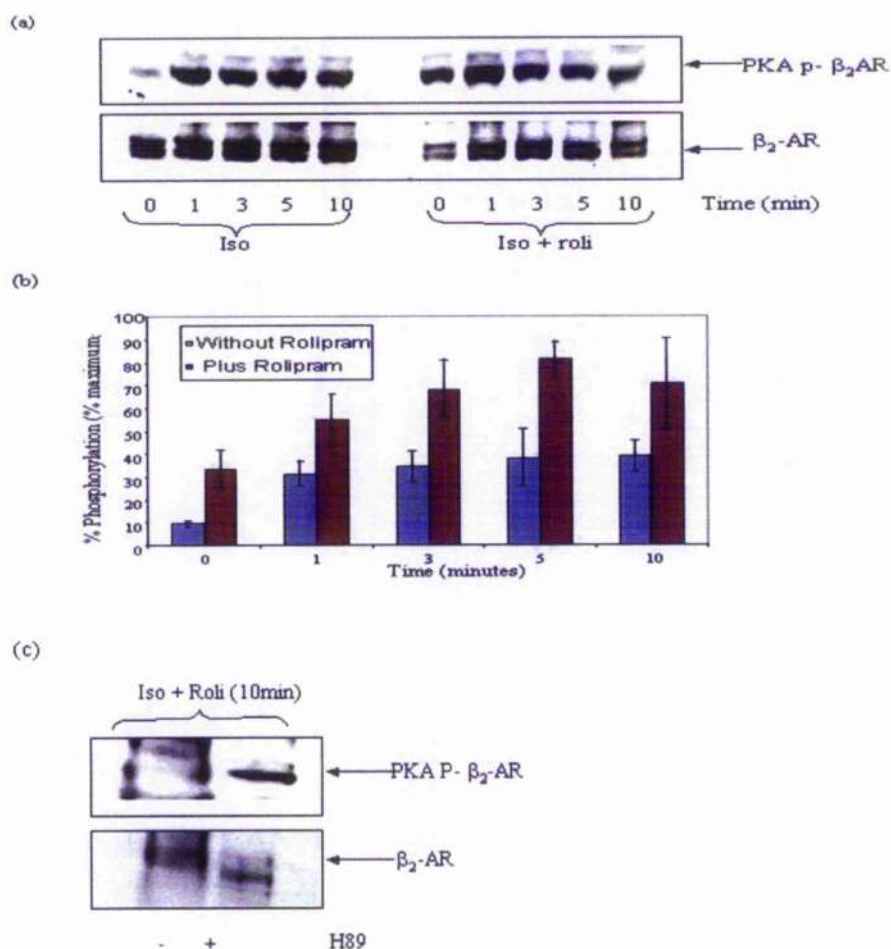


**Figure 3.18 PKA phosphorylation of  $\beta_2$ AR in HEKB2 cells.**

(a) HEKB2 cells were challenged with isoprenaline (10  $\mu$ M) for the indicated times either with or without rolipram (10  $\mu$ M) pre-treatment (10 min). Cells were harvested in 3T3 lysis buffer and normalized to have the equal protein levels in each time point. Clear lysates were subjected to SDS-PAGE and probed for PKA phosphorylation of the  $\beta_2$ AR at Ser345/346. The same blot was then stripped and probed with an anti- $\beta_2$ AR antibody. (b) Quantification of three experiments as in (a) (means  $\pm$  S.D.) with 100% as the maximal effect seen with isoprenaline and rolipram. Iso, isoprenaline; Roli, rolipram. (c) HEKB2 cells were pretreated with rolipram (10  $\mu$ M), with/without H89 (1  $\mu$ M) for 10 min, and then challenged with isoprenaline (10  $\mu$ M) for 10 min. Cell clear lysates were probed for PKA phosphorylation of the  $\beta_2$ AR at Ser345/346. The same blot was then stripped and probed with an anti- $\beta_2$ AR antibody.

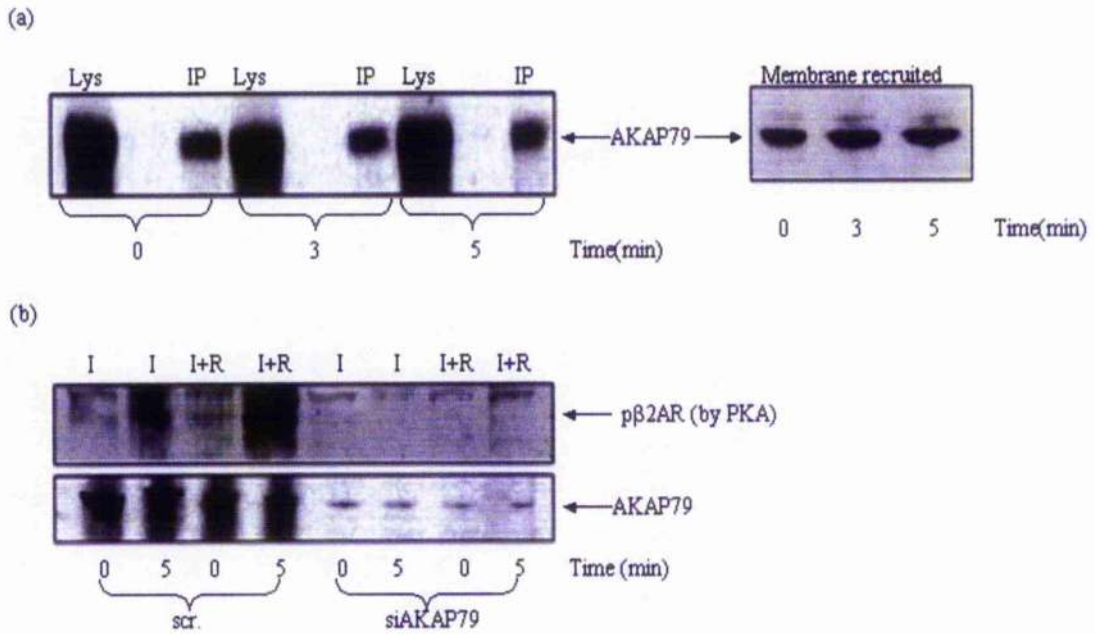


**Figure 3.19 AKAP79-mediated isoprenaline activation of phosphorylation of  $\beta_2$ AR in HEKB2 cells.**

(a) HEKB2 cells were challenged with isoprenaline (10  $\mu$ M) at the indicated time. In the left-hand panel, normalized cells lysates in 3T3 lysis buffer were subjected to immunoprecipitation with a specific anti-Flag antibody, followed by western blotting probed for AKAP79. In the right-hand panel, cells were harvested in KHEM buffer and subjected to membrane fractionation. Normalized membrane (P2) fractions were then probed for AKAP79. (b) HEKB2 cells were transfected with scrambled siRNA for control or siRNA to AKAP79. Following challenged with isoprenaline (10  $\mu$ M) alone or isoprenaline (10  $\mu$ M) plus Rolipram (10  $\mu$ M, 10 min pretreatment) as indicated, cells were harvested in 3T3 lysis buffer. Normalized clear cell lysates were then probed for phosphorylation of  $\beta_2$ AR by PKA. The same blot was stripped and blotted with an anti-AKAP79 antibody. Lys, lysate; IP, immunoprecipitation; scr, scrambled siRNA; siAKAP79, siRNA to AKAP79; I, isoprenaline; R, rolipram.

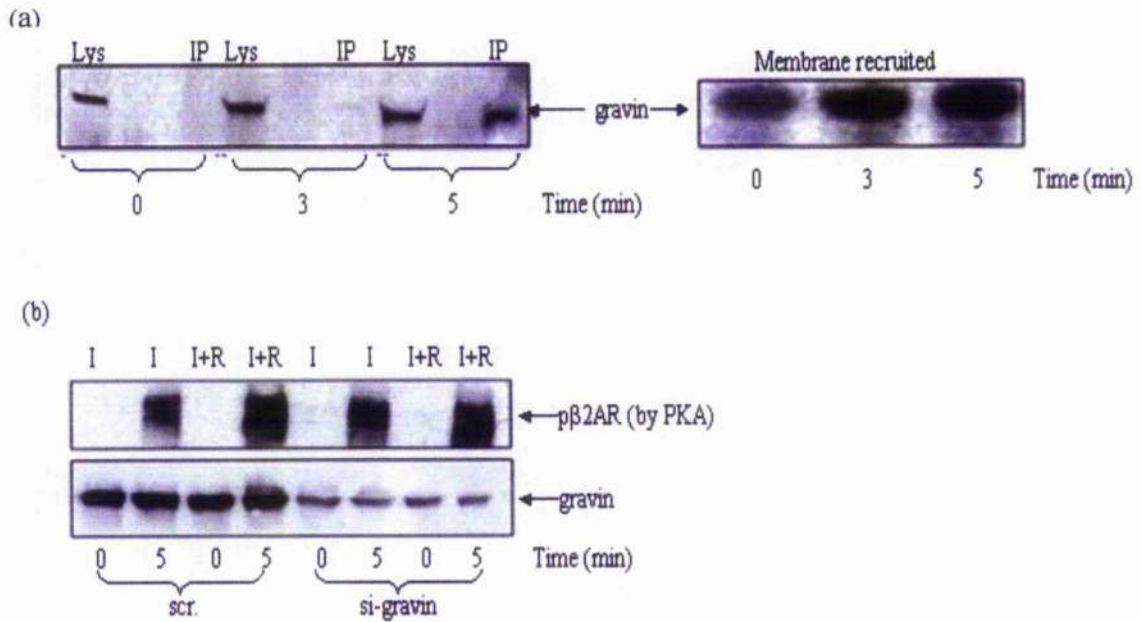


**Figure 3.20 Gravin-mediated isoprenaline activation of phosphorylation of  $\beta_2$ AR in HEKB2 cells.**

(a) HEKB2 cells were challenged with isoprenaline (10  $\mu$ M) at the indicated time. In the left-hand panel, normalized cells lysates in 3T3 lysis buffer were subjected to immunoprecipitation with a specific anti-Flag antibody, followed by western blotting probed for gravin (AKAP250). In the right-hand panel, cells were harvested in KHEM buffer and subjected to membrane fractionation. Normalized membrane (P2) fractions were then probed for gravin. (b) HEKB2 cells were transfected with scrambled siRNA for control or siRNA to gravin. Following challenged with isoprenaline (10  $\mu$ M) alone or isoprenaline (10  $\mu$ M) plus Rolipram (10  $\mu$ M, 10 min pretreatment) as indicated, cells were harvested in 3T3 lysis buffer. Normalized clear cell lysates were then probed for phosphorylation of  $\beta_2$ AR by PKA. The same blot was stripped and blotted with an anti-gravin antibody. Lys, lysate; IP, immunoprecipitation; scr, scrambled siRNA; si-gravin, siRNA to gravin; I, isoprenaline; R, rolipram.

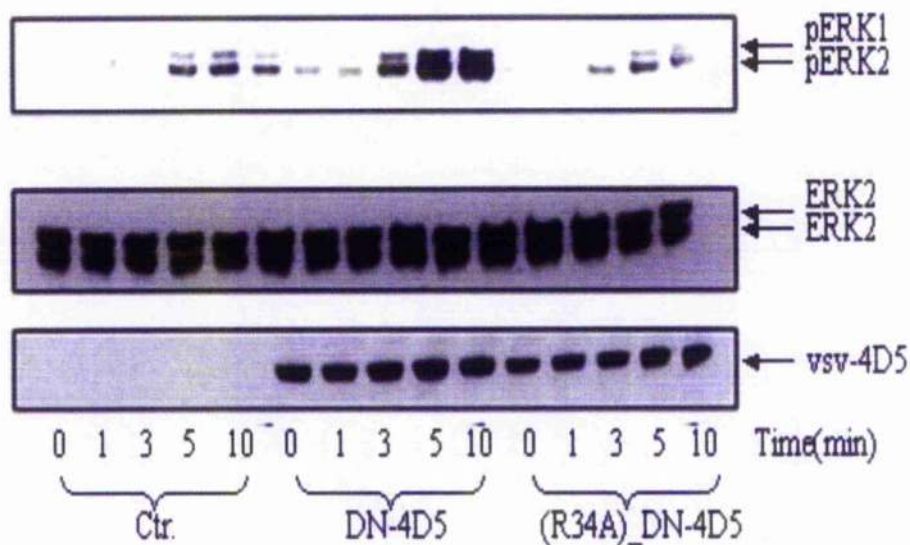
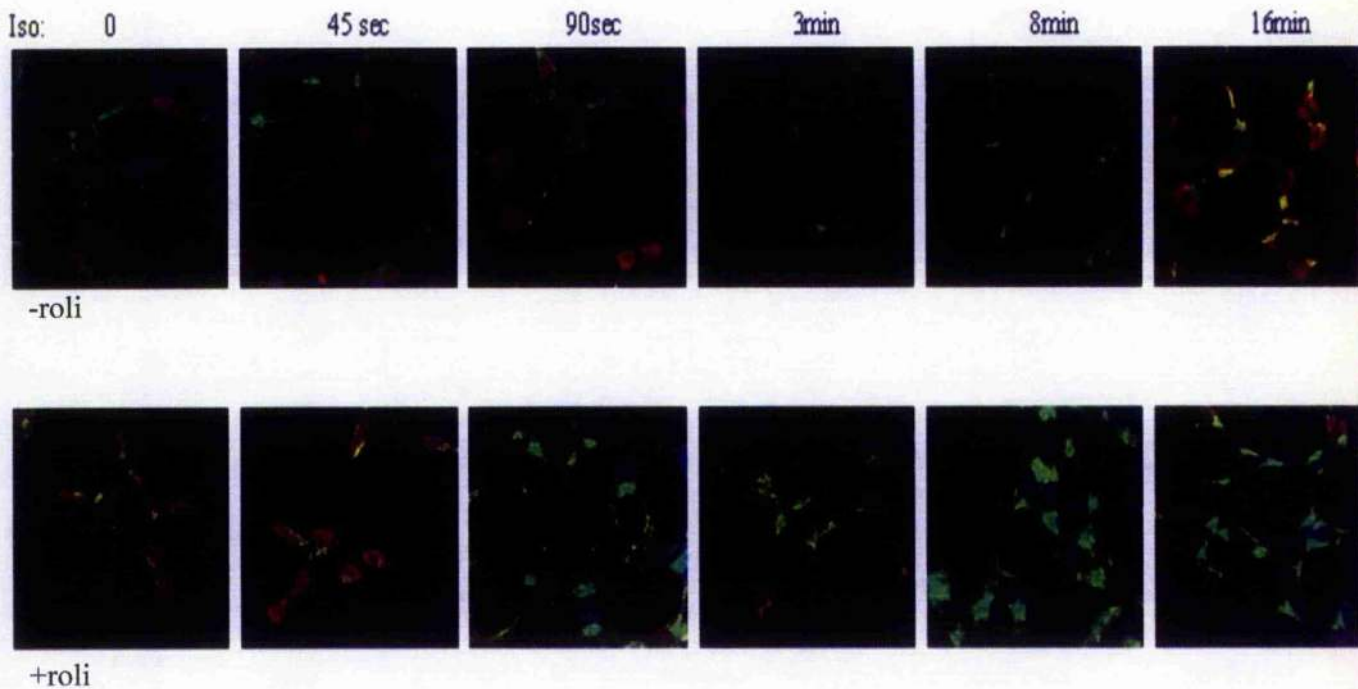


**Figure 3.21  $\beta$ -arrestin-scaffolded PDE4D5 is fundamental to regulate  $\beta_2$ AR switching.**

HEK293 cells were transfected, as indicated, with an empty vector (ctr.) and with vsv-epitope-tagged forms of either a dominant negative PDE4D5 (DN-4D5) or an Arg-34  $\rightarrow$ Ala mutant form of dominant negative PDE4D5 (R34A\_DN-4D5). Then cells were challenged with isoprenaline for a 0~10 min time course. Normalized cell lysates were immunoblotted for pERK1/2, total ERK1/2, and the vsv-epitope tag.



### 3.22 GRK2 phosphorylated $\beta_2$ AR trafficking in HEKB2 cells.

Cells were treated with isoprenaline alone (10 mM) or isoprenaline added together with rolipram (10 mM) or with rolipram alone in each case for the indicated times. Shown are merged fluorescent confocal images of fixed HEKB2 cells stably expressing GFP-tagged  $\beta_2$ AR (green) and stained to detect the GRK phosphorylated form (Ser<sup>355</sup>/Ser<sup>356</sup>) of the  $\beta_2$ AR (red) as well as nuclei [blue; DAPI (4,6-diamidino-2-phenylindole)]. Iso, isoprenaline; -Rol, without rolipram; +Rol, with rolipram pre-treatment.

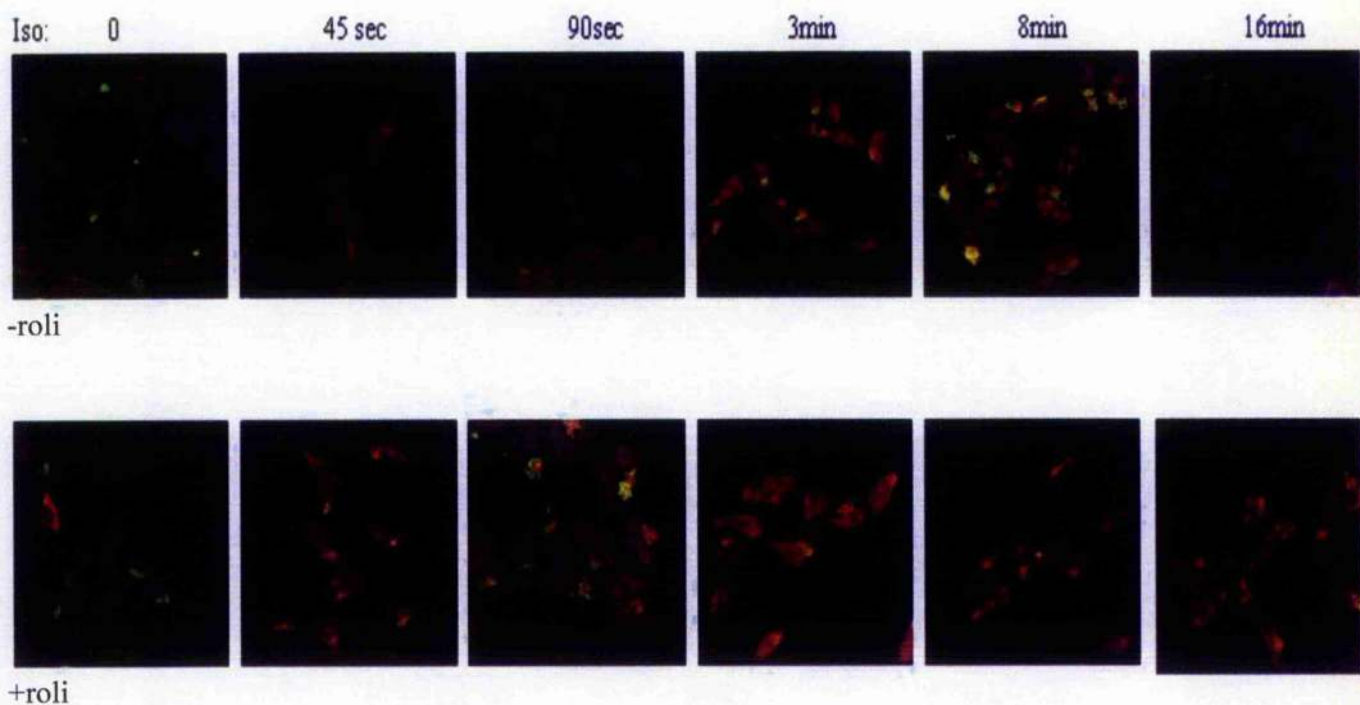


**Figure 3.23 PKA phosphorylated  $\beta_2$ AR trafficking in HEKB2 cells.**

Cells were treated with isoprenaline alone (10 mM) or isoprenaline added together with rolipram (10 mM) or with rolipram alone in each case for the indicated times. Shown are merged fluorescent confocal images of fixed HEKB2 cells stably expressing GFP-tagged  $\beta_2$ AR (green) and stained to detect the PKA phosphorylated form (Ser<sup>345</sup>/Ser<sup>346</sup>) of the  $\beta_2$ AR (red) as well as nuclei [blue; DAPI (4,6-diamidino-2-phenylindole)]. Iso, isoprenaline; -Rol, without rolipram; +Rol, with rolipram pre-treatment.

## **Chapter 4**

### **Analysis of Ubiquitination of PDE4D5 and its functions in HEKB2 cells**

## 4.1 Introduction

Ubiquitin (Ub) is a small polypeptide of 76 amino acids that can be covalently attached to other proteins (Hatakeyama and Nakayama 2003), forming an isopeptide bond between the activated C-terminal glycine of Ub and the  $\epsilon$ -amino group of a lysine residue in the substrate molecule. This occurs through a three-step process involving Ub-activating (E1), Ub-conjugating (E2) and Ub ligase (E3) enzymes (Pickart 2001) (Figure 4.1).

The intrinsic E3 ligase activity serves as the rate-limiting step of Ub modification of substrate proteins and plays a central role in determining the specificity of Ubiquitination. E3s are classified into two groups: the HECT (homology to E6-AP C-terminus) domain-containing E3s and the RING finger-containing E3s. The HECT domain proteins, such as E6-AP, are characterized by their ability to form a thioester intermediate with the activated Ub before transfer of Ub to substrates (Pickart 2001). In contrast, the RING finger-containing E3s, such as Mdm2, do not form a covalent bond with the activated Ub and instead catalyze ubiquitination by association with substrates (Pickart 2001).

Three types of Ub modification can exist on the substrate lysines: mono-ubiquitination, multi-ubiquitination and poly-ubiquitination (Figure 4.2). Mono-ubiquitination, which is defined by the addition of a single Ub to a substrate lysine, can serve as a novel endocytic signal (Hicke 2001; Haglund et al. 2003), whereas poly-ubiquitin chains, formed through one of the internal lysines within the Ub molecule in an iterative process, invariably acts to target substrate proteins for degradation by the proteasome (Pickart 2001). However, it also may serve to modulate diverse biological processes, such as cell cycle progression, apoptosis, antigen presentation and stress response (Weissman 2001). Multi-ubiquitination is formed by several attachments of single Ub to multiple lysine residues on the substrate.

An increasing body of evidence also suggests that the fate of a substrate that undergoes ubiquitination may depend on the type of lysine linkage (K29, K48 or K63) involved in forming poly-ubiquitin chains (Spence et al. 2000; Weissman 2001; Koegl

et al. 1999). For example, addition of ubiquitin chains using lysine 63 linkage on Ub generally leads to non-proteolytic events (eg DNA repair, endocytosis), whereas addition of Ub using position 48 signals for proteasome-mediated degradation.

Some short protein motifs and domains have been shown to bind Ub or substrate-bound Ub moieties and therefore have the potential to establish a network of protein-protein interactions (Pickart 2000). To date, it is clear that at least six conserved Ub binding modules exist (Schnell and Hicke 2003), the structures of five of which have been determined, including the UIM (Ub interacting motif) (Hofmann and Falquet 2001), UBA (Ub-associated domain) (Mueller et al. 2004), UEV (Ub E2 variant domain) (Pomillos et al. 2002), NZF (npl4 zinc finger domain) (Meyer et al. 2002), and CUE (coupling of Ub conjugation to ER degradation domain) (Ponting 2000). Each of these motifs can allow the binding of Ub *in vitro*, and the motifs are invariably used in a modular fashion to add Ub binding functionality to a large variety of multifunctional proteins *in vivo*.

The initial identification of the UIM originated from studies of the S5a subunit of the 19S regulator in the human 26S proteasome (Deveraux et al. 1994) and a more general UIM has been defined as a 20 residue sequence corresponding to the consensus: X-Ac-Ac-Ac-Ac-Φ-X-X-Ala-X-X-X-Ser-X-X-Ac-X-X-X-X, where Φ represents a large hydrophobic residue (typically Leu), Ac represents an acidic residue (Glu, Asp), and X represents residues that are less well conserved (Hofmann 2001). UIM occurs in a wide range of proteins, many of which are endocytic proteins that function in the pathway of endocytosis and vacuolar protein sorting (Hofmann 2001). Recently, a number of studies have suggested that UIMs can direct protein ubiquitination in substrates such as Eps15, Vps27p and Hrs (Miller et al. 2004; Polo et al. 2002; Klapisz et al. 2002; Oldham et al. 2002).

The prevalence of the UIM and its importance in a number of biological processes (Hofmann and Falquet 2001) has initiated the studies described here and in particular my observation by sequence analysis of the presence of a putative UIM motif in PDE4D.

The aims of this chapter are to identify a UIM motif in the C-terminal domain of the PDE4D5 isoform and show if it can act as an important modulator for the ubiquitination of this isoform. I show here that this motif acts as a ubiquitination signal for combined mono-ubiquitination and poly-ubiquitination. Although it is difficult to dissect the functional outcomes of these two ubiquitination types, I have shown here that the ubiquitination of PDE4D5 is important in modulating its binding to the signalling scaffold protein,  $\beta$ -arrestin.

Recent studies have revealed that  $\beta$ -arrestin serves as an adaptor to bring unknown E3-ligases to proximity of  $\beta_2$ ARs, leading to receptors ubiquitination (Shenoy et al. 2001). This finding, complete with the strong link between PDE4D5 and  $\beta$ -arrestin (Bojger et al. 2003) have prompted me to investigate the extent of the  $\beta$ -arrestin involvement in the ubiquitination of PDE4D5. Following the previous observations, I also show that  $\beta$ -arrestin is crucial for ubiquitination of PDE4D5 by acting as an adaptor for the Mdm2 E3 ligase.

## 4.2 Results

### 4.2.1 Isoprenaline-stimulated ubiquitination of PDE4D5 in HEKB2 cells

Sequence analysis of PDE4D5 reveals a short motif with high homology to a UIM (slight difference in the UIM position 9) at its C-terminal region (Figure 4.3). Indeed, this motif is conserved in all PDE4D subfamily members, but not in other PDE4 subfamilies. As UIM domains have been reported to be required for mono-ubiquitination of some proteins (Miller et al. 2004; Polo et al. 2002; Klapisz et al. 2002; Oldham et al. 2002), I set out to determine whether the putative UIM motif present in PDE4D5 modulates its own ubiquitination. To evaluate the possible Ub modification of PDE4D5, I first investigated whether VSV epitope-tagged PDE4D5 could undergo isoprenaline-induced ubiquitination in HEKB2 cells. Human VSV-tagged PDE4D5 was transiently transfected into HEKB2 cells. After 48hr, HEKB2 cells were stimulated with the  $\beta$ -adrenergic agonist isoprenaline for the indicated times and VSV-PDE4D5 was isolated by immunoprecipitation with VSV-agarose (Figure 4.4). The ubiquitinated VSV-PDE4D5 was detected by western blotting the IP samples using a specific Ub antibody, while VSV-PDE4D5 was detected with an anti-VSV antibody. As shown in Figure 4.4 a, a distinctive smear band, which is typical of

ubiquitinated proteins (Christianson and Green 2004; Mimnaugh and Neckers 2005), was observed in the anti-Ub immunoblot at 10 min agonist challenge. Such ubiquitination of PDE4D5 appeared to be due to either different-length ubiquitin chains attached to a single lysine site of PDE4D5, several different length polyubiquitin chains conjugated to multiple lysine residues within the protein, or the combination of both types of ubiquitin modification.

These data show that human VSV-PDE4D5 undergoes at least poly-ubiquitination in HEKB2 cells upon isoprenaline stimulation for 10 min. In order to exclude the artifacts that might result from the overexpression of VSV-PDE4D5, I also examined the endogenous PDE4D5 ubiquitination status upon  $\beta$  agonist challenge in HEKB2 cells. Here I showed that endogenous PDE4D5 in HEKB2 cells displayed an ubiquitination pattern similar to VSV-PDE4D5 as shown by the presence of smear band detected on the anti-ubiquitin immunoblot (Figure 4.4 c). This result suggests that the ubiquitination of VSV-PDE4D5 was not influenced by the presence of the VSV tag.

#### **4.2.2 UIM of PDE4D5 is critical for ubiquitination**

The PDE4 family is composed of 4 different genes, PDE4A, PDE4B, PDE4C, and PDE4D, which generate different isoforms due to the distinct translation starting sites and spliced variants (Houslay and Adams 2003). Each isoform is characterized a unique N-terminal region and the C-terminal region of each isoform is conserved within the same subfamily gene (Houslay and Adams 2003). Sequence analysis of PDE4D gene shows the presence of the UIM domain in their C-terminus (Figure 4.3), indicating that the various isoforms produced by of this gene might undergo ubiquitination. In contrast, no putative UIM was observed in the cognate region of the PDE4A, PDE4B and PDE4C genes (Fig 4.3). Thus, in order to assess whether PDE4A, PDE4B and PDE4C display a ubiquitination pattern, I studied the ubiquitination of transiently transfected VSV-tagged human PDE4A, VSV-tagged human PDE4B and VSV-tagged human PDE4C isoforms in HEKB2 cells. Here I showed that stimulation of HEKB2 cells with isoprenaline did not trigger ubiquitination of either PDE4A5, PDE4B1, PDE4B3, PDE4B4 or PDE4C1 (Figure 4.5). Interestingly, isoprenaline stimulation of HEKB2 cells also failed to induce ubiquitination of VSV-PDE4D3

(Figure 4.6 b). Looking into the PDE4D3 sequence, it contains the same UIM sequence as PDE4D5 (Figure 4.6 a). Therefore, molecular determinants other than UIM itself must contribute to decide upon ubiquitination, to allow for this isoform specificity within the PDE4D sub-family.

Fisher et al. (2003) have suggested that the conserved N-proximal acid patch within UIM seems to be most important in contributing Ub binding (Fisher et al. 2003). To determine if the acid patch 723EEE is involved in PDE4D5 ubiquitination, I created a triple point mutation at amino acids 723, 724 and 725 (723E) in the VSV-tagged PDE4D5 construct (Figure 4.7 a) and studied its ubiquitination using the in vivo ubiquitination assay. Here I showed that the mutation of this region in the UIM (723EEE→AAA) abrogated the ability of PDE4D5 to be ubiquitinated in HEKB2 cells upon challenge with isoprenaline (Figure 4.7 b). This indicates that PDE4D5 has a functional UIM and that the three glutamates at the N-terminal end of this UIM are critical for its functioning.

#### **4.2.3 Vasopressin-stimulated ubiquitination of PDE4D5 in HEKV2 cells**

GPCRs are categorized into Class A and Class B, based on their binding kinetics with  $\beta$ -arrestins (Oakley et al. 2000). The  $\beta_2$ AR and V<sub>2</sub>R, respectively, act as prototypes for these two groups of GPCRs. To evaluate the different effects of two GPCR types on the PDE4D5 ubiquitination, I used HEKV2 cells stably overexpressing vasopressin V<sub>2</sub> receptor to perform the in vivo ubiquitination assay. I transiently transfected HEKV2 cells with VSV-tagged PDE4D5 and stimulated them with vasopressin for different times. The VSV-PDE4D5 was isolated on the VSV-agarose and immunoblotted with a specific ubiquitin antibody as before. Strikingly, unlike the highly transient ubiquitination of 4D5 in HEKB2 cells, VSV-PDE4D5 underwent ubiquitination over a much longer time course in the HEK V<sub>2</sub> cells (Figure 4.8, left upper panel). This phenomenon is reminiscent of the ubiquitination of Class B receptors e.g. V<sub>2</sub>R (Martin et al. 2003) and  $\beta$ -arrestin in HEKV2 cells (Shenoy et al. 2001).

The same membrane was stripped and immunoblotted with VSV to confirm the equal pull-downed VSV-PDE4D5 (Figure 4.8, left lower panel). As was the case

in HEKB2 cells after isoprenaline treatment, the VSV-PDE4D5 723E mutant ablated PDE4D5s ability to be ubiquitinated upon vasopressin challenge in HEKV2 cells (Figure 4.8, middle panel). Control experiments were done in non-transfected V2 cells and no ubiquitination signal was detected in the VSV-immunoprecipitated samples (Figure 4.8, right panel).

#### 4.2.4 Requirement of $\beta$ -arrestin binding for PDE4D5 ubiquitination

Previous studies have shown that  $\beta$ -arrestin2 is necessary for  $\beta_2$ AR ubiquitination (Shenoy et al. 2001). In HEKB2 cells, it is also known that  $\beta$ arrestin preferentially binds to PDE4D under basal conditions and recruits PDE4D to the plasma membrane upon isoprenaline challenge (Perry et al. 2002). To test whether the association between PDE4D5 and  $\beta$ -arrestin is required for PDE4D5 ubiquitination, I compared the ubiquitination of wild type VSV-PDE4D5 with that of  $\beta$ -arrestin binding defective VSV-PDE4D5, in which a critical  $\beta$ -arrestin site was mutated to alanine (VSV-PDE4D5 E27A). In HEKB2 cells, isoprenaline treatment led to ubiquitination of wild type VSV-PDE4D5 but not the mutant VSV-PDE4D5 E27A (Figure 4.9 a, b).

As PDE4D5 is known to exist in a complex with the multi-function scaffold protein  $\beta$ -arrestin and it is know that  $\beta$ arrestin itself is modified by ubiquitin after  $\beta$ -adrenergic stimulation challenge (Shenoy et al. 2001), it is important to exclude the possibility that the detected ubiquitination in immunopurified PDE4D5 samples is in fact that of associated  $\beta$ -arrestin and not PDE4D5 per se. To this end, I performed the *in vivo* ubiquitination assay for  $\beta$ -arrestin. HEKB2 cells transfected with wild type VSV-PDE4D5 were stimulated with isoprenaline for different times. The endogenous  $\beta$ -arrestin was isolated on Protein G beads using a specific  $\beta$ -arrestin antibody and the IPs subjected to Western blotting with an antibody specifically against Ub. The ubiquitinated  $\beta$ -arrestin was detected as a smeared band on the Western blot at 15 min after isoprenaline challenge, consistent with the previous finding (Shenoy et al. 2001). Interestingly,  $\beta$ -arrestin ubiquitination occurred 5 min later than did the ubiquitination of VSV-PDE4D5 (Figure 4.9 c). Thus supports the notion that the ubiquitination of PDE4D5 and  $\beta$ -arrestin are indeed two separate processes.

#### **4.2.5 Interaction of the E3 Ub ligase Mdm2 with PDE4D5**

The finding that  $\beta$ -arrestin binding is required for PDE4D5 ubiquitination suggests that  $\beta$ -arrestin might serve as an adaptor protein that bridges PDE4D5 to the ubiquitination machinery. It has been shown that  $\beta$ -arrestin links RING finger E3 ligase Mdm2 to the  $\beta_2$ AR and initiates its ubiquitination. It is likely, therefore, that PDE4D5 is ubiquitinated in a similar manner. Work in this chapter has already shown that ablation of the ability of PDE4D5 to bind  $\beta$ -arrestin leads to its loss of ubiquitination (Figure 4.9 b). Here, I set out to examine if this observation came from a diminished/abolished association between PDE4D5 and Mdm2.

To assess the PDE4D5-Mdm2 association in HEKB2 cells, I transiently transfected HEKB2 cells with VSV-tagged wild type PDE4D5, a mutant PDE4D5 that does not bind to  $\beta$ -arrestin (PDE4D5 E27A), a mutant PDE4D5 that does not bind to RACK1 (PDE4D5 L29/30A) and a UIM mutant (PDE4D5 723E). I then evaluated their interactions with Mdm2 by immunoprecipitation and immunoblotting. Mdm2 associated more with VSV-PDE4D5 L29/30A and wild type VSV-PDE4D5, but less with VSV-PDE4D5 723E and least with VSV-PDE4D5 E27A (Figure 4.10 a). Recently, it was discovered that  $\beta$ -arrestin and RACK1 mutually interact with PDE4D5 (Bolger et al. 2006). This finding may explain the fact that Mdm2 associates more with PDE4D5 L29/30A as it has been shown to bind a larger pool of  $\beta$ arrestin than wild type PDE4D5. I also performed a reverse IP whereby the four different types of VSV-tagged PDE4D5 were isolated on the VSV-agarose and their association with Mdm2 was analyzed by immunoblotting the IP samples with a specific Mdm2 antibody. These results again showed that ablation of the interaction between PDE4D5 with  $\beta$ -arrestin (PDE4D5 E27A) severely attenuated the association between PDE4D5 and Mdm2 (Figure 4.10 b), confirming that PDE4D5-bound  $\beta$ arrestin is responsible for placing Ub E3 ligase Mdm2 in close proximity to PDE4D5, therefore mediating its ubiquitination (Figure 4.9).

#### **4.2.6 The ubiquitination signals of VSV-PDE4D5 are composed of mono-ubiquitination and poly-ubiquitination**

In vivo, three types of poly-ubiquitin chains can be formed by different types of linkages within Ub: namely K29, K48, and K63. These are found on a number of

ubiquitin-modified substrate proteins (Pickart 2001). Since each chain type may assume a different conformation (Varadan et al. 2002), it has been suggested that different types of ubiquitin conjugates have the potential to decide substrate proteins' fate. To test the type of poly-ubiquitin chain attached to VSV-PDE4D5 (Figure 4.4), and therefore better understand the functional outcome of PDE4D5 ubiquitin modification, three HA-tagged Ub mutants, K48R (lacking any K48-polyubiquitin chain), K63R (lacking any K63-polyubiquitin chain) or the triple mutant K29, K48, K63R (absence of the major polyubiquitin chains) were used. Mutants and HA-tagged wild type Ub were transiently co-transfected with VSV-PDE4D5 into HEKB2 cells and assayed for isoprenaline-stimulated ubiquitination. As shown in Figure 4.11, both wild type HA-Ub and HA-UbK63R displayed ubiquitination. However, the ability of PDE4D5 to be poly-ubiquitinated was severely attenuated when K48 was mutated to R, whereas little polyubiquitination signal on PDE4D5 immunoprecipitates was detected (Figure 4.11). In addition, when K29, K48 and K63 of HA-Ub were all mutated to arginine (R), the polyubiquitin chains on VSV-PDE4D5 were completely inhibited (Figure 4.11). Collectively, these findings indicated that the polyubiquitin chains on PDE4D5 upon isoprenaline stimulation were composed of K29-linked polyubiquitin chains, K48-linked polyubiquitin chains and K63-linked polyubiquitin chains, and that K48-linked polyubiquitin chains predominated. Notably, a distinct HA band separate from the high molecular weight smear was detected as the same molecular weight as VSV-PDE4D5, indicative of mono-ubiquitinated form of PDE4D5. Thus, prevention of the ubiquitin chain formation does not influence the single ubiquitin modification on PDE4D5 (Figure 4.11).

#### **4.2.7 Isoprenaline stimulates the association of VSV-PDE4D5 with proteasome 19S regulatory subunits 19S1, 19S2 and 19S5a in a time-dependent manner**

I have suggested above that PDE4D5 undergoes K48-linked polyubiquitination upon isoprenaline stimulation in HEKB2 cells. As it is well-known that proteins which possess K48-Ub chains target proteins to the proteasome (Pickart 2001), and some 19S regulatory subunits of 26 proteasome serve to recognize the multi-ubiquitin chains (Glickman 2000), I set out to examine whether ubiquitinated PDE4D5 associates with 19S subunits. To determine whether PDE4D5 can interact with 19S subunits, I expressed VSV-tagged wild type PDE4D5 in HEKB2 cells and stimulated the cells with isoprenaline for different times. Both cell lysates and the

isolated VSV-PDE4D5 on VSV-agarose from these lysates were separated by SDS-PAGE and Western blotted with a specific antibody raised against one of a variety of 19S subunits. Time-dependent increases in the association of PDE4D5 with 19S2 and 19S5a were observed, however, no interactions were detected between PDE4D5 and 19S1, 19S6 or 19S12 (Figure 4.12). To further confirm that this association is ubiquitin dependant, I sought to determine whether PDE4D5 ubiquitination mutant (PDE4D5 723E) would lose its ability to interact with 19S subunits. To this end the experiment was repeated after transient transfection of VSV-PDE4D5 723E into HEKB2 cells. As shown in Figure, stimulation of HEKB2 cells with isoprenaline did not have any effect on PDE4D5 723E association with 19S subunits (Figure 4.13). These results clearly indicate that polyubiquitin chains on PDE4D5 orchestrated by its UIM indeed serve to target PDE4D5 to the 19S regulatory subunits.

#### **4.2.8 Isoprenaline promotes PDE4D5 interaction with $\beta$ -arrestin in HEKB2 cells via a ubiquitination-dependent process**

To explore the biological function of PDE4D5 ubiquitination, I examined the effect of ubiquitin addition on the interaction of PDE4D5 with  $\beta$ -arrestin. It is well known that their association and subsequent translocation to the plasma membrane are crucial in the regulation of  $\beta_2$ AR desensitization (Perry et al. 2003; Lynch et al. 2005). Work described earlier in this chapter shows that the ubiquitination of PDE4D5 reached a peak at 10 min post isoprenaline challenge. Therefore, a broader time window would be beneficial to examine the effect of ubiquitination on PDE4D5 interaction with  $\beta$ -arrestin. Wild type VSV-PDE4D5 or mutant VSV-PDE4D5 723E was singly transfected into HEKB2 cells, and after 48hr, isoprenaline was administered for different times. Endogenous  $\beta$ -arrestin was isolated by immunoprecipitation and the  $\beta$ -arrestin-bound VSV-PDE4D5 or VSV-PDE4D5 723E was detected by Western blotting using an anti-VSV antibody. Clearly, under basal conditions,  $\beta$ -arrestin binds more to wild type PDE4D5 than to mutant PDE4D5 723E and the association between wild type PDE4D5 and  $\beta$ -arrestin (but not 4D5 723E) was noticeably enhanced up to 10 min isoprenaline treatment after which it started to decrease (Figure 4.14 a, b). Interestingly, the kinetics of this interaction between PDE4D5 and  $\beta$ -arrestin bore a striking resemblance to the kinetics of PDE4D5 ubiquitination (Figure 4.14 c, d, e). This suggests that the direct effect of Ub

modification of PDE4D5 is to strongly increase its binding to  $\beta$ -arrestin and therefore increase the amount of PDE4D5 which translocates to activated receptors with  $\beta$ -arrestin. This may have important consequences for the kinetics of receptor desensitization.

#### **4.2.9 In vitro ubiquitination assay on peptide array of PDE4D5 identifies two regions where the ubiquitin acceptors reside**

To date, it has proved impossible to accurately predict the sites of Ub on proteins as no clear consensus has been reported. Indeed, in many cases, a variety of lysines within locations having different sequences of substrate proteins are capable of functioning as Ub acceptor sites (King et al. 1996; Hou et al. 1994; Crook et al. 1996). Therefore, mutation of single lysine or a combination of several lysines to determine the actual lysine site that is ubiquitinated in PDE4D5 requires much effort. In the hope of circumvent this practical difficulty, I used a novel methodology by performing *in vitro* ubiquitination assays on peptide arrays that covered the entire PDE4D5 sequence. The peptide arrays consist of overlapping peptides (25 mers), sequentially shifted by 5 amino acids to include the complete PDE4D5 sequence, which were then spotted on nitrocellulose. The prevalent application of this peptide array analysis will be extensively explored in Chapter 6. *In vitro* ubiquitination of the full-length PDE4D5 array was achieved using a commercial kit and purified GST-Mdm2 was a kind gift from Professor Ron Hay at Dundee University. The membrane was then probed with an antibody against Ub. Positive Ub signals were noted as dark spots and negative Ub signals were observed as clear areas. Figure 4.15 shows that two separate regions of PDE4D5 provide the lysines as Ub acceptors: one area spans the amino acid sequence of peptide 10, 11, 12 and 13 (amino acids 46-85), another is spanning the sequence of peptide 28, 29 and 30 (amino acids 136-170) (Figure 4.15).

Scanning alanine mutagenesis in two-hybrid and pull-down assay is a commonly used analytical method to aid identification of motifs that define sites of interaction between proteins. Scanning alanine mutagenesis is combined with peptide array technology to further identify lysines involved in Region 1. Instead of the full-length sequence of PDE4D5, a family of peptides derived from a 25-mer parent peptide 10 whose sequence reflected amino acids 46-70 of PDE4D5 were used. These

peptides each had a single substitution of successive amino acids to alanine in the sequence to form the scanning peptide array. The *in vitro* ubiquitination assay on peptide 10 alanine scan array did not show any reduction of the ubiquitin signal (Figure 4.16), suggesting that single mutation of a lysine in this sequence of peptide 10 was not enough to ablate the modification. Other lysines within the same sequence may compensate for a single alanine substitution. In the case of peptide 10, two lysines are present (Figure 4.15 b). Control studies were performed with peptide 3 and 5 alanine scan arrays (Figure 4.16) and no ubiquitination was observed.

### 4.3 Discussion

In this chapter, it has been demonstrated that the ubiquitin-interacting motif (UIM) present on PDE4D5 confers its ability to undergo ubiquitination, by K48-linked and K63-linked polyubiquitin chains. Post-translational modification often serves to modulate the functions of substrate proteins (Jenson 2004). Here I show that ubiquitinated PDE4D5 displays an enhanced association with certain proteasome 19 regulatory subunits (Figure 4.12), as well as increased binding to  $\beta$ -arrestin (Figure 4.14). Changes in the proportion of  $\beta$ -arrestin-bound PDE4D5 can lead to a higher percentage of cAMP-degrading PDE4D5 recruited to the plasma membrane upon isoprenaline challenge in HEKB2 cells (Perry et al. 2002). The data presented here suggests that ubiquitination of this cAMP phosphodiesterase isoform may be required for efficient receptor desensitization as the modification would not only promote localized cAMP hydrolysis (down regulating further the PKA phosphorylation of the  $\beta_2$ AR) but also initiate the degradation of PDE4D5 after it has performed its essential function. Both of these actions would serve to reset the receptor for another round of agonist challenge.

The four PDE4 genes generate over 20 different isoforms, each of which is unique in their N-terminal region. In addition, the C-terminal regions from each of the four subfamilies are distinct, the role of which is still ill-understood (Houslay 2005). I, for the first time, show that one of the functions of these distinct extreme C-terminal of PDE4 isoforms is to direct their own ubiquitination via the UIM. PDE4A5, PDE4B1, PDE4B3 and PDE4B4 do not contain a UIM in their extreme C-terminus unlike PDE4D5, which might explain the differences observed in agonist mediated

ubiquitination of these species (Figure 4.5). Interestingly, although the UIM is present in PDE4D3, another long isoform of PDE4D gene subfamily, it does not confer the ability of PDE4D3 to be ubiquitinated in HEK293 cells upon  $\beta_2$ AR activation (Figure 4.6 b). This observation can be explained as such: there are molecular determinants, other than UIM, that are required for the ubiquitination of PDE4D3. One may argue that the lack of ubiquitination on the isoform PDE4A5, PDE4B1, PDE4B4 and PDE4D3 are due to the 'wrong' stimuli. Although I did not screen for other conditions of stimuli to test the possibilities of their ubiquitination, I preclude the possible artificial functional importance of UIM in PDE4D5 ubiquitination by mutating highly conserved acidic acids (glutamates) (723E), which completely abolished the ubiquitination of PDE4D5 (Figure 4.7 b).

It has been suggested that, *in vivo*, most UIMs tested biochemically display a preference binding to polyubiquitin chains, with respect to monoubiquitin (Polo et al. 2002). However, to date, in the case of UIM-dependent substrate protein self-ubiquitination, it exclusively appears to be monoubiquitin modification (Polo et al. 2002; Hofmann and Falquet 2001). My finding that PDE4D5 undergoes a UIM-dependent polyubiquitination therefore suggests a UIM-directed versatile Ub modification exists. This is consistent with Miller et al.'s finding (Miller et al. 2004) that the presence of an UIM does not exclusively promote monoubiquitination, but rather a mixture of mono-, multi- and polyubiquitination.

Two classes of GPCRs have been identified with respect to their distinct kinetics of  $\beta$ arrestin binding. The  $\beta_2$ AR belongs to Class A receptors, which bind  $\beta$ -arrestin transiently during endocytosis and have a slightly higher affinity for the  $\beta$ -arrestin2 isoform (Oakley et al. 2000). However, the  $V_2$ R, which is classified as Class B receptor, is able to bind  $\beta$ arrestin more stably and shows equal affinity for  $\beta$ -arrestin1 and  $\beta$ -arrestin2. I have examined the ubiquitination status of PDE4D5 in these two receptor systems and found strikingly different kinetics of deubiquitination of PDE4D5 with respect to the two classes of receptors. Stimulation of the  $\beta_2$ AR leads to transient PDE4D5 ubiquitination (Figure 4.4), whereas when  $V_2$ R is stimulated, PDE4D5 remains stably ubiquitinated (Figure 4.8). Interestingly, previous studies have shown that  $\beta$ -arrestin also exhibits similar kinetics of deubiquitination in these

two model receptor systems (Shenoy and Lefkowitz 2003). As PDE4D5 is known to preferentially bind to  $\beta$ -arrestin compared to other PDE4 isoforms (Bolger et al. 2003), this coincidence of the same pattern of ubiquitination in PDE4D5 and  $\beta$ -arrestin in the two receptor systems reflects the presence of an important factor that bridges these two proteins' namely ubiquitin modification.

I have shown that  $\beta$ -arrestin binding to PDE4D5 is required for PDE4D5 ubiquitination (Figure 4.9). This suggests that  $\beta$ -arrestin may serve as an adaptor that links PDE4D5 to the ubiquitination machinery. It has been known that the oncoprotein Mdm2, a negative regulator of p53, interacts with  $\beta$ -arrestin at endogenous level of the two proteins (Shenoy et al. 2001). Mdm2 contains a RING (really interesting new gene) domain at its C-terminus and catalyses the ubiquitination of  $\beta$ -arrestin. PDE4D5 ubiquitination, which in itself requires  $\beta$ -arrestin, is mediated by Mdm2 that is brought by the adaptor protein  $\beta$ -arrestin in close proximity to PDE4D5. The similar crucial role of  $\beta$ -arrestin in acting as adaptor for the Mdm2 E3 ligase has been underlined in the case of ubiquitination of Insuline-like Growth Factor-1 Receptor (IGF-1R) (Girnita et al. 2005). In addition, although the E3-ligase for ubiquitination of  $\beta_2$ AR is still unknown,  $\beta$ -arrestin is known to be required as an adaptor to bring E3-ligases to close proximity (Shenoy et al. 2001).

My findings indicate that Mdm2 only forms a complex with  $\beta$ -arrestin-bound PDE4D5 (Figure 4.10), and this may explain the loss of detection of PDE4D5 ubiquitination on PDE4D5 mutants that cannot bind to  $\beta$ -arrestin (Figure 4.9 b). More convincingly, 4D5 ubiquitination was attenuated when endogenous Mdm2 was knocked down using siRNA (data not shown). Interestingly, mutation of PDE4D5 UIM resulted in both a decreased association between PDE4D5 723E and Mdm2 (Figure 4.10) and an ablation of ubiquitinated PDE4D5 (Figure 4.7 b). This might suggest that in the case of PDE4D5, Mdm2 exerts its substrate specificity on the recognition code – UIM domain. In other words, Mdm2 might recognize the UIM on PDE4D5 and recruit the E2-conjugated Ub to the substrate protein, PDE4D5, therefore mediating its ubiquitination. If this is true, overexpression of another UIM-containing protein may lead to a decrease in PDE4D5 ubiquitination.

Ub has 7 lysine residues and at least five of them (K6, K11, K29, K48, and K63) can function as a linkage for polyubiquitin chains (Passmore and Barford 2004). It is now well accepted that different types of ubiquitin linkages have the potential to decide the modified proteins' fate (Weissman 2001). PDE4D5 has been shown to be conjugated with Ub-chains (Figure 4.7 b), therefore it is of importance to dissect which type of linkage mediates this modification as this may provide evidence as to the function of such an event. Although Ub contains seven lysine residues, they are not used with the same frequency in polyubiquitin chain assembly. The predominant linkages observed are Lys48-Gly76 (Chau et al. 1989), Lys29-Gly76 (Mastrandrea et al. 1999), and Lys63-Gly76 (Seibenhener et al. 2004), of which K48-linked chains appear to be the most frequently used signal. Mutation of K48 (so that K48-linked Ub chain can not occur) nearly abolished the detection of PDE4D5 ubiquitination to a similar degree as the triple K mutant (K29, 48, 63R), suggesting that K48-linked chain is predominantly present on PDE4D5 when PDE4D5 is ubiquitinated. Further study of K63-linked chain shows that blocking the formation of K63-linked ubiquitins also contributes to the ubiquitination signals of PDE4D5, as mutation of K63 to arginine also somewhat reduces PDE4D5 polyubiquitination (Figure 4.11). As the other lysine mutant ubiquitins were unavailable I did not study the possibility of their presence on PDE4D5. However, at least in the case of PDE4D5, K29, K48 and K63 are most important in forming the polyubiquitin chains as mutating of all these lysines totally ablated the detection of PDE4D5 polyubiquitination (Figure 4.11).

The canonical Ub signal, a K48-linked polyubiquitin chain, is known to target substrate proteins to the 26S proteasome degradation pathway (Layfield et al. 2003). The 26S proteasome comprises two main particles: the 20S core proteasome and 19S regulatory complex (Figure 4.17). The 19S regulatory particle confers substrate specificities (Glickman 2000) via the UIM-containing subunit 19S5a (also known as Rpn10) and recently, another subunit Rpt5 is suggested to have a role in recognizing polyubiquitinated proteins (Lam et al. 2002). The 18 subunits of each 19S cap can be grouped into the Lid and the Base (Figure 4.17), which are tethered by the two largest subunit S1/Rpn2 and S2/Rpn1 (Voges et al. 1999).

Due to the limited availability of commercial antibodies against 19S subunits, I picked one subunit from the Base (19S6), two from the Lid (19S12 and 19S5a) and

the two joint subunits (19S1 and 19S2) to study the interactions with PDE4D5 under conditions where PDE4D5 is ubiquitinated. Compared to the PDE4D5 Ub mutant 723E, wild type PDE4D5 associates with 19S1, 19S2 and 19S5a in a time-dependent manner (Figure 4.12 a, b, e). This suggests that ubiquitinated PDE4D5 are targeted to the 26S proteasome for degradation by these specific 19S subunits. It is well known that 19Sa recognizes polyubiquitin chains through its prototype UIM domains UIM1 (LALAL) and UIM2 (IAYAM) (Pickart 2000). Interestingly, the two proteins of the 19S regulatory complex, 19S1 and 19S2, have also been shown to contain a number of repeated sequences that resemble the LALAL or IAYAM found within the UIM1 and UIM2 regions of 19S5a (Young et al. 1998). Recently Rpn1 is indicated to recognize Ub-like proteins (Elsasser et al. 2002). The findings presented here, provide an independent experimental support that in addition to 19S5a, 19S2 can also recognize the ubiquitinated proteins in vivo and potentially target these proteins for 26S proteasome degradation.

Ub modifications have also been suggested to signal nonproteolytic, reversible events, such as changes in protein activity, subcellular localization or protein-protein interactions (Schnell, and Hicke 2003). It is clear from the data outlined above, that ubiquitination of PDE4D5 changes its ability to bind to  $\beta$ -arrestin (Figure 4.14). Recently, it has been shown that  $\beta$ -arrestin forms a complex with PDE4 enzymes, thereby providing a means of delivering a cAMP-degrading enzyme to the plasma membrane in an agonist-dependent fashion (Perry et al 2002). My findings suggest that ubiquitination of the PDE may be essential to promote efficient complex formation and translocation (Figure 4.14 a). It is apparent that in response to isoprenaline in HEK293 cells, the ability of wild type PDE4D5 to bind  $\beta$ -arrestin increases within 10 min, followed by a slight decrease afterwards. The kinetics of the PDE4D5 binding to  $\beta$ -arrestin coincidentally match that of the Ub modification of PDE4D5 (Figure 4.14 c). Indeed, the ubiquitination and deubiquitination of PDE4D5 may synchronize the kinetics of binding and release between PDE4D5 and  $\beta$ -arrestin. In addition, ablation of the ability of PDE4D5 ubiquitination by mutating the UIM region of PDE4D5 strongly diminished the time-dependent association of PDE4D5 with  $\beta$ -arrestin (Figure 4.14 e).

Compared to the relatively conserved phosphate acceptor site within substrates of kinases which direct binding and phosphorylation, no such consensus motif exists for ubiquitination. In many cases, any lysine within the substrate protein is capable to accept Ub (King et al. 1996; Hou et al. 1994; Crook et al. 1996). Recently, however, many groups have uncovered a higher chance of a number of specific positioned lysines that are ubiquitinated in the substrate proteins. These include: (1) lysines located within or adjacent to PEST sequence (Roth and Davis 2000; Marchal et al. 2000); (2) two adjacent lysine residues positioned 10 and 9 residues upstream of SCF <sup>$\beta$ -TrCP</sup> E3 substrates of the DSG(XX)<sub>2-7n</sub>S destruction motif (Kumar et al. 2004); (3) one or more of the lysines present in the region between two UIMs in the same substrate protein; (4) the lysines located at least 22 residues N-terminal to the UIM in an orientation-dependent manner (Miller et al. 2004). In order to make identification of acceptor lysine residues in PDE4D5 simple, I took advantage of the newly developed peptide array technology, (discussed in more detail in Chapter 6), to perform *in vitro* ubiquitination assays. Each spot on the peptide array of PDE4D5 represents a specific sequence of PDE4D5, presumably having some measure of secondary structure, therefore, given the full ubiquitination machinery and appropriate incubation temperature, Ub may be conjugated to the right lysine residues as it does *in vivo*. Immunoblotting the post-*in vitro* ubiquitinated peptide array with a specific Ub antibody identified two separate regions where the Ub-modified lysine residues were located. Surprisingly, Region1 (peptide10-13) is part of the  $\beta$ arrestin binding site of PDE4D5 (but not RACK1) (Figure 4.15 a; Figure 6.5). This suggests that the ubiquitination of PDE4D5 and the association between PDE4D5 and  $\beta$ -arrestin are intrinsically related. In order to ascertain the exact lysine residues that are ubiquitinated, I used peptide10-derived alanine scanning array that was subjected to *in vitro* ubiquitination. Since two lysine residues are present in the same peptide (peptide10), substitution of either of them did not abolish the ubiquitination signals, indicating that both of the lysines are indeed ubiquitinated (Figure 4.16 b). Further experiments need to be done on peptide 13-derived alanine scanning array to determine if the lysine within this sequence can also be ubiquitinated.

The second region of the positive ubiquitination sites on PDE4D5 extends from D136 through to R170 (Figure 4.16), where only one lysine resides. Therefore I

would propose investigating the peptide28-derived alanine scanning array under the in vitro ubiquitination conditions. Unexpectedly, this lysine (K140) is 14 residues C-terminal to the PDE4D5 PKA phosphorylation site, giving rise to a speculation that PKA phosphorylation of PDE4D5 on S126 might feed into the signal of its ubiquitination (Mackenzie et al. 2002). To evaluate this hypothesis, further experiments need to be done on PDE4D5 using mutants that either abolish or mimics phosphorylation of PDE4D5 by PKA and compare their ability to be ubiquitinated. Unfortunately, alanine scans of peptides D136 were unavailable during my time of study.

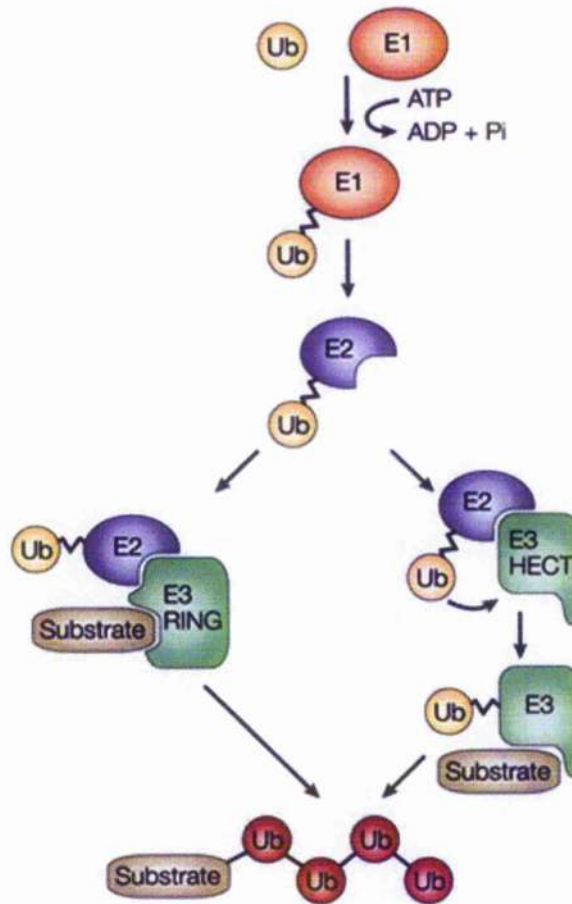
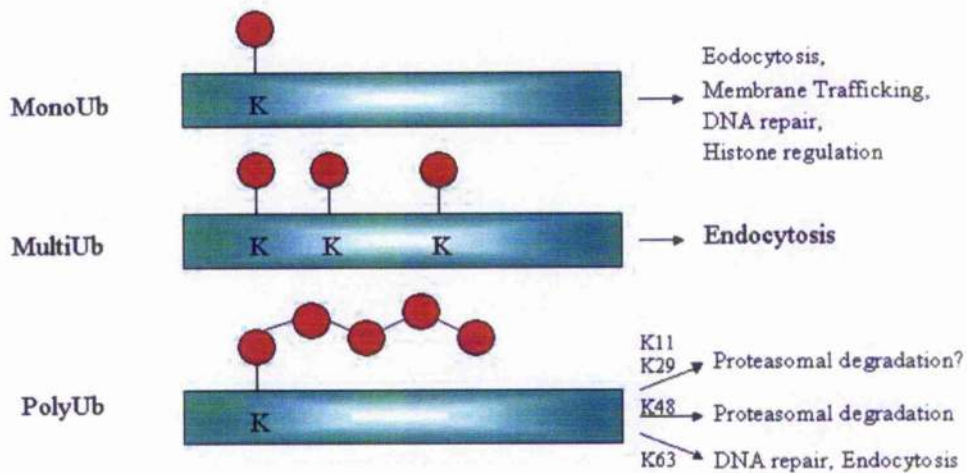


**Figure 4.1** The ubiquitination pathway.

Free ubiquitin (Ub) is activated in an ATP-dependent manner with the formation of a thiol-ester linkage between Ub activating enzyme E1 and the carboxyl terminus Gly76 of Ub. Ubiquitin is transferred to one of a number of different Ub conjugating enzymes (E2s). Ub ligases (E3s) catalyze the formation of an isopeptide bond between the  $\epsilon$ -amino group of a lysine residue in substrate proteins and the carboxyl terminus Gly76 of Ub. Two families of E3s are known. For HECT domain E3s, Ub is transferred to the active-site cysteine of the HECT domain followed by transfer to substrates. For RING E3s, Ub is transferred directly from the E2 to the substrate. (This schematic is adapted from Di Piore et al. 2001 Nature)



#### 4.2 Different forms of ubiquitin modification.

Monoubiquitination (MonoUb) is obtained by the attachment of a single Ub molecule (red circle) to a lysine residue (K), whereas multiubiquitination (MultiUb) is the result of addition of several single Ubs to different lysine residues in a protein. These modifications are implicated in cellular processes, including endocytosis and membrane trafficking. Polyubiquitination (PolyUb), however, is obtained by the formation of a polymeric chain of Ub molecules by the subsequent additions of Ub molecules to the preceding Ub. The functions of Lys48-linked ubiquitin chains target proteins for degradation by the 26S proteasome, whereas chain elongation via Lys63 is involved in several non-proteolytic functions, including signaling DNA repair, the stress response, endocytosis and signal transduction. The biological function of ubiquitin chains coupled via Lys11 and Lys29 remains to be determined, but it has been suggested by some group that the linkage through Lys11 or Lys29 may target proteins to the proteasome.

(a)

X-Ac-Ac-Ac-Ac-Q-X-X-Ala-X-X-X-Ser-X-X-Ac-X-X-X-X

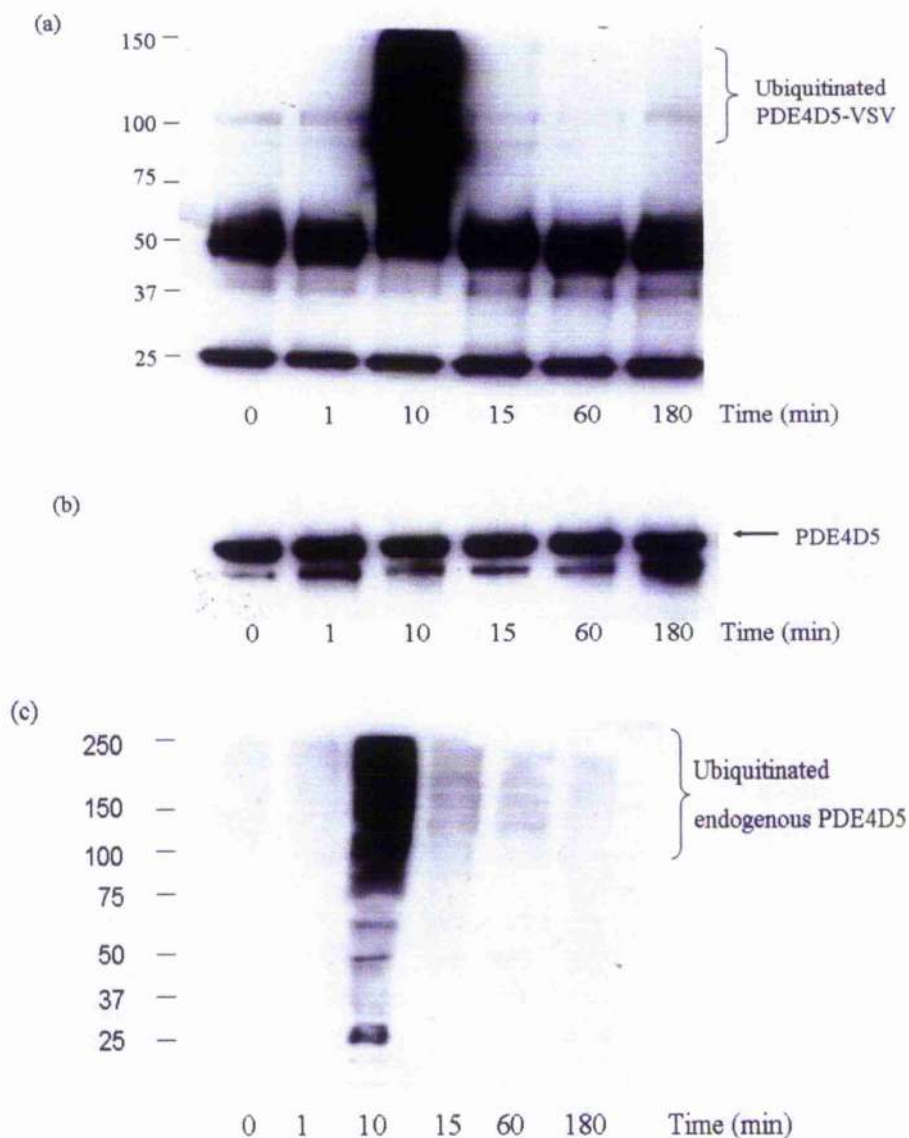
Hrs-A	Q E E E L Q L A L A L S Q S E A E E K
Hrs-B	Q E E E L Q L A L A L S Q S E A E E K
Vps27p-1	D E E E L I R K A I E I S L K E S R N S
Vps27p-2	E E D P D L K A A I Q E S L R E A E E A
Stam 1-A	K E E E D L A K A I E L S I K E Q R Q Q
Stam 1-B	K E E E D L A K A I E L S L K E Q R Q Q
Stam 2-A	K E D E D I A K A I E L S L Q E Q K Q Q
Stam 2-B	K E D E D I A K A I E L S L Q E Q K Q Q
Eps15-1	S E E D M I E W A K R E S E R E E E Q R
Eps15-2	Q E Q E D L E L A I A L S K S E I S E A
PDE4D	V E E E A V G E E E E S Q P E A C V I

(b)

	*	20	*	40	*	60	*	80					
PDE4A11 :	SMAQIPCTAQEALTAQGLSGVBEALDATIWEASPAQ	SLEVMACH	ASLEAELEAVYL	QQA	STGSAPVAR	DEFSSRE	EFVAVS	: 86					
PDE4B1 :	-----	SKHG	-----	GHYFSSSTKTCV	IPN	-----	RDSLGETDID	: 37					
PDE4C :	-----	EEEE	-----	GEETALAKEA	ELPPT	-----	ELTSPEA	: 28					
PDE4D5 :	-----	ENKDSGSQV	EDTSCSDSKT	CTQSSST	-----	EI	ELDEQVEEAVGEE	: 45					
			E	E	l	d	e						
	*	100	*	120	*	140	*	160					
PDE4A11 :	HSS	SALAQ	QSPLLPA	WRTL	LSVSEHAP	GLPGLP	STAAEVA	QREHQAA	KRACSACAGTF	GEDTSALP	APGGGGSG	GDPT	: 165
PDE4B1 :	DKS	-----	DT	-----	-----	-----	-----	-----	-----	-----	-----	-----	: 44
PDE4C :	GP	GDLE	EDN	QRT	-----	-----	-----	-----	-----	-----	-----	-----	: 42
PDE4D5 :	RS	Q	RA	CV	LD	RS	PDT	-----	-----	-----	-----	-----	: 61
	P	6d											

### 4.3 Characterization of the UIM.

(a) Alignment of C-terminal extreme sequence of PDE4D with the UIM-containing sequences of several endocytic proteins. Consensus UIM is indicated and delineated in red line. N-proximal acidic patch was shown in blue, hydrophobic residue is shown in pink, nearly invariable alanine is shown in green, conserved serine at position 13 is indicated in red and conserved glutamate at position 16 is indicated in violet. (b) Extreme C-terminal of PDE4A11, PDE4B1, PDE4C, and PDE4D5 were aligned by GENEDOC Software. Conserved amino acids within these four gene families are indicated by the letters at the bottom line. The red line delineates where the UIM is located.



#### 4.4 Isoprenaline-stimulated ubiquitination of PDE4D5.

(a) HEKB2 cells were transiently transfected with PDE4D5-VSV and the endogenous  $\beta_2$ ARs were stimulated for the indicated times. PDE4D5 was immunoprecipitated with VSV affinity beads, the bound protein sample was separated by SDS-PAGE and the presence of ubiquitinated forms in the immunoprecipitates (IP) was detected with a ubiquitin-specific antibody. (b) Shows the equal amount of PDE4D5 in the IP samples. (c) HEKB2 cells were stimulated with isoprenaline for the indicated times and endogenous PDE4D5 was immunoprecipitated with Protein-G beads by a specific PDE4D antibody. The presence of ubiquitinated forms in the IP samples was detected with a ubiquitin-specific antibody.

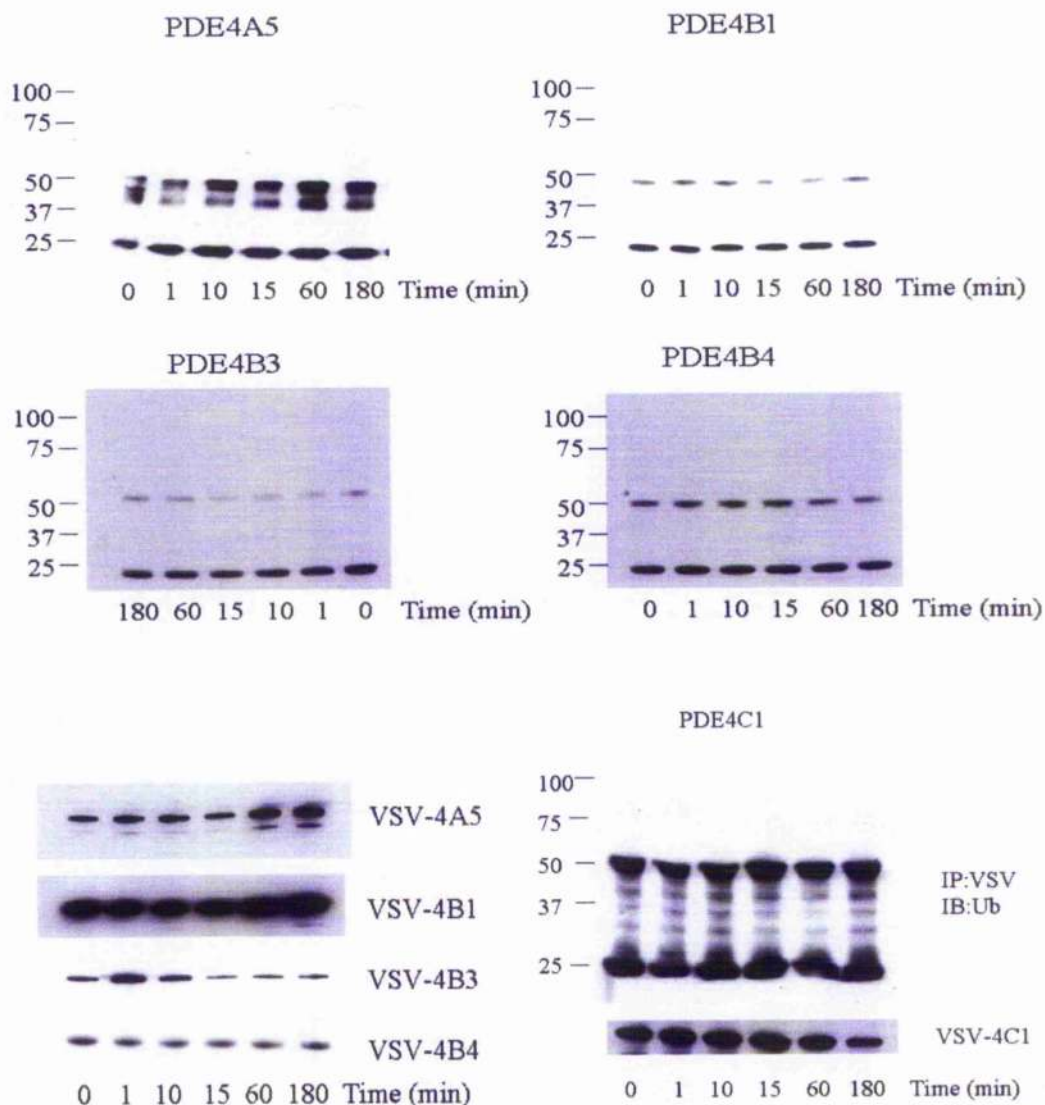


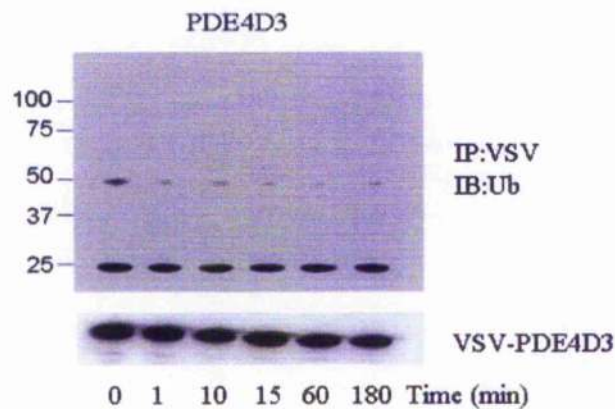
**Figure 4.5 Isoprenaline-stimulation of HEKB2 cells failed to lead to ubiquitination of PDE4A5, PDE4B1, PDE4B3, PDE4B4 and PDE4C1.**

HEKB2 cells were transiently transfected with one of the VSV-tagged PDE4 isoforms (PDE4A5, PDE4B1, PDE4B3, PDE4B4 and PDE4C1) and the endogenous  $\beta_2$ ARs were stimulated for the indicated times. PDE4 isoforms were immunoprecipitated with VSV affinity beads, and the presence of ubiquitinated forms in the immunoprecipitates (IP) was detected with a ubiquitin-specific antibody.

(a)



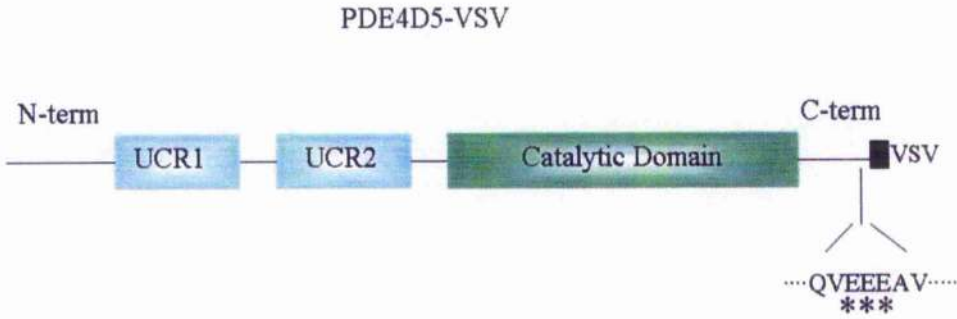
(b)



#### 4.6 Absence of ubiquitination of PDE4D3 in response to isoprenaline in HEKB2 cells.

(a) Sequence alignment of the extreme C-terminal residues of PDE4B1, PDE4D3 and PDE4D5, respectively. UIM domains are shown in red. (b) HEKB2 cells were transiently transfected with VSV-PDE4D3 and stimulated with isoprenaline at indicated times. Immunoprecipitation (IP) was performed with VSV affinity beads, and ubiquitination was assessed using a specific Ub antibody on the IP samples. Positions of the molecular mass markers (kDa) are indicated.

(a)



(b)

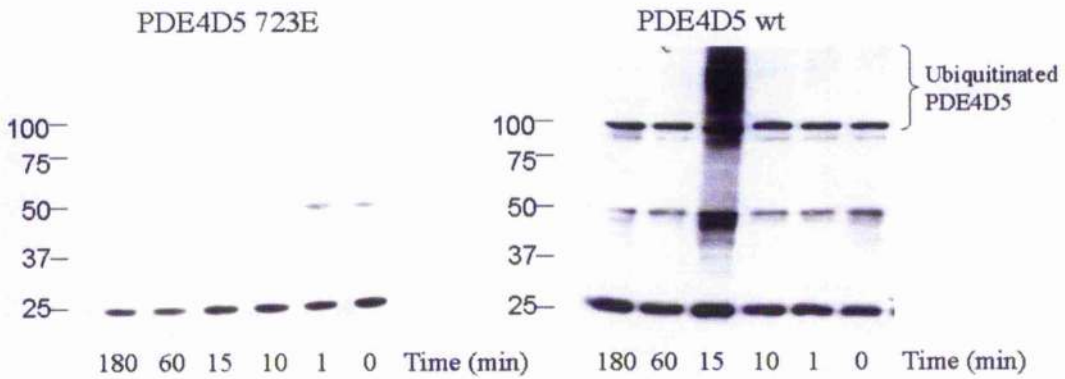


**Figure 4.7 The extreme C-terminal of PDE4D5 contains a UIM domain essential for ubiquitination.**

(a) Schematic representation of VSV-PDE4D5 ubiquitination mutant. Catalytic domain connects N-terminal region of PDE4D5 with its extreme C-terminal domain. The VSV tag is located at the C-terminus of the molecule (black box). Triple point mutations in the context of the full-length VSV-PDE4D5 are indicated (\*). (b) HEKB2 cells were transiently transfected with PDE4D5 723E-VSV and stimulated with isoprenaline at indicated times. Ubiquitination of the isolated PDE4D5 723-VSV on VSV affinity beads was assessed by Western blotting using a specific Ub antibody. Positive control was performed using VSV-tagged PDE4D5 wild type (PDE4D5 wt) transfected HEKB2 cells. Positions of the molecular mass markers (kDa) are indicated.

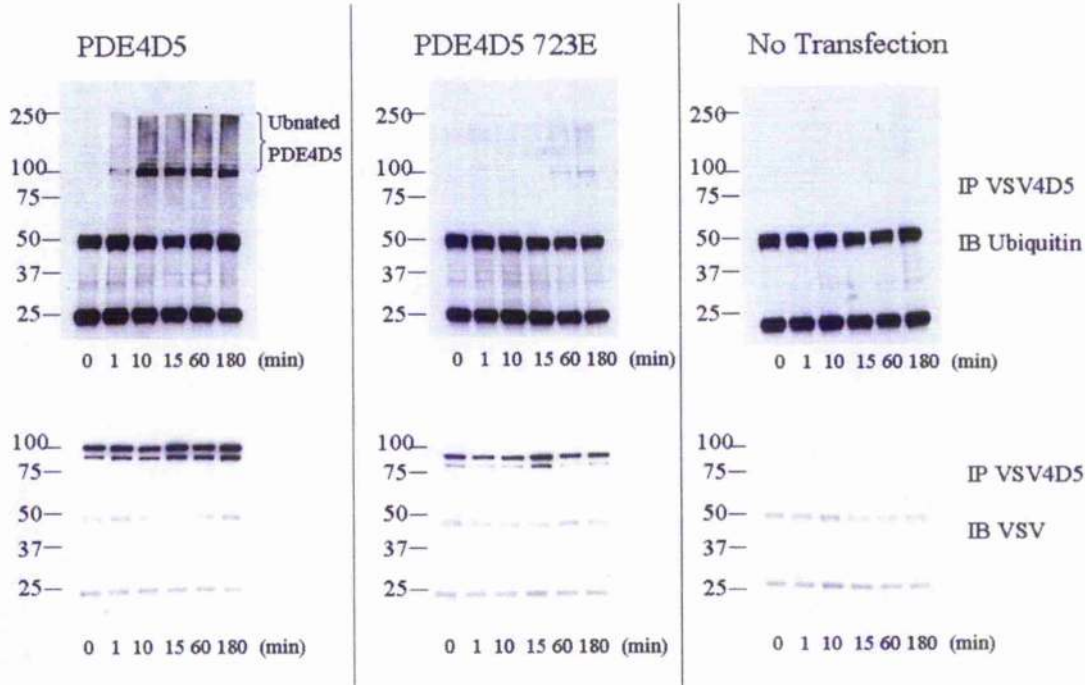


**Figure 4.8 Vasopressin-stimulated ubiquitination of PDE4D5-VSV in HEK293T cells.**

Left Panel: HEK293T cells were transiently transfected with PDE4D5-VSV and the endogenous  $V_2R$ s were stimulated with vasopressin for the indicated times. PDE4D5 was immunoprecipitated with VSV affinity beads, and the presence of ubiquitinated forms in the immunoprecipitates (IP) was detected with a Ub-specific antibody. The same blot was stripped and probed with an anti-VSV antibody to confirm the equal amount of PDE4D5 pull-downed in the IP samples. Middle Panel: Under the same conditions as Left Panel but with transfected VSV-PDE4D5 723E mutant, the ubiquitination status of VSV-PDE4D5 723E was assessed by probing the isolated PDE4D5 723E on the VSV agarose with a specific Ub antibody. Right Panel: control experiment was done in the non-transfected HEK293T cells. Positions of the molecular mass markers (kDa) are indicated.

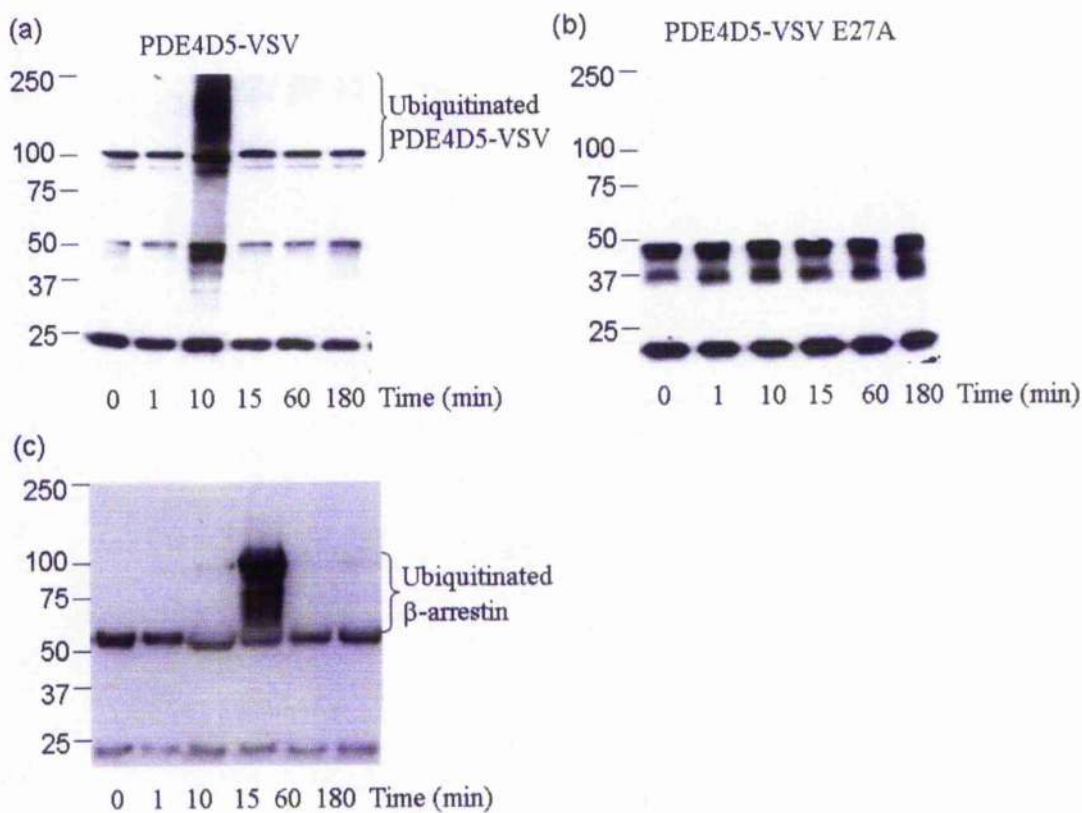
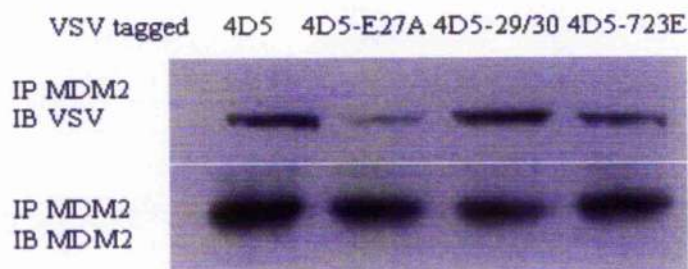


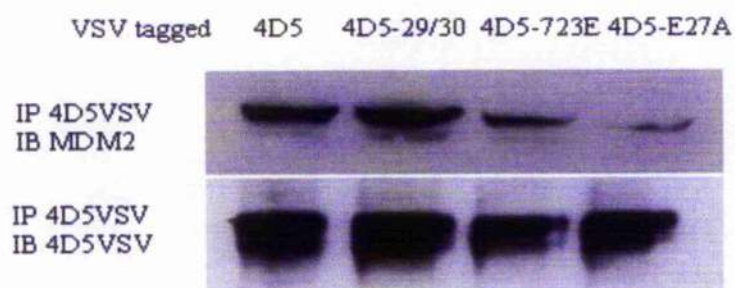
**Figure 4.9  $\beta$ -arrestin-mediated PDE4D5 ubiquitination in HEKB2 cells.**

(a) HEKB2 cells were transiently transfected with VSV-tagged wild type PDE4D5 and stimulated with isoprenaline at indicated times. Immunoprecipitation (IP) was performed with VSV-agarose, and ubiquitination of PDE4D5-VSV was assessed by Western blotting using a specific Ub antibody. (b) HEKB2 cells were transiently transfected with VSV-tagged PDE4D5 mutant that does not bind to  $\beta$ -arrestin (PDE4D5-VSV E27A) and stimulated with isoprenaline at indicated times. Immunoprecipitation was performed with VSV-agarose, and ubiquitination of PDE4D5-VSV E27A was assessed using a specific Ub antibody by Western blotting. (c) Endogenous  $\beta_2$ ARs were stimulated with isoprenaline for the indicated times. Endogenous  $\beta$ -arrestin was isolated on Protein-G beads with a specific anti- $\beta$ -arrestin antibody and ubiquitinated forms of  $\beta$ -arrestin in the IP samples were assessed by Western blotting using a specific Ub antibody. The positions of molecular mass marker (kDa) are indicated.

(a)

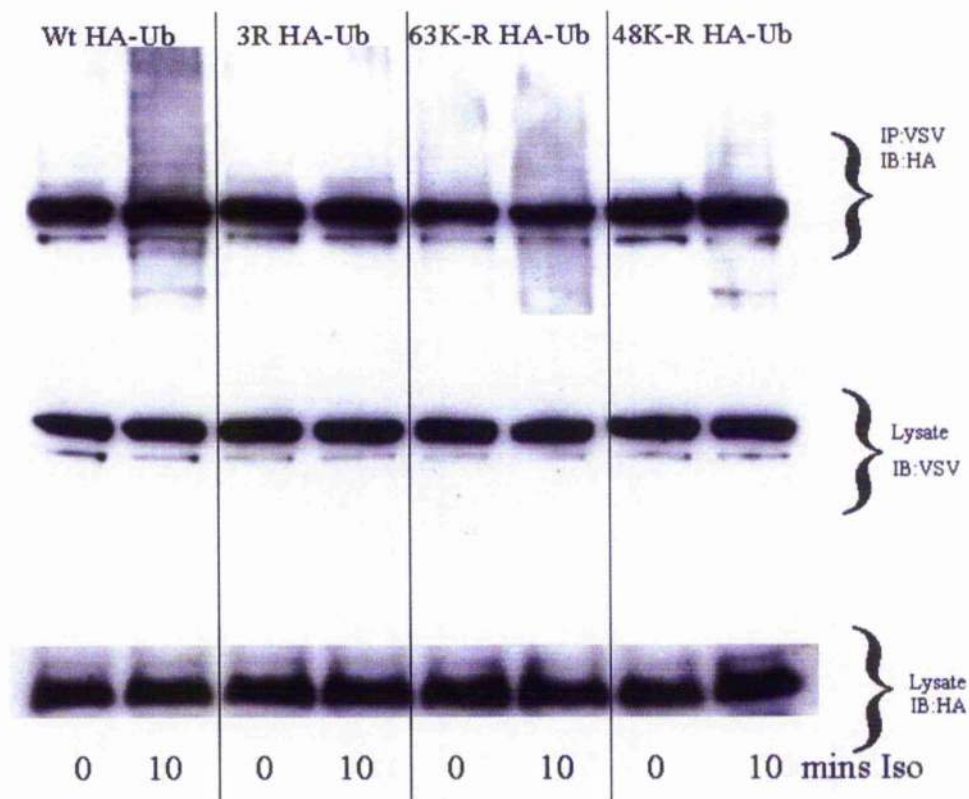


(b)



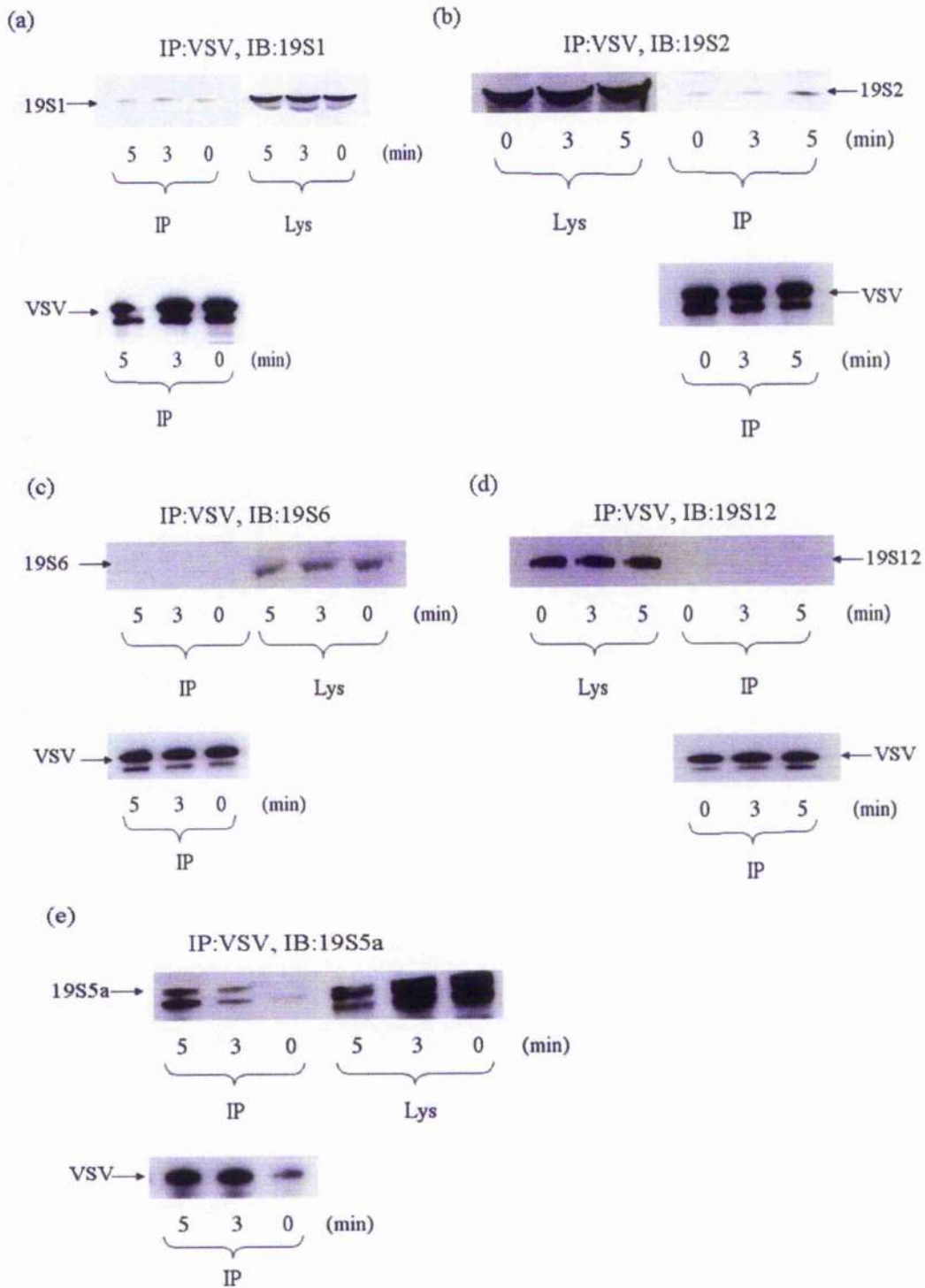
#### 4.10 PDE4D5 interacts with Mdm2 via a $\beta$ -arrestin-dependent manner.

HEKB2 cells were transiently transfected with VSV-tagged PDE4D5, PDE4D5 29/30 mutant (that blocks its binding to RACK1), PDE4D5 723E mutant (that blocks its ubiquitination) and PDE4D5 E27A mutant (that does not bind to  $\beta$ -arrestin), respectively. (a) Endogenous Mdm2 in HEKB2 cells were immunoprecipitated on Protein-G beads with an antibody specific to Mdm2 and the association of Mdm2 with those overexpressed proteins was determined by Western blotting analysis with VSV antibody. Equal amount of immunoprecipitated Mdm2 was verified by blotting the IP samples with Mdm2 antibody. (b) Different forms of VSV-tagged PDE4D5 in HEKB2 cells were isolated on VSV-agarose and the association of these different forms of VSV-tagged PDE4D5 was assessed by Western blotting analysis with a specific Mdm2 antibody. Equal amount of immunoprecipitated VSV-tagged different forms of PDE4D5 was verified by blotting each IP sample with VSV antibody.



#### 4.11 A mixture of K29-linked, K48-linked and K63-linked polyubiquitin chains on PDE4D5 in response to isoprenaline in HEKB2 cells.

HEKB2 cells were transiently transfected with VSV-tagged wild type PDE4D5 and one of the following HA-tagged Ub forms: wild type Ub (WT HA-Ub), or K29, 48, 63R mutant of Ub (3R HA-Ub), or K63R mutant of Ub (K63R HA-Ub) or K48R mutant of Ub (K48R HA-Ub). HEKB2 cells were then stimulated with isoprenaline for different times and harvested in 3T3 lysis buffer. An equal protein concentration of cell lysate was subject to immunoprecipitation (IP) with VSV-agarose and the ubiquitination forms of VSV-tagged PDE4D5 in the IP samples were determined by Western blotting analysis using a HA antibody. The expression of PDE4D5 constructs and Ub constructs were verified by blotting an aliquot of the transfected cell lysate (30  $\mu$ g) with VSV antibody and HA antibody, respectively.



#### **4.12 Isoprenaline-stimulated wild type PDE4D5 interaction with proteasome 19S1, 19S2 and 19S5a in a time-dependent manner in HEKB2 cells.**

HEKB2 cells transiently transfected with VSV-tagged wild type PDE4D5 were stimulated with isoprenaline for different times. PDE4D5 was isolated on VSV-agarose and its association with proteasome 19 regulatory complex subunits was assessed by Western Blotting analysis using specific antibodies against (a) 19S1, (b) 19S2, (c) 19S6, (d) 19S12 and (e) 19S5a, respectively. The expression of 19S subunits were verified by blotting an aliquot of the transfected cell lysate (30  $\mu$ g) with their corresponding antibody. Equal amount of immunoprecipitated PDE4D5 in each IP sample was determined by Western Blotting using a specific VSV antibody.

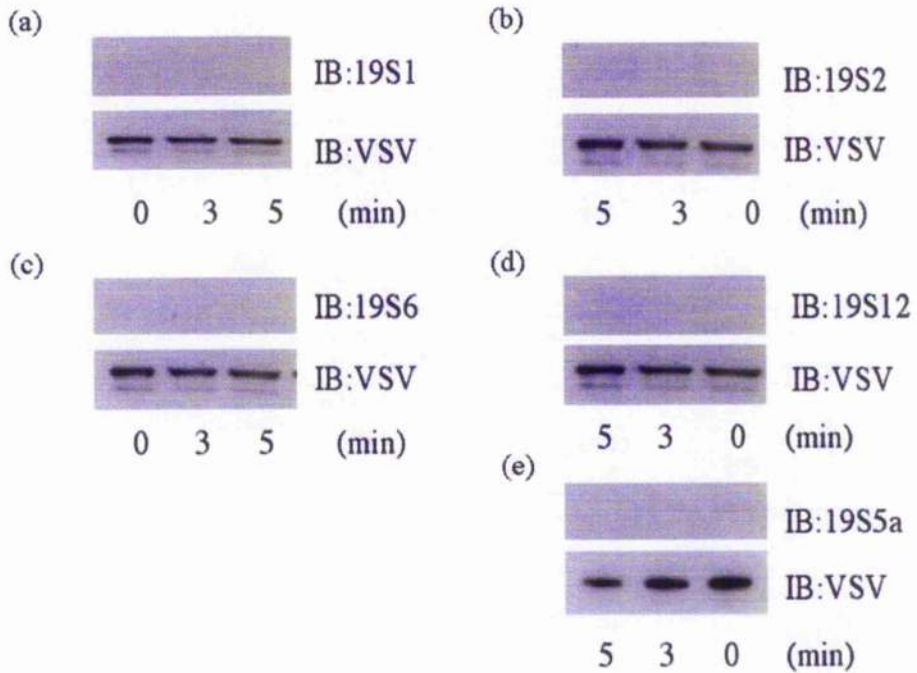


**Figure 4.13** Loss of ability of VSV-tagged PDE4D5 UIM mutant 723E to interact with proteasome 19S regulatory complex in HEKB2 cells in response to isoprenaline.

HEKB2 cells were transiently transfected with VSV-tagged PDE4D5 UIM mutant 723E, followed by stimulation with isoprenaline at indicated times. VSV-tagged PDE4D5 723E was isolated on VSV-agarose and the interaction between PDE4D5 723E and 19S regulatory complex subunits were assessed by Western blotting analysis using antibodies against (a) 19S1, (b) 19S2, (c) 19S6, (d) 19S12, and (e) 19S5a as indicated. A VSV antibody was used to confirm the equal amount of PDE4D5 723 in each set of IP samples.

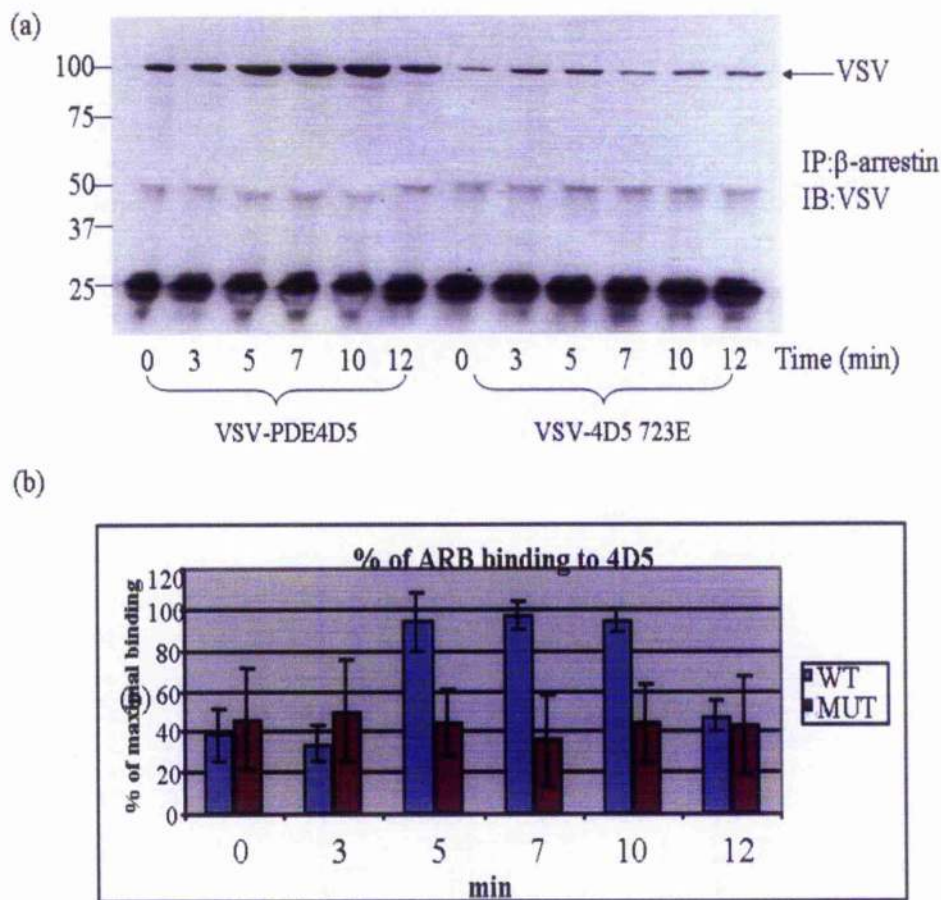


**Figure 4.14 Ubiquitination of PDE4D5 enhances its binding to  $\beta$ -arrestin.**

(a) HEKB2 cells transiently transfected with either VSV-tagged wild type PDE4D5 or its UIM mutant 723E were stimulated with isoprenaline for different times. Immunoprecipitation (IP) was performed with anti- $\beta$ -arrestin antibody to isolate endogenous  $\beta$ -arrestin in those transfected HEKB2 cells. The association of  $\beta$ -arrestin with either wild type PDE4D5 or UIM mutant 723E was assessed by Western blotting analysis on IP samples using a specific VSV antibody. (b) Quantification of three experiments as in (a) (means  $\pm$  S.D.) with 100% as the maximal effect seen with isoprenaline.

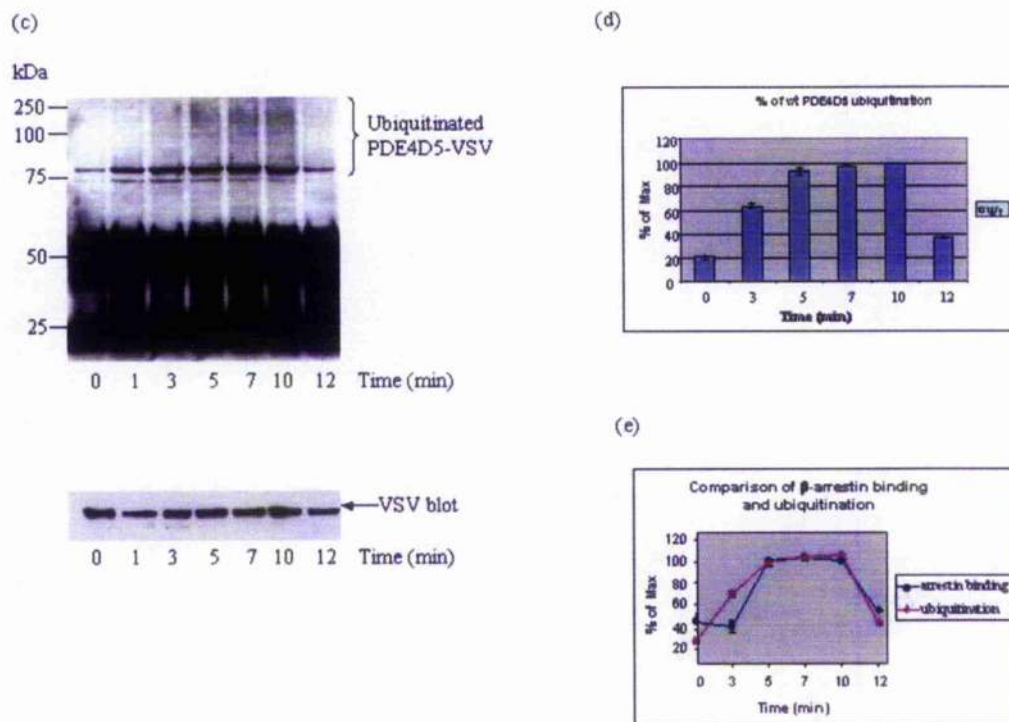
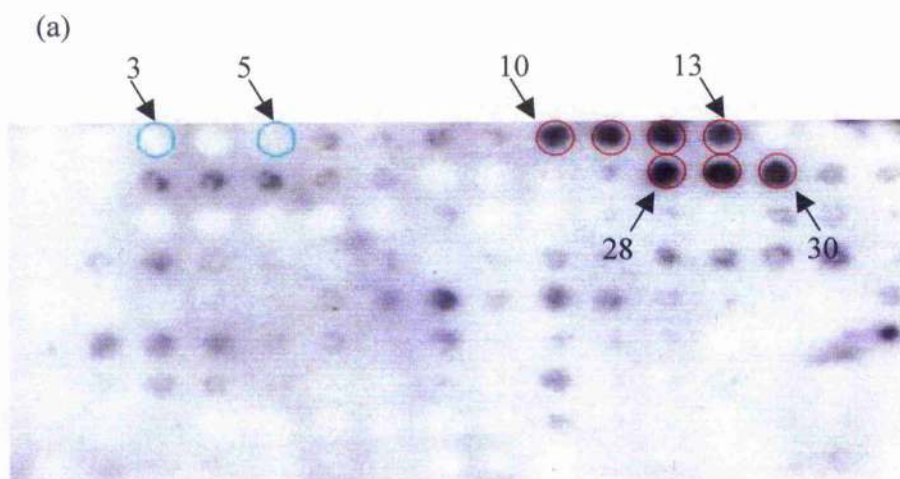


**Figure 4.14 Ubiquitination of PDE4D5 enhances its binding to  $\beta$ -arrestin.**

(c) HEKB2 cells were transiently transfected with wild type VSV-tagged PDE4D5 and stimulated with isoprenaline at indicated time. VSV-PDE4D5 was isolated on VSV-agarose and the ubiquitination of VSV-PDE4D5 on the VSV affinity beads was detected by Western blotting analysis using a specific Ub antibody. The levels of immunoprecipitated VSV-PDE4D5 were examined by immunoblotting with anti-VSV antibody. (d) Quantification of three experiments as in (c) (means  $\pm$  S.D.) with 100% as the maximal effect seen with isoprenaline. (e) Plot for comparison between the kinetics of isoprenaline-stimulated  $\beta$ -arrestin binding and that of isoprenaline-induced ubiquitination of PDE4D5, which is concluded from Figure 4.14 (b) and (d).



(b)

**Peptide 10-13**

AR**K**SVSP**K**LSPVISPRNSPRLLRMLLSSNIP**K**QRRFTVA

**Peptide 28-30**

DLSP**K**SMSRNSSIASDIHGDDLIVTPFAQVLASLR

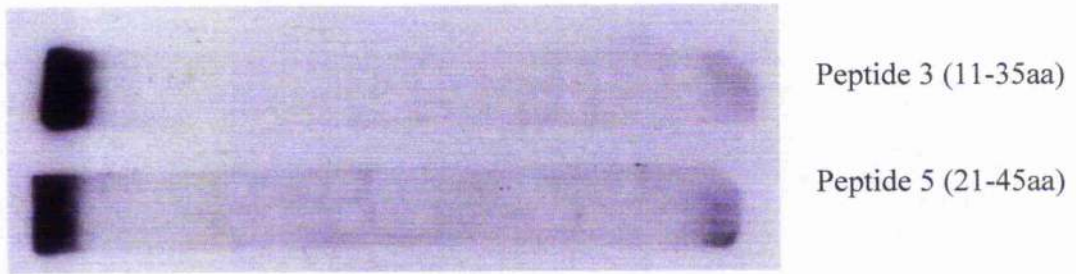
Peptide PKA site location (blue)

DPMTSPGSGLILQANFVHSQRRESFLYRSDSLDLSP**K**SMSRNSSIASDIH  
GDDLIVTPFAQV

**Figure 4.15** *In vitro* ubiquitination assay determines PDE4D5 putative ubiquitination sites.

(a) The PDE4D5 peptide array that underwent *in vitro* ubiquitination assay using a commercial Ubiquitination Kit was incubated with a specific Ub antibody and subject to ECL. Positive signals are scored as dark spots and negative signals are scored as blank spot. (b) Two regions that encompass the Ub acceptor sites amino acid sequences in sequential peptides on PDE4D5 peptide array are delineated. Ub acceptor sites are indicated in red. The amino acid sequence that contains both PKA phosphorylation consensus (marked in blue) and the second regions of ubiquitination sites (underlined) are also delineated.

(a)



(b)

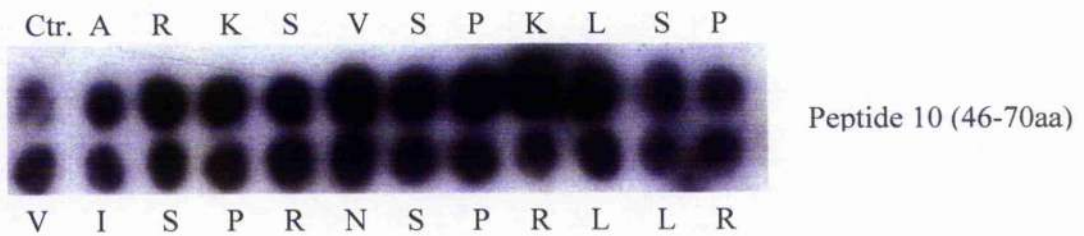


**Figure 4.16** The *in vitro* ubiquitination of sequential alanine substitution version of a peptide 10-derived peptide.

Here shows an array of peptides based on a 25mer parent peptide (Ctr, peptide 10 in Figure 4.15 a) of sequence Ala46-Arg68 in PDE4D5. Further spots reflect a scanning peptide array of this parent peptide where indicated amino acids were sequentially and individually substituted with alanine. Cellulose membrane was blocked before immunoblotting with a specific anti-ERK2 antibody. Ctr, control.

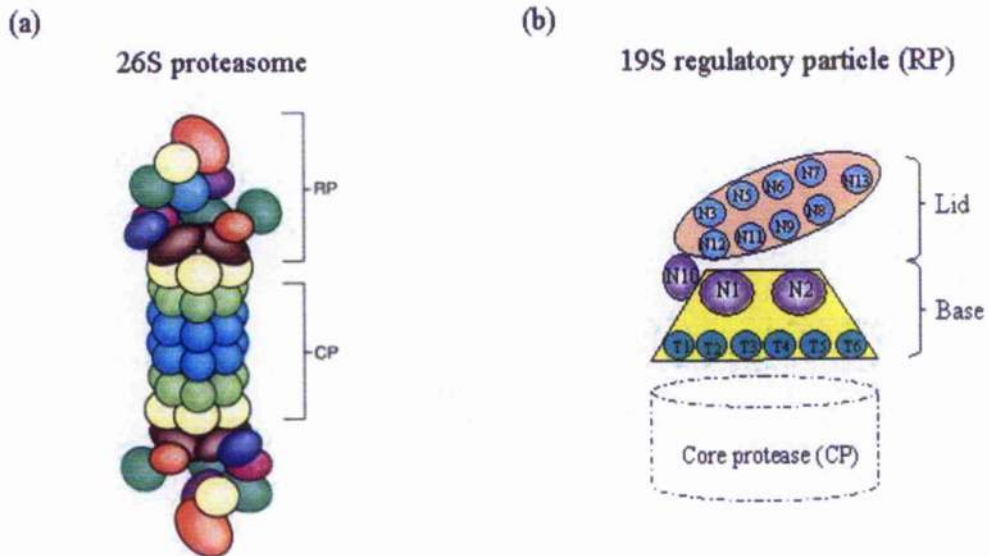


**Figure 4.17 Organization and structure of the 26S proteasome and 19S regulatory particles.**

(a) Organization of the 26S proteasome, which is composed of 19S regulatory particle (RP) and 20 core protease (CP). (b) Proposed organization of 19S regulatory particle with its Lid and Base subparticles. N, RP non-ATPase subunits; T, RP AAA-ATPase subunits.

## **Chapter 5**

### **Initial Exploration of Sumoylation of PDE4D5 in HEK293 cells**

## 5.1 Introduction

Reversible post-translational modifications are widely used to dynamically regulate protein functions (Hochstrasser 2000). This has been further supported in the study of my last chapter, where ubiquitination of PDE4D5 was shown to affect its binding affinity towards  $\beta$ -arrestin. In addition to Ub, several other ubiquitin-like proteins (Ubls) have recently been identified and suggested to be able to alter the function of their conjugated proteins (Hochstrasser 2000; Johnson 2004; Pickart and Eddins 2004). One Ubl in particular, the small ubiquitin-related modifier (SUMO), is perhaps the best-studied example of a post-translational modification after modification by Ub (see reviews: Seeler and Dejean 2003; Gill 2004; Verger et al. 2003; Muller et al. 2004; Hilgarth et al. 2004).

Small ubiquitin-related modifiers (SUMOs) are a group of proteins that conjugate to a wide range of proteins in the cell (Hay 2005). They are highly conserved from yeast to mammals. So far, only one SUMO gene has been identified in yeast species and invertebrate, whereas eight isoforms have been found in plants (Dohmen 2004). In human cells, four types of SUMO, termed SUMO-1, SUMO-2, SUMO-3 and SUMO-4 have been identified (Dohmen 2004). Human SUMO isoforms have a similar protein folding that is characterized by  $\beta\beta\alpha\beta\beta\alpha\beta$ , but they differ in their sequence identity. SUMO-2 and SUMO-3 are very similar in sequence (95% sequence identity for the human proteins), but SUMO-1 is only about 47% identical to SUMO-2 and SUMO-3 (Melchior 2000; Muller et al. 2004). Another difference between SUMO isoforms is their cellular status; for example, the majority of SUMO-1 exists in the conjugated form, whereas the SUMO-2 and SUMO-3 isoforms exist primarily as free proteins that are strongly subject to rapid conjugation that is distinct from SUMO-1 (Saitoh et al. 2000).

SUMO molecules conjugate to their target proteins through an isopeptide bond formed between the C-terminal glycine residue of SUMO and a lysine residue in the substrate. In most cases, the lysine residues are embedded in a consensus sequence composed of a characterized  $\psi$ KXE motif, where  $\psi$  represents a hydrophobic amino acid residue, including Leu, Ile, Val or Phe (Johnson 2004), and K is the site of SUMO conjugation. As is generally known, in a SUMO conjugation reaction SUMO

hydrolase first removes the four C-terminal amino acids of SUMO. This exposes a diglycine motif to facilitate SUMO conjugation. The SUMO molecule is then adenylated and covalently linked to a SUMO-activating E1 enzyme. Subsequently, SUMO is transferred to the SUMO-conjugating E2 enzyme Ubc9, which catalyzes the transfer of SUMO to its target proteins (Figure 5.1). To note, Ubc9 does not discriminate between SUMO isoforms and carries out all SUMO paralogues-mediated modification (Melchior 2000). Distinct from its counterpart in the ubiquitination pathway, the SUMO E2, Ubc9 can, in many cases, directly bind to substrate proteins via their sumoylation consensus sequence  $\psi$ KXE (Sampson et al. 2001). The E3 ligase, which stimulates SUMO conjugation to target proteins, including PIAS, RanBP2, and Pc2, has only been recently identified. Although not required for sumoylation in vitro (Bernier-Villamor et al. 2002), SUMO E3 ligases seem to modulate the efficiency of sumoylation of target proteins in vivo. This is especially of importance for substrates that lack SUMO attachment consensus sequences.

There are several models describing the functional consequences of SUMO modification: it may compete with ubiquitination and affect protein stabilities (Desterro et al. 1998), alter substrate protein subcellular localization (Wilson and Rangasamy 2001), affect transcriptional activities (Seeler and Dejean 2003), or mediate protein-protein interactions (Reverter and Lima 2005). Compared to the classic function of ubiquitination, which leads to the 26 proteasome-dependent degradation, the biological consequences of SUMO modification vary in a substrate-specific manner.

My alignment of the PDE4D5 amino acid sequence (Figure 5.2) reveals one conserved sumo modification consensus motif in its catalytic domain. This motif is considered to provide the potential site for recognition by the SUMO-conjugating E2, Ubc9 and therefore directs target protein sumoylation. In exploring here whether PDE4D5 is a substrate for sumo modification I found that PDE4D5 was indeed susceptible to SUMO modification if appropriate conditions were provided to aid in the detection of this modification. Mutations affecting sumoylation of PDE4D5 have significant functional consequences on its association with other binding partners, such as  $\beta$ -arrestins, RACK-1, and ERK2. These findings identify sumoylation as a

post-translational modification that affects the interaction of PDE4D5 with proteins that sequester it. This occurs in such a manner that is dependent on the presence of a lysine residue within the SUMO modification consensus sequence present in the PDE4D5 catalytic domain.

## 5.2 Results

### 5.2.1 Mutation of the potential target lysine residue located within SUMO modification consensus sequence in PDE4D5 ablates its sumoylation *in vitro*.

Wild type PDE4D5 contains a short motif, VKTE, in the N-terminal of its catalytic domain, which suggests that this PDE4 isoform may become SUMOylated. This motif fits the minimal SUMO modification consensus sequence  $\psi$ KXE (Figure 5.2). If this hypothesis is correct, the lysine residue (K323) within VKTE motif would be a strong candidate to provide a SUMO modification site. In another words, if VKTE provides the lysine to be modified by SUMO, mutation of this lysine residue to arginine would ablate any such modification. To test whether human PDE4D5 is modified by SUMO, I first performed site-directed mutagenesis on lysine 323 of PDE4D5, which is contained within the putative SUMO consensus sequence. This mutation (K323R) thus can be used as a negative control for detection of PDE4D5 sumoylation if lysine 323 is susceptible to SUMO modification.

An *in vitro* translational sumoylation study, performed by the Hay laboratory, using 35S-methionine wild type PDE4D5 DNA, SUMO-activating E1 enzyme (SAE1/SAE2), SUMO-conjugating E2 enzyme (Ubc9), SUMO isoforms, SUMO-1 or SUMO-2, both of which lack the four C-terminal amino acid residues, and an ATP regenerating system, was performed to determine whether PDE4D5 is modified by SUMO-1 or SUMO-2. After incubation for 4 hour at 37°C, Fractionate reaction products was analysed by 4-12% SDS-PAGE, subsequent staining and fixing, and subject to phosphoimager after the gels were dried. In the reaction that contained SUMO-activating E1 enzyme, SUMO-conjugating E2 enzyme Ubc9 and SUMO-1, proteins with a molecular mass larger than that of PDE4D5 were detected, suggesting that PDE4D5 is conjugated by SUMO-1 (Figure 5.3, lane 5). In the reaction that contained SUMO-2, instead of SUMO-1, together with SUMO E1, E2 enzymes, proteins with a mass larger than that of PDE4D5 were also detected, indicating that

PDE4D5 is attached to SUMO-2 (Figure 5.3, lane 6). However, these bands were not detected if ATP was not added to the reaction mixture (UN, Figure 5.3, lane 4), indicating that SUMO-activating E1 enzyme, Ubc9, and SUMO isoforms are necessary for PDE4D5 sumoylation *in vitro*. A similar finding was observed for the *in vitro* study of a positive control, sumoylation of Sp100, a transcription factor that has been shown to be able to undergo sumoylation under decent conditions (Figure 5.3, lane 2 and 3). On the other hand, when purified recombinant E1 enzymes (Aoa1 and Uba2 subunits), Ubc9 and SUMO-1 or SUMO-2 were mixed with the *in vitro* translated substrate proteins PDE4D5K323RK or PDE4D5K323RJ in the presence of ATP, SDS-PAGE and autoradiography did not reveal the slower migrating, sumoylated form of PDE4D5 (Figure 5.3, lane 7-12) as that of wild type PDE4D5. This suggests that mutation of lysine residue within VKTE motif of PDE4D5 ablates its ability to become sumoylated *in vitro*, and that lysine 323 in PDE4D5 indeed provides a site where SUMO can be attached to and modify.

## **5.2.2 Modification of PDE4D5 by SUMO-1 in cells**

### **5.2.2.1 Conditions that I have tried to detect sumoylation of PDE4D5 in cells.**

Although SUMO modification only occurs to a small fraction of substrate, its biological consequences seem to affect long-term fate of modified proteins (Hay 2005). Therefore, it appears that a history of SUMO modification makes a difference between the proteins modified and non-modified. *In vitro* data has suggested that PDE4D5 is a SUMO target. However, it cannot be simply presumed that PDE4D5 can also be modified by SUMO-1 or SUMO-2 *in vivo* in intact cells. Thus, I set out here to assess whether SUMO can modify PDE4D5, and if the sumoylation site is within VKTE motif.

In order to amplify the detection of SUMO modification of PDE4D5, I first overexpressed a small epitope VSV-tagged wild type PDE4D5 in HEKB2 cells, and used overexpressed VSV-K323R as a control. Cells were harvested in 3T3 lysis buffer. Immunoblotting of the immunoprecipitates obtained using anti-VSV agarose beads with SUMO-1 or SUMO-2 antibody failed to reveal the SUMO associated with the immunoprecipitants. Then I tried to co-overexpress VSV-PDE4D5 (wild type) and His<sub>6</sub>-tagged SUMO-1 (or SUMO-2), but the immunoprecipitate of VSV-PDE4D5 again did not reveal the interaction with either SUMO-1 or SUMO-2. As SUMO E2

Ubc9 has been shown to mediate SUMO transfer to its target, I wish to study if co-expression of VSV-PDE4D5 (wild type) and Ubc9 could help detect the sumoylation of PDE4D5 in HEKB2 cells. Unfortunately, signals for SUMO were not apparent in the VSV-pulled down immunoprecipitates.

HEKB2 cells have been stably transfected with  $\beta_2$ -adrenergic receptors. Thus, in order to preclude any potential artefacts resulting from the use of this cell line, I then also used COS-1 cells and HEK293 cells to study the interaction between VSV-PDE4D5 and SUMO under the same conditions. Again, I failed to detect any modification of PDE4D5 with SUMO.

As the SUMO modification of its target has been suggested to be mediated by some other post-translational modifications on the same substrate protein, and it has been shown that PDE4D long isoforms are susceptible to PKA mediated phosphorylation via increased cAMP levels, therefore, I set out here to assess if elevating the intracellular levels of cAMP would help detect the SUMO modification of PDE4D5 *in vivo*. HEKB2 cells or HEK293 cells were transfected with VSV-PDE4D5 or the SUMO mutant form of this isoform where the putative target lysine was mutated to arginine. The transiently transfected cells were challenged for 5 min with 10  $\mu$ M  $\beta$ -agonist isoprenaline or 100  $\mu$ M IBMX (a non-selective PDE inhibitors) / 100 $\mu$ M forskolin (that activates adenylyl cyclase directly so as to increase intracellular cAMP), respectively. The lysates in 3T3 lysis buffer were subject to immunoprecipitation with anti-VSV agarose. The following western blot using an anti-SUMO-1 antibody failed to detect endogenous SUMO-1 in the VSV-PDE4D5-containing precipitates.

In order to preclude the possibility that 3T3 lysis buffer obscured the detection of sumoylation of PDE4D5, I also used a non-detergent-containing buffer KHEM buffer to harvest cell under the test conditions mentioned above. Similar to the results obtained above, I could not detect any association between wild type PDE4D5 tagged with VSV and endogenous/transfected SUMO-1 or SUMO-2.

As SUMO-1 and SUMO-2 confer different patterns of conjugation onto substrate proteins, where SUMO-1 exists predominantly in its conjugating form, but SUMO-2/3 are dramatically subject to rapid conjugation upon heat shock and oxidative or ethanol stress (Saitoh et al; Manza et al. 2004). Therefore, I tried to assess if treatment of HEK293/HEKB2 cells with H<sub>2</sub>O<sub>2</sub> for 30 min would trigger the SUMO-2 modification of VSV-PDE4D5. The null interaction between VSV-PDE4D5 and endogenous SUMO-2 indicates that wild type PDE4D5 did not undergo sumoylation under oxidative stress conditions.

So far, all the possible conditions under which PDE4D5 might be modified by SUMO have been tried, except the consideration of the importance of SUMO E3 ligase. Only recently has it been appreciated that SUMO E3 ligases are important in regulating substrate selection, promoting the efficiency of target protein sumoylation *in vivo* (Hay 2005). As the failure of detection of SUMO modification of PDE4D5 *in vivo* might result from the weak activity of SUMO E3 ligase in those studied cells, especially when isopeptidase activity is high, I set out to examine if the overexpression of one of the SUMO E3 ligases, PIASy, would enhance the degree of PDE4D5 being modified by SUMO, to which its conjugation can be detected *in vivo*. In this set of experiments, HEK293 cells were cotransfected with VSV- tagged PDE4D5 (C-terminal epitope tag) and HA-tagged PIASy (N-terminal epitope tag), and harvested in the modified RIPA buffer that contains 25 μM NEM (a de-ubiquitinating enzyme) and 10 μM MG132 (proteasome inhibitor). The VSV-PDE4D5 was immunoprecipitated with anti-VSV agarose beads and immunoblotted with SUMO-1 (Figure 5.4). A sumoylated species was observed at about 125 kDa on the SDS gel. Overlaid VSV antibody on the same blot revealed two bands, one reflecting the size of unmodified wild type PDE4D5 (~105 kDa), another 25 kDa larger and corresponding to the previous SUMO-1 signal in the VSV-precipitates (Figure 5.4). This suggests that wild type PDE4D5 exists in a dual form, one being SUMO modified, another not. A form of PDE4D5, where lysine 323 has been mutated to arginine, was co-expressed with HA-PIASy in HEK293 cells. Failure to detect SUMO modification of VSV-K323R under the same experiment conditions as that of VSV-PDE4D5 (wild type) provides an independent support that lysine 323,

located within VKTE in PDE4D5, is the site of SUMO modification of PDE4D5 in intact cells (Figure 5.4).

### **5.2.3 Effects of SUMO-1 modification on PDE4D5 interaction with its binding partners.**

Sumoylation has previously been shown to affect protein-protein interactions (Matunis et al. 1998). As PDE4D5 has a number of binding partners, such as  $\beta$ -arrestins (Bolger et al. 2003), RACK-1 (Yarwood et al. 1999), ERK2 (MacKenzie et al. 2000) and AKAP188 (unpublished data), I set out to test whether sumoylation of PDE4D5 can affect its association with these various binding partners. Here, I performed two strategies to address this question. One was sequential immunoprecipitation, where VSV-PDE4D5 was transfected in HEK293 cells and PDE4D5 endogenous binding partners were sequentially immunoprecipitated from the lysates. Then both the lysates and immunoprecipitates were probed with anti-VSV antibody. Here, I show that wild type PDE4D5, either in the pre-IP lysates, or post-IP lysates, or in the individual IP samples, as indicated in Figure, appears in two forms: one is migrating faster and has the native size of 105 kDa; another is migrating slower and located about 25 kDa above the other (Figure 5.5 a). As it has been suggested that SUMO-1 migrates as an approximately 25 kDa species on SDS-PAGE, this larger mass of PDE4D5 is likely to be due to the addition of SUMO-1 onto VSV-PDE4D5. In order to confirm this, I stripped the blot and probed it with anti-SUMO-1 antibody. As shown here, only one band was evident in each sample lane and each band corresponded to the upper band of the VSV blot used to identify epitope-tagged PDE4D5 (Figure 5.5 b). This confirms the SUMO conjugated status of PDE4D5 in the sequential IP experiment. Interestingly, in all cases the amount of the sumoylated form of PDE4D5 detected in each immunoprecipitated species was greater than that of non-sumoylated form of PDE4D5 (Figure 5.5 a), suggesting that those PDE4D5 binding partners preferentially bind to the SUMO-conjugated form of PDE4D5. In another word, SUMO modification enhances the association of PDE4D5 with the known binding partners, namely  $\beta$ -arrestins, RACK-1, ERK2 and AKAP188 under the conditions that I performed these experiments.

Another strategy I performed to address the effect of sumoylation on PDE4D5 interaction is the comparison of the signals obtained from VSV-PDE4D5 or VSV-K323R associated binding partners. These experiments utilized VSV tagged wild type PDE4D5 and VSV tagged lysine 323 mutated form of PDE4D5. Under the experimental conditions utilised with PDE4D5 /K323R and PIASy (Figure 5.6 a), wild type PDE4D5 binds much more to  $\beta$ -arrestins, RACK-1, ERK2 and AKAP188 than its SUMO mutant (K323R), providing an independent support for the previous data obtained from the first strategy performance (Figure 5.6 b,c,d,e). These data suggest that SUMO modification of PDE4D5 enhances its interaction with certain of its binding partners.

### 5.3 Discussion

This investigation demonstrates that PDE4D5, a unique PDE4 isoform, exists in a dual form, one of which is SUMO-1 modified, another is not so modified (Figure 5.4, 5.5 a). I have presented evidence that this modification occurs both *in vitro* and *in vivo* in a HEK293 cell line engineered to express VSV-tagged PDE4D5. However, co-transfection with HA-tagged PIASy is required to identify SUMO-1 modification of PDE4D5. I have mapped the SUMO modification site on PDE4D5 to one consensus lysine (K323) in the N-terminal portion of catalytic domain of PDE4D5 (Figure 5.4). Sumoylation of PDE4D5 seems to affect its interaction with some other proteins (Figure 5.5 a). Alignment of four different PDE4 genes reveals that PDE4A and PDE4D both possess sumoylation consensus motif. Although, to date, I have not been able to show that PDE4A can be modified by SUMO-1, this at least suggests that SUMO modification might be not restricted to PDE4D gene family members, but also members of the PDE4A family. The effects of sumoylation of PDE4D5 isoform may be also important for regulation of all of the PDE4A/D family members, which contain the SUMO modification consensus motif.

Sumoylation is now known highly dynamic and reversible (Dohmen 2004), equilibrating between sumoylation and desumoylation. The major difficulties in identifying SUMO targets are: (1) these proteins are rapidly deconjugated by SUMO-specific proteases upon cell lysis in nondenaturing buffer (Melchior F. 2000); (2) only a small fraction of the substrate, frequently below 1% is sumoylated at any give time

(Johnson 2004). This might explain why I could not detect any sumoylated form PDE4D5 in the initial screen unless a lysis buffer containing SDS and NEM (modified RIPA buffer) was used in the analysis, which correlates with the characteristics of many SUMO-conjugated proteins (Chang et al. 2004; et al. 2002; Hofmann et al. 2000).

Although *in vitro* sumoylation of PDE4D5 has been shown to occur in the presence of SUMO-E, E2, Ubc9 and SUMO-1 (or SUMO-2) in the absence of a SUMO-E3 (Figure 5.3), the extent of detecting sumoylation of PDE4D5 in intact HEK293 cells was shown to increase in the presence of the PIASy, which serves as a SUMO-E3 ligase (Figure 5.4). This investigation demonstrates that PIASy is crucial for PDE4D5 sumoylation to be detected *in vivo* in the model system used here. PIASy, one of the isoform of PIAS proteins, has a SP-RING domain, which resembles RING finger motif found in many Ub E3s (Hochstrasser 2001) and is responsible for the direct binding to SUMO E2 conjugating enzyme Ubc9. Common to other PIAS proteins, PIASy contains a SIM (SUMO interacting motif) domain, which is implicated in binding to SUMO non-covalently (Minty et al. 2000). Therefore, it appears that introducing exogenous HA-PIASy into HEK293 cells increases the E3 ligase-dependent activity by efficiently bringing both E2 Ubc9 and SUMO isoforms in close proximity to PDE4D5, therefore making the sumoylation of PDE4D5 *in vivo* possible and detectable. Owing to the low amount of PDE4D5 expressed endogenously in HEK293, exogenously expressing VSV-PDE4D5, together with HA-PIASy, increases the amount of PDE4D5 being sumoylated.

Although the conditions under which sumoylation of PDE4D5 has been identified in several experiments were optimized and kept through all my *in vivo* experiments, the frequency of detecting sumoylated form of PDE4D5 is still relatively low, in another word, the chance of being able to detect PDE4D5 *in vivo* is variable. Thus a large number of evaluations were carried out in order to obtain definitive results. Therefore, the following functional analyses of sumoylation of PDE4D5 were performed in samples that were first tested and proven to produce positive sumoylation results.

PDE4D5 contains 745 amino acids and has an estimated molecular mass of

84.4 kDa. However, PDE4D5 normally migrates to positions significantly higher than 84.4 kDa in an SDS-PAGE gel at about 105 kDa. Moreover, although SUMO-1 has an estimated molecular mass of ~12 kDa, several previous studies have demonstrated that many SUMO-conjugated proteins usually have a size increase of ~20 kDa after conjugation by one SUMO-1 molecule (Johnson 2004). Under the optimized conditions, protein bands of 105 and 130 kDa were clearly detectable by immunoblot analysis with an anti-VSV antibody (Figure 5.5, lane 1). The size difference between these two bands implies that VSV-PDE4D5 is conjugated by one SUMO-1 molecule. As SUMO-1 does not have  $\psi$ KXE motif, or the possible acceptor lysines that are homologous to lysine 29, 48, 63 of Ub, this finding is consistent with previous observations that SUMO-1 does not form poly-SUMO chains (Secler and Dejean 2003). The evidence demonstrating that VSV-PDE4D5 is conjugated by SUMO-1 also comes from immunoprecipitation experiments. In the lysate prepared from HEK293 cells transfected with VSV-PDE4D5 and HA-PIASy, VSV-tagged PDE4D5 was immunoprecipitated and detected by an anti-SUMO-1 antibody (Figure 5.5 b) or VSV antibody (Figure 5.5 a). As is generally known, proteins are often sumoylated on the lysine residue of a  $\psi$ KXE sequence. In the N-terminal of catalytic domain of PDE4D5 resides such a consensus motif VKTE (Figure 5.2). Mutating the lysine residue of this site influenced PDE4D5 sumoylation, indicating this lysine residue is the actual site for SUMO modification (Figure 5.4 b). This result also eliminates the possibility that the proteins detected are non-specifically immunoprecipitated by anti-VSV agarose beads. Interestingly, when I tried to do the reverse IP, in which anti-SUMO-1 antibody was used to immunoprecipitate sumoylated form of PDE4D5, VSV-PDE4D5 did not come down together with the SUMO-1 antibody. This might be attributed to the fact that the SUMO-1 antibody used in this study can not be used for immunoprecipitation. Notably, the quantity of VSV-PDE4D5 that is sumoylated appears to be a small percentage of the total VSV-PDE4D5 (Figure 5.3; 5.4 a). However, in one rare case, I obtained high quantity of sumoylated form of PDE4D5 (Figure 5.5 a).

Sumoylation often affects the function of protein-protein interactions (Matunis et al. 1998; Johnson 2004). The sequential IP results demonstrate that the sumoylated form of VSV-PDE4D5 is more abundant than the non-sumoylated VSV-PDE4D5 (~105 kDa) in each IP sample, as the band at 130 kDa is observed more

intense than that at 105 kDa in immunoblot (Figure 5.5, lane 1). This phenomenon is possibly owing to the fact that sumoylated PDE4D5 preferentially interacted with various numbers of scaffolding/signalling proteins, such as  $\beta$ -arrestins, RACK-1, ERK2 and AKAP188.

Additionally, the availability of lysine323 in PDE4D5 largely affects the extent to which PDE4D5 interacts with a number of its binding partners, as sumoylated form of PDE4D5 accounts for a large proportion of the total PDE4D5 that is associated with the scaffolding or signalling proteins (Figure 5.5). In another word, wild type PDE4D5, composed of both sumoylated and non-sumoylated form, binds to its binding partners studied here more than that in only non-sumoylated form (K323R). As the signalling complexes containing PDE4D5 and its individual binding partners are sequestered in distinct focal points and serve as shaping cAMP gradients, the changes in the binding affinities of PDE4D5 towards its binding partners due to its sumoylation status thus provides a possible mechanism for fine-tuning the compartmentalization and desensitization of cAMP in the cells. The magnitude of the differences in binding affinity towards those binding partners between wild type PDE4D5 and the non-sumoylated form of PDE4D5 are considerably large and therefore potentially capable of representing a biologically important homeostatic mechanism.

To elucidate the meaning of the sumoylation of PDE4D5, it is important to know what kinds of signal can induce or suppress the sumoylation of PDE4D5. Although I have shown that SUMO E3 ligase PIASy is important, there still leaves a number of questions to be answered. (1) What is the SUMO isopeptidase involved? It is well known that the level of the sumoylation is a balance between the activities of sumoylation enzyme (E1, Ubc9, or SUMO E3 ligase PIASy) and SUMO-specific proteases. So far, there are three genes, SENP1, SENP2 (also known as Axam, Supr-1, SSP3, and SMT31P2), and SENP3 (SMT31P1), that have been shown to function as SUMO-specific proteases in mammals (Hay 2005; Melchior et al. 2003). Possibly the knockdown of one of the SUMO-specific protease in HEK293 cells using siRNA technique would reveal the answer, which application into the cells will surely make the detection of the SUMO modification of PDE4D5 easier and more reliable. (2) Is

sumoylation of PDE4D5 a constitutive process or a regulated one? If regulated, what signals trigger or inhibit the pathway? A number of post-translational modifications, such as those that can target the same acceptor lysine as SUMO (for example, ubiquitination and acetylation) or those that modify other residues, such as phosphorylation, have been suggested to regulate sumoylation either positively (Desterro et al. 1998; Everett et al. 1999; Muller et al. 2000; Yang et al. 2003) or negatively (Hietakangas et al. 2003; Sobko et al. 2002). Thus, it will be intriguing to see if phosphorylated or ubiquitinated forms of PDE4D5 transfected in cells will make a difference in its sumoylation status. (3) Are there any other macromolecules able to bind to PDE4D5 and regulate its SUMO modification? This is inspired by the fact that sumoylation of Mdm2 and p53 *in vivo* has been shown to be enhanced by association with the tumor suppressor ARF (Chen and Chen 2003), and that sumoylation of the transcriptional factor Sp3 was reduced when bound to DNA (Sapetschnig et al. 2002). I have already shown that sumoylation of PDE4D5 increases its binding to  $\beta$ -arrestins, RACK-1, ERK2 and AKAP18 $\delta$ , but it will be interesting to see if blocking the interactions between PDE4D5 and these binding partners using the mutants of PDE4D5 will affect the SUMO modification status of PDE4D5.

To further discuss the function of sumoylation of PDE4D5, it will be necessary to check its activity, its sub-cellular localization. Given the instability of SUMO modifications *in vivo*, the SUMO-1 fusion protein, which SUMO proteases cannot cleave, might provide an alternative means to elucidate the nature of sumoylation of PDE4D5.

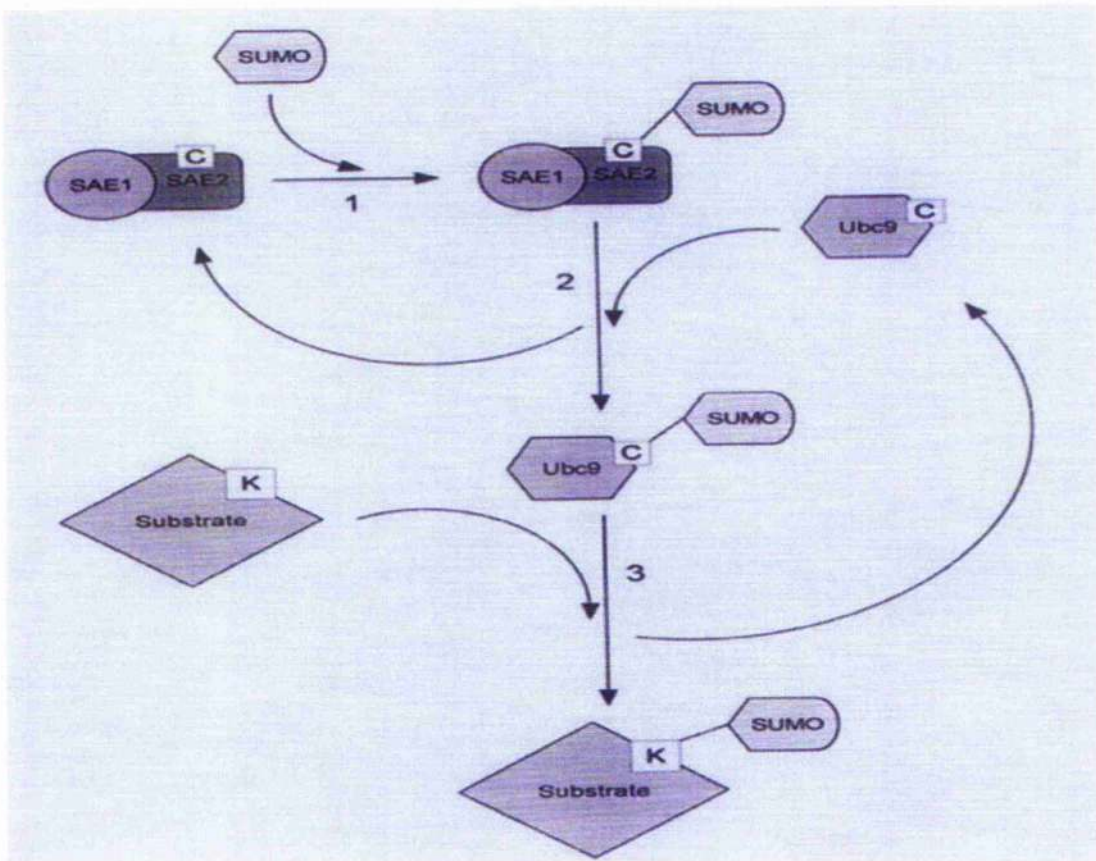


**Figure 5.1 Enzymatic conjugation mechanism of sumoylation.**

The SUMO precursor is cleaved by SUMO-specific proteases (SENPs) with C-terminal hydrolase activity to expose a C-terminal diglycine. In an ATP-dependent reaction, mature SUMO forms a thioester conjugate with the heterodimer SUMO E1 activating enzyme (in yeast is SAE1/SAE2, in mammals is Aos1/Uba2). SUMO is then transferred to the SUMO E2 conjugating enzyme Ubc9 and formed a thioester intermediate again. From Ubc9, SUMO is conjugated to a substrate protein via an isopeptide bond with a lysine residue (K). Recently several unrelated SUMO E3 ligases have been shown to crucial for substrate protein sumoylation in step 3. SUMO modification is reversible and SUMO is removed from substrates by SUMO specific proteases (SENPs) with isopeptidase activity. Schematic is taken from Wojcikiewicz 2004).

M A Q Q T S P D T L T V P E V D N P H C P N P W L N E D L V K S L R E N L L Q H E K S K T A R K S V  
 S P K L S P V I S P R N S P R L L R R M L L S S N I P K Q R R F T V A H T C F D V D N G T S A G R S  
 P L D P M T S P G S G L I L Q A N F V H S Q R R E S F L Y R S D S D Y D L S P K S M S R N S S I A S  
 D I H G D D L I V T P F A Q V L A S L R T V R N N F A A L T N L Q D R A P S K R S P M C N Q P S I N  
 K A T I T E E A Y Q K L A S E T L E E L D W C L D Q L E T L Q T R H S V S E M A S N K F K R M L N R  
 E L T H L S E M S R S G N Q V S E F I S N T F L D R Q H E V E I P S P T Q K E K E K K K R P M S Q I  
 S G V K K L M H S S S L T N S S I P R F G V K T E Q E D V L A K E L E D V N K W G L H V F R I A E L  
 S G N R P L T V I M H T I F Q E R D L L K T F K I P V D T L I T Y L M T L E D H Y H A D V A Y H N N  
 I H A A D V V Q S T H V L L S T P A L E A V F T D L E I L A A I F A S A I H D V D H P G V S N Q F L  
 I N T N S E L A L M Y N D S S V L E N H H L A V G F K L L Q E E N C D I F Q N L T K K Q R Q S L R K  
 M V I D I V L A T D M S K H M N L L A D L K T M V E T K K V T S S G V L L L D N Y S D R I Q V L Q N  
 M V H C A D L S N P T K P L Q L Y R Q W T D R I M E E F F R Q G D R E R E R G M E I S P M C D K H N  
 A S V E K S Q V G F I D Y I V H P L W E T W A D L V H P D A Q D I L D T L E D N R E W Y Q S T I P Q  
 S P S P A P D D P E E G R Q G Q T E K F Q F E L T L E E D G E S D T E K D S G S Q V E E D T S C S D  
 S K T L C T Q D S E S T E I P L D E Q V E E E A V G E E E E S Q P E A C V I D D R S P D T •

**Figure 5.2 PDE4D5 amino acid sequence alignment.**

The entire sequence of human PDE4D5 is illustrated here. Letters in red indicate  $\beta$ -arrestin binding sites on PDE4D5; letters in orange are the SUMO modification consensus motif ( $\psi$ KXE); letters in green indicate the potential ubiquitin interaction motif (UIM).

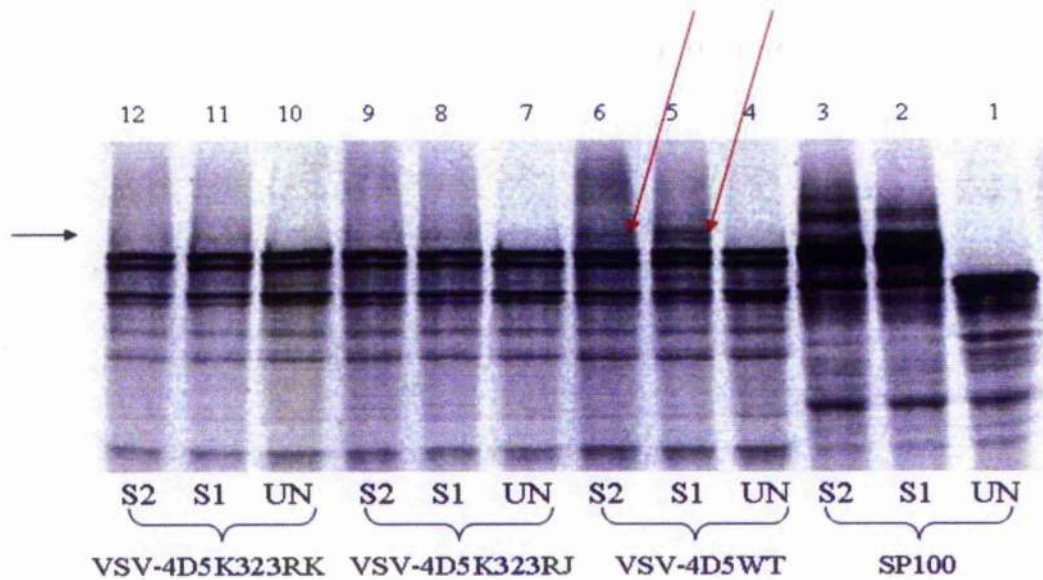


**Figure 5.3 PDE4D5 is a substrate for SUMO-1 and SUMO-2 conjugation *in vitro*.** *In vitro* expression of 35S labelled PDE4D5 and following *in vitro* SUMO modification of PDE4D5 were performed by the Hay laboratory in Dundee University. Fractionate reaction products were subject to SDS-PAGE gel and subsequent staining, fixing and drying. Results were analysed by phosphoimager. As a positive control, the PDE4D5 unrelated protein SP100, which has been shown to be modified by SUMO, was used (lane 1-3). For negative controls for all samples (UN), ATP regenerating system was omitted in the reactions.

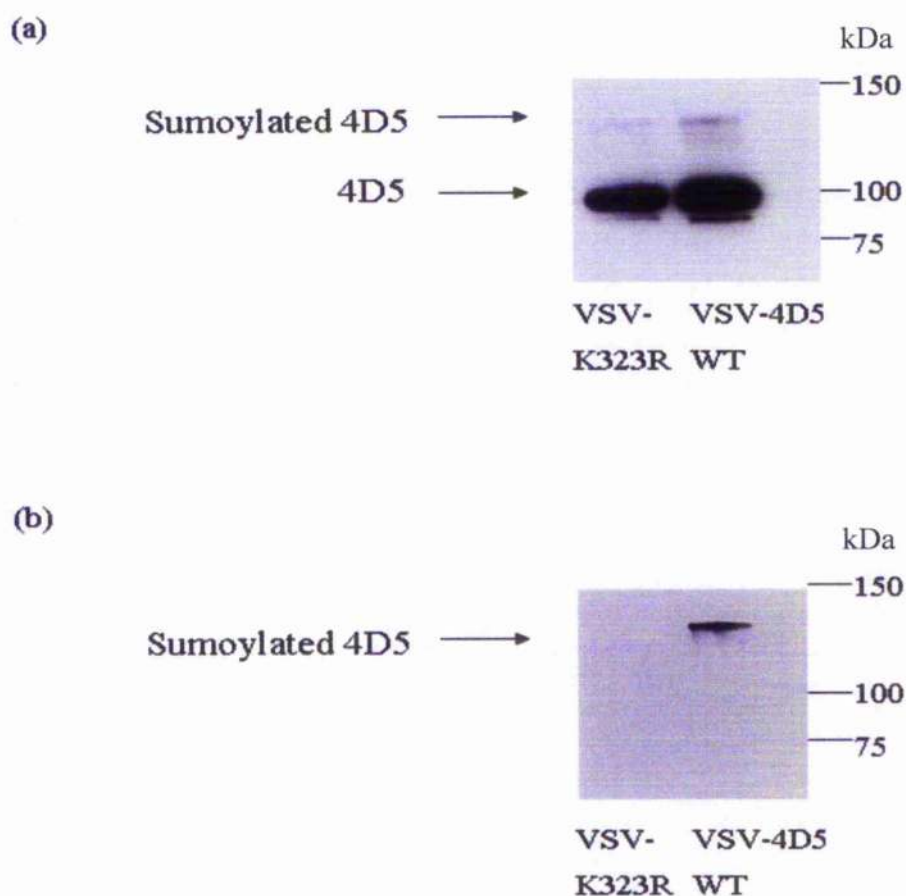
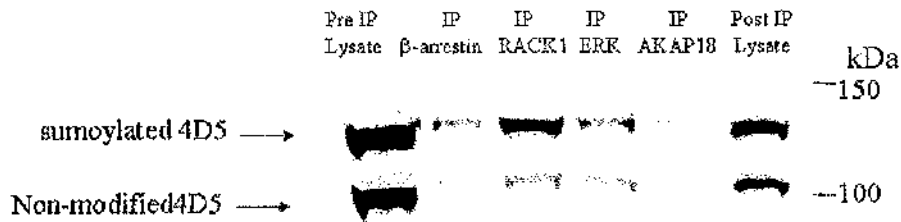


**Figure 5.4 Exogenously expressed VSV-tagged PDE4D5 is modified by SUMO-1 *in vivo*.**

HEK293 cells were transfected with VSV-PDE4D5 and HA-PIASy, and harvested in modified RIPA buffer containing 0.1% SDS and 25  $\mu$ M NEM. Clear cell lysates were immunoprecipitated with anti-VSV agarose beads. (a) Immunoprecipitates were analyzed by Western blotting with an anti-VSV monoclonal antibody. (b) The same membrane was then stripped and re-probed with an anti-SUMO-1 monoclonal antibody. The positions of free and putative SUMO-1 conjugated PDE4D5 are indicated. Molecular weight markers are shown on the right.

(a)



(b)

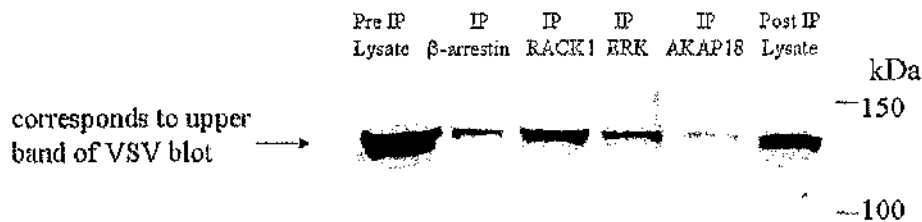


**Figure 5.5 Illustration of sumoylated form of PDE4D5 preferentially binding to  $\beta$ -arrestin, RACK-1, ERK2, and AKAP18.**

HEK293 cells were transfected with VSV-PDE4D5 and HA-PIASy. Cells were harvested in modified RIPA buffer containing SDS and NEM.  $\beta$ -arrestin, RACK1, ERK1/2, and AKAP18 $\delta$  were individually and sequentially immunoprecipitated with their corresponding antiserum. (a) The sequential IP samples run together with the pre-immunoprecipitate and post-immunoprecipitate samples were analyzed by Western blotting with an anti-VSV antibody. (b) The same blot was stripped and reprobed with SUMO-1. Running position of molecular weight markers and of SUMO-1 conjugated PDE4D5 are indicated.

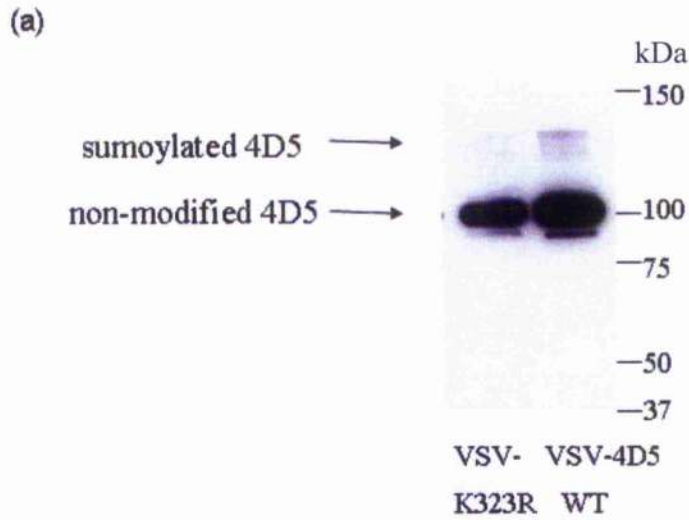


**Figure 5.6 SUMO-1 conjugation enhances PDE4D5 interaction with  $\beta$ -arrestins, RACK-1, ERK and AKAP18 $\delta$ .**

(a) Immunoprecipitation of VSV-tagged PDE4D5 was performed in HEK293 cells transfected with VSV-PDE4D5 and HA-PIASy. Sumoylation status of VSV-PDE4D5 was analyzed by Western blotting of the immunoprecipitates with anti-VSV antibody. VSV tagged 4D5K323R was used as a control. The position of conjugated and non-conjugated PDE4D5, as well as the protein molecular weight marker is indicated.

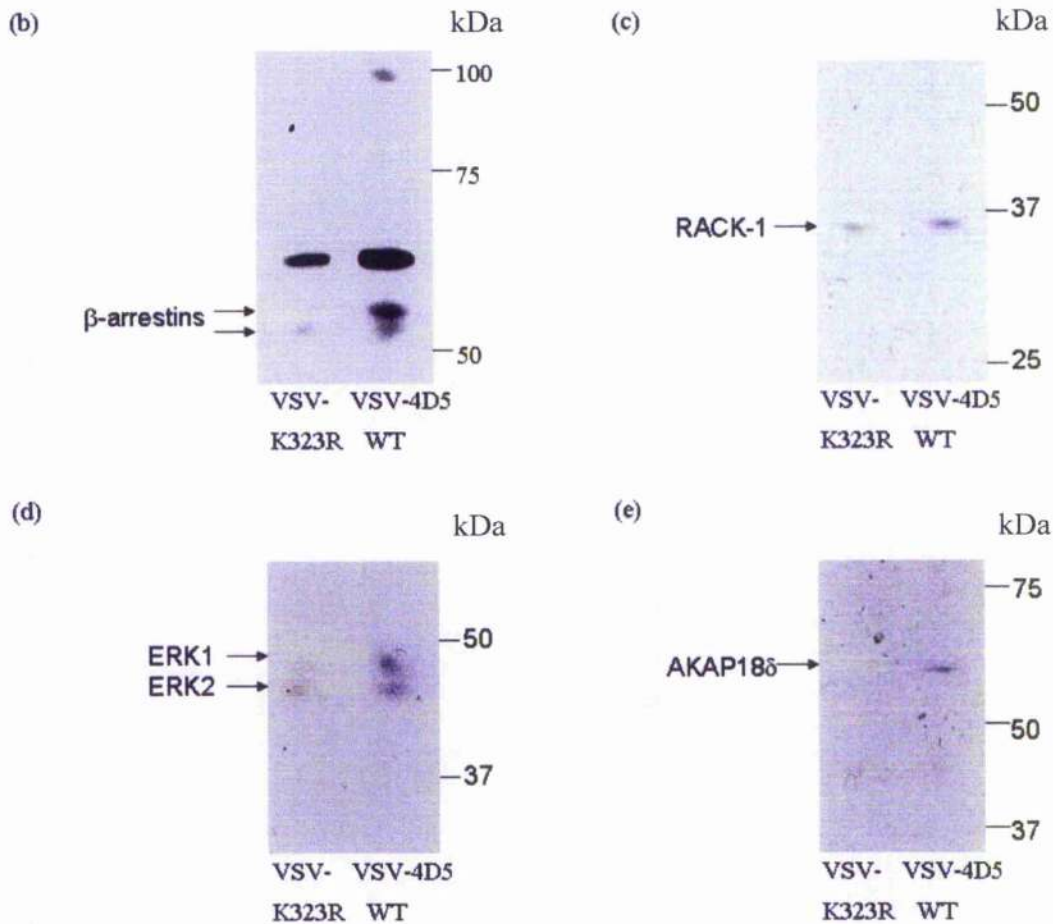


**Figure 5.6 SUMO-1 conjugation enhances PDE4D5 interaction with  $\beta$ -arrestins, RACK-1, ERK and AKAP18 $\delta$ .**

HEK293 cells were transfected with VSV-PDE4D5 and HA-PIASy and harvested in modified RIPA buffer containing SDS, NEM. Confirmation of the sumoylation of PDE4D5 was required prior the further explore of the interactions between PDE4D5 and  $\beta$ -arrestins, RACK-1, ERK1/2 or AKAP18 $\delta$  (see Figure 5.6 a). (b) Shows the difference between wild type PDE4D5 and SUMO mutant of PDE4D5 (K323R) in interacting with  $\beta$ -arrestins. This association was analyzed by Western blotting with anti- $\beta$ -arrestin antibody. (c) Shows the interaction of wild type PDE4D5 or SUMO mutant of PDE4D5 with RACK-1. (d) Shows the association between PDE4D5 or SUMO mutant of PDE4D5 and ERK1/2. (e) Shows the interaction of wild type PDE4D5 or its SUMO mutant with AKAP18 $\delta$ . Running position of protein molecular weight marker and the studied proteins that are associated with PDE4D5 are indicated.

## **Chapter 6**

### **Analysis of Binding Sites on PDE4D5 to $\beta$ -arrestin, ERK2 and Ubc9**

## 6.1 Introduction

Individual signaling pathways consist of a number of discrete components. In many instances individual members of a signaling pathway have been shown to interact with the components of other signaling pathways, therefore the two or more signaling systems are integrated and form highly intensive networks to achieve the integrated function of cells in one organism (Houslay and Milligan 1997). The complex formations, which involve protein-protein interactions, take place either between potential scaffolding/adaptor proteins and signaling proteins or between two different signaling proteins (Pawson and Scott 1997). The rapidity at which the reversible interactions can be altered depends on the concentration of constituents and their affinities for each other.

Our group (see for review: Houslay and Adams 2003) and, more recently, others have demonstrated that specific PDE4 isoforms can interact with a number of distinct proteins, including signal scaffolding proteins, like  $\beta$ -arrestins (Bolger et al. 2003), RACK (Yarwood et al. 1999), protein kinases like c-Src (McPhee et al. 1999), DISC1 (Miller et al. 2005), XAP2 (Bolger et al. 2003), myomegalin (Varadan et al. 2002), mAKAP (Dodge et al. 2001), AKAP450 (McCahill et al. 2005; Tasken et al. 2001) and ERK (MacKenzie et al. 2000). Such interactions are thought to provide the molecular machinery that is responsible for underpinning the formation of compartmentalized cAMP signaling (Houslay and Baillie 2003).

The signalling scaffold proteins,  $\beta$ -arrestin1 and  $\beta$ -arrestin2 can bind to a site within the highly conserved catalytic unit of PDE4 isoforms from all four subfamilies (Bolger et al. 2003). This interaction confers a new feature of the GPCR/ $\beta$ -arrestin desensitization system, whereby  $\beta$ -arrestin-delivered PDE4 appears to regulate the activity of PKA at the plasma membrane and thereby regulate the PKA phosphorylation status of the  $\beta_2$ AR itself (Lynch et al. 2005). A functional consequence of this is switching of signalling of the  $\beta_2$ AR from activation of adenylyl cyclase through Gs to activation of ERK through Gi (Baillie et al. 2003). Although all PDE4 isoforms have the potential to interact with  $\beta$ -arrestin and regulate  $\beta_2$ AR phosphorylation by PKA, it has been shown that invariably it is the PDE4D5 isoform that performs such a role (Bolger et al. 2003; Lynch et al. 2005). This is because the

unique 88-amino acid N-terminal region of this isoform contains an additional interaction site for interaction with  $\beta$ -arrestins, thereby conferring preferential recruitment of PDE4D5 to complexes with  $\beta$ -arrestin when this isoform is expressed in cells.

PDE4 isoforms of the B/C/D families provide a point of cross-talk that links ERK2 activation to the regulation of cAMP signaling (Houslay and Adams, 2003; Houslay and Kolch 2000). Thus activation of ERK through EGF challenge causes the rapid inhibition of long PDE4 isoforms that can trigger an increase in cAMP levels. A functional consequence of this is to allow for activation of PKA, which can subsequently elicit the phosphorylation and re-activation of long PDE4 isoforms (Hoffmann et al. 1999). That PDE4 isoforms are authentic substrates for ERK phosphorylation was the discovery that the PDE4 catalytic unit contains a consensus KIM docking site for MAP Kinases as well as a FQF motif that confers specificity for phosphorylation by ERK rather than JNK (MacKenzie et al. 2000). These sites are both located in the C-terminal of the catalytic unit of PDE4 and straddle the target serine residue for ERK2 phosphorylation, which are essential for *in vivo* binding and phosphorylation of PDE4 by ERK2.

In last chapter, I proposed that PDE4D5 contains a SUMO modification consensus sequence ( $\psi$ KXE) in the N-terminal portion of the PDE4 catalytic domain and that this sequence might be responsible for conferring sumoylation upon PDE4D5 (Figure 5.4). Ubc9, a single E2-type-conjugating enzyme (Melchior 2000), plays an important role in SUMO substrate recognition as it has been shown physically interacting with almost all known SUMO substrate in yeast two-hybrid assays (Sampson et al. 2001). Although some studies (Sampson et al. 2001) have demonstrated that Ubc9 directly recognizes substrate proteins, through their  $\psi$ KXE consensus sequence, it has not been generalized in all  $\psi$ KXE-containing proteins. This prompted me to assess the possible binding between PDE4D5 and Ubc9 and any involvement of the putative Ubc9 binding motif on PDE4D5.

Studies on protein-protein interaction have mainly been analyzed through immunoprecipitation, pull-down and yeast two-hybrid techniques as readouts. These

are then coupled to mutation and truncation to gain insight into the binding sequence. The generation of panels of mutants and truncates requires extensive amounts of work. Recently, however, peptide array analysis has been developed in order to provide a novel, powerful and rapid technology to identify potential sites of interaction between proteins (Kramer and Schneider-Mergener 1998). Here I employed this technique, together with traditional immunoprecipitation methodologies, to evaluate further the mode of interaction of  $\beta$ -arrestins, EKR2 and Ubc9 with PDE4D5.

## 6.2 Results

### 6.2.1 Analyses of PDE4D5 binding to $\beta$ -arrestins

PDE4D5 preferentially binds  $\beta$ -arrestins compared to other PDE4 isoforms (Bolger et al. 2003). Consequently, it is preferentially recruited to the GRK-phosphorylated  $\beta_2$ AR where it serves to degrade the cAMP in the local environment of the  $\beta_2$ AR (Bolger et al. 2003; Lynch et al. 2005). Such preferential binding of PDE4D5 is because it, uniquely, has two sites for interaction with  $\beta$ -arrestin2, one in its unique N-terminal region and another within the conserved PDE4 catalytic region (Bolger et al. 2003).

Although  $\beta$ -arrestin1 and  $\beta$ -arrestin2 are ~80% sequence identical (Miller et al. 2001, Figure 6.2), this does not guarantee that they both interact with PDE4D5 in the same manner. Therefore, I set out here to assess individual  $\beta$ -arrestin1 and  $\beta$ -arrestin2 binding sites on PDE4D5 by using the peptide array analyses.

#### 6.2.1.1 Purification of GST- $\beta$ -arrestin1 and GST- $\beta$ -arrestin2 fusion proteins

In order to carry out the peptide array analyses I first expressed the full-length  $\beta$ -arrestin1 and  $\beta$ -arrestin2 fused with GST in *E. Coli* and purified them as described in the Materials and Methods. After each step, equal amount of samples were collected and all were run in the same SDS-PAGE gel to help trace the progress of this purification. This gel was then subject to Coomassie Blue to visualize the proteins, followed by extensive washes in de-staining buffer to get rid of the background. Here, I show that both  $\beta$ -arrestin1 and  $\beta$ -arrestin2 recombinant proteins are reasonably homogenous, with the size of 73 kDa and 75 kDa, respectively on the gel (Figure 6.3).

### 6.2.1.2 Peptide arrays identify sites in PDE4D5 that interacts with $\beta$ arrestin2

As a novel and powerful technology, peptide array analysis is used here to identify potential sites of interaction between PDE4D5 and  $\beta$ -arrestin2. In this, overlapping peptides (25 mers), shifted along by 5 amino acids in the sequence and representing the entire sequence of PDE4D5 were 'spot-synthesized' and immobilized on cellular membranes (Kramer and Schneider-Mergener 1998; Frank 2002). The membrane was then overlaid with recombinant  $\beta$ -arrestin2-GST protein and probed with antiserum to  $\beta$ -arrestin. A control study was performed with GST alone, which did not bind to PDE4D5 peptide array. Positive interactions were indicated by darkspots and negative interactions were indicated by clear areas (Figure 6.4). Here the peptide array analysis identified two potential binding regions for  $\beta$ -arrestin2 on PDE4D5, one located in the N-terminal region of PDE4D5 and the other in the common catalytic region (Figure 6.5). Previous progressive N-terminal truncation analysis inferred that amino acids 70 through 88 in PDE4D5 were important for  $\beta$ -arrestin2 binding (Bolger et al. 2003). The evident interaction of  $\beta$ -arrestin2 with peptide 13, which encompasses amino acid 61-85 of PDE4D5, is entirely consistent with this (Figure 6.5). However, I show here that  $\beta$ -arrestin2 may actually bind a much wider part of the unique N-terminal region of PDE4D5, extending from amino acid 11 through to 85, as indicated by the positive signal from peptide spots 3 through to 13 (Figure 6.5). Thus, my peptide array analysis suggests that  $\beta$ -arrestin2 may bind to an extended surface across the unique N-terminal region of PDE4D5.

Previous analyses also indicated that  $\beta$ -arrestin2 was able to bind to the C-terminal portion of PDE4D5 catalytic region, namely the EKFQFELTLEE sequence, which extends from amino acid 668 through to 678 (Bolger et al. 2003). This sequence is cognate to that found in other PDE4 isoforms, and therefore considered as the common binding site for  $\beta$ -arrestin2 (Bolger et al. 2003). Here, my peptide array analysis provides an independent support for this finding (Figure 6.5), because  $\beta$ -arrestin2 is clearly shown to interact with four sequentially located peptides (132-135) in the PDE4D5 array library whose sequence share the common motif EKFQFELTLEE. Consistent with the importance of the components of such a motif, peptide 131, which lacks the LEEDG sequence found in peptide 132, and peptide 136, which lacks the FQFEL sequence, show no binding to PDE4D5, and peptide 135 that

lacks the GQTEK sequence appears to show a considerable diminution in the signal for interaction of  $\beta$ -arrestin2 compared to peptide 134.

#### **6.2.1.3 Peptide arrays identify sites in PDE4D5 that interacts with $\beta$ -arrestin1**

The peptide array data obtained from the detection of PDE4D5 binding to  $\beta$ -arrestin2 supports and extends previous studies, therefore validating the application of this approach to assess PDE4D5 binding to proteins.

To date there is no evidence detailing the  $\beta$ -arrestin1 binding sites on PDE4D5. I wished to see if  $\beta$ -arrestin1 interacts with PDE4D5 in the same manner as  $\beta$ -arrestin2. Here I show that  $\beta$ -arrestin1 binds to PDE4D5 on the same sites as  $\beta$ -arrestin2 and exhibits exactly the same interaction pattern (Figure 6.5). This might be explained by the high sequence homology between  $\beta$ -arrestin1 and  $\beta$ -arrestin2 (~80%) (Miller et al. 2001, Figure 6.2).

#### **6.2.1.4 Scanning substitution identifies individual amino acids on PDE4D5 that require for it to interact with $\beta$ -arrestin2**

Scanning alanine mutagenesis in yeast two-hybrid and pull-down assays is a commonly used analytical method to identify the sites of interaction between proteins. Recently, a new, but cognate, procedure where the peptide array analysis is applied has been developed in our laboratory. This involves the sequential single substitution of successive amino acids in the sequence of the 25 progeny of parent peptide of interest to alanine to form the scanning peptide array (Figure 6.4). Identical procedures are carried out, as described above, for detection of interaction. This approach aids in the identification of particular amino acids where substitution for alanine can negate interaction of the 25-mer peptide with overlaid GST-fusion proteins.

Since  $\beta$ -arrestin1 and  $\beta$ -arrestin2 show the same binding sites on PDE4D5 (Figure 6.5), I chose  $\beta$ -arrestin2 as a representative to further evaluate the interactions between PDE4D5 and  $\beta$ -arrestin2.

During the time when I was studying the interaction between PDE4D5 and  $\beta$ -

arrestins, the interaction between RACK1 and PDE4D5 was analyzed by my colleague (George Baillie) using the same peptide array technique. The peptide spot indicating the binding PDE4D5 with RACK1-GST came out positive in the N-terminal region of PDE4D5. This is consistent with previous truncation and mutation data identifying an interaction site for RACK1 in the unique N-terminal region of PDE4D5 (Steele et al. 2001). However, interestingly, this peptide spot (spot 5) falls into the N-terminal PDE4D5 binding region for  $\beta$ -arrestin2 that I identified in my studies (Figure 6.5). I set out then to perform further analysis of peptide spot 5 to identify important amino acids used by PDE4D5 to interact with either  $\beta$ -arrestin2 or RACK1. Thus, I used alanine scanning substitution of the 25-mer peptide representing amino acids 22-45 (spot 5) of PDE4D5 to define the  $\beta$ -arrestin2-PDE4D5 interaction. This alanine scan demonstrated that the interaction was either ablated (L33, R34) or severely attenuated (N26, E27, D28, L29, V30) when the indicated amino acids were changed to alanine (Figure 6.6 a). These data might help explain why  $\beta$ -arrestin2 and RACK1 bind in a mutually exclusive fashion to PDE4D5.

In order to gain further insight into the interaction of  $\beta$ -arrestin2 with PDE4D5 catalytic domain, again I used scanning alanine substitution, this time of a peptide representing amino acids E660-F685 (spot 133 on parent peptide array) within the catalytic unit of PDE4D5 (Figure 6.6 b). The alanine scanning array of parent spot 133 was overlaid with  $\beta$ -arrestin2-GST, followed by the detection of  $\beta$ -arrestin2 using antiserum specific to  $\beta$ -arrestin on the array. Here I show that substitution, with alanine, of any one of F670, F672, E673, L674 and L676 led to either ablation or severe attenuation of the interaction with  $\beta$ -arrestin2 (Figure 6.6 b). This shows considerably agreement with the prediction of the importance of this region for the binding to  $\beta$ -arrestin 2 as deduced from bioinformatic analysis (Bolger et al. 2003).

## **6.2.2 Analysis of PDE4D5 association with ERK2**

### **6.2.2.1 Expression and purification of GST-ERK2 fusion proteins**

Full length ERK2 fused with GST was expressed in *E. Coli* and subject to purification as described in the Materials and Methods. A small sample from each step was mixed with 2x sample buffer and loaded in 4-12% SDS-PAGE gel. The progression of this purification and the purity of the GST-ERK2 fusion proteins was

visualized with 2 hour-Coomassie Blue staining, followed by extensive wash in de-staining buffer. I show here that GST-ERK2 recombinant protein was purified to homogeneity, with a size of some 67 kDa on the gel (Figure 6.7).

#### **6.2.2.2 Selective immunoprecipitation identifies the association between PDE4D5 and ERK2**

PDE4D3 has been shown to have FQF and KIM docking sites for extracellular signal-related kinase 2 (ERK2) (p42<sup>MAPK</sup>) (MacKenzie et al. 2000), which confers PDE4 binding to ERK2 and is essential for ERK2 to phosphorylate PDE4 in intact cells. PDE4D5 is a long PDE4D isoform that differs from PDE4D3 solely by virtue of its unique N-terminal region arising through alternative mRNA splicing (Bolger et al. 1997). It thus shares with PDE4D3 a consensus site for phosphorylation by ERK2, in this case S651 in the motif PQSP, as well as the two EKR docking motifs (Hoffmann et al. 1999). Although S651 on PDE4D5 has been proven to provide a substrate for C-terminal catalytic domain phosphorylation by ERK2 (Hoffmann et al. 1999), the potential binding region of PDE4D5 with ERK2 has not been validated through direct experimentation. Therefore, I set out here to examine the domains and specifically, the amino acids that are important for ERK2 interaction with PDE4D5.

In order to evaluate potential ERK2 binding to PDE4D5, I examined immunopurified complexes from HEK293 cells. Transfected PDE4D5-VSV was immunoprecipitated with VSV affinity beads, followed by western blotting to probe for ERK2. Control experiments were done with the equal amount of proteins from lysates of cells that were not transfected to express PDE4D5-VSV. Here, I identified endogenous ERK2 co-immunoprecipitating with PDE4D5 (Figure 6.8). This shows that PDE4D5 can directly bind to ERK2. A specific VSV antibody was also used to probe the immunoprecipitates to confirm the pull-down of recombinant PDE4D5-VSV.

#### **6.2.2.3 Peptide array analysis identifies the interaction sites for ERK2 on PDE4D5**

To explore further the ERK2 binding sites on PDE4D5, I again performed peptide array analyses. Full length PDE4D5 peptide library was overlaid with 10 µg/ml of purified recombinant ERK2-GST protein. Bound GST-ERK2 was then

detected with an anti-ERK2 antibody, the procedure of which is identical to that employed using western blotting. A control study was also performed with GST alone, which did not bind to the PDE4D5 peptide array. That MAP Kinase docking element facilitates the substrate phosphorylation by MAPK was firstly formulated by Michael Karin (Karin 1995) and this idea is now well accepted and proven. The KIM domain potentially allows interaction of either JNK or ERK, however, the presence of the FQF domain confers specificity for ERK docking. Such an FQF domain is generally located some 5-30 residues carboxyl-terminal to the ERK2 phosphorylation site (see Review: Sharrocks et al. 2000). In PDE4D5, the putative ERK2 specificity motif, namely the FQF motif, is located some 19 amino acids COOH-terminal to S651, the target for ERK2 phosphorylation (MacKenzie et al. 2000; Houslay and Adams 2003). Here, my peptide array analysis provides additional experimental support for such a contention (Figure 6.9). Thus, the ERK2 probe clearly interacts with four, sequentially located peptides (131-134) in the PDE4D5 array whose sequence contains the FQF motif. Consistent with the importance of such a motif, I show here that there was no interaction of ERK2 with peptide 130, which lacks the QF, the second and the third amino acid in the FQF sequence (Figure 6.9). This indicates that the last two amino acids in FQF are crucial to allow for PDE4D5 interaction with ERK2. Additionally, there appears an evident ablation in the signal for interaction of ERK2 with peptide 135, which lacks the first two amino acids FQ, indicating the importance of these two amino acids for ERK2 to bind PDE4D5 (Figure 6.9). Combined together, the peptide array analysis suggests that the sequence of PDE4D5, extending from amino acid 650 through to 690 contributes its ERK2 binding, in which FQF integrity seems crucial, consistent with previous hypothesis (MacKenzie et al. 2000).

However, a KIM domain is clearly present in the catalytic domain of PDE4D5, located some 122 amino acids C-terminal to the ERK phosphorylation site S651, and has been shown to be functional by mutation analysis (MacKenzie et al. 2000). Despite this, no peptides that represent partial or entire KIM domain of PDE4D5 were observed to interact with GST-ERK2 when probing PDE4D5 with ERK2-GST in the peptide array analysis (Figure 6.9). This suggests that the peptides in the array do not fold appropriately to form a functional KIM binding site and that other interactions are necessary in the folded protein so as to present an effective KIM site. Indeed, the KIM site is clearly isolated on an exposed beta-hairpin loop in the

folded intact catalytic unit (Houslay and Adams 2003). It may be that attributes from a folded catalytic unit are required for the KIM motif to be presented appropriately in the form of a beta-hairpin loop. This does signify that peptide arrays can have limitations in identifying binding sites that require complex folded structures.

#### **6.2.2.4 Scanning substitution identifies individual amino acids in the PDE4D5 required for it to interact with ERK2**

My peptide array analyses have demonstrated that the sequence in peptide 133, as well as binding  $\beta$ -arrestin2, is also involved in the binding of ERK2 (Figure 6.9). In order to define this interaction further for ERK, I again used alanine scan substitution. This time of the 25-mer peptide, representing amino acids E660 to E685 in PDE4D5. GST-ERK2 fusion proteins were incubated with this alanine scan array of original peptide 133, followed by detection with an anti-ERK2 specific antibody. This demonstrated that the interaction was either ablated (G662, R663, F670, F672, E673, L674, T675, L676, E677) or severely attenuated (E661, Q664, G665, E678, D679) when the indicated amino acids were changed to alanine (Figure 6.10). These cover a broad span of PDE4D5 C-terminal catalytic domain that also binds  $\beta$ -arrestin2 and includes the amino acids that seem to be essential for  $\beta$ -arrestin2 binding to PDE4D5, such as F670, F672, E673, L674, and L676 (Figure 6.6 b). These data suggest that ERK2 and  $\beta$ -arrestin2 might compete for interaction within the catalytic unit of PDE4D5.

Odyssey analysis provides another novel and sensitive technology to assess the interactions between proteins. Odyssey system uses two infra red detection channels that can be used to detect the signal of two different antisera with different wavelength tags to analyze simultaneously signals. This can be used to analyze interactions involving the array peptides with two proteins of interest. This extension from its traditional application of probing SDS-PAGE gels, allows me to show here that Odyssey analysis is ideal to evaluate binding of  $\beta$ -arrestin2 and ERK2 to PDE4D5 peptide arrays.

The alanine scan array of PDE4D5 peptide 133 was exposed to equal molar amount of  $\beta$ -arrestin2 and ERK2-GST fusion proteins and the binding of these

proteins to the PDE4D5 peptide alanine scan array was achieved using both an anti- $\beta$ -arrestin2 rabbit antibody and an anti-ERK2 mouse antibody, each linked to distinct secondary antiserum labeled with different wavelength probes. I here identified  $\beta$ -arrestin2 (green) and ERK2 (red) associating with specific peptide spots representing the alanine scanning substitution array in single channel analyses using the Odyssey system (Figure 6.11 a). I then combined signals from both channels as an overlay. Analysis using merged channels identified peptide spots with predominant or solely  $\beta$ -arrestin2-PDE4D5 complexes (indicated in green), those with predominant or solely ERK2-PDE4D5 complex (indicated in red) and those with mixed populations of  $\beta$ -arrestin2-PDE4D5 and ERK2-PDE4D5 (indicated in yellow). Those not interacting with either  $\beta$ -arrestin2 or ERK2 gave a null result (black) (Figure 6.11 b). Interestingly, it shows there that only with F670, F672, L674 and I.676 was the binding of these two fusion proteins simultaneously ablated (Figure 6.11 b; black). This indicates that these amino acids provide a common docking site on the PDE4 catalytic unit for both  $\beta$ -arrestin2 and ERK2.

### **6.2.3 Analyses of PDE4D5 binding to Ubc9**

#### **6.2.3.1 Selective immunoprecipitation analyses indicate PDE4D5 binds to Ubc9**

Analysis of the PDE4D5 sequence led me note that its catalytic domain contains an eligible SUMO modification consensus site, namely  $\psi$ KXE, which is of VKTE (Johnson 2004). Many of the SUMO target proteins that contain this minimal sequence have been shown to directly interact with SUMO-conjugating enzyme Ubc9 (Sampson et al. 2001) through this motif. Thus, I set out to examine if this was the case for PDE4D5 by employing immunoprecipitation experiments to address this possibility.

Endogenous PDE4D3 and PDE4D5 were selectively immunopurified from HEKB2 cells with an antiserum specific to PDE4D. Control experiments were performed using HEKB2 cells subject to PDE4D knockout using siRNA. Doing this I found endogenous Ubc9 was detected in the immunopurified complex from HEKB2 cells, but not in control cells where the expression of PDE4D was ablated by siRNA-mediated knockdown (Figure 6.12). No such association between PDE4D5 and Ubc9

was detected when pre-immune serum was used together with Protein G beads as a control (Figure 6.12). These data suggest that PDE4D, represented by PDE4D3 and PDE4D5 in HEKB2 cells, can interact with Ubc9. However, these data do not prove that this occurs in a direct manner, as other linker proteins may be present in immunoprecipitates from whole cell lysates. Further pull-down studies using Ubc9-GST and PDE4D5-MBP are therefore required to show if the direct interaction exists.

### **6.2.3.2 Purification of GST-Ubc9 fusion proteins**

Recombinant Ubc9 protein fused with GST was expressed in *E. Coli* and subject to purification as described in the Materials and Methods. Equal small amount of samples from each step was taken and mixed with 2x Sample Buffer, followed by electrophoresis performed on 4-12% gel. The progression of the purification, as well as the purity of GST-Ubc9 proteins in each step were visualized by 2hr Coomassie Blue staining and the following extensive wash in de-staining buffer. I show here that GST-Ubc9 recombinant protein is purified as homogenous protein, with the size of some 40 kDa on the gel (Figure 6.13).

### **6.2.3.3 Peptide arrays identify sites in the PDE4D5 that interacts with Ubc9**

Although the immunoprecipitation data obtained above demonstrates, for the first time, association between PDE4D5 and Ubc9, it does not provide evidence of direct interaction and does not indicate the nature of any putative binding site for Ubc9 on PDE4D5 if binding was direct. Therefore, I again used peptide array analysis to provide evidence for a possible direct interaction and to provide details as to what region of PDE4D5 might interact with Ubc9. Here, I show that the Ubc9 probe clearly interacts with two distinct regions in PDE4D5, both of which are located C-terminal to the PDE4D5 potential sumoylation site at K323.

Region 1 is composed of spot 75, 76 and 77, whose amino acids extend from 371 through to 405. Region 2 is composed of spot 132, 133, 134 and 135, whose amino acids extend from 655 through to 695. The second binding region is reminiscent of that for both  $\beta$ -arrestin2 and ERK2 binding, whose sequence contains the EK~~F~~Q~~F~~ELTLEE motif and extends from amino acids 656 to 695. The integrity of the EK~~F~~Q~~F~~ELTLEE motif seems important for the Ubc9 binding on PDE4D5 as I show

here that there was no reaction of Ubc9 with PDE4D5 peptide 131, which lacks the LEEDG sequence found in peptide 132 (Figure 6.14). This indicates that at least certain of these amino acids are crucial to allow for PDE4D5 interaction with Ubc9. Additionally, there seems a considerable diminution in the signal for interaction of Ubc9 with peptide 135 compared to peptide 134 (Figure 6.14), implying the importance of amino acids within the QTEK sequence. Interestingly, Ubc9 shows no interaction with peptide 136 whose sequence does not contain the FQF domain. These data indicate that FQF domain is required for PDE4D5 to interact with Ubc9.

#### **6.2.3.4 Alanine scanning substitution identifies individual amino acids in the PDE4D5 catalytic region that may contribute to a binding site for Ubc9**

In order to gain further insight into the interaction of Ubc9 with the PDE4D5 catalytic unit, I used scanning alanine substitution of a peptide representing amino acids P376 to N400 of PDE4D5 (from parent peptide 76, which shows strongest interaction) and a peptide representing amino acids E660 to E685 (from parent peptide 133, which has been shown to interact with  $\beta$ -arrestin2 and ERK2) of PDE4D5 (Figure 6.15). These two alanine scanning arrays were incubated with GST-Ubc9 and then probed with a specific anti-Ubc9 antibody. Here, I show that in the spot 76 alanine scanning array, interaction with GST-Ubc9 was either ablated (Y383, Y391) or severely attenuated (L387, E388, D394, Y397, N400) when the indicated amino acids were changed to alanine (Figure 6.15 upper panel). This suggests that these amino acids may be important for Ubc9 binding to PDE4D5. In the spot 133 alanine scan array, I show that substitution, with alanine, of any one of F670, F672, E673, L674, L676 and E677 led either to ablation or severe attenuation of the interaction of GST-Ubc9 with PDE4D5 (Figure 6.15 lower panel). This result has strong similarity to the mode through which both  $\beta$ -arrestin2 and ERK2 interact with PDE4D5 at this site. Specifically, my data suggests that a core, common binding surface for  $\beta$ -arrestin2, ERK2 and Ubc9 is provided by F670, F672, L674 and L676. Thus it is likely that  $\beta$ -arrestin2, ERK2 and Ubc9 bind in a mutually exclusive fashion to PDE4D5, providing the molecular basis for sequestered distinct 'pools' of PDE4D5.

#### **6.2.4 Analyses of $\beta$ -arrestin2 binding to Ubc9**

Analysis of the sequence of full-length  $\beta$ -arrestin2 led me to note a potential

sumoylation site at K295 residue located with a SUMO consensus sequence ( $\psi$ KXE), which takes the form of LKHE in  $\beta$ -arrestin2. This minimal consensus sequence, reminiscent of that in PDE4D5 (VKTE; see above), might also be able to interact with Ubc9 and thus promote  $\beta$ -arrestin2 sumoylation of  $\beta$ -arrestin2. Therefore, I set out here to evaluate any potential interaction between  $\beta$ -arrestin2 and Ubc9.

#### **6.2.4.1 Peptide array and scanning substitution array identify sites in the $\beta$ -arrestin2 that may allow interaction with Ubc9**

I probed  $\beta$ -arrestin2 peptide arrays with Ubc9-GST and discerned clear interactions between Ubc9 and two separate regions on  $\beta$ -arrestin2. Region 1 is composed of the amino acids from spot 36 to 39, whose sequence extends from amino acid 176 through to 215. Region 2 is indicated by interactions with spot 74 and spot 75, whose sequence spans amino acid 366 through to amino acid 395 in  $\beta$ -arrestin2. Region 1 extends from the C-terminal part of the  $\beta$ -arrestin2 N-domain through to the N-terminal portion of its C-domain, whilst Region 2 is located in the C-domain.

In contrast to the two putative regions of PDE4D5 that bind Ubc9, the two putative interaction sites on  $\beta$ -arrestin2 for Ubc9 straddle the potential target sumoylation K295 residue within the consensus  $\psi$ KXE motif (LKHE, Figure 6.16). Such potential binding sites may then promote sumoylation at the K295 site. It would be interesting to assess if this is the case as it has been previously shown that ERK2 uses this strategy to dock on PDE4D3, which facilitates the phosphorylation of PDE4D3 on the straddled serine residue (S579) (MacKenzie et al. 2000). Compared to spots 74 and 75, the adjacent spots 73 and 76 did not show any interaction with Ubc9. This indicates that the sequence IVFED found in spot 74, but not in spot 73, and the sequence 'TNLIE found in spot 75 but not 76, may also contribute to the binding of Ubc9 to  $\beta$ -arrestin2.

In order to gain further insight into specific amino acids that might be directly implicated in the interaction of  $\beta$ -arrestin2 with Ubc9 I, again, employed alanine scanning substitution analysis. In this instance I analysed the region bounded by amino acid 186 through amino acid 210 and the region extending from amino acid 371 through to 395. In the first binding region, I showed that substitution of any of

F191, S197, L204, E207, L208, Y209 and Y210 ablated interaction with Ubc9, while substitution of single L192, S194, D195, R196, L198, L200 or D205 severely compromised Ubc9 binding. In the second binding region, I demonstrated that F376, Y380, F388, D390, F391, L394 and R395 were important for Ubc9 binding, as their single substitution to alanine either ablated or severely attenuated the binding to Ubc9 (Figure 6.17). Due to the time left for me to finish my PhD, I did not perform any mutagenesis of these potential sites to confirm their binding importance, but it is essential that this is done.

### 6.3 Discussion

A key feature of PDE4 family members is their ability to interact with a variety of signaling or signaling scaffolding proteins (Houslay and Adams 2003). Members of all four PDE4 sub-families have been shown to bind to  $\beta$ -arrestin in pull down assays (Perry et al. 2002) and the binding regions were subsequently mapped to their conserved catalytic domains in two-hybrid assays (Bolger et al. 2003). However, PDE4D5, a long PDE4 isoform, has been shown to bind preferentially to  $\beta$ -arrestin because it has an additional site within its unique N-terminal region that can bind to  $\beta$ -arrestin. Thus  $\beta$ -arrestin-tethered PDE4D5 is preferentially delivered to agonist-stimulated, GRK-phosphorylated  $\beta_2$ ARs where it serves to degrade local cAMP (Lynch et al. 2005). In the studies described here, I have used a novel methodology to show that PDE4D5 is able to bind to  $\beta$ -arrestin through a broad surface on its unique N-terminal region, as well as through a domain in its catalytic unit. I also show that the region in the catalytic region of PDE4D5 that  $\beta$ -arrestin binds to is likely to form a multi-functional docking site as both ERK2 and Ubc9 also bind to this region. My studies suggest that the binding of  $\beta$ -arrestin, ERK2 and Ubc9 to PDE4D5 will be mutually exclusive and thus these interacting proteins may act to sequester distinct pools of PDE4D5 that each has particular functional roles.

PDE4D5 has a unique 88 amino acid N-terminal domain that is able to interact with the signaling scaffolding protein  $\beta$ -arrestin (Bolger et al. 2003). Previous studies, using progressive N-terminal truncation analyses, inferred that amino acids 70 through to 88 in PDE4D5 were involved in its unique binding to  $\beta$ -arrestin compared to other PDE4 isoforms (Bolger et al. 2003). However, using a novel peptide array

approach, I show here that  $\beta$ -arrestin can actually interact over an extended surface of the unique N-terminal region of PDE4D5. This surface appears to extend from amino acids 11 through to 85 in PDE4D5 (Figure 6.5). Interestingly, it has been previously shown that RACK1, an exclusive binding partner of PDE4D5, interacts with PDE4D5 N-terminal region via RAID1, whose sequence spans amino acids 23 through to 44 (Bolger et al. 2002). Therefore, it appears that  $\beta$ -arrestin and RACK1 might compete to bind to PDE4D5 in this region and interact with PDE4D5 in an exclusive manner. Although I did not perform further the experiments to prove this hypothesis, work done at the same time in the Houslay laboratory has provided evidence to prove that this is indeed the case (Bolger et al. 2006).

Previously, analysis of N-terminal truncation (Bolger et al. 2003) indicated that only when the last 18 amino acids of the 88 amino acid N-terminal region of PDE4D5 were deleted was the increased interaction with  $\beta$ -arrestin delimited. The peptide array analysis reported here is not only consistent with this portion of PDE4D5 being involved, but also implies that part of the previously N-terminal truncated portion also might provide an interacting surface. Thus, it might be expected to see that progressive N-terminal truncation within this newly-identified  $\beta$ -arrestin-interacting region of PDE4D5 will likely yield constructs with gradually diminishing affinities for  $\beta$ -arrestin2.

During my investigation, others in the Houslay Laboratory assessed competition between RACK1 and  $\beta$ -arrestin for binding to PDE4D5 (Bolger et al., 2006). In my studies I focused on the amino acids 21-45 (peptide 5; Figure 6.5), which includes RAID1 and to which  $\beta$ -arrestin also binds. Scanning array analysis of peptide 5 indicated a number of amino acids within a motif of  $^{26}\text{NEDLVxxLR}^{34}$ , as being important for PDE4D5- $\beta$ -arrestin interaction (Figure 6.6 a). Interestingly, previous N-terminal truncation of this sub-region had not been shown to overtly compromise PDE4D5- $\beta$ -arrestin interaction in either two-hybrid or immunoprecipitation studies (Bolger et al. 2003), whilst certain point mutations within this region could (Bolger et al 2006). This seeming discrepancy can be explained if mutation of certain amino acids in this sub-region acted to trigger extensive changes in the conformation of the N-terminal portion of PDE4D5 as a

whole such that  $\beta$ -arrestin binding site there was ablated/compromised. Thus, whilst mutations in this sub-region can cause loss of  $\beta$ -arrestin binding, its deletion does not ablate binding. It may, of course, affect affinities for interaction. However, such binding analyses would require a great deal of resource to undertake.

Previous truncation analyses indicated that  $\beta$ -arrestin binding region within the PDE4 catalytic unit was located between amino acid 662 and 683 of PDE4D5 (Bolger et al. 2003). Here, my peptide array analysis shows that  $\beta$ -arrestin2 interacts with the catalytic domain of PDE4D5 in a sequence that spans Ala655-Glu694 (Figure 6.5), which contains the EKFQFELTLEE motif conserved in all PDE4 sub-families.

The alanine scanning peptide array analysis clearly provides a rapid and effective way of identifying the potential amino acids that are important for protein-protein interaction, which has been shown to provide a powerful approach in the present studies. Scanning alanine substitution arrays identified F670, F672, E673, L674 and L676 in PDE4D5 as being involved in this interaction (Figure 6.6 b). Indeed, this region was previously implicated as being located in sub-domain 3 of the PDE4 catalytic unit as deduced from the bioinformatic analysis (Bolger et al. 2003). Interestingly, the presence of an FQF motif has been demonstrated in all authentic ERK substrates and suggested to be recognized specifically by ERK but not JNK (Sharrocks et al. 2000). Such an FQF motif is found in helix-17 of the PDE4 catalytic unit and shown to provide a docking site for ERK interaction and essential for its in vivo phosphorylation (MacKenzie et al. 2000). My peptide array analysis provides an independent experimental support for such a contention (Figure 6.9). Here I show that PDE4D5 binds to ERK2 through a sequence that encompasses amino acids 650-690 of PDE4D5, which contains the EKFQFELTLEE motif that was also found in  $\beta$ -arrestin binding (Figure 6.5). In addition to this FQF motif, another putative ERK docking site, namely the KIM motif, the consensus sequence of which is proposed as (V/L)X<sub>2</sub>(R/K)(R/K)X<sub>3-6</sub>L and is found in various ERK transcription factor substrates, has also been suggested to mediate the interaction of PDE4D with ERK2 (MacKenzie et al. 2000). In the case of PDE4D3, mutation of the core residues of KIM (K455/K456) stops its association with ERK2 (MacKenzie et al. 2000). In PDE4D5, the KIM motif is located 122 residues N-terminal to the ERK target Ser651 residue,

which can be recognized by all MAP kinases. However, this region, the entire sequence of which is found in peptides 104 and 105 did not seem to interact with ERK2-GST in the peptide array analysis. This is in contrast with the observation of PDE4D3 interaction with ERK2, where both KIM and FQF are crucial for their binding and mutation of either of them would lead to the loss of interaction (MacKenzie et al. 2000). As the peptide array technique bears limitations whereby the peptides sometimes are not able to fold properly on the cellulose membranes, therefore negating the potential protein interactions, it is likely that the KIM-containing peptide of PDE4D5 did not fold properly to form a binding surface as in the crystal structure this motif is on a defined beta-hairpin loop and so such a structure may be needed to present the residues appropriately. Therefore, it is necessary to see if the truncation or mutagenesis studies in co-immunoprecipitation and two-hybrid assays produce the same results.

As the focus of the present study was on the possible competition between  $\beta$ -arrestin2 and ERK2 for binding to PDE4D5, I focused on amino acids 660-685 (peptide 133; Figure 6.9), which includes FQF and to which  $\beta$ -arrestin2 also binds (Figure 6.5). Interestingly, alanine scanning of this region indicates a series of amino acids that appear to be important for the PDE4D5-ERK2 interaction (Figure 6.10). Unexpectedly, the amino acids that are crucial for PDE4D5- $\beta$ -arrestin binding are subset of those important for PDE4D5-ERK2 binding (Figure 6.6 b and 6.10). This suggests a potential for competition. In order to explore this, I performed peptide competitive binding experiment on PDE4D5 alanine substitution array (660-685) by using Odyssey system. This analysis shows that under conditions when  $\beta$ -arrestin2 and ERK2 are present at identical molar concentration in the assay, F670, F672, L674 and L676 are all crucial for the binding of PDE4D5 to both  $\beta$ -arrestin2 and ERK2, additionally supporting the hypothesis that  $\beta$ -arrestin2 and ERK2 compete to bind PDE4D5 (Figure 6.11).

Both peptide array analysis (Figure 6.14) and co-immunoprecipitation assays (Figure 6.12) demonstrate that PDE4D5 can bind to the SUMO-conjugating enzyme, Ubc9 (Hay 2005). Peptide array analysis identifies two regions on PDE4D5 that are involved in its ability to bind to Ubc9, both of which are located downstream to the

putative SUMO modification consensus motif  $\psi$ KXE, with the form of VKTE in PDED4D5 (Figure 6.14). Intriguingly, the second interaction domain falls into the region of sequence that spans amino acids 655-695, to which both  $\beta$ -arrestin2 and ERK2 bind (Figure 6.5 and 6.9). This implies that by interacting with this sub-domain on PDE4D5,  $\beta$ -arrestin2, ERK2 and Ubc9 might compete for the same docking site. Alanine scanning substitution arrays of this sequence, which extends amino acid 660-685, supported such a hypothesis as substitution of any amino acid within the cluster F670, F672, L674 and L676 led to the evident ablation of the interaction between PDE4D5 and Ubc9. This concurred with observations assessing binding of both  $\beta$ -arrestin and ERK2 to this scanning array set (Figure 6.15).

As shown here, the region representing amino acids E660 to E685 in PDE4D5 shows remarkable importance for the binding of  $\beta$ -arrestin, ERK2 and Ubc9. Further insight into the mode of the folding of this region might be gained by 3-D analysis of the crystal structure. At present, there is little structural literature available for the region cognate to the portion from Phe670 to Leu676 of PDE4D5. However, two crystal structures for a truncated PDE4B2 enzyme, namely (1F0J) (Xu et al. 2000) and 1XM6 (Card et al. 2004), extend as far as residues 672 and 677 cognate in PDE4D5, respectively. The PDE4D C-terminal stretch, involving amino acids 324-677 in PDE4D5, shows 85% sequence identity to the cognate region in PDE4B. This allowed our collaborators to build a structural homology model of this portion of PDE4D using the PDE4B structures as templates (Figure 6.18). Both templates taken together indicate that the sequence corresponding to <sup>660</sup>EEGRQGQTEKFQFELTLE<sup>677</sup> in PDE4D5 formed an  $\alpha$ -helix-containing structure (helix-17) that is separated from helix-16 by a flexible linker. However, the alignment of helix-17 within the catalytic domains in both templates is different. In the 1F0J structure, which is for a truncated PDE4B the helical region equivalent to PDE4D5 316-672, does not make any packing contacts with the core catalytic domain of its parent protein molecule, although it juxtaposes a symmetry-related molecule in the crystal structure (Xu et al. 2000). This might suggest that helix-17 is connected to the compact core of the catalytic unit by a flexible linker region rather than packing tightly onto the core catalytic domain. Interestingly, in the 1XM6 structure, which is for a truncated PDE4B enzyme equivalent to PDE4D5 295-692, helix-17 is folded across the mouth of the catalytic

pocket, trapping the PDE4 inhibitor, mesopram inside (Card et al. 2004). This would likely be a catalytically inactive form and exemplifying an extreme case. However, it is consistent with helix-17 being able to be mobile rather than fixed, which would be important for a multi-functional docking region. Consequently, two models for PDE4D5 containing this region were constructed. In the model based upon 1F0J (Figure 18), helix-17 is conformationally mobile and does not interact with the catalytic domain. The residues involved in  $\beta$ -arrestin2, ERK2, and Ubc9 binding, namely Phe670, Phe672, Leu674 and Leu676 form a semi-circular patch on an exposed surface located upon one side of the C-terminal part of helix-17. It is therefore likely that this part of the surface of helix-17 physically interacts with, as appropriate, either  $\beta$ -arrestin or ERK2 or Ubc9. On the other hand, the PDE4D model based on the 1XM6 structure presents the ability of helix-17 to fold across the opening of the catalytic site. In this arrangement, a key residue needed for the binding of each of  $\beta$ -arrestin, ERK2 and Ubc9, namely Leu674 is entirely packed against the catalytic domain (Figure 6.18). This partially occludes the surface implicated in binding of  $\beta$ -arrestin, ERK2 and Ubc9. Therefore, it seems likely that if helix-17 does normally abut the catalytic site, then some modification needs to trigger its movement away from this surface so as to expose helix-17 for interaction of these proteins and to allow access of cAMP substrate and inhibitors to the active site. Thus a model based on 1F0J, which provides an open docking site for  $\beta$ -arrestin2, ERK2 and Ubc9 to compete for binding and appears to be most likely to reflect the normal state of PDE4D5. The flexibility of helix-17 linker may be needed so that it can adopt different conformations when docking of these other molecules occur that have a second interaction site elsewhere on the PDE4D5 surface. It may also allow for regulation of binding and also for selectivity in binding, especially if regulated in some way, such as by phosphorylation.

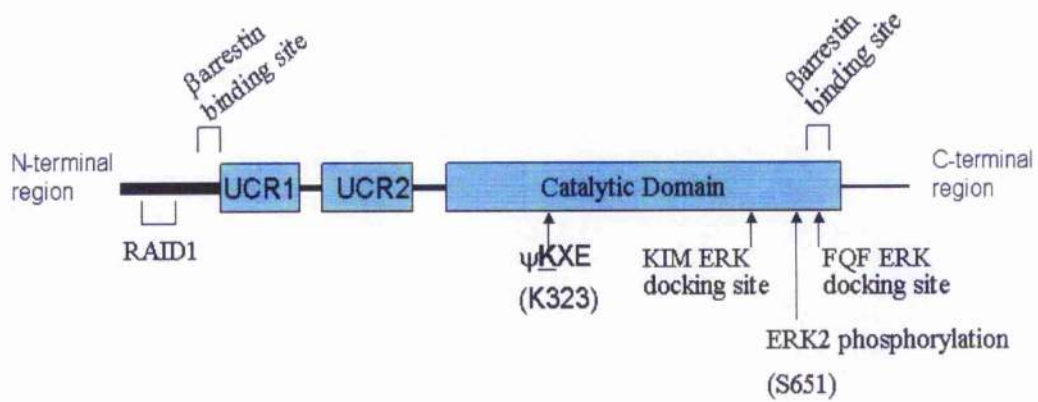


**Figure 6.1 Schematic of long isoform PDE4D5.**

Long isoform PDE4D5 is unique in its N-terminal region which is responsible for its interaction with other proteins and subcellular localization. The figure depicts the regions where PDE4D5 uses to bind to a variety of proteins. RAID1, RACK1 Interacting Domain1; UCR1, Upstream Conserved Region 1; UCR2, Upstream of Conserved Region 2;  $\psi$ KXE, SUMO modification consensus sequence.

```

B-arrestin : -MGDK 20 40 60 80 : 82
B-arr2 : HGEK 83
          GTRVFKR 89N KLTVTLGKRDFVDH6D VDPVDGVVLVDP YLR R4VSVTLTCAFYRGREDLDVGL3ERKDLF6A

B-arrestin : 100 120 140 160 : 165
B-arr2 : TY 166
          Q FPP P 4P TRLQ RL64KLG2HA DF F IP NLPCVTLQPGFEDTGRACGVDSR64AFCA LEEK HKRNSVR

B-arrestin : 180 200 220 240 : 248
B-arr2 : LVIRKVSQAPR4PGPQF3AETTR FLMSD4 LNLEASLDKR6YYRGEF6 VVVVVTNN3 KTVKKIK6SVRQYADICLF TAQ

B-arrestin : 260 280 300 320 : 331
B-arr2 : YKCFVA E DD V PSSTFCVYT6TP L INREKRGALDGLKLEHEDTNLASST664RGAH4E6LGI6VSY4VKVKLVSER

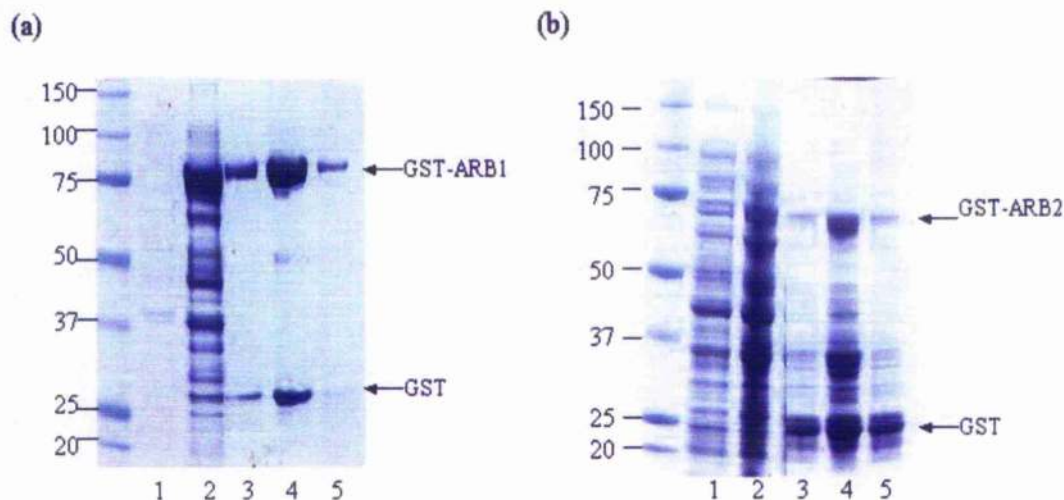
B-arrestin : 340 360 380 400 : 407
B-arr2 : GODV VELFF LHHKPF P PE PVDNLIIE DYN DDDIVFEDFAR RLKQMKDD 2

B-arrestin : --- : 410
B-arr2 : --- : -

```

**Figure 6.2** Sequence alignments of the residues of full-length  $\beta$ -arrestin1 and  $\beta$ -arrestin2.

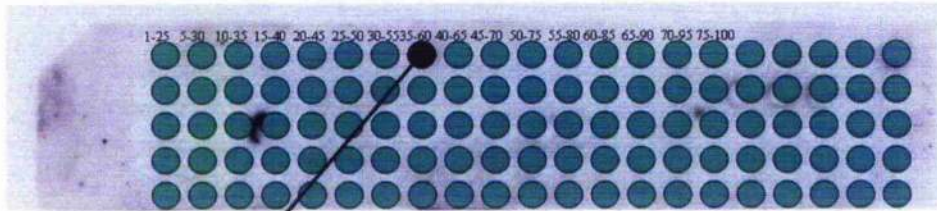
The full-length sequence of human  $\beta$ -arrestin1 and full-length  $\beta$ -arrestin2 are aligned by ClustalW software. Conserved amino acids are indicated in black and the varied amino acids are indicated in grey. B-arrestin,  $\beta$ -arrestin1; B-arr2,  $\beta$ -arrestin2.



### 6.3 Over-expression and purification of recombinant proteins of GST-β-arrestin1 and GST-β-arrestin2.

GST-β-arrestin1 and GST-β-arrestin2 were over-expressed at 37°C in *E. Coli* DH5α cells by induction with 1mM IPTG. Samples from different stages of the Glutathione Sepharose column purification process (see section 2.2.5) were separated on a 4-12% SDS-PAGE gel stained with Coomassie brilliant blue. Expression of GST-β-arrestin1 and GST-β-arrestin2 are indicated as arrows. Free GST present in the final elute is also indicated as arrows. Molecular weight markers are shown with sizes indicated in kDa. The listing numbers are indicated as follows: 1, before induction; 2, 5 hr after induction; 3, before elution with glutathione buffer; 4, glutathione sepharose beads alone; 5, after elution with glutathione buffer. The observed molecular weight of full-length (a) GST-β-arrestin1 on SDS-PAGE is ~75 kDa; full-length (b) GST-β-arrestin2 on SDS-PAGE is ~73 kDa.

Stage1 : initial screen... GST overlay and blotting



YGMVCSAYDNV NKVRVAIKKISPFHEQTYC

Stage2 : alanine scanning... GST overlay and blotting



- 1 YGMVCSAYDNV NKVRVAIKKISPFHEQTYC
- 2 AGMVCSAYDNV NKVRVAIKKISPFHEQTYC
- 3 YAMVCSAYDNV NKVRVAIKKISPFHEQTYC
- 4 YGAVCSAYDNV NKVRVAIKKISPFHEQTYC
- 5 YGMACSA YDNV NKVRVAIKKISPFHEQTYC
- 6 YGMVASA YDNV NKVRVAIKKISPFHEQTYC
- 7 YGMVCAA YDNV NKVRVAIKKISPFHEQTYC
- 8 YGMVCSA YDNV NKVRVAIKKISPFHEQTYC
- 9 YGMVCSAADNV NKVRVAIKKISPFHEQTYC
- 10 YGMVCSAYANV NKVRVAIKKISPFHEQTYC

**Figure 6.4 Detection of protein-protein interaction by using Peptide Array Analysis and subsequent Alanine Substitution Analysis.**

Upper panel shows how peptide array analysis works. GST fusion protein was overlaid onto the cellulose membrane that contains the overlapping peptides (25 mers), each shifted along by 5 amino acids in the whole sequence of the protein of interest. This interaction was detected with the antiserum against the protein that was fused with GST. Spots were blank, indicative of null interaction. Spots were dark, indicating the positive interaction. The numbers ahead of each peptide indicate their order in the array. Lower panel shows how alanine substitution analysis works. The amino acids from the parent peptide shown positive in upper panel were singly and successively substituted to alanine, except the amino acid alanine which needed changing to be aspartic acid. Similar to the procedure of peptide array analysis, GST-fused protein was overlaid and detected by its specific antiserum. The wild type parent peptide was used as a control (1).

```

1  IMAQQTSPDTLTVPEVDNPHCPNPWL(1-25)
2   SPDTLTVPEVDNPHCPNPWLNEDLV(6-30)
3    TVPEVDNPHCPNPWLNEDLVKSLRE(11-35)
4     DNPCHPNPWLNEDLVKSLRENLLQH(16-40)
5      PNPWLNEDLVKSLRENLLQHEKSKT(21-45)
6       NEDLVKSLRENLLQHEKSKTARKSV(26-50)
7        KSLRENLLQHEKSKTARKSVSPKLS(31-55)
8         NLLQHEKSKTARKSVSPKLSVISP(36-60)
9          EKSKTARKSVSPKLSVISPSPR(41-65)
10           ARKSVSPKLSVISPSPRLLRRM(46-70)
11            SPKLSVISPSPRLLRRMLLSSN(51-75)
12             PVISPRSPRLLRRMLLSSNPKQR(56-80)
13              RNSPRLRRMLLSSNPKQRRTVA(61-85)
14               LLRRMLLSSNPKQRRTVAHTCFD(66-90)
15                LLSSNPKQRRTVAHTCFD(71-95)

```

```

130 STIPQSPSPAPDDPEEGRQQQTEKF(646-670)
131  SPPSPAPDDPEEGRQQQTEKFQFELT(651-675)
132   APDDPEEGRQQQTEKFQFELTLEEDG(656-680)
133    EEGRQQQTEKFQFELTLEEDGESDTE(661-685)
134     QQTEKFQFELTLEEDGESDTEKDSGS(666-690)
135      FQFELTLEEDGESDTEKDSGSQVEED(671-695)
136       TLEEDGESDTEKDSGSQVEEDTSCSD(676-700)
137        GESDTEKDSGSQVEEDTSCSDKTLQ(681-705)

```

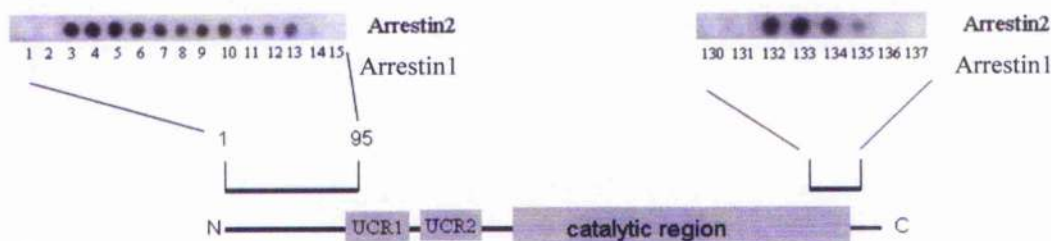


**Figure 6.5 Probing PDE4D5 peptide array for  $\beta$ -arrestin2 interaction sites.**

PDE4D5 is shown schematically with its unique N-terminal region, UCR1, UCR2, catalytic region and C-terminal domain. Cellulose membrane containing overlapping peptides and representing the entire sequence of PDE4D5 was blocked in 5% milk before being overlaid with recombinant  $\beta$ -arrestin2-GST or  $\beta$ -arrestin1-GST. The detection was performed using immunoblotting with a specific anti- $\beta$ -arrestin antibody. Shown here are the only sections in the array that generate dark spots (positive interactions).

(a)



(b)



**Figure 6.6 The binding of  $\beta$ -arrestin2 to sequential alanine substituted version of a RAID1-containing peptide.**

(a) Here shows an array of peptides based on a 25mer parent peptide (Ctr, peptide 5 in Figure 6.5) of sequence Asn22-Thr45 in PDE4D5. Further spots reflect a scanning peptide array of this parent peptide where indicated amino acids were sequentially and individually substituted with alanine. Cellulose membrane was blocked before overlaid with GST- $\beta$ -arrestin, followed by immunoblotting with a specific anti-arrestin2 antibody. (b) Cellulose membrane containing the control (peptide 133, representing the sequence Glu660-Glu685 in PDE4D5 in Figure 6.5) and the alanine-sequentially and singly substituted (derived) peptides were overlaid with  $\beta$ -arrestin2-GST after being blocked with milk. This array was then subject to immunoblotting using anti- $\beta$ -arrestin antibody. Wild type peptide (Ctr) plus progeny with the indicated residue substituted for alanine were marked under the spots. Ctr, control.

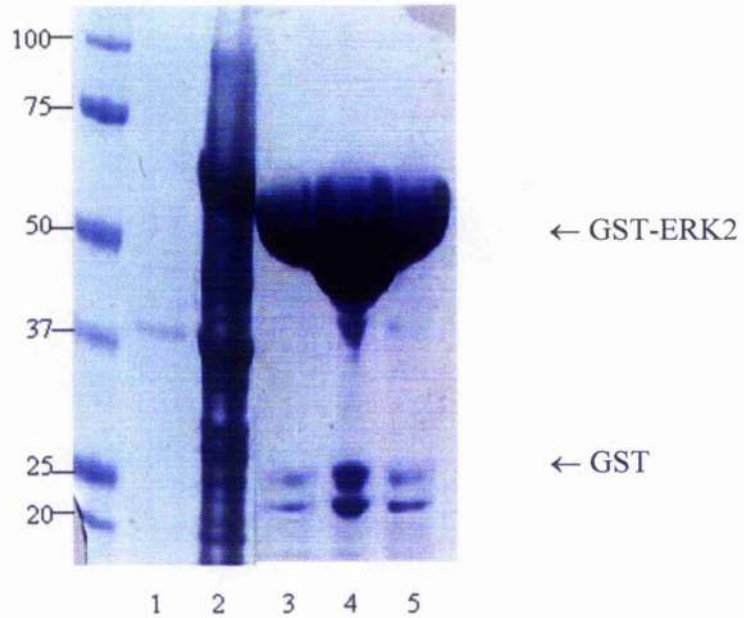


**Figure 6.7 Purification of recombinant protein of GST-ERK2.**

GST-ERK2 was over-expressed at 37°C in *E. Coli* DH5 $\alpha$  cells by induction with 1mM IPTG. Samples from different stages of the Glutathione Sepharose column purification process (see section 2.2.5) were separated on a 4-12% SDS-PAGE gel stained with Coomassie brilliant blue. Expression of GST-ERK2 is indicated as arrows. Free GST present in the final elute is also indicated as arrows. Molecular weight markers are shown with sizes indicated in kDa. The listing numbers are indicated as follows: 1, before induction; 2, 5 hr after induction; 3, before elution with glutathione buffer; 4, glutathione sepharose beads alone; 5, after elution with glutathione buffer. The observed molecular weight of full-length GST-ERK2 on SDS-PAGE is ~60 kDa, which corresponds closely with its calculated molecular weight of 67 kDa.

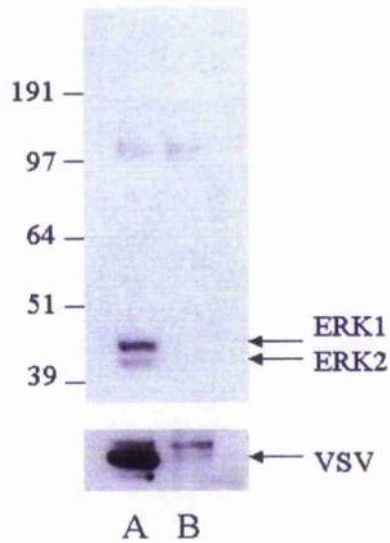


**Figure 6.8 Association of PDE4D5 with ERK2 in HEKB2 cells.**

Intact HEKB2 cells (control cells, lane B) and those transfected with VSV-tagged PDE4D5 (lane A) were harvested in 3T3 lysis buffer and subject to immunoprecipitation with VSV affinity beads. The association of PDE4D with ERK2 was detected by probing the immunoprecipitates with a specific anti-ERK1/2 antibody, which was followed by probing the same membrane with a specific VSV antibody to confirm the pull-down. Molecular weight markers are shown with sizes indicated in kDa.

130STIPQSPSPAPDDPEEGRQGQTEKF(646-670)  
 131 SPSAPDDPEEGRQGQTEKFQFELT(651-675)  
 132 PDDPEEGRQGQTEKFQFELTLEEDG(656-680)  
 133 EGRQGQTEKFQFELTLEEDGESDTE(661-685)  
 134 QTEKFQFELTLEEDGESDTEKDSGS(666-690)  
 135 QFELTLEEDGESDTEKDSGSQVEED(671-695)

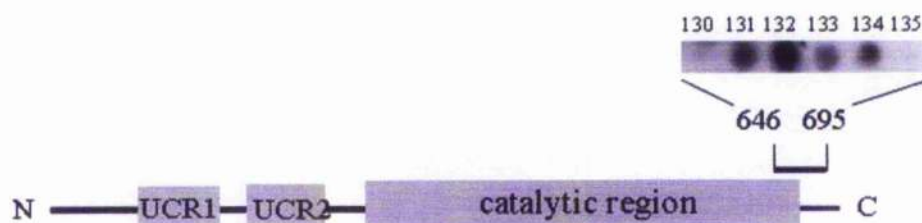


**Figure 6.9 Probing PDE4D5 peptide array for ERK2 interaction sites.**

PDE4D5 is shown schematically with its unique N-terminal region, UCR1, UCR2, catalytic region and C-terminal domain. Cellulose membrane containing overlapping peptides and representing the entire sequence of PDE4D5 was blocked in 5% milk before being overlaid with recombinant ERK2-GST. The detection was performed using immunoblotting with a specific anti-ERK2 antibody. Shown here are the only sections in the array that generate dark spots (positive interactions).



**Figure 6.10 The binding of ERK2 to sequential alanine substituted version of a FQF-containing peptide.**

Here shows an array of peptides based on a 25mer parent peptide (Ctr, peptide 132 in Figure 6.9) of sequence Glu660-Glu685 in PDE4D5. Further spots reflect a scanning peptide array of this parent peptide where indicated amino acids were sequentially and individually substituted with alanine. Cellulose membrane was blocked before overlaid with GST-ERK2, followed by immunoblotting with a specific anti-ERK2 antibody. Ctr, control.

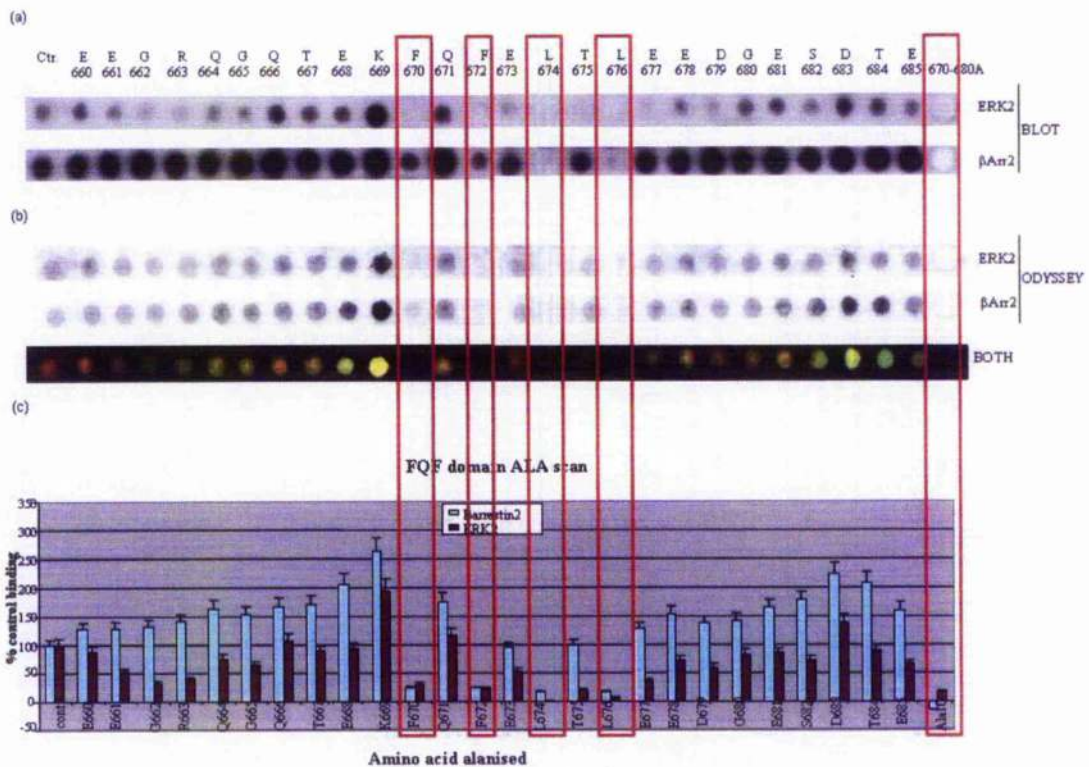


**Figure 6.11 The binding of  $\beta$ -arrestin2 and ERK2 to sequential alanine substituted version of a FQF-containing peptide.**

(a) Comparison of  $\beta$ -arrestin2 and ERK2 binding to an alanine scan array of PDE4D5 whose sequence reflects amino acids 660-685, as shown in Figure 6.6b and Figure 6.10, by using ECL developing reagent. (b) As (a) but except that signals were detected with Odyssey system, the peptide array was screened for interaction with recombinant  $\beta$ -arrestin2-GST, or ERK2-GST as shown in black-and-white, and simultaneous interaction with recombinant  $\beta$ -arrestin2-GST and recombinant ERK2-GST as shown in color. (c) Shows the quantitative data from three independent experiments by using ECL reagent. Data were expressed as fold in control peptide signal. Red boxes indicated the most important amino acids that are essential for both  $\beta$ -arrestin2 and ERK2 binding to PDE4D5 within a peptide spanning from Glu660 to Glu 685. 670-680A is used as a negative control.

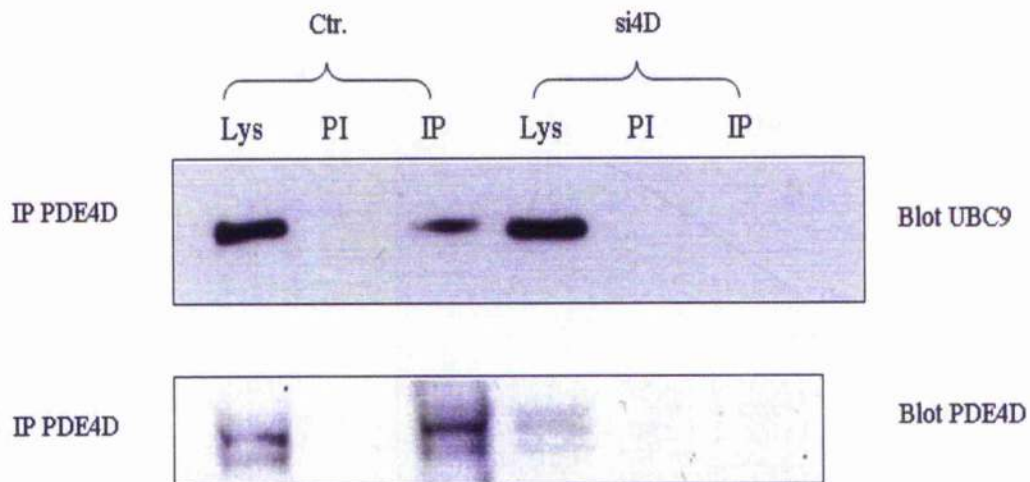


**Figure 6.12 Association of PDE4D with Ubc9 in HEKB2 cells.**

Intact HEKB2 cells (control cells) and those transfected with siRNA specific to PDE4D were harvested in 3T3 lysis buffer and subject to immunoprecipitation with a specific anti-PDE4D antibody. The association of PDE4D with Ubc9 was detected by probing the immunoprecipitates with a specific anti-Ubc9 antibody. Lower panel shows the efficient ablation of PDE4D when a siRNA specific to PDE4D was transfected in. Lys, lysates; PI, pre-immune; IP, immunoprecipitation.

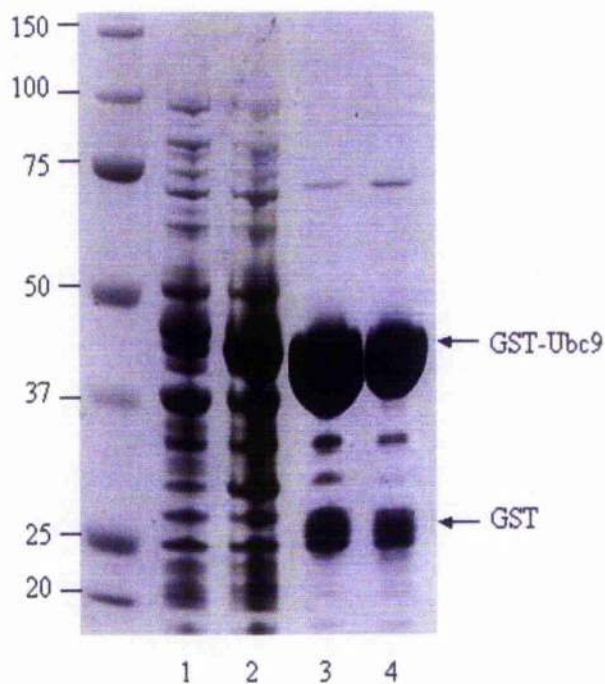


**Figure 6.13 Purification of recombinant protein of GST-Ubc9.**

GST-Ubc9 was over-expressed at 37°C in *E. Coli* DH5 $\alpha$  cells by induction with 1mM IPTG. Samples from different stages of the Glutathione Sepharose column purification process (see section 2.2.5) were separated on a 4-12% SDS-PAGE gel stained with Coomassie brilliant blue. Expression of GST-Ubc9 is indicated as arrows. Free GST present in the final elute is also indicated as arrows. Molecular weight markers are shown with sizes indicated in kDa. The listing numbers are indicated as follows: 1, before induction; 2, 5 hr after induction; 3, before elution with glutathione buffer; 4, after elution with glutathione buffer. The observed molecular weight of full-length GST-Ubc9 on SDS-PAGE is ~43 kDa, which corresponds closely with its calculated molecular weight of 45 kDa.

```

73HTIFQERDLLKTFKIPVDTLITYLM(361-385)
74  ERDLLKTFKIPVDTLITYLMTLEDH(366-390)
75    KTFKIPVDTLITYLMTLEDHYHADV(371-395)
76      PVDTLITYLMTLEDHYHADVA YHNN(376-400)
77        ITYLMTLEDHYHADVA YHNNIHAAD(381-405)
78          TLEDHYHADVA YHNNIHAADV VVQST(386-410)
79            YHADVA YHNNIHAADV VVQSTHVLLS(391-415)

130STIPQSPSPAPDDPEEGRQGQTEKF(646-670)
131  SPSAPDDPEEGRQGQTEKFQFELT(651-675)
132    PDDPEEGRQGQTEKFQFELTLEEDG(656-680)
133      EGRQGQTEKFQFELTLEEDGESDTE(661-685)
134        QTEKFQFELTLEEDGESDTEKDSGS(666-690)
135          QFELTLEEDGESDTEKDSGSQVEED(671-695)
136            LEEDGESDTEKDSGSQVEEDTSCSD(676-700)

```

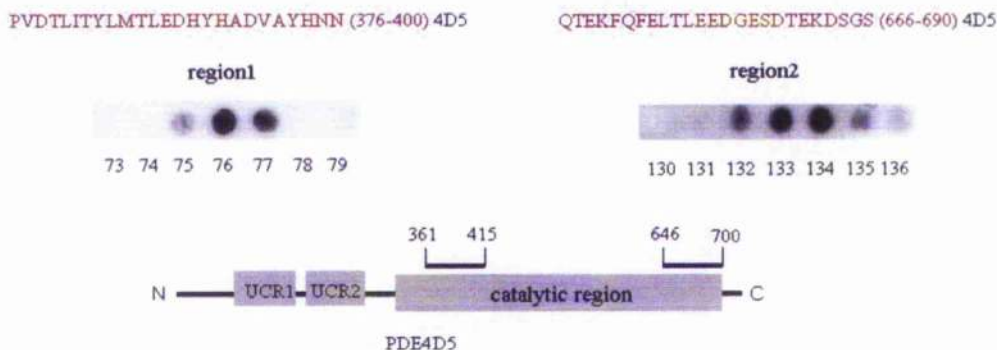
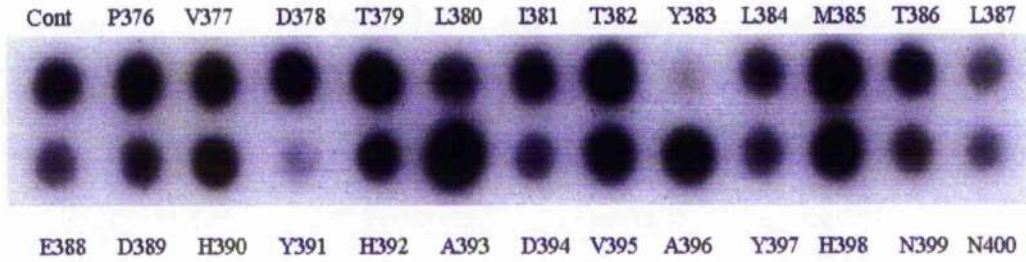


**Figure 6.14 Probing PDE4D5 peptide array for Ubc9 interaction site.**

PDE4D5 is shown schematically with its unique N-terminal region, UCR1, UCR2, catalytic region and C-terminal tail. The entire sequence of PDE4D5, represented by spots on cellulose membranes containing overlapping peptides, each shifted along by 5 amino acids in the PDE4D5 sequence, was overlaid with recombinant Ubc9-GST protein, blocked prior to detection by immunoblotting. Shown are sections of membranes indicating positive interaction peptide spots (black) bounded by null interaction peptide spots (clear). The numbers associated with the peptides indicate their order in the array. The sequences of PDE4D5 that shows positive binding to Ubc9 are indicated in red.

(a)



(b)

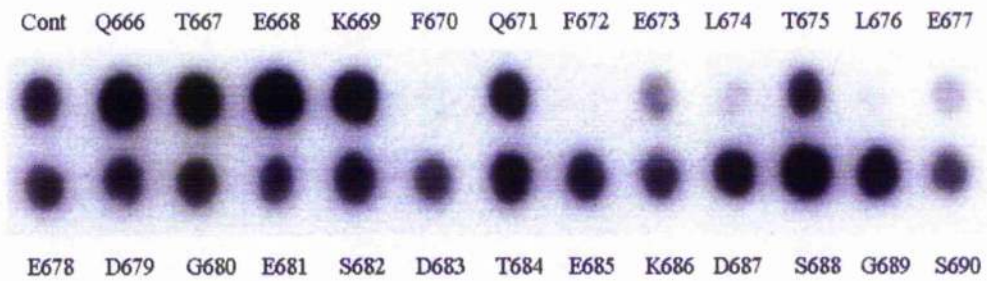


**Figure 6.15 The binding of Ubc9 to sequential alanine substituted versions of Ubc9-interacting PDE4D5 peptides.**

(a) Shows an array of peptides based on a parent peptide (spot 76 in original PDE4D5 peptide array) whose sequence reflects amino acids 376-400 of PDE4D5. This alanine substitution array was probed with recombinant Ubc9-GST and interaction was detected by immunoblotting with an anti-Ubc9 antibody. The wild type parent peptide (spot 76) was used as a control. (b) Shows an array of peptides based on a parent peptide (spot 134 in original PDE4D5 peptide array) whose sequence reflects amino acids 666-690 of PDE4D5. This alanine substitution array was probed with recombinant Ubc9-GST and interaction was again detected by immunoblotting with an anti-Ubc9 antibody. The wild type parent peptide (spot 134) was used as a control. Cont, control.

34RLVIRKVFQFAPEKPGPQPSAETTRH(166-190)  
 35 KVFQFAPEKPGPQPSAETTRHFLMSD(171-195)  
 36 PEKPGPQPSAETTRHFLMSDRSLHL(176-200)  
 37 PQPSAETTRHFLMSDRSLHLEASLD(181-205)  
 38 ETTRHFLMSDRSLHLEASLDKELY(186-210)  
 39 FLMSDRSLHLEASLDKELYHGEPL(191-215)  
 40 RSLHLEASLDKELYHGEPLNPNVH(196-220)  
 41 EASLDKELYHGEPLNPNVHVTNNS(201-225)

72PRPQSAAPETDVPVDNLIEFDTNY(356-380)  
 73 AAPETDVPVDNLIEFDTNYATDDD(361-385)  
 74 DVPVDNLIEFDTNYATDDDIVFED(366-390)  
 75 TNLIEFDTNYATDDDIVFEDFARLR(371-395)  
 76 FDTNYATDDDIVFEDFARLRKGMK(376-400)  
 77 ATDDDIVFEDFARLRKGMKDDD(381-405)

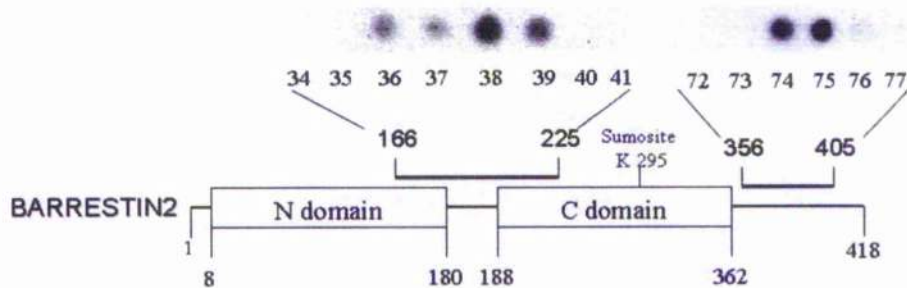


**Figure 6.16 Probing  $\beta$ -arrestin2 peptide array for Ubc9 interaction sites.**

$\beta$ -arrestin2 is shown schematically with its N-domain and C domain. Cellulose membrane containing overlapping peptides and representing the entire sequence of  $\beta$ -arrestin2 was blocked in 5% milk before being overlaid with recombinant Ubc9-GST. The detection was performed using immunoblotting with a specific anti-Ubc9 antibody. Shown here are the only sections in the array that generate dark spots (positive interactions) bounded by clear spots (null interactions). The numbers associated with the peptides indicate their order in the array. The potential sumoylation site on  $\beta$ -arrestin2 is indicated on the  $\beta$ -arrestin2 schematic

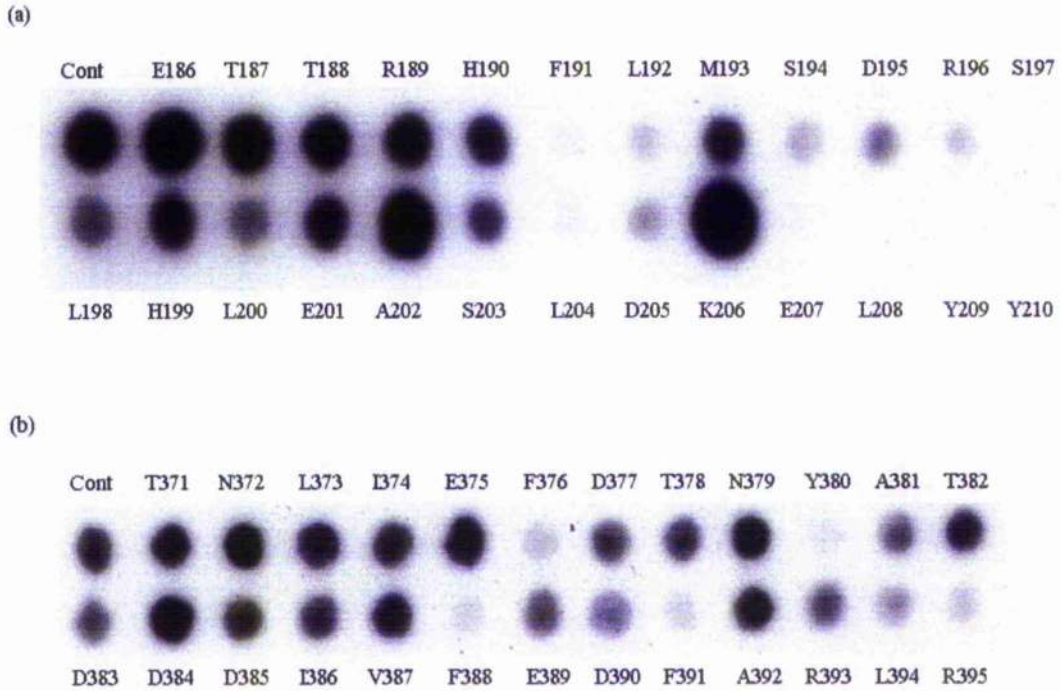
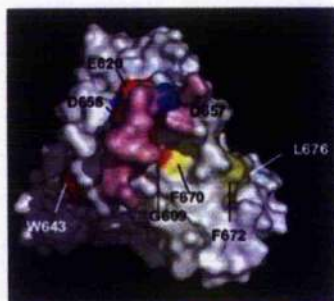


**Figure 6.17 The binding of Ubc9 to sequential alanine substituted versions of Ubc9-interacting  $\beta$ -arrestin2 peptides.**

(a) Shows an array of peptides based on a parent peptide (spot 38 in original  $\beta$ -arrestin2 peptide array) whose sequence reflects amino acids 186-210 of  $\beta$ -arrestin2. This alanine substitution array was probed with recombinant Ubc9-GST and interaction was detected by immunoblotting with an anti-Ubc9 antibody. The wild type parent peptide (spot 38) was used as a control. (b) Shows an array of peptides based on a parent peptide (spot 75 in original  $\beta$ -arrestin2 peptide array) whose sequence reflects amino acids 371-395 of  $\beta$ -arrestin2. This alanine substitution array was probed with recombinant Ubc9-GST and interaction was again detected by immunoblotting with an anti-Ubc9 antibody. The wild type parent peptide (spot 75) was used as a control. Cont, control.

(a)



(b)

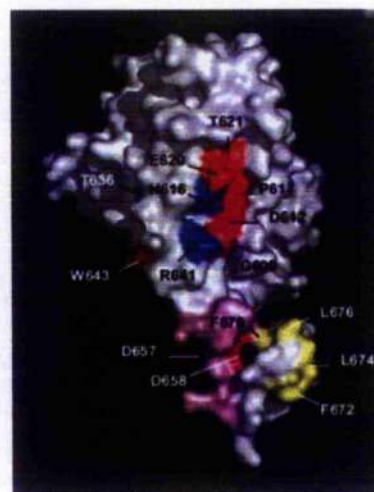


**Figure 6.18 Predicted structure of catalytic domain in PDE4D.**

The structure of PDE4D catalytic domain is modeled based upon the existence of its conserved counterpart in PDE4B, whose structure has been resolved. (a) Shows the derived 1XM6 structure in which the predicted  $\alpha$  helix-17 ( $^{670}\text{FQFELTL}^{676}$ ) in PDE4D5 is indicated to fold across the opening of the catalytic site and in so doing occlude the surface implicated in  $\beta$ -arrestin2, ERK2 or Ubc9 interaction. (b) Shows the derived 1F0J structure in which the predicted  $\alpha$  helix-17 ( $^{670}\text{FQFELTL}^{676}$ ) in PDE4D5 stays in the open area away from its core catalytic domain. Amino acids whose alanine substitution leads to loss of RACK1 interaction are shown in red and those that leads to clear attenuation are shown in blue. Amino acids whose alanine substitution leads to loss of  $\beta$ -arrestin2 interaction are shown in yellow. The flexible linker region between helix 16 and 17 are shown in pink.

## **Chapter 7**

### **General Discussion**

## General Discussion

The cAMP signaling pathway controls a wide range of cellular processes, the specificity of which is facilitated by three dimensional organization of signaling proteins, such as ACs, AKAPs and PDEs within cells (Houslay and Adams 2003; Wong and Scott 2004; Tasken and Aandahl 2004). Pivotal in shaping and controlling intracellular cAMP gradients, PDEs provide the sole means to degrade cAMP.

PDE4 genes generate over 20 isoforms, each of which is characterized by their unique N-terminal region, which can mediate protein-protein interactions and confer intracellular targeting (Houslay et al. 2005). An emerging theme in PDE4 action is that individual isoforms are sequestered to particular signaling complexes, therefore allowing regulation of the activity of the cAMP effector proteins, targeted PKA, plasma-membrane bound CNGCs or localized EPACs (Baillie et al. 2005).

It is well established that phosphorylation of  $\beta_2$ AR by two types of protein kinases, PKA and GRK can result in receptor desensitization (Kohout and Lefkowitz 2002). PKA phosphorylation of the  $\beta_2$ AR causes the receptor to switch from its predominant coupling to  $G_s$ , which activates adenylyl cyclase, to another G-protein protein, namely  $G_i$ , thereby allowing for activation of the ERK pathway (Lefkowitz et al. 2002). GRK phosphorylated  $\beta_2$ AR binds with high affinity to membrane recruited  $\beta$ -arrestin. Such binding of  $\beta$ -arrestin to the  $\beta_2$ AR prevents further coupling to  $G\alpha_s$  and targets the  $\beta_2$ AR for endocytosis (Lefkowitz and Shenoy 2005). Recently, a new facet of this desensitization system has been identified (Perry et al. 2002), in that  $\beta$ -arrestin, when translocated to the receptor in response to agonist stimulation, has been shown to be in complex with PDE4. This results in efficient  $\beta_2$ AR desensitization with concomitant interdiction of coupling, preventing cAMP synthesis and also increasing local cAMP degradation (Perry et al. 2002; Bolger et al. 2003).

In the course of this work, I have extended our knowledge of the properties of one particular long PDE4 isoform, PDE4D5. PDE4B and PDE4D together contribute more than 90% of the total PDE4 activity in HEKB2 cells (Lynch et al. 2005). However, it is PDE4D5 alone, which contributes only 24% of total PDE4

activity in these cells, that has been identified, by RNA silencing and overexpression of catalytically inactive (dominant negative) PDE4D5, as the functionally relevant PDE interacting with  $\beta$ -arrestin to control PKA phosphorylation of the  $\beta_2$ AR and consequentially switching of its signaling to activation of ERK pathway (Lynch et al. 2005; Bolger et al. 2003).

Using co-immunoprecipitation, I have shown that AKAP79 associates with the  $\beta_2$ AR in a constitutive manner in HEKB2 cells. In contrast to this, the AKAP gravin is only associated with the  $\beta_2$ AR receptor subsequent to challenge of cells with isoprenaline. Further studies using siRNA technology to achieve knockdown of specific AKAPs show that the ability of isoprenaline to trigger PKA-mediated phosphorylation of the  $\beta_2$ AR, and consequential activation of ERK, is ablated upon knockdown of AKAP79 but not upon knockdown of gravin. Such data indicate that  $\beta$ -arrestin-recruited PDE4D5 gates the potential of a discrete pool of AKAP79-tethered PKA to phosphorylate the associated  $\beta_2$ AR. It is this important process that is required for the switching of  $\beta_2$ AR coupling from  $G_s$  to  $G_i$  and the consequential ERK activation. Although the role of the recruited gravin is still not understood, the fact that selective knockdown of gravin did not have any effect on PKA phosphorylated  $\beta_2$ AR indicates that membrane-bound forms of gravin serve a role distinct from that of AKAP79 in regulating the PKA phosphorylation of the  $\beta_2$ AR, at least in HEKB2 cells.

It has been established that engineering a single point mutation within the catalytic domain of PDE4D5 can generate a catalytically inactive form of PDE4D5 that retains its ability to bind to  $\beta$ -arrestin (Baillie et al. 2003). This catalytically inactive species is able to exert a dominant negative role, displacing the active endogenous counterpart and enhancing the isoprenaline-stimulated phosphorylation of ERK. Here I confirm this data, and also show that mutating Arg34 to Ala within this dominant negative PDE4D5 ablates its ability to bind  $\beta$ -arrestin thereby preventing its ability to enhance isoprenaline-stimulated ERK phosphorylation. This data indicates that  $\beta$ -arrestin-mediated delivery of PDE4D5 participates in a unique desensitization process. The localized rate of cAMP degradation is increased, AKAP79-anchored receptor-bound PKA is deactivated and the  $\beta_2$ AR is uncoupled from  $G_i$ . Alterations in

the expression and availability of both AKAP79 and  $\beta$ -arrestin-bound PDE4D5 might confer cell-type specific remodeling of the switching of  $\beta_2$ AR signaling to ERK.

In contrast to the  $\beta$ -arrestin-delivered PDE4D5 isoform-specific regulation of  $\beta_2$ AR phosphorylation by PKA (Lynch et al. 2005), I have suggested that the regulation of GRK2 phosphorylation by PKA is, seemingly, regulated by a mixed pool of PDE4 activity rather than a single isoform. This may be because GRK2 is located through the cytosol and thus subject to phosphorylation by cytosolic PKA, thus being regulated by bulk cAMP levels. Using immunoprecipitation, I have shown that inactivation of PDE4 by the PDE4 selective inhibitor, rolipram enhances the isoprenaline-induced PKA phosphorylation of GRK2, leading to increased GRK2 membrane recruitment. In addition, siRNA-mediated knockdown of either PDE4B or PDE4D subfamilies, which provide 30% and 60% of the total PDE4 activity in HEKB2 cells, respectively, also enhanced the isoprenaline-induced PKA phosphorylation of GRK2. In contrast to this, inhibition of PDE3, which provides 40% of the total PDE activity in HEKB2 cells failed to affect PKA phosphorylation of GRK2. This implies that, in response to isoprenaline, the actions of PDE4B and PDE4D may act synergistically on the same cAMP pool, indeed a combination of knockdown of both PDE4B and PDE4D, whilst not additive in effect, did achieve a similar increase in isoprenaline-induced PKA phosphorylation of GRK2 to rolipram. This is however distinct from the pool of cAMP regulated by PDE3, implying its function may be to regulate a spatially discrete pool of cAMP. Indeed, PDE3 is exclusively membrane-bound, and in many cell types, it has been shown that selective inhibition of PDE3 and PDE4 leads to very different functional outcomes (Maurice et al. 2003; Huang et al. 2001).

It has previously been shown by others that PKA phosphorylation of GRK2 increases its ability to interact with  $G\beta\gamma$  and, in consequence, increases the membrane recruitment of GRK2 (Cong et al. 2001; Lodowski et al. 2003). Here my data lends further support to this. With further time and resources I would like to examine the role of  $G\beta\gamma$  in the rolipram enhanced isoprenaline-induced GRK2 membrane translocation either by engineering a  $G\beta\gamma$  mutant which would prevent its binding to GRK2, or by employing an engineered HEKB2 cell line that lacks endogenous  $G\beta\gamma$ .

Interestingly, in the presence of rolipram, the isoprenaline-induced membrane recruitment of GRK was not only accelerated but was also transient in nature. Such transience was abolished when the cells were pretreated with the MEK inhibitor UO126, suggesting an enhanced ERK activation involved in releasing the membrane-bound GRK2. As discussed above, previous studies have shown that PDE4 inhibition promotes PKA phosphorylation of the  $\beta_2$ AR and the switching of its signaling to ERK (Lynch et al. 2005; Baillie 2003). Here I confirm these results and extend them in showing an increase in the membrane fraction of ERK phosphorylated GRK2 that is more transient when rolipram is present in addition to isoprenaline. This parallels the transient nature of the GRK2 membrane translocation in the presence of both isoprenaline and rolipram. Therefore, PDE4 appears to control the scope of the actions of GRK2 in the early stage of  $\beta_2$ AR desensitization. In the process of membrane recruitment of GRK2, PDE4 regulates PKA phosphorylation of GRK2 and the subsequent GRK2 translocation to the membrane. Once GRK2 forms in complex with the receptor, the switching of  $\beta_2$ AR G-protein coupling from  $G_s$  to  $G_i$ , regulated by PDE4D5 causes activation of ERK that acts to phosphorylate and deactivate GRK2, promoting its release from the plasma membrane back to the cytosol. Following membrane translocation of GRK2,  $\beta$ -arrestin/PDE4D complexes are recruited to the membrane (Perry et al. 2002) and desensitization commences. I show here that the time-dependent transient and concomitant membrane recruitment of both  $\beta$ -arrestin and PDE4D5 occur more rapidly in isoprenaline-challenged cells that have been pretreated with rolipram, consistent with the GRK2 membrane recruitment time course.

Interestingly, in the absence of isoprenaline, inhibition of PDE4 alone by rolipram is sufficient to cause PKA phosphorylation of GRK2, with consequential effects on GRK2 membrane recruitment and GRK2-mediated phosphorylation of the  $\beta_2$ AR. In contrast however, rolipram alone had no effect on ERK activation nor was ERK phosphorylated GRK2 detected in the plasma membrane following rolipram treatment. I would suggest that GRK2 phosphorylation by PKA is initiated in the cytosol thus allowing its control by global changes in cAMP that can be regulated by PDE4 isoenzymes also located within the cytosol. Indeed, single PDE4B or PDE4D subfamily knockdown failed to elicit the PKA phosphorylation of GRK2. This

indicates that the cAMP threshold to activate PKA is set such that it needs either stimulation of adenylyl cyclase or the ablation of both PDE4B and PDE4D subfamilies in order to breach this threshold to activate PKA. Indeed, knockdown of both PDE4B and PDE4D together did achieve an increase in the PKA phosphorylated status of GRK2 in resting (unstimulated) cells.

In contrast, activation of the ERK2 pathway requires agonist stimulated AKAP79-tethered PKA phosphorylation of  $\beta_2$ AR at the plasma membrane. Following agonist stimulation  $\beta$ -arrestin and PDE4D5, in complex, are recruited to the membrane where PDE4D5 is able to control a localized pool of cAMP thereby regulating PKA phosphorylation of the receptor and consequential activation of the ERK pathway. This hypothesis has been partially proved by Lynch et al. (2005), as in resting HEK293 cells, knockdown of either PDE4B or PDE4D in the absence of agonist, by siRNA, failed to induce the PKA phosphorylation of the  $\beta_2$ AR (Lynch et al. 2005). This study, however did not examine the effect of knocking down both PDE4B and PDE4D on phosphorylation of the  $\beta_2$ AR by PKA in the absence of agonist and should be addressed in the future.

It is widely recognized that reversible post-translational modifications often regulate dynamic protein function. Previous studies have shown PDE4D5 to be phosphorylated both by PKA at Ser126, which serves to activate PDE4D5 (Sette et al. 1994; MacKenzie et al. 2002) and by ERK2 at Ser651, which, conversely, inhibits enzyme activity (Hoffmann et al. 1999; MacKenzie et al. 2000; Baillie et al. 2001). Post-translational modifications of specific proteins often occur in response to extracellular stimuli. It has been established (Perry et al. 2002; Lynch et al. 2005) that PDE4D5, in complex with  $\beta$ -arrestin, is recruited to the plasma membrane in response to isoprenaline stimulation of the  $\beta_2$ AR where it regulates localized cAMP levels. I therefore set out to examine if PDE4D5 underwent post-translational modification following agonist treatment. If this modification did occur I wished to examine its effect on downstream signaling and the interaction of PDE4D5 with other proteins, for example  $\beta$ -arrestin. Sequence analysis revealed a ubiquitin interaction motif (UIM domain) located within the extreme C-terminus of PDE4D5, prompting my investigation. UIM domains have been suggested to direct ubiquitination as well as to

interact with ubiquitin (Miller et al. 2004). I thus examined whether PDE4D5 was ubiquitinated in response to isoprenaline treatment in HEKB2 cells. Indeed I show here that PDE4D5 does indeed become ubiquitinated, in both HEKB2 cells in response to isoprenaline stimulation and also in HEKV2 cells in response to vasopressin stimulation. This ubiquitination of PDE4D5 appears to be dependent upon the integrity of its UIM domain as, when the critical acidic patch within this domain was mutated, ubiquitination of PDE4D5 in response to agonist was severely attenuated. In agreement with this, several isoforms of PDE4A, PDE4B and PDE4C, which lack a UIM domain within their extreme C-termini, did not undergo ubiquitination in response to isoprenaline challenge of HEK cells expressing these species. Thus, it would appear that ubiquitination of PDE4 isoenzymes requires at least the presence of one UIM domain. PDE4D3, however, which does contain an UIM domain within its extreme C-terminus failed to undergo ubiquitination in HEKB2 cells in response to isoprenaline. This suggests that an UIM domain alone is insufficient to promote ubiquitination, as will be further discussed below.

$\beta$ -arrestins are important adapter and scaffold proteins in GPCR signaling (Lefkowitz and Whalen 2004). It has been shown that  $\beta$ -arrestin is involved in  $\beta_2$ AR and V<sub>2</sub>R ubiquitination processes and that it can act as an E3 ligase adapter (Shenoy et al. 2001; Martin et al. 2003). Meanwhile,  $\beta$ -arrestin itself has also been shown to undergo ubiquitination, via an action involving the E3 ligase Mdm2 (Shenoy et al. 2001), which plays an important role in controlling the ubiquitination of p53 (Fang et al. 2000). My data here demonstrates that ablation of PDE4D5 binding to  $\beta$ -arrestin completely abolishes the detection of PDE4D5 ubiquitination in response to isoprenaline in HEKB2 cells. This suggests two possibilities. Firstly it is known that a percentage of PDE4D5 forms a complex with  $\beta$ -arrestin in HEKB2 cells. It may be that the ubiquitination signal observed following immunoprecipitation of PDE4D5 from agonist stimulated HEKB2 cells is in fact ubiquitinated  $\beta$ -arrestin that has been pulled down in complex with PDE4D5. Secondly, it is possible that  $\beta$ -arrestin interacting with PDE4D5 is acting in its capacity as an E3 ligase adaptor protein and, as has been reported for its function in the ubiquitination of the  $\beta_2$ AR (Girnita et al. 2005), acts to locate E3 ligase in close proximity to PDE4D5 thereby enabling its ubiquitination. I have shown here that the ubiquitination of PDE4D5 and  $\beta$ -arrestin

occurs with very disparate time courses. This, coupled to the lack of the ubiquitination signal seen in the PDE4D5 UIM mutant that is still able to bind to  $\beta$ -arrestin, suggests that it is ubiquitination of PDE4D5 and not  $\beta$ -arrestin that is observed. To further investigate the possibility that PDE4D5 is indeed ubiquitinated upon isoprenaline stimulation, I chose to evaluate first the key E3 ligase, Mdm2, which has been reported to interact with  $\beta$ -arrestin and function to ubiquitinate it, as well as various proteins including p53 (Fang et al. 2000; Girnita et al. 2005; Lin et al. 2002). The observation that a mutant of PDE4D5, which is unable to interact with arrestin (E27), severely diminished ubiquitination of PDE4D5 upon isoprenaline treatment, suggests that the presence of arrestin is key. This might be because arrestin acts to deliver the E3 ligase, Mdm2 to act on complexed PDE4D5.

Indeed, in HEKB2 cells when Mdm2 is knocked down by specific siRNA, then wild type PDE4D5 failed to undergo ubiquitination in response to isoprenaline. This shows that Mdm2 is crucial for the ubiquitination of PDE4D5. Together, these data suggest that only PDE4D5 in complex with  $\beta$ -arrestin and therefore with Mdm2 can be modified by Ub moieties. Interestingly, in PDE4D5 mutated in its UIM domain, which compromised its ability to undergo ubiquitination, the level of associated Mdm2 was much reduced in comparison to wild type PDE4D5. As Mdm2 binds to  $\beta$ -arrestin (Shenoy et al. 2001) and this is the suggested mode of delivery to initiate PDE4D5 ubiquitination, it seems that mutation of the UIM domain of PDE4D5 might lower the amount of associated  $\beta$ -arrestin and hence reduce the amount of associated Mdm2. In order to address this hypothesis, I have checked the relative levels of  $\beta$ -arrestin that binds to the UIM mutated form to the wild type form of PDE4D5. The result that UIM mutated form of PDE4D5 binds to less  $\beta$ -arrestin than wild type PDE4D5 supports such a hypothesis.

In order to explore the effect of ubiquitination on PDE4D5 function, I explored the interaction of wild type and the UIM mutated form of PDE4D5 with  $\beta$ -arrestin. Using immunoprecipitation, I showed that more wild type PDE4D5 interacts with  $\beta$ -arrestin than PDE4D5 UIM mutant which loses the ability to undergo ubiquitination. Additionally the interaction of PDE4D5 and  $\beta$ -arrestin was transient in nature, peaking at 10 minutes after isoprenaline stimulation. However this was not

seen in the PDE4D5 UIM mutant transfected HEKB2 cells. These results imply that ubiquitination of PDE4D5 increases the proportion of the PDE4D5/ $\beta$ -arrestin complex within the cells, which might be of important in positively mediating the desensitization of  $\beta_2$ ARs. Thus, further work is required to define if ubiquitination is involved in the degree to which the PDE4D5/ $\beta$ -arrestin signaling complex is able to translocate to the plasma membrane and thereby attenuate  $G_s \rightarrow G_i$  switching. To answer this, I would first measure the ability of the UIM mutant PDE4D5 to translocate to the membrane fraction in complex with  $\beta$ -arrestin and compare this with wild type PDE4D5. Secondly I would propose to compare the degree of ERK activation in HEKB2 cells transfected with either wild type PDE4D5 or PDE4D5 UIM mutant. As  $\beta$ -arrestin-delivered PDE4D5 functions in attenuating ERK activation in response to isoprenaline in HEKB2 cells (Lynch et al. 2005), it would be expected that less ERK activation occurs in the UIM mutant transfected cells compared to wild type transfected cells.

Ubiquitin is a small molecule that contains seven lysine residues, each of which can be targeted by another ubiquitin in an iterative process to form distinct types of Ub chains (Pickart 2001). *In vitro*, K11, K29, K48 and K63 all can form Ub-Ub linkages. Poly-ubiquitin chains formed through K48 of two adjacent Ub are a well-characterized signal for targeting proteins for proteasomal degradation (Weissman 2001). Using HA-tagged Ub mutants, I show that PDE4D5 is modified largely by K48-linked Ub chains, as well as by a single Ub / mono-ubiquitination. This suggests that PDE4D5 might be targeted to proteasomes for degradation following ubiquitination. Indeed, I have demonstrated that wild type PDE4D5 interacts with 19S regulatory subunit S2 and S5a in a time-dependent manner when  $\beta_2$ AR is activated by isoprenaline. In the PDE4D5 UIM mutant that is unable to undergo ubiquitination, however, no interaction is observed. This supports the hypothesis that K48-linked Ub chain formed on PDE4D5 may target PDE4D5 to proteasomes. Further studies need to be done to confirm this. With further time, I would examine the half-life of PDE4D5 WT and UIM mutant forms by pulse-chase experiments.

I have demonstrated by *in vitro* ubiquitination that three lysine residues in the

unique N-terminal region of PDE4D5 are the putative ubiquitination sites. In order to examine their relative importance in conjugating ubiquitin, further work is required in which I would propose to examine the effect of single or combined selective mutation of these lysine residues on ubiquitination of PDE4D5. This *in vitro* data does, however, clearly explain the lack of ubiquitination in PDE4D3. This is because in the unique N-terminal regions of PDE4D3 and PDE4D5 it is only PDE4D5 which contains a putative ubiquitination site, explaining the inability of PDE4D3 to be ubiquitinated despite the presence of the UIM domain within its C-terminal region (Figure 6.1). Thus, in addition to functioning in protein-protein interaction and targeting PDE4 isoforms to distinct subcellular compartments (Houslay and Adams 2003), the N-terminal region of PDE4 family also serves to gate the process of ubiquitination in the case of PDE4D5.

It could be argued that the difference in the ubiquitination signals between PDE4D5 and PDE4D3 might be due to the preferential binding of PDE4D5 to  $\beta$ -arrestin (Bolger et al. 2003), and the consequential presence of Mdm2 within the complex. However, the complete absence of the ubiquitination signal from PDE4D3 abrogates this argument as at least the mono-ubiquitination signal or a faint poly-ubiquitination signal should be present as PDE4D3 is still binding to  $\beta$ -arrestin albeit to a lesser extent, in HEKB2 cells (Bolger et al. 2003). It is likely therefore that there is threshold of minimal  $\beta$ -arrestin binding for initiating ubiquitination. This would explain both the absence of ubiquitination of the PDE4D5 UIM mutant compared to wild type PDE4D5 and also the lack of ubiquitination of PDE4D3 and PDE4D5 in the absence of agonist stimulation.

Mutation of the UIM domain in PDE4D5 results in no ubiquitination and reduced  $\beta$ -arrestin binding. Simply concluding from this coincidence that ablation of ubiquitination leads to the reduced  $\beta$ -arrestin binding seems inappropriate because the reduced binding affinity might result from the consequential conformational changes in PDE4D5 when its UIM region is mutated, rather than the effect of lack of ubiquitination, albeit the latter might also be the case. In order to resolve this enigma, independent blockage of ubiquitination of wild type PDE4D5 and subsequent investigation of the association between PDE4D5 and  $\beta$ -arrestin are needed. This

could be done through three independent actions: (i) deploying the HA-tagged 3R ubiquitin mutant; (ii) knockdown of the crucial E3 ligase Mdm2 by virtue of siRNA reagent; or (iii) mutation of the key K residues in the N-terminal region of PDE4D5 that are responsible for accepting the ubiquitin moieties.

Following the ubiquitination, I investigated another similar molecule-mediated post-translational modification-sumoylation. Unlike ubiquitination, the conditions to detect sumoylation of PDE4D5 are highly stringent. Overexpression of E3 ligase PIASy together with WT PDE4D5 leads to sumoylation of PDE4D5, suggesting that E3 ligase PIASy is critical in forming PDE4D5-SUMO conjugates. Although there are a number of other isoforms (Hay 2005) within the PIAS family, my initial data suggests that it is only overexpression of the PIASy isoform, which can cause sumoylation of PDE4D5. Sequential immunoprecipitation experiments have shown that  $\beta$ -arrestin, RACK1, ERK2 and AKAP18 $\delta$  bind to both non-sumoylated and sumoylated forms of PDE4D5 within cells, with preferential binding to the sumoylated form. To note, in contrast to this dual binding of  $\beta$ -arrestin in a cellular setting where sumoylation of PDE4D5 is gettable and this post-translational modification increases the binding of  $\beta$ -arrestin to PDE4D5, in a cell-free system where this post-translational modification of PDE4D5 is negated in the peptide array studies, GST- $\beta$ -arrestin only interacts with non-sumoylated form of PDE4D5 (Figure 6.5), which corresponds to the interaction of  $\beta$ -arrestin with the 4D5 K323R mutant in the cell system. This suggest that  $\beta$ -arrestin can interact with PDE4D5, regardless of its sumoylation status, however, it preferentially binds to the sumoylated form of PDE4D5 that constitutes a portion, even though  $\sim$  1%, of the total pool of PDE4D5.

Sumoylation has been shown to be a highly dynamic process and one that controls the intracellular targeting of modified proteins, often targeting the modified protein to the nucleus. My hypothesis is that that wild-type PDE4D5 might shuttle between the cytosol and nucleus, dependent on its sumoylation status. To address this hypothesis, further work is required in examining localization of the protein by cell fractionation studies and confocal microscopy. From such studies I would hope to gain insight into the functional effect of sumoylated PDE4D5 on gene expression. In addition, SUMO-modified PDE4D5 sequestered in different signaling complexes may

well disseminate the distinct signals upstream and relay these signals to distinct intracellular compartments.

Initial experiments undertaken to study sumoylation effects on the interaction between PDE4D5 with  $\beta$ -arrestin, revealed an increased binding of  $\beta$ -arrestin to the sumoylated form of PDE4D5 (Figure 5.6 a), the form of which is about 1% of the total PDE4D5. However, in previous studies carried out by others, it has been suggested that ~ 7% of total PDE4D5 seems to interact with  $\beta$ -arrestin. The disparity between these two percentages might be due to the cell system used. In the previous study, the authors used HEK293 cells and evaluated the endogenous PDE4D5 that is in complex with endogenous  $\beta$ -arrestin. However, in the cell context where PDE4D5-VSV and PIASy-HA were co-transfected in HEK293 cells, the proportion of PDE4D5 that is sequestered by  $\beta$ -arrestin has not been tested. Therefore, it would be very useful to verify the proportion of the PDE4D5 interacting with  $\beta$ -arrestin under these conditions so as to reasonably compare the two proportions of PDE4D5, one sumoylated, another bound to  $\beta$ -arrestin.

The function of the sumoylation of PDE4D5 is not understood. However, initial studies have shown that the sumoylation site is located within a catalytic domain of PDE4D5 that has been suggested to be involved in dimerization. This implies that a potential relationship between sumoylation and dimerization may exist. Therefore, it would be interesting to determine if they synergize or antagonize on a specific effect, such as subcellular distribution, or change of activity. It has also been reported that sumoylation can prevent ubiquitination in some cases (Desterro et al. 1998), suggesting that this may be the case for PDE4D5. Thus, in the future work I would like to examine the relationship between the ubiquitination and sumoylation of PDE4D5.

Post-translational modification of PDE4D5, by ubiquitination and sumoylation, has been successfully shown through the experiments described here, however, caution with respect to the proportion of the PDE4D5 population actually subjected to these regulatory events need to be taken. Compared to the strong ubiquitin signals at 10 min after isoprenaline challenge with a specific ubiquitin

antibody (Figure 4.4 a), signals above the natural size of PDE4D5-VSV at the same time point in the same immunoprecipitant with the VSV antibody were hardly observed (Figure 4.4 b). This may indicate that only a very small portion of PDE4D5 underwent ubiquitination, and the reason that the ubiquitinated PDE4D5 was so robustly detected in Figure 4.4 a is perhaps due to the high sensitivity of the ubiquitin antibody used. Similarly, sumoylated forms of PDE4D5 may also only constitute a small subpopulation of total PDE4D5 (Figure 5.4 a). To further verify the functional importance of these two post-translational modifications on PDE4D5, experiments to identify the actual proportion of the total PDE4D5 modified are needed. This can be done by full immunoprecipitation of PDE4D5 in the cell system studied, followed by comparison of the modified form to the total PDE4D5.

Both ubiquitination and sumoylation of some proteins are involved in the pathology of neuronal diseases, such as Alzheimer's disease (Seibenhener et al. 2004), Parkinson's disease (Nakaso et al. 2004) and Huntington's disease (Nagaoka et al. 2004; Dohmen 2004). PDE4 has been implicated in impaired memory (Houslay and Adams 2003). Therefore, my finding with respect with the above two types of post-translational modification might add new insight relating PDE4 to the pathogenesis of neuronal diseases.

In support of the possible modification of PDE4D5 by SUMO, I show that, in addition to the existing PDE4D5-binding partners  $\beta$ -arrestin and ERK2, Ubc9, which is known as a SUMO E2 conjugating enzyme and function to recognize target proteins and facilitate the SUMO attachment (Desterro et al. 1997; Johnson 2004; Melchior 2000), is able to interact with PDE4D5 in intact HEK293 cells under basal conditions. It would be very interesting, in the future, to examine if the interaction between PDE4D5 and Ubc9 can be changed by the alterations of other parameters, such as an increase in intracellular cAMP levels.

In order to examine the binding mechanisms of interacting proteins on PDE4D5 more closely, I have employed a novel peptide array methodology. I have mapped  $\beta$ -arrestin binding on PDE4D5 to two sites, one within the N-terminal region (T11-85A) and the second a <sup>670</sup>FQFELTJ<sup>676</sup>-spanning catalytic domain. The N-

terminal interaction site overlaps the known RACK binding site, further supporting the hypothesis that  $\beta$ -arrestin and RACK1 exclusively interact with PDE4D5 (Bolger et al. 2006). Within the C-terminal binding site scanning alanine substitution arrays identified F670, F672, E673, L674 and L676, located in subdomain-3 of the catalytic unit of PDE4D5 as crucial in  $\beta$ -arrestin binding. Within this motif is a FQF motif which has previously been implicated as an ERK2 docking site on PDE4 isoenzymes (Houslay and Adams 2003). In addition to  $\beta$ -arrestin binding I show that this short motif is also crucial for Ubc9 binding to PDE4D5. In addition, Ubc9 has an additional interaction site (K371-D405) downstream of the SUMO consensus site (K323) of PDE4D5. Therefore, both  $\beta$ -arrestin and Ubc9 can straddle PDE4D5 at two distinct sites, one of which on the catalytic domain is identical. Like the exclusive interaction pattern of  $\beta$ -arrestin and RACK1 on PDE4D5 (Bolger et al. 2006), my finding suggests that  $\beta$ -arrestin and Ubc9 are likely to perform a similar competitive binding to PDE4D5. If this binding is mutually exclusive then it would suggest that  $\beta$ -arrestin bound PDE4D5 can be ubiquitinated but not sumoylated. This is because ubiquitination would strengthen  $\beta$ -arrestin interaction, stopping Ubc9 binding and therefore preventing sumoylation. It would be interesting to see if this was indeed the case. Due to the shared FQF binding domain it is likely that ERK2 also competes with  $\beta$ -arrestin and Ubc9 to bind PDE4D5. Thus these various proteins likely sequester different pools of PDE4D5 and in so doing add to the complexity of compartmentalization of cAMP signaling in cells. It is highly likely that overexpression of ERK2 or Ubc9 in HEK293 cells may reduce the extent of the  $\beta$ -arrestin-mediated  $\beta_2$ AR desensitisation in response to  $\beta$  agonist as their overexpression might compete the endogenous  $\beta$ -arrestin binding to PDE4D5.

Peptide array based analysis provides only initial identification of potential interaction sites between proteins, mutation studies need to be carried out in order to confirm the binding sites on PDE4D5. Further work is required in order to assess the inter-relationships between PDE4D5 and  $\beta$ -arrestin, Ubc9 and ERK2. I would propose to examine the binding of these proteins with PDE4D5 after each of the others is knocked down using siRNA. This would be very interesting as it could provide evidence as to whether endogenous levels of particular scaffolds have consequences for the signaling through other scaffolding proteins. It has been shown that Ubc9 is

ubiquitously expressed in both cytoplasm and nucleoplasm (Melchior 2000; Dohmen 2004), and  $\beta$ -arrestin2 shuttles between the cytosol and nucleus (Scott et al. 2002; Wang et al. 2003). It would be interesting to examine whether a dynamic association between these proteins with PDE4D5 exists and if this alters their role in signal transduction. It has been shown that Ubc9 directs sumoylation of many proteins (Hay 2005), and I have demonstrated PDE4D5 can undergo sumoylation. Therefore, a siRNA-mediated knockdown of Ubc9 in HEK293 cells would then be useful to confirm the importance of Ubc9 in mediating PDE4D5 sumoylation.

In the work presented in this thesis, I have extended the appreciation of the concept that PDE4D5 has multifunctional roles in cells each of which is associated with the ability of PDE4D5 to be sequestered in distinct signaling complexes via distinct scaffolding proteins. In addition to the existing binding partners  $\beta$ -arrestin, RACK1 and ERK2, I have added Ubc9 to the PDE4D5 'partnership list'. It appears that distinct pools of PDE4D5 sequestered by particular scaffolds are exposed to different post-translational modifications and that control compartmentalized signal transduction. Thus, anchored PDE4D5 may be dynamically recruited to different areas of cells to provide cross-talk with other signaling pathways and reprogramme the signal transduction. For example, only when PDE4D5 is complexed to  $\beta$ -arrestin is it able to be ubiquitinated and this has potential to modify the regulation of  $\beta_2$ AR desensitization. Ubc9-sequestered PDE4D5, however, is subject to SUMO modification and consequential integration with other binding proteins. As such, my data highlight the necessity for better identification and characterization of these partnerships.

The design of peptide compounds that can sterically block these particular interactions is likely to be extremely useful to determine the functional importance of the distinct properties of PDE4D5. Furthermore, these peptides-derived compounds might be used as PDE4 isoform-specific inhibitors to block unwanted aspects of their *in vivo* functions, therefore achieving a major goal in drug research to improve the therapeutic ratio while reduce the side effects seen in the current available PDE4 inhibitors.

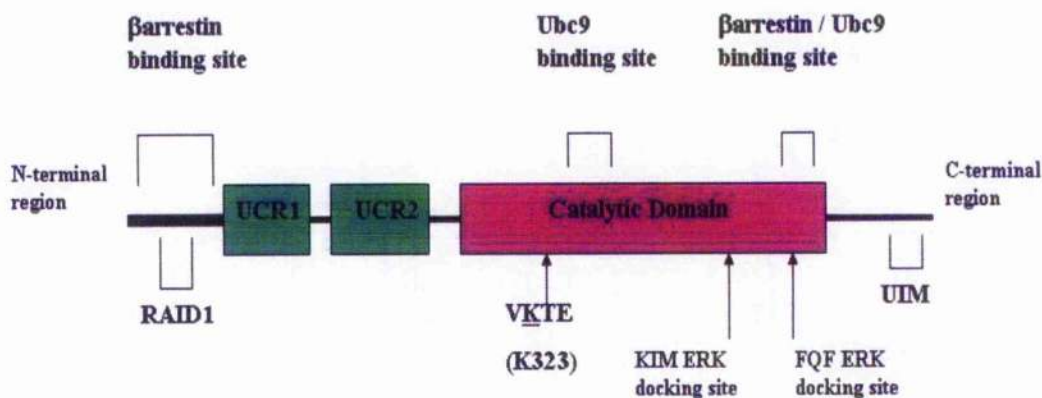


**Figure 7.1 Schematic of PDE4D5.**

N-terminal domain of PDE4D5 contains both  $\beta$ -arrestin binding site and RACK-1 binding site. The catalytic domain of PDE4D5 possesses a potential SUMO lysine, two Ubc9 binding sites, one  $\beta$ -arrestin binding site and two ERK docking sites, whereas the extreme C-terminus of PDE4D5 contains a Ubiquitin Interaction Motif. All the binding units are indicated in open squares or arrows.

## References

- Abrahamsen H., Baillie G., Ngai J., Vang T., Nika K., Ruppelt A., Mustelin T., Zaccolo M., Houslay M. and Tasken K. (2004) TCR- and CD28-mediated recruitment of phosphodiesterase 4 to lipid rafts potentiates TCR signaling. *The Journal of Immunology* **173**(8), 4847-4858.
- Ahmed T., Frey S. and Frey J.U. (2004) Regulation of the phosphodiesterase PDE4B3-isotype during long-term potentiation in the area dentata in vivo. *Neuroscience* **124**(4), 857-867.
- Aizawa T., Wei H., Miano J.M., Abe J., Berk B.C. and Chen Yan. (2003) Role of phosphodiesterase 3 in NO/cGMP-mediated antiinflammatory effects in vascular smooth muscle cells. *Circulation Research* **93**(5), 406-413.
- Antoni F.A. (2000) Molecular diversity of cAMP signaling. *Frontiers in Neuroendocrinology* **21**(2), 103-132.
- Ariga M., Neitzert B., Nakae S., Mottin G., Bertrand C., Pruniaux M.P., Jin S.L. and Conti M. (2004) Nonredundant function of phosphodiesterases 4D and 4B in neutrophil recruitment to the site of inflammation. *The Journal of Immunology* **173**(12), 7531-7538.
- Arp J., Kirchhof M.G., Baroja M.L., Nazarian S.H., Chau T.A., Strathdee C.A., Ball E.H. and Madrenas J. (2003) Regulation of T-cell activation by phosphodiesterase 4B2 requires its dynamic redistribution during immunological synapse formation. *Molecular and Cellular Biology* **23**(22), 8042-8057.
- Arshavsky V.Y., Lamb T.D. and Pugh, E.N. Jr. (2002) G proteins and phototransduction *Annual Review of Physiology* **64**, 153-187.
- Artemyev N.O., Arshavsky V.Y. and Cote R.H. (1998) Photoreceptor phosphodiesterase: interaction of inhibitory gamma subunit and cyclic GMP with

specific binding sites on catalytic subunits. *Methods* **14**(1), 93-104.

Asirvatham A.L., Galligan S.G., Schillace R.V., Davey M.P., Vasta V., Beavo J.A. and Carr D.W. (2004) A-kinase anchoring proteins interact with phosphodiesterases in T lymphocyte cell lines. *Journal of Immunology* **173**(8), 4806-4814.

Attramadal H., Arriza J.L., Aoki, C., Dawson T.M., Codina J., Kwatra M.M., Snyder S.H., Caron M.G. and Lefowitz R.J. (1992) Beta-arrestin2, a novel member of the arrestin/beta-arrestin gene family. *The Journal of Biological Chemistry* **267**(25), 17882-17890.

Azzi M., Charest P.G., Angers S., Rousseau G., Kohout T., Bouvier M. and Pifleyro G. (2003) Beta-arrestin-mediated activation of MAPK by inverse agonists reveals distinct active conformations for G protein-coupled receptors. *Proc Natl Acad Sci U. S. A.* **100**(20), 11406–11411.

Babol K. and Blasiak J. (2005) Beta3-adrenergic receptor. *Postepy Biochemii* **51**(1), 80-87.

Baillie G.S. and Houslay M.D. (2005) Arrestin times for compartmentalised cAMP signalling and phosphodiesterase-4 enzymes. *Current Opinion in Cell Biology* **17**(2), 129-134.

Baillie G.S., Huston E., Scotland G., Hodgkin M., Gall I., Peden A.H., MacKenzie C., Houslay E.S., Currie R., Pcttitt T.R., Walmsley A.R., Wakelam M.J., Warwicker J. and Houslay M.D.. (2002) TAPAS-1, a novel microdomain within the unique N-terminal region of the PDE4A1 cAMP-specific phosphodiesterase that allows rapid, Ca<sup>2+</sup>-triggered membrane association with selectivity for interaction with phosphatidic acid. *The Journal of Biological Chemistry* **277**(31), 28298-28309.

Baillie G.S., MacKenzie S.J. and Houslay M.D. (2001) Phorbol 12-myristate 13-acetate triggers the protein kinase A-mediated phosphorylation and activation of the PDE4D5 cAMP phosphodiesterase in human aortic smooth muscle cells through a route involving extracellular signal regulated kinase (ERK). *Molecular Pharmacology*

60(5), 1100-1111.

Baillie G.S., Mackenzie S.J., McPhee I. and Houslay M.D. (2000) Sub-family selective actions in the ability of Erk2 MAP kinase to phosphorylate and regulate the activity of PDE4 cAMP-specific phosphodiesterases. *British Journal of Pharmacology* **131**(4), 811–819.

Baillie G.S., Scott J.D. and Houslay M.D. (2005) Compartmentalisation of phosphodiesterases and protein kinase A: opposites attract. *FEBS Letter* **579**(15), 3264-3270.

Baillie G.S., Sood A., McPhee I., Gall I., Perry S.J., Lefkowitz R.J. and Houslay M.D. (2003) beta-Arrestin-mediated PDE4 cAMP phosphodiesterase recruitment regulates beta-adrenoceptor switching from Gs to Gi. *Proc Natl Acad Sci U. S. A.* **100**(3), 940-945.

Bajpai M., Fiedler S.E., Huang Z., Vijayaraghavan S., Olson G.E., Livera G., Conti M. and Carr D.W. (2006) AKAP3 selectively binds PDE4A isoforms in bovine spermatozoa. *Biology of Reproduction* **74**(1), 109-118.

Ballard S.A., Gingell C.J., Tang K., Turner I.A., Price M.E. and Naylor A.M. (1998) Effects of sildenafil on the relaxation of human corpus cavernosum tissue in vitro and on the activities of cyclic nucleotide phosphodiesterase isozymes. *The journal of Urology* **159**(6), 2164-2171.

Barber R., Baillie G.S., Bergmann R., Shepherd M.C., Sepper R., Houslay M.D. and Hecke G.V. (2004) Differential expression of PDE4 cAMP phosphodiesterase isoforms in inflammatory cells of smokers with COPD, smokers without COPD, and nonsmokers. *American Journal of Physiology. Lung Cellular and Molecular Physiology* **287**(2), L332-343.

Barnes A.P., Livera G., Huang P., Sun C., O'Neal W.K., Conti M., Stutts M.J. and Milgram S.L. (2005) Phosphodiesterase 4D forms a cAMP diffusion barrier at the apical membrane of the airway epithelium. *The Journal of Biological Chemistry*

**280(9)**, 7997-8003.

Barnette M.S. and Underwood D.C. (2000) New phosphodiesterase inhibitors as therapeutics for the treatment of chronic lung disease. *Current Opinion in Pulmonary Medicine* **6(2)**, 164-169.

Bayer P., Arndt A., Metzger S., Mahajan R., Melchior F., Jaenicke R. and Becker J. (1998) Structure determination of the small ubiquitin-related modifier SUMO-1. *Journal of Molecular Biology* **280(2)**, 275-286.

Bayewitch M.L., Avidor-Reiss T., Levy R., Pfeuffer T., Nevo I., Simonds W.F. and Vogel Z. (1998) Inhibition of adenylyl cyclase isoforms V and VI by various Gbetagamma subunits. *The FASEB Journal* **12(11)**, 1019-1025.

Beard M.B., Huston E., Campbell L., Gall L., McPhee I., Yarwood S., Scotland G. and Houslay M.D. (2002) In addition to the SH3 binding region, multiple regions within the N-terminal noncatalytic portion of the cAMP-specific phosphodiesterase, PDE4A5, contribute to its intracellular targeting. *Cellular Signalling* **14(5)**, 453-465.

Beard M.B., O'Connell J.C., Bolger G.B. and Houslay M.D. (1999) The unique N-terminal domain of the cAMP phosphodiesterase PDE4D4 allows for interaction with specific SH3 domains. *FEBS Letters* **460(1)**, 173-177.

Beard M.B., Olsen A.E., Jones R.E., Erdogan S., Houslay M.D. and Bolger G.B. (2000) UCR1 and UCR2 domains unique to the cAMP-specific phosphodiesterase family form a discrete module via electrostatic interactions. *The Journal of Biological Chemistry* **275(14)**, 10349-10358.

Beavo J.A. (1995) Cyclic nucleotide phosphodiesterases: functional implications of multiple isoforms. *Physiological Reviews* **75(4)**, 725-748.

Beavo J.A. and Brunton L.L. (2002) Cyclic nucleotide research -- still expanding after half a century. *Nature reviews. Molecular cell biology* **3(9)**, 710-8.

Bender A.T. and Beavo J.A. (2006) Cyclic nucleotide phosphodiesterases: molecular regulation to clinical use. *Pharmacological Reviews* **58**(3), 488-520.

Berman D.M. and Gilman A.G. (1998) Mammalian RGS proteins: barbarians at the gate. *The Journal of Biological Chemistry* **273**(3), 1269-1272.

Bernier-Villamor V., Sampson D.A., Matunis M.J. and Lima C.D. (2002) Structural basis for E2-mediated SUMO conjugation revealed by a complex between ubiquitin-conjugating enzyme Ubc9 and RanGAP1. *Cell* **108**(3), 345-356.

Bevan S., Porteous L., Sitzer M. and Markus H.S. (2005) Phosphodiesterase 4D gene, ischemic stroke, and asymptomatic carotid atherosclerosis. *Stroke* **36**(5), 949-953.

Bohren K.M., Nadkarni V., Song J.H., Gabbay K.H. and Owerbach D. (2004) A M55V polymorphism in a novel SUMO gene (SUMO-4) differentially activates heat shock transcription factors and is associated with susceptibility to type I diabetes mellitus. *The Journal of Biological Chemistry* **279**(26), 27233-27238.

Bolger G., Michaeli T., Martins T., St. John T., Steiner B., Rodgers L., Riggs M., Wigler M and Ferguson K. (1993) A family of human phosphodiesterases homologous to the dunce learning and memory gene product of *Drosophila melanogaster* are potential targets for antidepressant drugs. *Molecular and Cellular Biology* **13**(10), 6558-6571.

Bolger G.B., McCahill A., Huston E., Cheung Y.F., McSorley T., Baillie G.S. and Houslay M.D. (2003) The unique amino-terminal region of the PDE4D5 cAMP phosphodiesterase isoform confers preferential interaction with beta-arrestins. *The Journal of Biological Chemistry* **278**(49), 49230-49238.

Bolger G.B., McCahill A., Yarwood S.J., Steele M.R., Warwicker J. and Houslay M.D. (2002) Delineation of RAID1, the RACK1 interaction domain located within the unique N-terminal region of the cAMP-specific phosphodiesterase, PDE4D5. *BMC Biochemistry* **3**, 24.

Bolger G.B., Peden A.H., Steele M.R., MacKenzie C., McEwan D.G., Wallace D.A., Huston E., Baillie G.S. and Houslay M.D. (2003) Attenuation of the activity of the cAMP-specific phosphodiesterase PDE4A5 by interaction with the immunophilin XAP2. *The Journal of Biological Chemistry* **278**(35), 33351-33363.

Bos J.L. (2003) Epac: a new cAMP target and new avenues in cAMP research. *Nature Reviews. Molecular Cell Biology* **4**(9), 733-738.

Bos J.L., De Bruyn K., Enserink J., Kuiperij B., Rangarajan S., Rehmann H., Riedl J., de Rooij J., van Mansfeld F. And Zwartkruis F. (2003) The role of Rap1 in integrin-mediated cell adhesion. *Biochemical Society Transactions* **31**(1), 83-86.

Brink C.B., Harvey B.H., Bodenstein J., Venter D.P. and Oliver D.W. (2004) Recent advances in drug action and therapeutics: relevance of novel concepts in G-protein-coupled receptor and signal transduction pharmacology. *British Journal of Clinical Pharmacology* **57**(4), 373-387.

Broderick K.E., Kean L., Dow J.A., Pyne N.J. and Davis S.A. (2004) Ectopic expression of bovine type 5 phosphodiesterase confers a renal phenotype in *Drosophila*. *The Journal of Biological Chemistry* **279**(9), 8159-8168.

Brunton L.L. (2003) PDE4: arrested at the border. *Science's STKE* **204**, PE44.

Brunton L.L., Hayes J.S. and Mayer S.E. (1998) Functional compartmentation of cAMP and protein kinase in heart. *Advances in Cyclic Nucleotide Research* **14**, 391-397.

Burnouf C. and Pruniaux M.P. (2002) Recent advances in PDE4 inhibitors as immunoregulators and anti-inflammatory drugs. *Current Pharmaceutical Design* **8**(14), 1255-1296.

Burns F., Rodger I.W. and Pyne N.J. (1992) The catalytic subunit of protein kinase A triggers activation of the type V cyclic GMP-specific phosphodiesterase from guinea-pig lung. *Biochemical Journal* **283**(Pt 2), 487-91.

Busch C.J., Liu H., Graveline A.R. and Bloch K.D. (2006) Nitric oxide induces phosphodiesterase 4B expression in rat pulmonary artery smooth muscle cells. *American Journal of Physiology. Lung Cellular and Molecular Physiology* **290**(4), L747-L753.

Buxton I.L., and Brunton L.L. (1983) Compartments of cyclic AMP and protein kinase in mammalian cardiomyocytes. *The Journal of Biological Chemistry* **258**(17), 10233-10239.

Cali J.J., Zwaagstra J.C., Mons N., Cooper D.M. and Krupinski J. (1994) Type VIII adenylyl cyclase. A Ca<sup>2+</sup>/calmodulin-stimulated enzyme expressed in discrete regions of rat brain. *The Journal of Biological Chemistry* **269**(16), 12190-12195.

Card G.L., England B.P., Suzuki Y., Fong D., Powell B., Lee B., Luu C., Tabrizizad M., Gillette S., Ibrahim P.N., Artis D.R., Bollag G., Milburn M.V., Kim S.H., Schlessinger J. and Zhang K.Y. (2004) Structural basis for the activity of drugs that inhibit phosphodiesterases. *Structure* **12**(12), 2233-2247.

Carlisle Michel J.J., Dodge K.L., Wong W., Mayer N.C., Langeberg L.K., Scott J.D. (2004) PKA-phosphorylation of PDE4D3 facilitates recruitment of the mAKAP signaling complex. *Biochemical Journal* **381**(Pt 3), 587-592.

Castro A., Jerez M.J., Gil C. and Martinez A. (2004) Cyclic nucleotide phosphodiesterases and their role in immunomodulatory responses: advances in the development of specific phosphodiesterase inhibitors. *Medical Research Reviews* **25**(2), 229-244.

Chang B.Y., Harte R.A. and Cartwright C.A. (2002) RACK1: a novel substrate for the Src protein-tyrosine kinase. *Oncogene* **21**(50), 7619-7629.

Chang L.K., Lee Y.H., Cheng T.S., Hong Y.R., Lu P.J., Wang J.J., Wang W.H., Kuo C.W., Li S.S. and Liu S.T. (2004) Post-translational modification of Rta of Epstein-Barr virus by SUMO-1. *The Journal of Biological Chemistry* **279**(37), 38803-38812.

Chau V., Tobias J.W., Bachmair A., Marriott D., Ecker D.J., Gonda D.K. and Varshavsky A. (1989) A multiubiquitin chain is confined to specific lysine in a targeted short-lived protein. *et al. Science* **243**(4898), 1576-1583.

Choi E.J., Xia Z., Storm D.R. (1992) Stimulation of the type III olfactory adenylyl cyclase by calcium and calmodulin. *Biochemistry* **31**(28), 6492-6498.

Christianson J.C. and Green W.N. (2004) Regulation of nicotinic receptor expression by the ubiquitin-proteasome system. *The EMBO Journal* **23**, 4156-4165.

Claing A., Laporte S.A., Caron M.G. and Lefkowitz R.J. (2002) Endocytosis of G protein-coupled receptors: roles of G protein-coupled receptor kinases and beta-arrestin proteins. *Progress in Neurobiology* **66**(2), 61-79.

Cong M., Perry S.J., Lin F.T., Fraser I.D., Hu L.A., Chen W., Pitcher J.A., Scott J.D. and Lefkowitz R.J. (2001) Regulation of membrane targeting of the G protein-coupled receptor kinase 2 by protein kinase A and its anchoring protein AKAP79. *The Journal of Biological Chemistry* **276**(18), 15192-15199.

Conti M., Richter W., Mehats C., Livera G., Park J.Y. and Jin C. (2003) Cyclic AMP-specific PDE4 phosphodiesterases as critical components of cyclic AMP signaling. *The Journal of Biological Chemistry* **278**(8), 5493-5496.

Cooper D.M. (2003) Regulation and organization of adenylyl cyclases and cAMP. *Biochemical Journal* **375**(Pt 3), 517-529.

Cooper D.M. and Crossthwaite A.J. (2006) Higher-order organization and regulation of adenylyl cyclases. *Trends in Pharmacological Sciences* **27**(8), 426-31.

Cooper D.M., Schell M.J., Thorn P. and Irvine R.F. (1998) Regulation of adenylyl cyclase by membrane potential. *The Journal of Biological Chemistry* **273**(42), 27703-27707.

Corbin J.D. and Francis S.H. (1999) Cyclic GMP phosphodiesterase-5: target of

sildenafil. *The Journal of Biological Chemistry* **274**(20), 13729-13732.

Cote R.H. (2004) Characteristics of photoreceptor PDE (PDE6): similarities and differences to PDE5. *International Journal of Impotence Research* **16** Suppl 1:S28-33.

Crook T., Ludwig R.L., Marston N.J., Willkomm D. and Vousden K.H. (1996) Sensitivity of p53 lysine mutants to ubiquitin-directed degradation targeted by human papillomavirus E6. *Virology* **217**(1), 285-292.

D'Sa C., Tolbert L.M., Conti M. and Duman R.S. (2002) Regulation of cAMP-specific phosphodiesterases type 4B and 4D (PDE4) splice variants by cAMP signaling in primary cortical neurons. *Journal of Neurochemistry* **81**(4), 745-757.

Daaka Y., Luttrell L.M., Lefkowitz R.J. (1997) Switching of the coupling of the beta2-adrenergic receptor to different G proteins by protein kinase A. *Nature* **390**(6655), 88-91.

Dal Piaz V. and Giovannoni M.P. (2000) Phosphodiesterase 4 inhibitors, structurally unrelated to rolipram, as promising agents for the treatment of asthma and other pathologies. *European Journal of Medicinal Chemistry* **35**(5), 463-480.

Danchin A. (1993) Phylogeny of adenylyl cyclases. *Advances in Second Messenger and Phosphoprotein Research* **27**, 109-162.

De Rooij J., Rehmann H., van Triest M, Cool R.H., Wittinghofer A. and Bos J.L. (2000) Mechanism of regulation of the Epac family of cAMP-dependent RapGEFs. *The Journal of Biological Chemistry*. **275**(27), 20829-20836.

Degerman E., Belfrange P. and Manganiello V.C. (1997) Structure, localization, and regulation of cGMP-inhibited phosphodiesterase (PDE3). *The Journal of Biological Chemistry* **272**(11), 6823-6826.

Desterro J.M., Rodriguez M.S. and Hay R.T. (1998) SUMO-1 modification of I $\kappa$ B $\alpha$  inhibits NF- $\kappa$ B activation. *Molecular Cell* **2**(2), 233-239.

Deveraux Q., Ustrell V., Pickart C. and Rechsteiner M. (1994) A 26 S protease subunit that binds ubiquitin conjugates. *The Journal of Biological Chemistry* **269**(10), 7059-7061.

Di Fiore P.P., Polo S. and Hofmann K. (2003) When ubiquitin meets ubiquitin receptors: a signalling connection. *Nature Reviews. Molecular Cell Biology* **4**(6), 491-497.

Ding B., Abe J., Wei H., Huang Q., Walsh R.A., Molina C.A., Zhao A., Sadoshima J., Blaxall B.C., Berk B.C. and Yan C. (2005) Functional role of phosphodiesterase 3 in cardiomyocyte apoptosis: implication in heart failure. *Circulation* **111**(19), 2469-2476.

Diviani D., Baisamy L. and Appert-Collin A. (2006) AKAP-Lbc: A molecular scaffold for the integration of cyclic AMP and Rho transduction pathways *European Journal of Cell Biology* **85**(7), 603-610.

Dodge K.L., Khouangsathiene S., Kapiloff M.S., Mouton R., Hill E.V., Houslay M.D., Langeberg L.K. and Scott J.D. (2001) mAKAP assembles a protein kinase A/PDE4 phosphodiesterase cAMP signaling module. *The EMBO Journal* **20**(8), 1921-1930.

Dohmen R.J. (2004) SUMO protein modification. *Biochimica et Biophysica Acta* **1695**(1-3), 113-131.

Dryja T.P., Rucinski D.E., Chen S.H. and Berson E.L. (1999) Frequency of mutations in the gene encoding the alpha subunit of rod cGMP-phosphodiesterase in autosomal recessive retinitis pigmentosa. *Investigative Ophthalmology and Visual Science* **40**(8), 1859-1865.

Duda D.M. and Schulman B.A. (2005) Tag-team SUMO wrestling. *Molecular Cell* **18**(6), 612-614.

Dumaz N. and Marais R. (2005) Integrating signals between cAMP and the RAS/RAF/MEK/ERK signalling pathways. Based on the anniversary prize of the Gesellschaft für Biochemie und Molekularbiologie Lecture delivered on 5 July 2003

at the Special FEBS Meeting in Brussels. *The FEBS Journal* **272**(14), 3491-3504.

Dupre D.J., Rola-Pleszczynski M. and Stankova J. (2004) Inverse agonism: more than reverting constitutively active receptor signaling. *Biochemistry and Cell Biology* **82**(6), 676-680.

Eardley I. and Cartledge J. (2002) Tadalafil (Cialis) for men with erectile dysfunction. *International Journal of Clinical Practice* **56**(4), 300-304.

Edmondson SD, Mastracchio A, He J, Chung CC, Forrest MJ, Hofsess S, MacIntyre E, Metzger J, O'Connor N, Patel K, *et al.* (2003) Benzyl vinylogous amide substituted aryldihydropyridazinones and aryldimethylpyrazolones as potent and selective PDE3B inhibitors. *Bioorganic and Medicinal Chemistry Letters* **13**(22), 3983-3987.

Elorza A., Sarnago S. and Mayor F. Jr. (2000) Agonist-dependent modulation of G protein-coupled receptor kinase 2 by mitogen-activated protein kinases. *Molecular Pharmacology* **57**(4), 778-783.

Elsasser S., Gali R.R., Schwickart M., Larsen C.N., Leggett D.S., Müller B., Feng M.T., Tubing F., Dittmar G.A. and Finley D. (2002) Proteasome subunit Rpn1 binds ubiquitin-like protein domains. *Nature Cell Biology* **4**(9), 725-730.

Engels P., Sullivan M., Muller T. and Lubbert H. (1995) Molecular cloning and functional expression in yeast of a human cAMP-specific phosphodiesterase subtype (PDE IV-C). *FEBS Letters* **358**(3), 305-310.

Fagan K.A., Graf R.A., Tolman S., Schaack J. and Cooper D.M. (2000) Regulation of a Ca<sup>2+</sup>-sensitive adenylyl cyclase in an excitable cell. Role of voltage-gated versus capacitative Ca<sup>2+</sup> entry. *The Journal of Biological Chemistry* **275**(51), 40187-40194.

Fan Chung K. (2006) Phosphodiesterase inhibitors in airways disease *European Journal of Pharmacology* **533**(1-3), 110-117.

Fang S., Jensen J.P., Ludwig R.L., Vousden K.H. and Weissman A.M. (2000) Mdm2 is

a RING finger-dependent ubiquitin protein ligase for itself and p53. *The Journal of Biological Chemistry* **275**(12), 8945-8951.

Fawcett L., Baxendale R., Stacey P., McGrouther C., Harrow I., Soderling S., Hetman J., Beavo J.A. and Phillips S.C. (2000) Molecular cloning and characterization of a distinct human phosphodiesterase gene family: PDE11A. *Proc. Natl. Acad. Sci. U.S.A.* **97**(7), 3702-3707.

Ferguson, S. S. (2001) Evolving concepts in G protein-coupled receptor endocytosis: The role in receptor desensitization and signaling. *Pharmacological. Reviews* **53**(1), 1-24.

Fesenko E.E., Kolesnikov S.S. and Lyubarsky A.L. (1985) Induction by cyclic GMP of cationic conductance in plasma membrane of retinal rod outer segment. *Nature* **313**(6000), 310-313.

Fidock M., Miller M. and Lanfear J. (2001) Isolation and differential tissue distribution of two human cDNAs encoding PDE1 splice variants. *Cell Signalling* **14**(1), 53-60.

Fisher D.A., Smith J.F., Pillar J.S., St. Denis S.H. and Cheng J.B. (1998) Isolation and characterization of PDE8A, a novel human cAMP-specific phosphodiesterase. *Biochemical and Biophysical Research Communications* **246**(3), 570-577.

Fisher R.D., Wang B., Alam S.L., Higginson D.S., Robinson H., Sundquist W.I. and Hill C.P. (2003) Structure and ubiquitin binding of the ubiquitin-interacting motif. *The Journal of Biological Chemistry* **278**(31), 28976-28984.

Fleming Y.M., Frame M.C. and Houslay M.D. (2004) PDE4-regulated cAMP degradation controls the assembly of integrin-dependent actin adhesion structures and REF52 cell migration. *Journal of Cell Science* **117**(Pt 11), 2377-2388.

Frame M., Wan K.F., Tate R., Vandenabeele P. and Pyne N.J. (2001) The gamma subunit of the rod photoreceptor cGMP phosphodiesterase can modulate the

proteolysis of two cGMP binding cGMP-specific phosphodiesterases (PDE6 and PDE5) by caspase-3. *Cellular Signalling* **13**(10), 735-741.

Frame M.J., Tate R., Adams D.R., Morgan K.M., Houslay M.D., Vandenberg P. and Pyne N.J. (2003) Interaction of caspase-3 with the cyclic GMP binding cyclic GMP specific phosphodiesterase (PDE5a1). *European Journal of Biochemistry* **270**(5), 962-970.

Francis S.H., Colbran J.L., McAllister-Lucas L.M. and Corbin J.D. (1994) Zinc interactions and conserved motifs of the cGMP-binding cGMP-specific phosphodiesterase suggest that it is a zinc hydrolase. *The Journal of Biological Chemistry* **269**(36), 22477-22480.

Francis S.H., Turko I.V. and Corbin J.D. (2001) Cyclic nucleotide phosphodiesterases: relating structure and function. *Progress in Nucleic Acid Research and Molecular Biology* **65**, 1-52.

Fraser I.D., Cong M., Kim J., Rollins E.N., Daaka Y., Lefkowitz R.J. and Scott J.D. (2000) Assembly of an A kinase-anchoring protein-beta(2)-adrenergic receptor complex facilitates receptor phosphorylation and signaling. *Current Biology* **10**(7), 409-412.

Freedman N.J., Liggett S.B., Drachman D.F., Pei G., Caron M. and Lefkowitz R.J. (1995) Phosphorylation and desensitization of the human beta 1-adrenergic receptor. Involvement of G protein-coupled receptor kinases and cAMP-dependent protein kinase. *The Journal of Biological Chemistry* **270**(30), 17953-17961.

Fujishige K., Kotera J., Michibata H., Yuasa K., Takebayashi S., Okumura K. and Omori K. (1999) Cloning and characterization of a novel human phosphodiesterase that hydrolyzes both cAMP and cGMP (PDE10A). *The Journal of Biological Chemistry* **274**(26), 18438-18445.

Gal A., Orth U., Baehr W., Schwinger E. and Rosenberg T. (1994) Heterozygous missense mutation in the rod cGMP phosphodiesterase beta-subunit gene in autosomal

dominant stationary night blindness. *Nature Genetics* 7(4), 551.

Gardner C, Robas N, Cawkill D and Fidock M (2000) Cloning and characterization of the human and mouse PDE7B, a novel cAMP-specific cyclic nucleotide phosphodiesterase. *Biochemical and Biophysical Research Communications* 272(1), 186-192.

Gardner L.A., Delos Santos N.M., Matta S.G., Whitt M.A. and Bahouth S.W. (2004) Role of the cyclic AMP-dependent protein kinase in homologous resensitization of the beta1-adrenergic receptor. *The Journal of Biological Chemistry* 279(20), 21135-21143.

Geijsen N., Spaargaren M, Raaijmakers J.A., Lammers J.W., Koenderman L. and Coffey P.J. (1999) Association of RACK1 and PKCbeta with the common beta-chain of the IL-5/IL-3/GM-CSF receptor. *Oncogene* 18(36), 5126-5130.

Giembycz M. (2000) PDE4D-deficient mice knock the breath out of asthma. *Trends in Pharmacological Sciences* 21(8), 291-292.

Giembycz M.A. (2000) Phosphodiesterase 4 inhibitors and the treatment of asthma: where are we now and where do we go from here? *Drugs* 59(2), 193-212.

Giembycz M.A. (2005) Life after PDE4: overcoming adverse events with dual-specificity phosphodiesterase inhibitors. *Current Opinion in Pharmacology* 5(3), 238-244.

Gilckman M.H. and Ciechanover A. (2002) The ubiquitin-proteasome proteolytic pathway: destruction for the sake of construction. *Physiological Reviews* 82(2), 373-428.

Gill G. (2004) SUMO and ubiquitin in the nucleus: different functions, similar mechanisms? *Genes and Development* 18(17), 2046-2059.

Giorgi M., Modica A., Pompili A., Pacitti C. and Gasbarri A. (2004) The induction of cyclic nucleotide phosphodiesterase 4 gene (PDE4D) impairs memory in a water

maze task. *Behavioural Brain Research* **154**(1), 99-106.

Girnita L., Shenoy S.K., Sehat B., Vasilcanu R., Girnita A., Lefkowitz R.J. and Larsson O. (2005)  $\beta$ -Arrestin is crucial for ubiquitination and down-regulation of the insulin-like growth factor-1 receptor by acting as adaptor for the MDM2 E3 ligase. *The Journal of Biological Chemistry* **280**(26), 24412-24419.

Glickman M.H. (2000) Getting in and out of the proteasome. *Seminars in Cell and Developmental Biology* **11**(3), 149-158.

Goraya T.A. and Cooper D.M. (2005)  $\text{Ca}^{2+}$ -calmodulin-dependent phosphodiesterase (PDE1): current perspectives. *Cell Signalling* **17**(7), 789-797.

Goraya T.A., Masada N., Ciruela A. and Cooper D.M. (2004) Sustained entry of  $\text{Ca}^{2+}$  is required to activate  $\text{Ca}^{2+}$ -calmodulin-dependent phosphodiesterase 1A. *The Journal of Biological Chemistry* **279**(39), 40494-40504.

Gretarsdottir S., Thorleifsson G., Reynisdottir S.T. et al. (2003) The gene encoding phosphodiesterase 4D confers risk of ischemic stroke. *Nature Genetics* **35**(2), 131-138.

Gu C. and Cooper D.M. (2000)  $\text{Ca}^{2+}$ ,  $\text{Sr}^{2+}$ , and  $\text{Ba}^{2+}$  identify distinct regulatory sites on adenylyl cyclase (AC) types VI and VIII and consolidate the apposition of capacitative cation entry channels and  $\text{Ca}^{2+}$ -sensitive ACs. *The Journal of Biological Chemistry* **275**(10), 6980-6986.

Guipponi M., Scott H.S., Kudoh J., Kawasaki K., Shibuya K., Shintani A., Asakawa S., Chen H., Lalioti M.D., Rossier C., Minoshima S., Shimizu N. and Antonarakis S.E. (1998) Identification and characterization of a novel cyclic nucleotide phosphodiesterase gene (PDE9A) that maps to 21q22.3: alternative splicing of mRNA transcripts, genomic structure and sequence. *Human Genetics* **103**(4), 386-392.

Haglund K., Di Fiore P.P. and Dikic I. (2003) Distinct monoubiquitin signals in receptor endocytosis. *Trends in Biochemical Sciences* **28**(11), 598-603.

Hansen G., Jin S. Umetsu D.T. and Conti M. (2000) Absence of muscarinic cholinergic airway responses in mice deficient in the cyclic nucleotide phosphodiesterase PDE4D. *Proc. Natl. Acad. Sci. U.S.A.* **97**(12), 6751-6756.

Harding V.B., Jones L.R., Lefkowitz R.J., Koch W.J. and Rockman H.A. (2001) Cardiac beta ARK1 inhibition prolongs survival and augments beta blocker therapy in a mouse model of severe heart failure. *Proc. Natl. Acad. Sci. U.S.A.* **98**(10), 5809-5814.

Härndahl L., Jing X.J., Ivarsson R., Degerman E., Ahrén B., Manganiello V.C., Renström E. and Holst L.S. (2002) Important role of phosphodiesterase 3B for the stimulatory action of cAMP on pancreatic beta-cell exocytosis and release of insulin. *The Journal of Biological Chemistry* **277**(40), 37446-37455.

Hatakeyama S. and Nakayama K.I. (2003) Ubiquitylation as a quality control system for intracellular proteins. *Journal of Biochemistry (Tokyo)* **134**(1), 1-8.

Hay R.T. (2005) SUMO: a history of modification. *Molecular Cell* **18**(1), 1-12.

Hayashi, M., Matsushima, K., Ohashi, H., Tsunoda, H., Murase, S., Kawarada, Y. and Tanaka, T. (1998) Molecular cloning and characterization of human PDE8B, a novel thyroid-specific isozyme of 3',5'-cyclic nucleotide phosphodiesterase. *Biochemical and Biophysical Research Communications* **250**(3), 751-756.

Hayes J.S. and Brunton L.L. (1982) Functional compartments in cyclic nucleotide action. *Journal of Cyclic Nucleotide Research* **8**(1), 1-16.

Heijink I.H., Vellenga E., Oostendorp J., de Monchy J.G., Postma D.S. and Kauffman H.F. (2005) Exposure to TARC alters beta2-adrenergic receptor signaling in human peripheral blood T lymphocytes. *American Journal of Physiology. Lung Cellular and Molecular Physiology* **289**(1), L53-L59.

Hepler J.R. and Gilman A.G. (1992) G proteins. *Trends in Biochemical Sciences* **17**(10), 383-387.

Hershko A. and Ciechanover A. (1998) The ubiquitin system. *Annual Review of Biochemistry* **67**, 425-479.

Hicke L. (2001) Protein regulation by monoubiquitin. *Nature Reviews. Molecular Cell Biology* **2**(3), 195-201.

Hilgarth R.S., Murphy L.A., Skaggs H.S., Wilkerson D.C., Xing H. and Sarge K.D. (2004) Regulation and function of SUMO modification. *The Journal of Biochemistry* **279**(52), 53899-53902.

Hochstrasser M. (2000) Evolution and function of ubiquitin-like protein-conjugation systems. *Nature Cell Biology* **2**(8), E153-E157.

Hoffmann R., Baillie G.S., MacKenzie S.J., Yarwood S.J. and Houslay M D. (1999) The MAP kinase ERK2 inhibits the cyclic AMP-specific phosphodiesterase HSPDE4D3 by phosphorylating it at Ser579. *The EMBO Journal* **18**(4), 893-903.

Hoffmann R., Wilkinson I.R., MCCALLUM J.F., Engels P. and Houslay M.D. (1998) cAMP-specific phosphodiesterase HSPDE4D3 mutants which mimic activation and changes in rolipram inhibition triggered by protein kinase A phosphorylation of Ser-54: generation of a molecular model. *Biochemical Journal* **333**(Pt 1), 139-149.

Hofmann H., Floss S., Stamminger T. (2000) Covalent modification of the transactivator protein IE2-p86 of human cytomegalovirus by conjugation to the ubiquitin-homologous proteins SUMO-1 and hSMT3b. *Journal of Virology* **74**(6), 2510-2524.

Hofmann K. and Falquet L. (2001) A ubiquitin-interacting motif conserved in components of the proteasomal and lysosomal protein degradation systems. *Trends in Biochemical Sciences* **26**(6), 347-350.

Horton Y.M., Sullivan M. and Houslay M.D. (1995) Molecular cloning of a novel splice variant of human type IVA (PDE-IVA) cyclic AMP phosphodiesterase and localization of the gene to the p13.2-q12 region of human chromosome 19.

*Biochemical Journal* **308**(Pt 2), 683-691.

Hou D., Cenciarelli C, Jensen J.P., Nguygen H.B. and Weissman A.M. (1994) Activation-dependent ubiquitination of a T cell antigen receptor subunit on multiple intracellular lysines. *The Journal of Biological Chemistry* **269**(19), 14244-14247.

Houslay M.D. (2001) PDE4 cAMP-specific phosphodiesterases. *Progress in Nucleic Acid Research and Molecular Biology* **69**, 249-315.

Houslay M.D. (2005) The long and short of vascular smooth muscle phosphodiesterase-4 as a putative therapeutic target. *Molecular Pharmacology* **68**(3), 563-567.

Houslay M.D. and Adams D.R. (2003) PDE4 cAMP phosphodiesterases: modular enzymes that orchestrate signalling cross-talk, desensitization and compartmentalization. *Biochemical Journal* **370**(Pt 1), 1-18.

Houslay M.D. and Baillie G.S. (2003) The role of ERK2 docking and phosphorylation of PDE4 cAMP phosphodiesterase isoforms in mediating cross-talk between the cAMP and ERK signalling pathways. *Biochemical Society Transactions* **31**(Pt 6), 1186-1190.

Houslay M.D. and Kolch W. (2000) Cell-type specific integration of cross-talk between extracellular signal-regulated kinase and cAMP signaling. *Molecular Pharmacology* **58**(4), 659-68.

Houslay M.D. and Milligan G. (1997) Tailoring cAMP-signalling responses through isoform multiplicity. *Trends in Biochemical Sciences* **22**(6), 217-224.

Houslay M.D., Schafer P. and Zhang K.Y. (2005) Keynote review: phosphodiesterase-4 as a therapeutic target. *Drug Discovery Today* **10**(22), 1503-1519.

Houslay M.D., Sullivan V. and Bolger, G.B. (1998) The multienzyme PDE4 cyclic adenosine monophosphate-specific phosphodiesterase family: intracellular targeting,

regulation, and selective inhibition by compounds exerting anti-inflammatory and antidepressant actions. *Advances in Pharmacology* **44**, 225-342.

Huai Q., Colicelli J. and Ke H. (2003) The crystal structure of AMP-bound PDE4 suggests a mechanism for phosphodiesterase catalysis. *Biochemistry* **42**(45), 13220-13226.

Huai Q., Wang H., Sun Y., Kim H.Y., Liu Y. and Ke H. (2003) Three-dimensional structures of PDE4D in complex with roliprams and implication on inhibitor selectivity. *Structure* **11**(7), 865-873.

Huang C., Hepler J.R., Chen L.T., Gilman A.G., Anderson, R.G. and Mumby S.M. (1997) Organization of G proteins and adenylyl cyclase at the plasma membrane. *Molecular Biology of the Cell* **8**(12), 2365-2378.

Huang Z., Ducharme Y., Macdonald D. and Robichaud A. (2001) The next generation of PDE4 inhibitors. *Current Opinion in Chemical Biology*. **5**(4), 432-438.

Hunter T. (1995) Protein kinases and phosphatases: the yin and yang of protein phosphorylation and signaling. *Cell* **80**(2), 225-236.

Iffland A. (2005) Structural determinants for inhibitor specificity and selectivity in PDE2A using the wheat germ in vitro translation system. *Biochemistry* **44**(23), 8312-8325.

Jacoby E., Bouhelal R., Gerspacher M., Seuwen K. (2006) The 7 TM G-protein-coupled receptor target family. *ChemMedChem* **1**(8), 761-782.

Jahns R., Boivin V. and Lohse M.J. (2006) beta(1)-Adrenergic receptor function, autoimmunity, and pathogenesis of dilated cardiomyopathy. *Trends in Cardiovascular Medicine* **16**(1), 20-24.

Jesen O.N. (2004) Modification-specific proteomics: characterization of post-translational modifications by mass spectrometry. *Current Opinion in Chemical*

*Biology* **8**(1), 33-41.

Jin S.L. and Conti M. (2002) Induction of the cyclic nucleotide phosphodiesterase PDE4B is essential for LPS-activated TNF- $\alpha$  responses. *Proc. Natl. Acad. Sci. U.S.A.* **99**(11), 7628-7633.

Jin S.L., Lan L., Zoudilova M. and Conti M. (2005) Specific role of phosphodiesterase 4B in lipopolysaccharide-induced signaling in mouse macrophages. *The Journal of Immunology* **175**(3), 1523-1531.

Jin S.L., Richard F.J., Kuo W.P., D'Ercole A.J. and Conti M. (1999) Impaired growth and fertility of cAMP-specific phosphodiesterase PDE4D-deficient mice. *Proc. Natl. Acad. Sci. U.S.A.* **96**(21), 11998-12003.

Jin S.L., Swinnen J.V. and Conti M. (1992) Characterization of the structure of a low Km, rolipram-sensitive cAMP phosphodiesterase. Mapping of the catalytic domain. *The Journal of Biological Chemistry* **267**(26), 18929-18939.

Joazeiro C.A. and Weissman A.M. (2000) RING finger proteins: mediators of ubiquitin ligase activity. *Cell* **102**(5), 549-552.

Jockers R., Angers S., Silva A.D., Benaroch P., Strosberg A.D., Bouvier M. and Marullo S. (1999) Beta(2)-adrenergic receptor down-regulation. Evidence for a pathway that does not require endocytosis. *The Journal of Biological Chemistry* **274**(41), 28900-28908.

Johnson E.S. (2004) Protein modification by SUMO. *Annual Review of Biochemistry* **73**, 355-382.

Johnson J.A., Gray M.O., Chen C.H. and Mochly-Rosen D. (1996) A protein kinase C translocation inhibitor as an isozyme-selective antagonist of cardiac function. *The Journal of Biological Chemistry* **271**(40), 24962-24966.

Johnson M. (2006) Molecular mechanisms of beta(2)-adrenergic receptor function,

response, and regulation. *The Journal of Allergy and Clinical Immunology* **117**(1), 18-24.

Johnston L.A., Erdogan S., Cheung Y.F., Sullivan M., Barber R., Lynch M.J., Baillie G.S., Heeke G.V., Adams D.R., Huston E. and Houslay M.D. (2004) Expression, intracellular distribution and basis for lack of catalytic activity of the PDE4A7 isoform encoded by the human PDE4A cAMP-specific phosphodiesterase gene. *Biochemical Journal* **380**(Pt 2), 371-384.

Kagey M.H., Melhuish T.A. and Wotton D. (2003) The polycomb protein Pc2 is a SUMO E3. *Cell* **113**(1), 127-137.

Kakiuchi S. and Yamazaki R. (1970) Calcium dependent phosphodiesterase activity and its activating factor (PAF) from brain studies on cyclic 3',5'-nucleotide phosphodiesterase. *Biochemical and Biophysical Research Communications* **41**(5), 1104-1110.

Kandel E.R. and Schwartz J.H. (1982) Molecular biology of learning: modulation of transmitter release. *Science* **218**(4571), 433-443.

Kanelis V., Rotin D. and Forman-Kay J.D. (2001) Solution structure of a Nedd4 WW domain-ENaC peptide complex. *Nature Structural Biology* **8**(5), 407-412.

Kapiloff M.S., Jackson N. and Airhart N. (2001) mAKAP and the ryanodine receptor are part of a multi-component signaling complex on the cardiomyocyte nuclear envelope. *Journal of Cell Science* **114**(Pt 17), 3167-3176.

Karin M. (1995) The regulation of AP-1 activity by mitogen-activated protein kinases. *The Journal of Biological Chemistry* **270**(28), 16483-16486.

Karpen J.W. and Rich T.C. (2001) The fourth dimension in cellular signaling. *Science* **293**(5538), 2204-2205.

Kaupp U.B. and Seifert R. (2002) Cyclic nucleotide-gated ion channels. *Physiological*

*Reviews* **82**(3), 769-824.

Kiely P.A., Leahy M., O'Gorman D. and O'Connor R. (2005) RACK1-mediated integration of adhesion and insulin-like growth factor I (IGF-I) signaling and cell migration are defective in cells expressing an IGF-I receptor mutated at tyrosines 1250 and 1251. *The Journal of Biological Chemistry* **280**(9), 7624-7633.

Kiely P.A., Sant A. and O'Connor R. RACK1 is an insulin-like growth factor 1 (IGF-1) receptor-interacting protein that can regulate IGF-1-mediated Akt activation and protection from cell death. (2002) *The Journal of Biological Chemistry* **277**(25), 22581-22589.

King R.W., Glotzer M. and Kirschner M.W. (1996) Mutagenic analysis of the destruction signal of mitotic cyclins and structural characterization of ubiquitinated intermediates. *Molecular Biology of the Cell* **7**(9), 1343-1357.

Kirsh O., S  ller J.S., Pichler A., Gast A., M  ller S., Miska E., Mathieu M., Harel-Bellan A., Kouzarides T., Melchior F. and Dejean A. (2002) The SUMO E3 ligase RanBP2 promotes modification of the HDAC4 deacetylase. *The EMBO Journal* **21**(11), 2682-2691.

Kitamura T., Kitamura Y., Kuroda S., Hino Y., Ando M., Kotani K., Konishi H., Matsuzaki H., Kikkawa U., Ogawa W. and Kasuga M. (1999) Insulin-induced phosphorylation and activation of cyclic nucleotide phosphodiesterase 3B by the serine-threonine kinase Akt. *Molecular and Cellular Biology* **19**(9), 6286-6296.

Klapisz E., Sorokina I., Lemeer S., Pijnenburg M., Verkleij A.J. and van Bergen en Henegouwen P.M. (2002) A ubiquitin-interacting motif (UIM) is essential for Eps15 and Eps15R ubiquitination. *The Journal of Biological Chemistry* **277**(34), 30746-30753.

Klauck K.M., Faux M.C., Labudda K., Langeberg L.K., Jaken S. and Scott J.D. (1996) Coordination of three signaling enzymes by AKAP79, a mammalian scaffold protein,

*Science* **271**(5255), 1589–1592.

Klemke M., Pasolli H. A., Kehlenbach R.H., Offermanns S., Schultz G. and Huttner W.B. (2000) Characterization of the extra-large G protein alpha-subunit XLalphas. II. Signal transduction properties. *The Journal of Biological Chemistry* **275**(43), 33633-33640.

Kobayashi, T., Gamanuma, M., Sakaki, T., Yamashita, Y., Yuasa, K., Kotera, J. and Omori, K. (2003) Molecular comparison of rat cyclic nucleotide phosphodiesterase 8 family: unique expression of PDE8B in rat brain. *Gene* **319**, 21-31.

Koegl M., Hoppe T., Schlenker S., Ulrich H.D., Mayer T.U. and Jentsch S. (1999) novel ubiquitination factor, E4, is involved in multiubiquitin chain assembly. *Cell* **96**(5), 635-44.

Kohout T.A. and Lefkowitz R.J. (2003) Regulation of G protein-coupled receptor kinases and arrestins during receptor desensitization. *Molecular Pharmacology* **63**(1), 9-18.

Kotaja N., Karvonen U., Janne O.A. and Palvimo J.J. (2002) PIAS proteins modulate transcription factors by functioning as SUMO-1 ligases. *Molecular and Cellular Biology* **22**(14), 5222-5234.

Kozasa T. (2004) The structure of GRK2-G beta gamma complex: intimate association of G-protein signaling modules. *Trends in Pharmacological Sciences* **25**(2), 61-63.

Kramer A. and Schneider-Mergener J. (1998) Synthesis and screening of peptide libraries on continuous cellulose membrane supports. *Methods in Molecular Biology* **87**, 25-39.

Krasel C., Dammeier S., Winstel R., Brockmann J., Mischak H. and Lohse M.J. (2001) Phosphorylation of GRK2 by protein kinase C abolishes its inhibition by calmodulin. *The Journal of Biological Chemistry* **276**(3), 1911-1915.

Krupinski J., Coussen F., Bakalyar H.A., Tang W.J., Feinstein P.G., Orth K., Slaughter C., Reed R.R. and Gilman A.G. (1989) Adenylyl cyclase amino acid sequence: possible channel- or transporter-like structure. *Science* **244**(4912), 1558-1564.

Kulkarni S.K. and Patil C.S. (2004) Phosphodiesterase 5 enzyme and its inhibitors: update on pharmacological and therapeutical aspects. *Methods and findings in Experimental and Clinical Pharmacology* **26**(10), 789-799.

Kumar K.G, Krolewski J.J. and Fuchs S.Y. (2004) Phosphorylation and specific ubiquitin acceptor sites are required for ubiquitination and degradation of the IFNAR1 subunit of type I interferon receptor. *The Journal of Biological Chemistry* **279**(45), 46614-46620.

Lam Y.A., Lawson T.G., Velayutham M., Zweier J.L. and Pickart C.M. (2002) A proteasomal ATPase subunit recognizes the polyubiquitin degradation signal. *Nature* **416**(6882), 763-767.

Lam Y.A., Xu W., Demartino G.N. and Cohen R.E. (1997) Editing of ubiquitin conjugates by an isopeptidase in the 26S proteasome. *Nature* **385**(6618), 737-740.

Lamba S. and Abraham W.T. (2000) Alterations in adrenergic receptor signaling in heart failure. *Heart Failure Reviews* **5**(1), 7-16.

Laporte, S. A., Oakley, R. H., Holt, J. A., Barak, L. S. and Caron, M. G. (2000). The interaction of beta-arrestin with the AP-2 adaptor is required for the clustering of beta 2-adrenergic receptor into clathrin-coated pits. *The Journal of Biological Chemistry* **275**(30), 23120 –23126.

Lawler O.A., Miggin S.M. and Kinsella B.T. (2001) Protein kinase A-mediated phosphorylation of serine 357 of the mouse prostacyclin receptor regulates its coupling to G(s)-, to G(i)-, and to G(q)-coupled effector signaling. *The Journal of Biological Chemistry* **276**(36), 33596-33607.

Layfield R., Cavey J.R. and Lowe J. (2003) Role of ubiquitin-mediated proteolysis in

the pathogenesis of neurodegenerative disorders. *Ageing Research Reviews* **2**(4), 343-356.

Le Jeune I.R., Shepherd M., Van Hecke G., Houslay M.D. and Hall I.P. (2002) Cyclic AMP-dependent transcriptional up-regulation of phosphodiesterase 4D5 in human airway smooth muscle cells. Identification and characterization of a novel PDE4D5 promoter. *The Journal of Biological Chemistry* **277**(39), 35980-35989.

Lee M.E., Markowitz J., Lee J.O. and Lee H. (2002) Crystal structure of phosphodiesterase 4D and inhibitor complex. *FEBS Letters* **530**(1-3), 53-58.

Lee R., Wolda S., Moon E., Esselstyn J., Hertel C. and Lerner A. (2002) PDE7A is expressed in human B-lymphocytes and is up-regulated by elevation of intracellular cAMP. *Cell Signalling* **14**(3), 277-284.

Lefkowitz R.J. and Shenoy S.K. (2005) Transduction of receptor signals by beta-arrestins. *Science* **308**(5721), 512-517.

Lefkowitz R.J. and Whalen E.J. (2004) beta-arrestins: traffic cops of cell signaling. *Current Opinion in Cell Biology* **16**(2), 162-168.

Lefkowitz R.J., Pierce K.L. and Luttrell L.M. (2002) Dancing with different partners: protein kinase a phosphorylation of seven membrane-spanning receptors regulates their G protein-coupling specificity. *Molecular Pharmacology* **62**(5), 971-974.

Lefkowitz R.J., Rockman H.A. and Koch W.J. (2000) Catecholamines, cardiac beta-adrenergic receptors, and heart failure. *Circulation* **101**(14), 1634-1637.

Lehnart S.E., Wehrens X.H., Reiken S., Warrier S., Belevych A.E., Harvey R.D., Richter W., Jin S.L., Conti M. and Marks A.R. (2005) Phosphodiesterase 4D deficiency in the ryanodine-receptor complex promotes heart failure and arrhythmias. *Cell* **123**(1), 25-35.

Leroy M.J., Degerman E., Taira M., Murata T., Wang L.H., Movsesian M.A., Meacci

- E. and Manganiello V.C. (1996) Characterization of two recombinant PDE3 (cGMP-inhibited cyclic nucleotide phosphodiesterase) isoforms, RcGIP1 and HcGIP2, expressed in NIH 3006 murine fibroblasts and Sf9 insect cells. *Biochemistry* **35**(31), 10194-10202.
- Li S.J. and Hochstrasser M. (1999) A new protease required for cell-cycle progression in yeast. *Nature* **398**(6724), 246-251.
- Lim J., Pahlke G. and Conti M. (1999) Activation of the cAMP-specific phosphodiesterase PDE4D3 by phosphorylation. Identification and function of an inhibitory domain. *The Journal of Biological Chemistry* **274**(28), 19677-19685.
- Lin F., Wang H. and Malbon C.C. (2000) Gravin-mediated formation of signaling complexes in beta 2-adrenergic receptor desensitization and resensitization. *The Journal of Biological Chemistry* **275**(25), 19025-19034.
- Lin H.K., Wang L., Hu Y.C., Altuwaijri S. and Chang C. (2002) Phosphorylation-dependent ubiquitylation and degradation of androgen receptor by Akt require Mdm2 E3 ligase. *The EMBO Journal* **21**(15), 4037-4048.
- Lin X., Liang M., Liang Y.Y., Brunnicardi F.C. and Feng X.H. (2003) SUMO-1/Ubc9 promotes nuclear accumulation and metabolic stability of tumor suppressor Smad4. *The Journal of Biological Chemistry* **278**(33), 31043-31048.
- Lipworth B.J. (2005) Phosphodiesterase-4 inhibitors for asthma and chronic obstructive pulmonary disease. *Lancet* **365**(9454), 167-175.
- Liu H. and Maurice D.H. (1999) Phosphorylation-mediated activation and translocation of the cyclic AMP-specific phosphodiesterase PDE4D3 by cyclic AMP-dependent protein kinase and mitogen-activated protein kinases. A potential mechanism allowing for the coordinated regulation of PDE4D activity and targeting. *The Journal of Biological Chemistry* **274**(15), 10557-10565.
- Lochhead A., Nekrasova E., Arshavsky V.Y. and Pyne N.J. (1997) The regulation of

the cGMP-binding cGMP phosphodiesterase by proteins that are immunologically related to gamma subunit of the photoreceptor cGMP phosphodiesterase. *The Journal of Biological Chemistry* **272**(29), 18397-403.

Lodowski D.T., Pitcher J.A., Capel W.D., Lefkowitz R.J. and Tesmer J.J. (2003) Keeping G proteins at bay: a complex between G protein-coupled receptor kinase 2 and Gbetagamma. *Science* **300**(5623), 1256-1262.

Luo X., Zeng W., Xu X., Popov S., Davignon I., Wilkie T.M., Mumby S.M. and Muallem S. (1999) Alternate coupling of receptors to Gs and Gi in pancreatic and submandibular gland cells. *The Journal of Biological Chemistry* **274**(25), 17684-17690.

Luttrell L.M. (2006) Transmembrane signaling by G protein-coupled receptors. *Methods in Molecular Biology* **332**, 3-49.

Luttrell L.M. and Lefkowitz R.J. (2002) The role of beta-arrestins in the termination and transduction of G-protein-coupled receptor signals. *Journal of Cell Science* **115**(Pt 3), 455-465.

Lynch M.J., Baillie G.S., Mohamed A., Li X., Maisonneuve C., Klussmann E., Heeke V. G. and Houslay M.D. (2005) RNA silencing identifies PDE4D5 as the functionally relevant cAMP phosphodiesterase interacting with beta arrestin to control the protein kinase A/AKAP79-mediated switching of the beta2-adrenergic receptor to activation of ERK in HEK293B2 cells. *The Journal of Biological Chemistry* **280**(39), 33178-33189.

MacKenzie S.J., Baillie G.S., McPhee I., Bolger G.B. and Houslay M.D. (2000) ERK2 mitogen-activated protein kinase binding, phosphorylation, and regulation of the PDE4D cAMP-specific phosphodiesterases. The involvement of COOH-terminal docking sites and NII2-terminal UCR regions. *The Journal of Biological Chemistry* **275**(22), 16609-16617.

MacKenzie S.J., Baillie G.S., McPhee I., MacKenzie C., Seamons R., McSorley T.,

Millen J., Beard M.B., Heeke V.G. and Houslay M.D. (2002) Long PDE4 cAMP specific phosphodiesterases are activated by protein kinase A-mediated phosphorylation of a single serine residue in Upstream Conserved Region 1 (UCR1). *British Journal of Pharmacology* **136**(3), 421-433.

MacKenzie S.J., Yarwood S.J., Peden A.H., Bolger G.B., Vernon R.G. and Houslay M.D. (1998) Stimulation of p70S6 kinase via a growth hormone-controlled phosphatidylinositol 3-kinase pathway leads to the activation of a PDE4A cyclic AMP-specific phosphodiesterase in 3T3-F442A preadipocytes. *Proc.Natl. Acad. Sci. U.S.A.* **95**(7), 3549-3554.

Malbon C.C., Tao J. and Wang H.Y. (2004) AKAPs (A-kinase anchoring proteins) and molecules that compose their G-protein-coupled receptor signalling complexes. *Biochemical Journal* **379**(Pt 1), 1-9.

Manganiello V.C., Taira M., Degerman E. and Belfrage P. (1995) Type III cGMP-inhibited cyclic nucleotide phosphodiesterases (PDE3 gene family). *Cell Signalling* **7**(5), 445-455.

Manza L.L., Codreanu S.G., Stamcr S.L., Smith D.L., Wells K.S., Roberts R.L., Liebler D.C. (2004) Global shifts in protein sumoylation in response to electrophile and oxidative stress. *Chemical Research in Toxicology* **17**(12), 1706-1715.

Marchal C., Haguenaue-Tsapis R. and Urban-Grimal D. (2000) Casein kinase I-dependent phosphorylation within a PEST sequence and ubiquitination at nearby lysines signal endocytosis of yeast uracil permease. *The Journal of Biological Chemistry* **275**(31), 23608-23614.

Marinissen M.J. and Gutkind J.S. (2001) G-protein-coupled receptors and signaling networks: emerging paradigms. *Trends in Pharmacological Sciences* **22**(7), 368-376.

Martin N.P., Lefkowitz R.J. and Shenoy S.K. (2003) Regulation of V2 vasopressin receptor degradation by agonist-promoted ubiquitination. *The Journal of Biological Chemistry* **278**(46), 45954-45959.

Martin N.P., Whalen E.J., Zamah M.A., Pierce K.L. and Lefkowitz R.J. (2004) PKA-mediated phosphorylation of the beta1-adrenergic receptor promotes Gs/Gi switching. *Cell Signalling* **16**(12), 1397-1403.

Martinez S.E., Wu A.Y., Glavas N.A., Tang X.B., Turley S., Hol W.G. and Beavo J.A. (2002) The two GAF domains in phosphodiesterase 2A have distinct roles in dimerization and in cGMP binding. *Proc. Natl. Acad. Sci. U.S.A.* **99**(20), 13260-13265.

Marx S.O., Reiken S., Hisamatsu Y., Jayaraman T., Burkhoff D., Rosembliit N. and Marks A.R. (2000) PKA phosphorylation dissociates FKBP12.6 from the calcium release channel (ryanodine receptor): defective regulation in failing hearts. *Cell* **101**(4), 365-376.

Masciarelli S., Horner K., Liu C., Park S.H., Hinckley M., Hockman S., Nedachi T., Jin C., Conti M. and Manganiello V. (2004) Cyclic nucleotide phosphodiesterase 3A-deficient mice as a model of female infertility. *The Journal of Clinical Investigation* **114**(2), 196-205.

Mastrandrea L.D., You J., Nilcs E.G. and Pickart C.M. (1999) E2/E3-mediated assembly of lysine 29-linked polyubiquitin chains. *The Journal of Biological Chemistry* **274**(38), 27299-27306.

Matunis M.J. and Pickart C.M. (2005) Beginning at the end with SUMO. *Nature Structural and Molecular Biology* **12**(7), 565-566.

Matunis M.J., Coutavas E. and Blobel G. (1996) A novel ubiquitin-like modification modulates the partitioning of the Ran-GTPase-activating protein RanGAP1 between the cytosol and the nuclear pore complex. *The Journal of Cell Biology* **135**(6Pt 1), 1457-1470.

Matunis M.J., Wu J. and Blobel G. (1998) SUMO-1 modification and its role in targeting the Ran GTPase-activating protein, RanGAP1, to the nuclear pore complex. *The Journal of Cell Biology* **140**(3), 499-509.

Maudsley S., Martin B. and Luttrell L.M. (2005) The origins of diversity and specificity in G protein-coupled receptor signaling. *The Journal of Pharmacological and Experimental Therapeutics* **314**(2), 485-494.

Maurice D.H., Palmer D., Tilley D.G., Dunkerley H.A., Netherton S.J., Raymond D.R., Elbatarny H.S. and Jimmo S.L. (2003) Cyclic nucleotide phosphodiesterase activity, expression, and targeting in cells of the cardiovascular system. *Molecular Pharmacology* **64**(3), 533-546.

McAllister-Lucas L.M., Haik T.L., Colbran J.L., Sonnenburg W.K., Seger D., Turko I.V., Beavo J.A., Francis S.H. and Corbin J.D. (1995) An essential aspartic acid at each of two allosteric cGMP-binding sites of a cGMP-specific phosphodiesterase. *The Journal of Biological Chemistry* **270**(51), 30671-30679.

McCahill A., McSorley T., Huston E., Hill E.V., Lynch M.J., Gall I., Keryer G., Lygren B., Tasken K., Hেকে V.G. and Houslay M.D. (2005) In resting COS1 cells a dominant negative approach shows that specific, anchored PDE4 cAMP phosphodiesterase isoforms gate the activation, by basal cyclic AMP production, of AKAP-tethered protein kinase A type II located in the centrosomal region. *Cell Signalling* **17**(9), 1158-1173.

McCahill A., Warwicker J., Bolger G.B., Houslay M.D. and Yarwood S.J. (2002) The RACK1 scaffold protein: a dynamic cog in cell response mechanisms. *Molecular Pharmacology* **62**(6), 1261-1273.

McConnachie G., Langeberg L.K. and Scott J.D. (2006) AKAP signaling complexes: getting to the heart of the matter. *Trends in Molecular Medicine* **12**(7), 317-323.

McPhec I., Cochran S. and Houslay M.D. (2001) The novel long PDE4A10 cyclic AMP phosphodiesterase shows a pattern of expression within brain that is distinct from the long PDE4A5 and short PDE4A1 isoforms. *Cell Signalling* **13**(12), 911-918.

McPhec I., Pooley L., Lobban M., Bolger G., Houslay M.D. (1995) Identification, characterization and regional distribution in brain of RPDE6 (RNPDE4A5), a novel

splice variant of the PDE4A cyclic AMP phosphodiesterase family. *Biochemical Journal* **310**(3), 965-974.

McPhee I., Yarwood S.J., Scotland G., Huston E., Beard M.B., Ross A.H., Houslay E.S. and Houslay M.D. (1999) Association with the SRC family tyrosyl kinase LYN triggers a conformational change in the catalytic region of human cAMP-specific phosphodiesterase HSPDE4A4B. Consequences for rolipram inhibition. *The Journal of Biological Chemistry* **274**(17), 11796-11810.

Mehats C., Jin S.L., Wahlstrom J., Law E., Umetsu D.T. and Conti M. (2003) PDE4D plays a critical role in the control of airway smooth muscle contraction. *The FASEB Journal* **17**(13), 1831-1841.

Melchior F. (2000) SUMO--nonclassical ubiquitin. *Annual Review of Cell and Developmental Biology* **16**, 591-626.

Melchior F., Schergaut M., Pichler A. (2003) SUMO: ligases, isopeptidases and nuclear pores. *Trends in Biochemical Sciences* **28**(11), 612-618.

Meschia J.F., Brott T.G., Brown R.D. Crook R., Worrall B.B., Kissela B., Brown W.M., Rich S.S., Case L.D., Evans E.W., Hague S., Singleton A., Hardy J. et al. (2005) Phosphodiesterase 4D and 5-lipoxygenase activating protein in ischemic stroke. *Annals of Neurology* **58**(3), 351-361.

Meyer H.H., Wang Y. and Warren G. (2002) Direct binding of ubiquitin conjugates by the mammalian p97 adaptor complexes, p47 and Ufd1-Npl4. *The EMBO Journal* **21**(21), 5645-5652.

Michaeli T., Bloom T.J., Martins T., Loughney K., Ferguson K., Riggs M., Rodgers L., Beavo J.A. and Wigler M. (1993) Isolation and characterization of a previously undetected human cAMP phosphodiesterase by complementation of cAMP phosphodiesterase-deficient *Saccharomyces cerevisiae*. *The Journal of Biochemistry* **268**(17), 12925-12932.

Michel J.J. and Scott J.D. (2002) AKAP mediated signal transduction. *Annual Review of Pharmacology and Toxicology* **42**, 235-257.

Millar J.K., Pickard B.S, Mackie S., James R., Christie S., Buchanan S.R., Malloy M.P., Chubb J.E., Huston E., Baillie G.S., Thomson P.A., Hill E.V., Brandon N.J., Rain J.C., Camargo L.M., Whiting P.J., Houslay M.D., Blackwood D.H., Muir W.J. and Porteous D.J. (2005) DISC1 and PDE4B are interacting genetic factors in schizophrenia that regulate cAMP signaling. *Science* **310**(5751), 1187-1191.

Miller S.L., Malotky E. and O'Bryan J.P. (2004) Analysis of the role of ubiquitin-interacting motifs in ubiquitin binding and ubiquitylation. *The Journal of Biological Chemistry* **279**(32), 33528-33537.

Milligan G. (2003) Constitutive activity and inverse agonists of G protein-coupled receptors: a current perspective. *Molecular Pharmacology* **64**(6), 1271-1276.

Mimnaugh E.G. and Neckers L.M. (2005) Measuring ubiquitin conjugation in cells. *Methods in Molecular Biology* **301**, 223-241.

Miyauchi Y., Yogosawa S., Honda R., Nishida T. and Yasuda H. (2002) Sumoylation of Mdm2 by protein inhibitor of activated STAT (PIAS) and RanBP2 enzymes. *The Journal of Biological Chemistry* **277**(51), 50131-50136.

Mongillo M., McSorley T., Evellin S., Sood A., Lissandron V., Terrin A., Huston E., Hannawacker A., Lohse M.J., Pozzan T., Houslay M.D. and Zaccolo M. (2004) Fluorescence resonance energy transfer-based analysis of cAMP dynamics in live neonatal rat cardiac myocytes reveals distinct functions of compartmentalized phosphodiesterases. *Circulation Research* **95**(1), 67-75.

Moore A.R. and Willoughby D.A. (1995) The role of cAMP regulation in controlling inflammation. *Clinical and Experimental Immunology* **101**(3), 387-389.

Movsesian M.A. (2002) PDE3 cyclic nucleotide phosphodiesterases and the compartmentation of cyclic nucleotide-mediated signalling in cardiac myocytes. *Basic*

*Research in Cardiology* **97** Suppl 1, 183-190.

Mueller T.D., Kamionka M. and Falquet L. (2004) Specificity of the interaction between ubiquitin-associated domains and ubiquitin. *The Journal of Biological Chemistry* **279**(12), 11926-11936.

Muller S., Hoegge C., Pyrowolakis G. and Jentsch S. (2001) SUMO, ubiquitin's mysterious cousin. *Nature Reviews. Molecular Cell Biology* **2**(3), 202-210.

Muller S., Ledl A. and Schmidt D. (2004) SUMO: a regulator of gene expression and genome integrity. *Oncogene* **23**(11), 1998-2008.

Murray F., MacLean M.R. and Pyne N.J. (2002) Increased expression of the cGMP-inhibited cAMP-specific (PDE3) and cGMP binding cGMP-specific (PDE5). *British Journal of Pharmacology* **137**(8), 1187-1194.

Nakagawa K. and Yokosawa H. (2002) PIAS3 induces SUMO-1 modification and transcriptional repression of IRF-1. *FEBS Letters* **530**(1-3), 204-208.

Nakamura T. and Gold G.H. (1987) A cyclic nucleotide-gated conductance in olfactory receptor cilia. *Nature* **325**(6103), 442-444.

Namekata K., Nishimura N. and Kimura H. (2002) Presenilin-binding protein forms aggresomes in monkey kidney COS-7 cells. *Journal of Neurochemistry* **82**(4), 819-827.

Netherton S.J. and Maurice D.H. (2005) Vascular endothelial cell cyclic nucleotide phosphodiesterases and regulated cell migration: implications in angiogenesis. *Molecular Pharmacology* **67**(1), 263-272.

Newlon M.G., Roy M., Morikis D., Hausken Z.E., Coghlan V., Scott J.D. and Jennings P.A. (1999) The molecular basis for protein kinase A anchoring revealed by solution NMR. *Nature Structural Biology* **6**(3), 222-227.

Nikolaev V.O., Bunemann M., Hein L., Hannawacker A. and Lohse M.J. (2004) Novel single chain cAMP sensors for receptor-induced signal propagation. *The Journal of Biological Chemistry* **279**(36), 37215-37218.

O'Donnell J.M. and Zhang H.T. (2004) Antidepressant effects of inhibitors of cAMP phosphodiesterase (PDE4). *Trends in Pharmacological Sciences* **25**(3), 158-163.

Oakley R.H., Laporte S.A., Holt J.A., Caron M.G. and Barak L.S. (2000) Differential affinities of visual arrestin, beta arrestin1, and beta arrestin2 for G protein-coupled receptors delineate two major classes of receptors. *The Journal of Biological Chemistry* **275**(22), 17201-17210.

Oberholte R., Ratzliff J., Baecker P.A., Daniels D.V., Zuppan P., Jarnagin K. and Shelton E.R. (1997) Multiple splice variants of phosphodiesterase PDE4C cloned from human lung and testis. *Biochimica et Biophysica Acta* **1353**(3), 287-297.

Oger S., Mchats C., Barnette M.S., Ferre F., Cabrol D. and Leroy M.J. (2004) Anti-inflammatory and utero-relaxant effects in human myometrium of new generation phosphodiesterase 4 inhibitors. *Biology of Reproduction* **70**(2), 458-464.

Oldham C.E., Mohny R.P., Miller S.L.H., Hanes R.N. and O'Bryan J.P. (2002) The ubiquitin-interacting motifs target the endocytic adaptor protein epsin for ubiquitination. *Current Biology* **12**(13), 1112-1116.

Ostrom R.S., Violin J.D., Coleman S. and Insel P.A. (2000) Selective enhancement of beta-adrenergic receptor signaling by overexpression of adenylyl cyclase type 6: colocalization of receptor and adenylyl cyclase in caveolae of cardiac myocytes. *Molecular Pharmacology* **57**(5), 1075-1079.

Owens R.J., Lumb S., Rees-Milton K., Russell A., Baldock D., Lang V., Crabbe T., Ballesteros M. and Perry M.J. (1997) Molecular cloning and expression of a human phosphodiesterase 4C. *Cell Signalling* **9**(8), 575-585.

Papa F.R. and Hochstrasser M. (1993) The yeast DOA4 gene encodes a

deubiquitinating enzyme related to a product of the human *trc-2* oncogene. *Nature* **366**(6453), 313-319.

Passmore L.A. and Barford D. (2004) Getting into position: the catalytic mechanisms of protein ubiquitylation. *Biochemical Journal* **379**(Pt 3), 513-525.

Patrucco E., Notte A., Barberis L., Selvetella G., Maffei A., Brancaccio M., Marengo S., Russo G., Azzolino O., Rybalkin S.D., Silengo L., Altruda F., Wetzker R., Wymann M.P., Lembo G. and Hirsch E. (2004) PI3Kgamma modulates the cardiac response to chronic pressure overload by distinct kinase-dependent and -independent effects. *Cell* **118**(3), 375-387.

Penn R.B., Pronin A.N. and Benovic J.L. (2000) Regulation of G protein-coupled receptor kinases. *Trends in Cardiovascular Medicine* **10**(2), 81-89.

Perry S.J. and Lefkowitz R.J. (2002) Arresting developments in heptahelical receptor signaling and regulation. *Trends in Cell Biology* **12**(3), 130-138.

Perry S.J., Baillic G.S., Kohout T.A., McPhee I., Magiera M.M., Ang K.L., Miller W.E., McLean A.J., Conti M., Houslay M.D. and Lefkowitz R.J. (2002) *Science* **298**(5594), 834-836.

Petrofski J.A. and Koch W.J. (2003) The beta-adrenergic receptor kinase in heart failure. *Journal of Molecular and Cellular Cardiology* **35**(10), 1167-1174.

Pichler A., Gast A., Seeler J.S., Dejean A. and Melchior F. (2002) The nucleoporin RanBP2 has SUMO1 E3 ligase activity. *Cell* **108**(1), 109-120.

Pickart C.M. (2000) Ubiquitin in chains. *Trends in Biochemical Sciences* **25**(11), 544-548.

Pickart C.M. (2001) Mechanisms underlying ubiquitination. *Annual Review of Biochemistry* **70**, 503-533.

Pickart C.M. and Eddins M.J. (2004) Ubiquitin: structures, functions, mechanisms. *Biochimica et Biophysica Acta* **1695**(1-3), 55-72.

Pierce K.L., Premont R.T. and Lefkowitz R.J. Seven-transmembrane receptors. (2002) Nature Reviews. *Molecular Cell Biology* **3**(9), 639-650.

Pitcher J.A., Tesmer J.J., Freeman J.L., Capel W.D., Stone W.C. and Lefkowitz R.J. (1999) Feedback inhibition of G protein-coupled receptor kinase 2 (GRK2) activity by extracellular signal-regulated kinases. *The Journal of Biological Chemistry* **274**(49), 34531-34534.

Polo S., Sigismund S., Faretta M., Guidi M., Capua M.R., Bossi G, Chen H., De Camilli P. and Di Fiore P.P. (2002) A single motif responsible for ubiquitin recognition and monoubiquitination in endocytic proteins. *Nature* **416**(6879), 451-455.

Ponting C.P. (2000) Proteins of the endoplasmic-reticulum-associated degradation pathway: domain detection and function prediction. *Biochemical Journal* **351**(Pt 2), 527-535.

Pornillos O., Alam S.L., Rich R.L., Myszka D.G., Davis D.R. and Sundquist W.I. (2002) Structure and functional interactions of the Tsg101 UEV domain. *The EMBO Journal* **21**(10), 2397-2406.

Pornillos O., Alam S.L., Rich R.L., Myszka D.G., Davis D.R. and Sundquist W.I. Pronin A.N., Loudon R.P. and Benovic J.L. (2002) Characterization of G protein-coupled receptor kinases. *Methods in Enzymology* **343**, 547-559.

Qiu Y.H., Chen C.N., Malone T., Richter L., Beckendorf S.K. and Davis R.L. (1991) Characterization of the memory gene *dunce* of *Drosophila melanogaster*. *Journal of Molecular Biology* **222**(3), 553-565.

Rall T. W. and Sutherland E. W. (1958) Fractionation and characterization of a cyclic adenine ribonucleotide formed by tissue particles. *The Journal of Biological Chemistry* **232**(2), 1077-1091.

Rapacciuolo A., Suvarna S., Barki-Harrington L., Luttrell L.M., Cong M., Lefkowitz R.J. and Rockman H.A. (2003) Protein kinase A and G protein-coupled receptor kinase phosphorylation mediates beta-1 adrenergic receptor endocytosis through different pathways. *The Journal of Biological Chemistry* **278**(37), 35403-35411.

Rehmann H., Prakash B., Wolf E., Rueppel A., De Rooij J., Bos J.L. and Wittinghofer A. (2003) Structure and regulation of the cAMP-binding domains of Epac2. *Nature Structural Biology* **10**(1), 26-32.

Reiter E. and Lefkowitz R.J. (2006) GRKs and beta-arrestins: roles in receptor silencing, trafficking and signaling. *Trends in endocrinology and metabolism* **17**(4), 159-65.

Ren D., Navarro B., Perez G., Jackson A.C., Hsu S., Shi Q., Tilly J.L. and Clapham D.E. (2001) A sperm ion channel required for sperm motility and male fertility. *Nature* **413**(6856), 603-609.

Rena G., Begg F., Ross A., MacKenzie C., McPhee I., Campbell L., Huston E., Sullivan M. and Houslay M.D. (2001) Molecular cloning, genomic positioning, promoter identification, and characterization of the novel cyclic amp-specific phosphodiesterase PDE4A10. *Molecular Pharmacology* **59**(5), 996-1011.

Reneland R.H., Mah S., Kammerer S., Hoyal C.R., Marnellos G., Wilson S.G., Sambrook P.N., Spector T.D., Nelson M.R. and Braun A. (2005) Association between a variation in the phosphodiesterase 4D gene and bone mineral density. *BMC Medical Genetics* **6**, 9.

Reverter D. and Lima C.D. (2005) Insights into E3 ligase activity revealed by a SUMO-RanGAP1-Ubc9-Nup358 complex. *Nature* **435**(7042), 687-692.

Rich T.C., Fagan K.A., Tse T.E., Schaack J., Cooper D.M. and Karpen J.W. (2001) A uniform extracellular stimulus triggers distinct cAMP signals in different compartments of a simple cell. *Proc. Natl. Acad. Sci. U.S.A.* **98**(23), 13049-13054.

Richter W and Conti M. (2004) The oligomerization state determines regulatory properties and inhibitor sensitivity of type 4 cAMP-specific phosphodiesterases. *The Journal of Biological Chemistry* **279**(29), 30338-30348.

Richter W., Jin S.L. and Conti M. (2005) Splice variants of the cyclic nucleotide phosphodiesterase PDE4D are differentially expressed and regulated in rat tissue. *Biochemical Journal* **388**(Pt 3), 803-811.

Robichaud A., Stamatiou P.B., Jin S.L., Lachance N., MacDonald D., Laliberté F., Liu S., Huang Z., Conti M. and Chan C.C. (2002) Deletion of phosphodiesterase 4D in mice shortens alpha(2)-adrenoceptor-mediated anesthesia, a behavioral correlate of emesis. *The Journal of Clinical Investigation* **110**(7), 1045-1052.

Rochais F., Vandecasteele G., Lefebvre F., Lugnier C., Lum H., Mazet J.L., Cooper D.M. and Fischmeister R. (2004) Negative feedback exerted by cAMP-dependent protein kinase and cAMP phosphodiesterase on subsarcolemmal cAMP signals in intact cardiac myocytes: an in vivo study using adenovirus-mediated expression of CNG channels. *The Journal of Biological Chemistry*. **279**(50), 52095-52105.

Rockman H.A., Koch W.J. and Lefkowitz R.J. (2002) Seven-transmembrane-spanning receptors and heart function. *Nature* **415**(6868), 206-212.

Ron D., Chen C.H., Caldwell J., Jamieson L., Orr E. and Mochly-Rosen D. (1994) Cloning of an intracellular receptor for protein kinase C: a homolog of the beta subunit of G proteins. *Proc. Natl. Acad. Sci. U.S.A.* **91**(3), 839-843.

Ron D., Jiang Z., Yao L., Vagts A., Diamond I. and Gordon A. (1999) Coordinated movement of RACK1 with activated betaIIIPKC. *The Journal of Biological Chemistry* **274**(38), 27039-27046.

Rosman G.J., Martins T.J., Sonnenburg W.K., Beavo J.A., Ferguson K. and Loughney K. (1997) Isolation and characterization of human cDNAs encoding a cGMP-stimulated 3',5'-cyclic nucleotide phosphodiesterase. *Gene* **191**(1), 89-95.

Roth A.F. and Davis N.G. (2000) Ubiquitination of the PEST-like endocytosis signal of the yeast a-factor receptor. *The Journal of Biological Chemistry* **275**(11), 8143-8153.

Rybalkin S.D., Rybalkina I., Beavo J.A. and Bornfeldt K.E. (2002) Cyclic nucleotide phosphodiesterase 1C promotes human arterial smooth muscle cell proliferation. *Circulation Research* **90**(2), 151-157.

Rybin V.O., Xu X., Lisanti M.P. and Steinberg S.F. (2000) Differential targeting of beta -adrenergic receptor subtypes and adenylyl cyclase to cardiomyocyte caveolae. A mechanism to functionally regulate the cAMP signaling pathway. *The Journal of Biological Chemistry* **275**(52), 41447-41457.

Sachdev S., Bruhn L., Sieber H., Pichler A., Melchior F. and Grosschedl R. (2001) PIASy, a nuclear matrix-associated SUMO E3 ligase, represses LEF1 activity by sequestration into nuclear bodies. *Genes and Development* **15**(23), 3088-3103.

Saenz de Tejada L., Angulo J., Cucvas P., Fernandez A., Moncada I., Allona A., Lledo E., Korschner H.G., Niewohner U., Haning H., Pages E. and Bischoff E. (2001) The phosphodiesterase inhibitory selectivity and the in vitro and in vivo potency of the new PDE5 inhibitor vardenafil. *International Journal of Impotence Research*. **13**(5), 282-290.

Saitoh H. and Hinchey J. (2000) Functional heterogeneity of small ubiquitin-related protein modifiers SUMO-1 versus SUMO-2/3. *The Journal of Biological Chemistry* **275**(9), 6252-6258.

Sampson D.A., Wang M. and Matunis M.J. (2001) The small ubiquitin-like modifier-1 (SUMO-1) consensus sequence mediates Ubc9 binding and is essential for SUMO-1 modification. *The Journal of Biological Chemistry* **276**(24), 21664-21669.

Sanz M.J., Alvarez A., Piqueras L., Cerdá M., Issekutz A.C., Lobb R.R., Cortijo J. and Morcillo E.J. (2005) Rolipram inhibits leukocyte-endothelial cell interactions in vivo through P- and E-selectin downregulation. *British Journal of Pharmacology* **135**(8),

1872-1881.

Scapin G., Patel S.B., Chung C., Varnerin, Edmondson S.D., Mastracchio A., Parmee E.R., Singh S.B., Becker J.W., Van der Ploeg L.H. and Tota M.R. (2004) Crystal structure of human phosphodiesterase 3B: atomic basis for substrate and inhibitor specificity. *Biochemistry* **43**(20), 6091-6100.

Scheffner M., Nuber U. and Huibregtse J.M. (1995) Protein ubiquitination involving an E1-E2-E3 enzyme ubiquitin thioester cascade. *Nature* **373**(6509), 81-83.

Schermuly R.T., Ghofrani H.A., Enke B., Weismann N., Grimminger F., Seeger W., Schudt C. And Walmrath D. (1999) Low-dose systemic phosphodiesterase inhibitors amplify the pulmonary vasodilatory response to inhaled prostacyclin in experimental pulmonary hypertension. *American Journal of Respiratory and Clinical Care Medicine* **160**(5 Pt 1), 1500-1506.

Schmidt D. and Muller S. (2002) Members of the PIAS family act as SUMO ligases for c-Jun and p53 and repress p53 activity. *Proc. Natl. Acad. Sci. U.S.A.* **99**(5), 2872-2877.

Schnell J.D. and Hicke L. (2003) Non-traditional functions of ubiquitin and ubiquitin-binding proteins. *The Journal of Biological Chemistry* **278**(38), 35857-35860.

Scott A.I., Perini A.F., Shering P.A. and Whalley L.J. (1991) *European Journal of Clinical Pharmacology* **40**(2), 127-129.

Scott J.D. (2003) A-kinase-anchoring proteins and cytoskeletal signalling events. *Biochemical Society Transactions* **31**(Pt 1), 87-89.

Scott J.D., Dell'Acqua M.L., Fraser I.D., Tavalin S.J. and Lester L.B. (2000) Coordination of cAMP signaling events through PKA anchoring. *Advances in Pharmacology* **47**, 175-207.

Sebastiani G., Morissette C, Lagace C., Boule M., Ouellette M.J., McLaughlin R.W.,

Lacombe D., Gervais F. and Tremblay P. (2005) The cAMP-specific phosphodiesterase 4B mediates Abeta-induced microglial activation. *Neurobiology of Aging* **27**(5), 691-701.

Seeler J.S. and Dejean A. (2003) Nuclear and unclear functions of SUMO. *Nature Reviews. Molecular Cell Biology* **4**(9), 690-699.

Seibenhener M.L., Babu J.R., Geetha T., Wong H.C., Krishna N.R. and Wooten M.W. (2004) Sequestosome 1/p62 is a polyubiquitin chain binding protein involved in ubiquitin proteasome degradation. *Molecular and Cellular Biology* **24**(18), 8055-8068.

Sette C. and Conti M. (1996) Phosphorylation and activation of a cAMP-specific phosphodiesterase by the cAMP-dependent protein kinase. Involvement of serine 54 in the enzyme activation. *The Journal of Biological Chemistry* **271**(28), 16526-16534.

Sette C., Vicini E. and Conti M. (1994) The ratPDE3/IVd phosphodiesterase gene codes for multiple proteins differentially activated by cAMP-dependent protein kinase. *The Journal of Biological Chemistry* **269**(28), 18271-18274.

Seybold J., Newton R., Wright L., Finney P.A., Suttorp N., Barnes P.J., Adcock I.M. and Giembycz M.A. (1998) Induction of phosphodiesterases 3B, 4A4, 4D1, 4D2, and 4D3 in Jurkat T-cells and in human peripheral blood T-lymphocytes by 8-bromo-cAMP and Gs-coupled receptor agonists. Potential role in beta2-adrenoreceptor desensitization. *The Journal of Biological Chemistry* **273**(32), 20575-20588.

Sharma R.K. (1991) Phosphorylation and characterization of bovine heart calmodulin-dependent phosphodiesterase. *Biochemistry* **30**(24), 5963-5968.

Sharrocks A.D., Yang S.H. and Galanis A. (2000) Docking domains and substrate-specificity determination for MAP kinases. *Trends in Biochemical Sciences* **25**(9), 448-453.

Shenoy S.K. and Lefkowitz R.J. (2003) Multifaceted roles of beta-arrestins in the regulation of seven-membrane-spanning receptor trafficking and signalling.

*Biochemical Journal* **375**(Pt 3), 503-515.

Shenoy S.K. and Lefkowitz R.J. (2003) Trafficking patterns of beta-arrestin and G protein-coupled receptors determined by the kinetics of beta-arrestin deubiquitination. *The Journal of Biological Chemistry* **278**(16), 14498-14506.

Shenoy S.K., McDonald P.H., Kohout T.A. and Lefkowitz R.J. (2001) Regulation of receptor fate by ubiquitination of activated beta 2-adrenergic receptor and beta-arrestin. *Science* **294**(5545), 1307-1313.

Shepherd et al. (2004) Remodelling of the PDE4 cAMP phosphodiesterase isoform profile upon monocyte-macrophage differentiation of human U937 cells. *British Journal of Pharmacology* **142**(2), 339-351.

Shiina T., Kawasaki A., Nagao T. and Kurose H. (2000) Interaction with beta-arrestin determines the difference in internalization behavior between beta1- and beta2-adrenergic receptors. *The Journal of Biological Chemistry* **275**(37), 29082-29090.

Smith F.D., Langeberg L.K. and Scott J.D. (2006) The where's and when's of kinase anchoring. *Trends in Biochemical Sciences* **31**(6), 316-323.

Smith P.G., Wang F., Wilkinson K.N., Savage K.J., Klein U., Neuberger D.S., Bollag G., Shipp M.A. and Aguiar R.C. (2005) The phosphodiesterase PDE4B limits cAMP-associated PI3K/AKT-dependent apoptosis in diffuse large B-cell lymphoma. *Blood* **105**(1), 308-316.

Smith S.J., Cieslinski L.B., Newton R., Donnelly L.E., Fenwick P.S., Nicholson A.G., Barnes P.J., Barnette M.S. and Giembycz M.A. (2004) Discovery of BRL 50481 [3-(N,N-dimethylsulfonamido)-4-methyl-nitrobenzene], a selective inhibitor of phosphodiesterase 7: in vitro studies in human monocytes, lung macrophages, and CD8+ T-lymphocytes. *Molecular Pharmacology* **66**(6), 1679-1689.

Snyder P.B., Florio V.A., Ferguson K. and Loughney K. (1999) Isolation, expression

and analysis of splice variants of a human Ca<sup>2+</sup>/calmodulin-stimulated phosphodiesterase (PDE1A). *Cell Signalling* **11**(7), 535-544.

Soderling S.H., Bayuga S.J. and Beavo J.A. (1999) Isolation and characterization of a dual-substrate phosphodiesterase gene family: PDE10A. *Proc. Natl. Acad. Sci. U.S.A.* **96**(12), 7071-7076.

Sondek J., Bohm A., Lambright D.G., Hamm H.E. and Sigler P.B. (1996) Crystal structure of a G-protein beta gamma dimer at 2.1A resolution. *Nature* **379**(6563), 369-374.

Souness J.E., Aldous D. and Sargent C. (2000) Immunosuppressive and anti-inflammatory effects of cyclic AMP phosphodiesterase (PDE) type 4 inhibitors. *Immunopharmacology* **47**(2-3), 127-162.

Spence J., Gali R.R., Dittmar G., Sherman F., Karin M. and Finley D. (2000) Cell cycle-regulated modification of the ribosome by a variant multiubiquitin chain. *Cell* **102**(1), 67-76.

Spence J., Sadis S., Haas A.L. and Finley D. (1995) A ubiquitin mutant with specific defects in DNA repair and multiubiquitination. *Molecular and Cellular Biology* **15**(3), 1265-1273.

Spengler M.L., Kurapatwinski K., Black A.R., Azizkhan-Clifford J. (2002) SUMO-1 modification of human cytomegalovirus IE1/IE72. *Journal of Virology* **76**(6), 2990-2996.

Stacey et al. (1998) Molecular cloning and expression of human cGMP-binding cGMP-specific phosphodiesterase (PDE5). *Biochemical and Biophysical Research Communications* **247**(2), 2492-2454.

Steele M.R., McCahill A., Thompson D.S., MacKenzie C., Isaacs N.W., Houslay M.D. and Bolger G.B. (2001) Identification of a surface on the beta-propeller protein RACK1 that interacts with the cAMP-specific phosphodiesterase PDE4D5. *Cell*

*Signalling* 13(7), 507-513.

Steiner A.A. and Branco L.G. (2003) Fever and anapyrexia in systemic inflammation: intracellular signaling by cyclic nucleotides. *Frontiers in Bioscience* 8, s1398-1408.

Sterne-Marr R., Gurevich V.V., Goldsmith P., Bodine R.C., Sanders C., Donoso L.A. and Benovic J.L. (1993) Polypeptide variants of beta-arrestin and arrestin3. *The Journal of Biological Chemistry* 268(21), 15640-15648.

Sturton G. and Fitzgerald M. (2002) Phosphodiesterase 4 inhibitors for the treatment of COPD. *Chest* 121(5 Suppl), 192S-196S.

Sullivan M., Olsen A.S. and Houslay M.D. (1999) Genomic organisation of the human cyclic AMP-specific phosphodiesterase PDE4C gene and its chromosomal localisation to 19p13.1, between RAB3A and JUND. *Cell. Signalling* 11(10), 735-742.

Sullivan M., Rena G., Begg F., Gordon L., Olsen A.S. and Houslay M.D. (1998) Identification and characterization of the human homologue of the short PDE4A cAMP-specific phosphodiesterase RD1 (PDE4A1) by analysis of the human HSPDE4A gene locus located at chromosome 19p13.2. *Biochemical Journal* 333(Pt 3), 693-703.

Sun Y., Cheng Z., Ma L. and Pei G. (2002) Beta-arrestin2 is critically involved in CXCR4-mediated chemotaxis, and this is mediated by its enhancement of p38 MAPK activation. *The Journal of Biological Chemistry* 277(51), 49212-49219.

Sunahara R., Dessauer C. and Gilman A. (1996) Complexity and diversity of mammalian adenylyl cyclases. *Annual Review of Pharmacology and Toxicology* 36, 461-480.

Sunahara R.K. and Taussig R. (2002) Isoforms of mammalian adenylyl cyclase: multiplicities of signaling. *Molecular Interventions* 2(3), 168-184.

Sutherland E.W. and Rall T.W. (1960) Formation of adenosine-3,5-phosphate (cyclic

adenylate) and its relation to the action of several neurohormones or hormones. *Acta Endocrinologica* **34**(Suppl 50), 171-174.

Swinnen J.V., Joseph D.R. and Conti M. (1989) The mRNA encoding a high-affinity cAMP phosphodiesterase is regulated by hormones and cAMP. *Proc. Natl. Acad. Sci. U.S.A.* **86**(21), 8197-8201.

Swinnen J.V., Tsikalas K.E. and Conti M. (1991) Properties and hormonal regulation of two structurally related cAMP phosphodiesterases from the rat Sertoli cell. *The Journal of Biological Chemistry* **266**(27), 18370-18377.

Tachibana H., Naga Prasad S.V., Lefkowitz R.J., Koch W.J. and Rockman H.A. (2005) Level of beta-adrenergic receptor kinase 1 inhibition determines degree of cardiac dysfunction after chronic pressure overload-induced heart failure. *Circulation* **111**(5), 591-597.

Tanaka K., Suzuki T., Hattori N. and Mizuno Y. (2004) Ubiquitin, proteasome and parkin. *Biochimica et Biophysica Acta* **1695**(1-3), 235-247.

Tang K.M., Jang E.K. and Haslam R.J. (1997) Expression and mutagenesis of the catalytic domain of cGMP-inhibited phosphodiesterase (PDE3) cloned from human platelets. *Biochemical Journal* **323**(Pt 1), 217-224.

Tao J., Wang H.Y. and Malbon C.C. (2003) Protein kinase A regulates AKAP250 (gravin) scaffold binding to the beta2-adrenergic receptor. *The EMBO Journal* **22**(24), 6419-6429.

Tasken K. and Aandahl E.M. (2004) Localized effects of cAMP mediated by distinct routes of protein kinase A. *Physiological Reviews* **84**(1), 137-167.

Tasken K.A., Collas P., Kemmner W.A., Witczak O., Conti M. and Tasken K. (2001) Phosphodiesterase 4D and protein kinase a type II constitute a signaling unit in the centrosomal area. *The Journal of Biological Chemistry* **276**(25), 21999-22002.

Tatham M.H. (2001) Polymeric chains of SUMO-2 and SUMO-3 are conjugated to protein substrates by SAE1/SAE2 and Ubc9. *The Journal of Biological Chemistry* **276**, 35368-35374.

Tatham M.H., Jaffray E., Vaughan O.A., Desterro J.M., Botting C.H., Naismith J.H. and Hay R.T. (2001) Polymeric chains of SUMO-2 and SUMO-3 are conjugated to protein substrates by SAE1/SAE2 and Ubc9. *The Journal of Biological Chemistry* **276**(38), 35368-35374.

Thornton C., Tang K.C., Phamluong K., Luong K., Vagts A., Nikanjam D., Yaka R. and Ron D. (2004) Spatial and temporal regulation of RACK1 function and N-methyl-D-aspartate receptor activity through WD40 motif-mediated dimerization. *The Journal of Biological Chemistry* **279**(30), 31357-31364.

Tilley D. and Maurice D.H. (2005) Vascular smooth muscle cell phenotype-dependent phosphodiesterase 4D short form expression: role of differential histone acetylation on cAMP-regulated function. *Molecular Pharmacology* **68**(3), 596-605.

Torras-Llort M. and Azorin F. (2003) Functional characterization of the human phosphodiesterase 7A1 promoter. *Biochemical Journal* **373**(Pt 3), 835-843.

Tran T.M., Friedman J., Qunaibi E., Baameur F., Moore R.H. and Clark R.B. (2004) Characterization of agonist stimulation of cAMP-dependent protein kinase and G protein-coupled receptor kinase phosphorylation of the beta2-adrenergic receptor using phosphoserine-specific antibodies. *Molecular Pharmacology* **65**(1), 196-206.

Vandecasteele G., Rochais F., Abi-Gerges A. and Fischmeister R. (2006) Functional localization of cAMP signalling in cardiac myocytes. *Biochemical Society Transactions* **34**(Pt 4), 484-488.

Vandecasteele G., Verde I., Rucker-Martin C., Donzeau-Gouge P. and Fischmeister R. (2001) Cyclic GMP regulation of the L-type Ca(2+) channel current in human atrial myocytes. *The Journal of Physiology* **533**(Pt 2), 329-340.

VanDemark A.P. and Hill C.P. (2002) Structural basis of ubiquitylation. *Current Opinion in Structural Biology* **12**(6), 822-830.

Varadan R., Walker O, Pickart C. and Fushman D. (2002) Structural properties of polyubiquitin chains in solution. *Journal of Molecular Biology* **324**(4), 637-647.

Verde I., Pahlke G, Salanova M., Zhang G, Wang S., Coletti D., Onuffer J., Jin S.L. and Conti M. (2001) Myomegalin is a novel protein of the golgi/centrosome that interacts with a cyclic nucleotide phosphodiesterase. *The Journal of Biological Chemistry* **276**(14), 11189-11198.

Verger A., Perdomo J. and Crossley M. (2003) Modification with SUMO. A role in transcriptional regulation. *EMBO Reports* **4**(2), 137-142.

Voges D., Zwinkl P. and Baumeister W. (1999) The 26 proteasome: a molecular machine designed for controlled proteolysis. *Annual reviews in Biochemistry* **68**, 1015-1068.

von Zastrow M. and Kobilka B.K. (1994) Antagonist-dependent and antagonist-independent steps in the mechanism of adrenergic receptor internalization. *The Journal of Biological Chemistry* **269**(28), 18448-18452.

Vossler M.R., Yao H., York R.D., Pan M.G., Kim C.S. and Stork P.J. (1997) cAMP activates MAP kinase and Elk-1 through a B-Raf- and Rap1-dependent pathway. *Cell* **89**(1), 73-82.

Wallace D.A., Johnston L.A., Huston E., MacMaster D., Houslay T.M., Cheung Y.F., Campbell L., Millen J.E., Smith R.A., Gall I., Knowles R.G., Sullivan M. and Houslay M.D. (2005) Identification and characterization of PDE4A11, a novel, widely expressed long isoform encoded by the human PDE4A cAMP phosphodiesterase gene. *Molecular Pharmacology* **67**(6), 1920-1934.

Wan K.F., Sambhi B.S., Frame M., Tate R. and Pyne N.J. (2001) The inhibitory gamma subunit of the type 6 retinal cyclic guanosine monophosphate phosphodiesterase is a

novel intermediate regulating p42/p44 mitogen-activated protein kinase signaling in human embryonic kidney 293 cells. *The Journal of Biological Chemistry* **276**(41), 37802-37808.

Wang D., Deng C., Bugaj-Gaweda B., Kwan M., Gunwaldsen C., Leonard C., Xin X., Hu Y., Unterbeck A. and De Vivo M. (2003) Cloning and characterization of novel PDE4D isoforms PDE4D6 and PDE4D7. *Cell Signalling* **15**(9), 883-891.

Wang G., Yang J. and Huijbrechtse J.M. (1999) Functional domains of the Rsp5 ubiquitin-protein ligase. *Molecular and Cellular Biology* **19**(1), 342-352.

Wang H., Lee Y. and Malbon C.C. (2004) PDE6 is an effector for the Wnt/Ca<sup>2+</sup>/cGMP-signalling pathway in development. *Biochemical Society Transactions* **32**(Pt 5), 792-796.

Wang P., Wu P., Egan R.W. and Billah M.M. (2003) Identification and characterization of a new human type 9 cGMP-specific phosphodiesterase splice variant (PDE9A5). Differential tissue distribution and subcellular localization of PDE9A variants. *Gene* **314**, 15-27.

Waterman H., Levkowitz G., Alroy I. and Yarden Y. (1999) Ubiquitin ligase activity and tyrosine phosphorylation underlie suppression of growth factor signaling by c-Cbl/Sli-1. *Molecular Cell* **4**(6), 1029-1040.

Wechsler J., Choi Y.H., Krall J., Ahmad F., Manganiello V.C. and Movsesian M.A. (2002) Isoforms of cyclic nucleotide phosphodiesterase PDE3A in cardiac myocytes. *The Journal of Biological Chemistry* **277**(41), 38072-38078.

Wei H., Ahn S., Shenoy S.K., Karnik S.S., Hunyady L., Luttrell L.M. and Lefkowitz R.J. (2003) Independent beta-arrestin 2 and G protein-mediated pathways for angiotensin II activation of extracellular signal-regulated kinases 1 and 2. *Proc. Natl. Acad. Sci. U.S.A.* **100**(19), 10782-10787.

Weissman A.M. (2001) Themes and variations on ubiquitylation. *Nature Reviews*.

*Molecular Cell Biology* **2**(3), 169-178.

Westphal R.S., Tavalin S.J., Lin J.W., Alto N.M., Fraser I.D., Langeberg L.K., Sheng M. and Scott J.D. (1999) Regulation of NMDA receptors by an associated phosphatase-kinase signaling complex. *Science* **285**(5424), 93-96.

Wilkinson K.D. (2000) Ubiquitination and deubiquitination: targeting of proteins for degradation by the proteasome. *Seminars in Cell and Developmental Biology* **11**(3), 141-148.

Wilson V.G. and Rangasamy D. (2001) Intracellular targeting of proteins by sumoylation. *Experimental Cell Research* **271**(1), 57-65.

Xia Z., Choi E.J., Wang F. and Storm D.R. (1992) The type III calcium/calmodulin-sensitive adenylyl cyclase is not specific to olfactory sensory neurons. *Neuroscience Letters* **144**(1-2), 169-173.

Xiang Y., Naro F., Zoudilova M., Jin S.L., Conti M. and Kobilka B. (2005) Phosphodiesterase 4D is required for beta2 adrenoceptor subtype-specific signaling in cardiac myocytes. *Proc. Natl. Acad. Sci. U.S.A.* **102**(3), 909-914.

Xiang Y., Rybin V.O., Steinberg S.F., Kobilka B. Xiang Y., Rybin V.O., Steinberg S.F. and Kobilka B. (2002) *The Journal of Biological Chemistry* **277**(37), 34280-34286.

Xu R.X., Hassell A.M., Vanderwall D., Lambert M.H., Holmes W.D., Luther M.A., Rocque W.J., Milburn M.V., Zhao Y., Ke II. and Nolte R.T. (2000) Atomic structure of PDE4: insights into phosphodiesterase mechanism and specificity. *Science* **288**(5472), 1822-1825.

Yaka R., Thornton C., Vagts A.J., Phamluong K., Bonci A. and Ron D. (2002) NMDA receptor function is regulated by the inhibitory scaffolding protein, RACK1. *Proc. Natl. Acad. Sci. U.S.A.* **99**(8), 5710-5715.

Yan C., Zhao A.Z., Bentley J.K. and Beavo J.A. (1996) The calmodulin-dependent

phosphodiesterase gene PDE1C encodes several functionally different splice variants in a tissue-specific manner. *The Journal of Biological Chemistry* **271**, 25699-25706.

Yang Q., Paskind M., Bolger G., Thompson W. J., Repaske D. R., Cutler L. S. and Epstein P. M. (1994) A novel cyclic GMP stimulated phosphodiesterase from rat brain. *Biochemical and Biophysical Research Communications* **205**(3), 1850-1858.

Yang S.H. and Sharrocks A.D. (2004) SUMO promotes HDAC-mediated transcriptional repression. *Molecular Cell* **13**(4), 611-617.

Yang Y., Fang S., Jensen J.P., Weissman A.M. and Ashwell J.D. (2000) Ubiquitin protein ligase activity of IAPs and their degradation in proteasomes in response to apoptotic stimuli. *Science* **288**(5467), 874-877.

Yarwood S.J., Steele M.R., Scotland G., Houslay M.D. and Bolger G.B. (1999) The RACK1 signaling scaffold protein selectively interacts with the cAMP-specific phosphodiesterase PDE4D5 isoform. *The Journal of Biological Chemistry* **274**(21), 14909-14917.

Yedovitzky M., Mochly-Rosen D., Johnson J.A., Gray M.O., Ron D., Abramovitch E., Cerasi E. and Neshler R. (1997) Translocation inhibitors define specificity of protein kinase C isoenzymes in pancreatic beta-cells. *The Journal of Biological Chemistry* **272**(3), 1417-1420.

Young P., Deveraux Q., Beal R.E., Pickart C.M. and Rechsteiner M. (1998) Characterization of two polyubiquitin binding sites in the 26 S protease subunit 5a. *The Journal of Biological Chemistry* **273**(10), 5461-5467.

Yuasa K., Kotera J., Fujishige K., Michibata H., Sasaki T. and Omori K. (2000) Isolation and characterization of two novel phosphodiesterase PDE11A variants showing unique structure and tissue-specific expression. *The Journal of Biological Chemistry* **275**(40), 31469-31479.

Zaccolo M. and Pozzan T. (2002) Discrete microdomains with high concentration of

cAMP in stimulated rat neonatal cardiac myocytes. *Science* **295**(5560), 1711-1715.

Zaccolo M., Magalhaes P. and Pozzan T. (2002) Compartmentalisation of cAMP and Ca(2+) signals. *Current Opinion in Cell Biology* **14**(2), 160-166.

Zhang H.T., Huang Y., Suvarna N.U., Deng C., Crissman A.M., Hopper A.T., De Vivo M., Rose G.M. and O'Donnell J.M. (2005) Effects of the novel PDE4 inhibitors MEM1018 and MEM1091 on memory in the radial-arm maze and inhibitory avoidance tests in rats. *Psychopharmacology* **179**(3), 613-619.

Zhang J., Ma Y., Taylor S.S. and Tsien R.Y. (2001) Genetically encoded reporters of protein kinase A activity reveal impact of substrate tethering. *Proc. Natl. Acad. Sci U.S.A.* **98**(26), 14997-15002.

Zhang K.Y., Card G.L., Suzuki Y., Artis D.R., Fong D., Gillette S., Hsieh D., Neiman J., West B.L., Zhang C., Milburn M.V., Kim S.H., Schlessinger J. and Bollag G. (2004) A glutamine switch mechanism for nucleotide selectivity by phosphodiesterases. *Molecular Cell* **15**(2), 279-286.